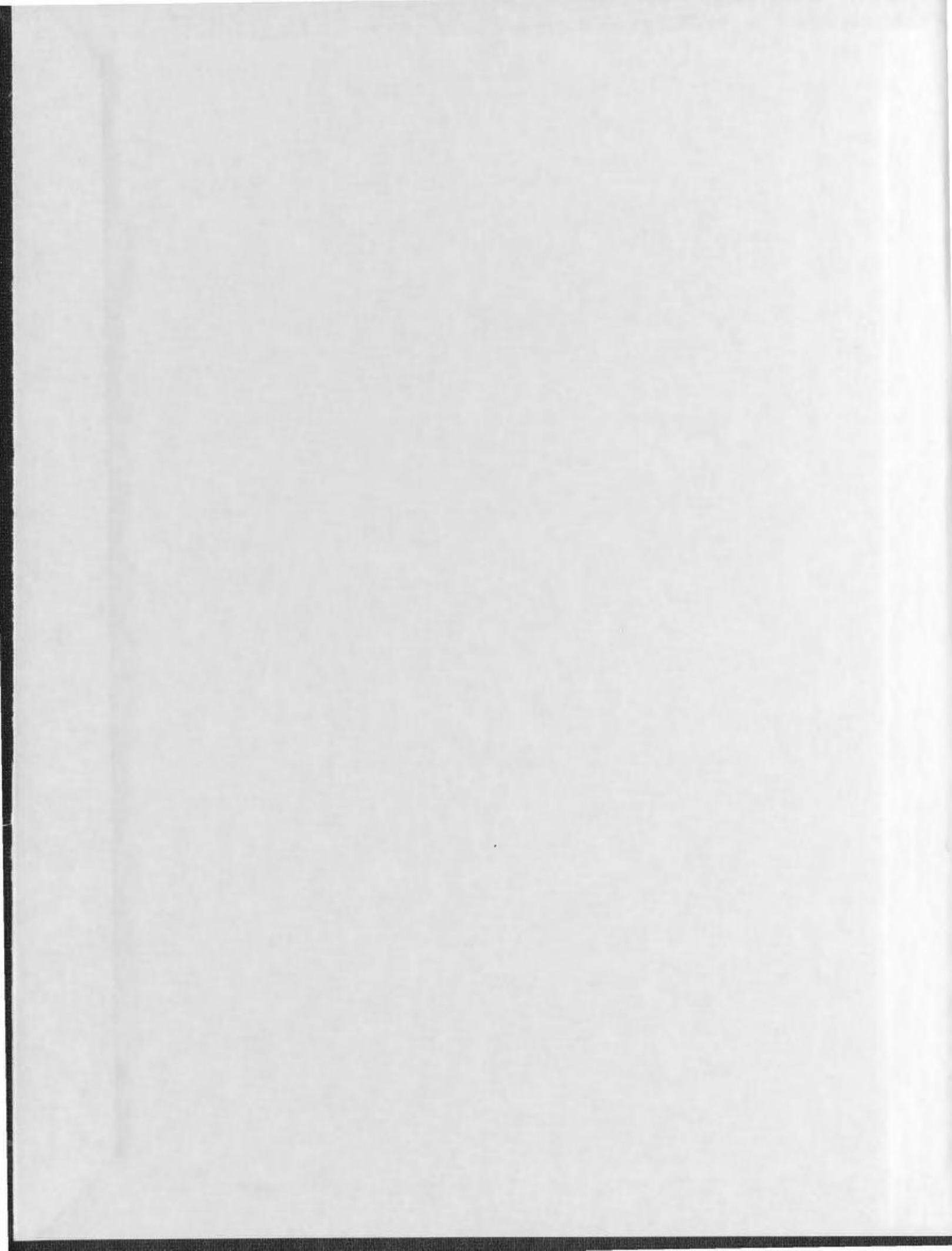MIXED-LAYER ILLITE/SMECTITE DIAGENESIS IN
THE RIFT AND POST-RIFT SEDIMENTS OF THE
JEANNE D'ARC BASIN, OFFSHORE
NEWFOUNDLAND, CANADA

IFTIKHAR A. ABID

INFORMATION TO USERS

MIXED-LAYER ILLITE/SMECTITE DIAGENESIS IN THE RIFT AND POST-RIFT SEDIMENTS OF THE JEANNE D'ARC BASIN, OFFSHORE NEWFOUNDLAND, CANADA

© Iftikhar A. Abid, B.Sc. (Hons.), M.Sc.

A thesis submitted to the School of Graduate
Studies in partial fulfillment of the
requirements for the degree of
Doctor of Philosophy

Department of Earth Sciences
Memorial University of Newfoundland
April 1996

St. John's   Newfoundland

Canada

ABSTRACT

Mixed-layer illite/smectite (I/S) clays were analyzed from 22 deep exploration wells from the Jeanne d'Arc Basin, where large commercial hydrocarbon reserves have been discovered. This basin has been subdivided into 4 areas (Southern, Trans-Basin Fault, Northern, and Outer Ridge Complex) based on general geology and characteristics of I/S-depth profiles.

The mineralogy of fine-grain clays (<0.1µm) consists of mainly mixed-layer I/S with minor amounts of kaolinite, illite, and chlorite. Smectite and/or smectite-rich I/S clays were supplied to the Jeanne d'Arc Basin during Upper Jurassic to Tertiary time. At present smectite-rich I/S clays occur only in shallow samples irrespective of their geologic age. The proportion of illite-layers, as well as their ordering in I/S, increase with depth and temperature. The random to R1-ordered I/S transition occurs between depth intervals of 1940m to 3720m and crosses several stratigraphic boundaries. The R1 to R3-ordered I/S transition is generally observed below 4000m depth. Basin-wide I/S data indicate that smectite-rich I/S clays have been illitized in both rift and post-rift sediments of the Jeanne d'Arc Basin due to diagenesis.

The majority of I/S clays in samples with vitrinite reflectance (R_o) values less than 0.5% are highly expandable and randomly interstratified. However, for R_o values greater than 0.66% only illite-rich ordered I/S is observed. The random to R1-ordered I/S transition generally occurs within the upper "oil window" level of organic maturity (0.50-

0.66%R_o). The relationships observed in this study should be expected in other wells of the Jeanne d'Arc Basin and may provide useful information to investigate the thermal maturity of sediments.

The $\delta^{18}O$ values of I/S clays range from 17.9‰ to 25.8‰ (SMOW), and calculated pore-fluid compositions vary from 1.5‰ to 11.6‰. In the Trans-Basin Fault area, high $\delta^{18}O$ pore-fluid values are present at shallower depths and coincide with a narrow transition from random to R1-ordered I/S and reflect vertical migration of deep-basinal fluids along the fault zones. These fluids appear to be responsible for the rapid I/S-depth transition observed. In contrast pore-fluid $\delta^{18}O$ in the Northern area increases progressively with depth, suggesting there was no significant vertical migration of deep basinal fluids in this area.

In the regional context I/S-depth profiles reflect the influence of such factors as temperature, fluid migration, basin structure, lithology, and salt diapirism. These observations illustrate that I/S-depth profiles should be expected to vary within the same sedimentary basin due to a variety of geological factors. A single well cannot always be considered representative of a particular basin.

ACKNOWLEDGEMENTS

iv

I thank my parents who have been sources of encouragement throughout my education. Finally, this thesis is dedicated to Asma Saleem (my wife) who has been my greatest supporter.

TABLE OF CONTENTS

LIST OF TABLES

LIST OF FIGURES

xiv

CHAPTER I

INTRODUCTION AND BACKGROUND

1.1 OBJECTIVES

The primary objective of this investigation is to characterize the composition of mixed-layer illite/smectite (I/S) from the argillaceous sediments in the Jeanne d'Arc Basin in order to place constraints on I/S diagenesis in the basin. The aim is to use several wells (16) (Table 1.1) together with additional control samples (6 wells) from different parts of the basin in order to see how I/S diagenesis may vary in response to variable geological features (i.e. burial depth, temperature, faults, lithology, stratigraphy) in the basin. Such a study will help to better understand the evolution of the basin and processes that affect illitization.

The Jeanne d'Arc is the only basin along the east coast of Canada where commercial oil reserves have been discovered (Fig. 1.1). No one has attempted, so far, to study mixed-layer I/S diagenesis on a regional scale in this basin. The large number of deep drill holes in the Jeanne d'Arc Basin provides adequate material and an excellent opportunity to undertake a basin-wide study of I/S in both rift and post-rift sediments and to compare the results with other sedimentary basins.

The second objective of this thesis is to compare

1
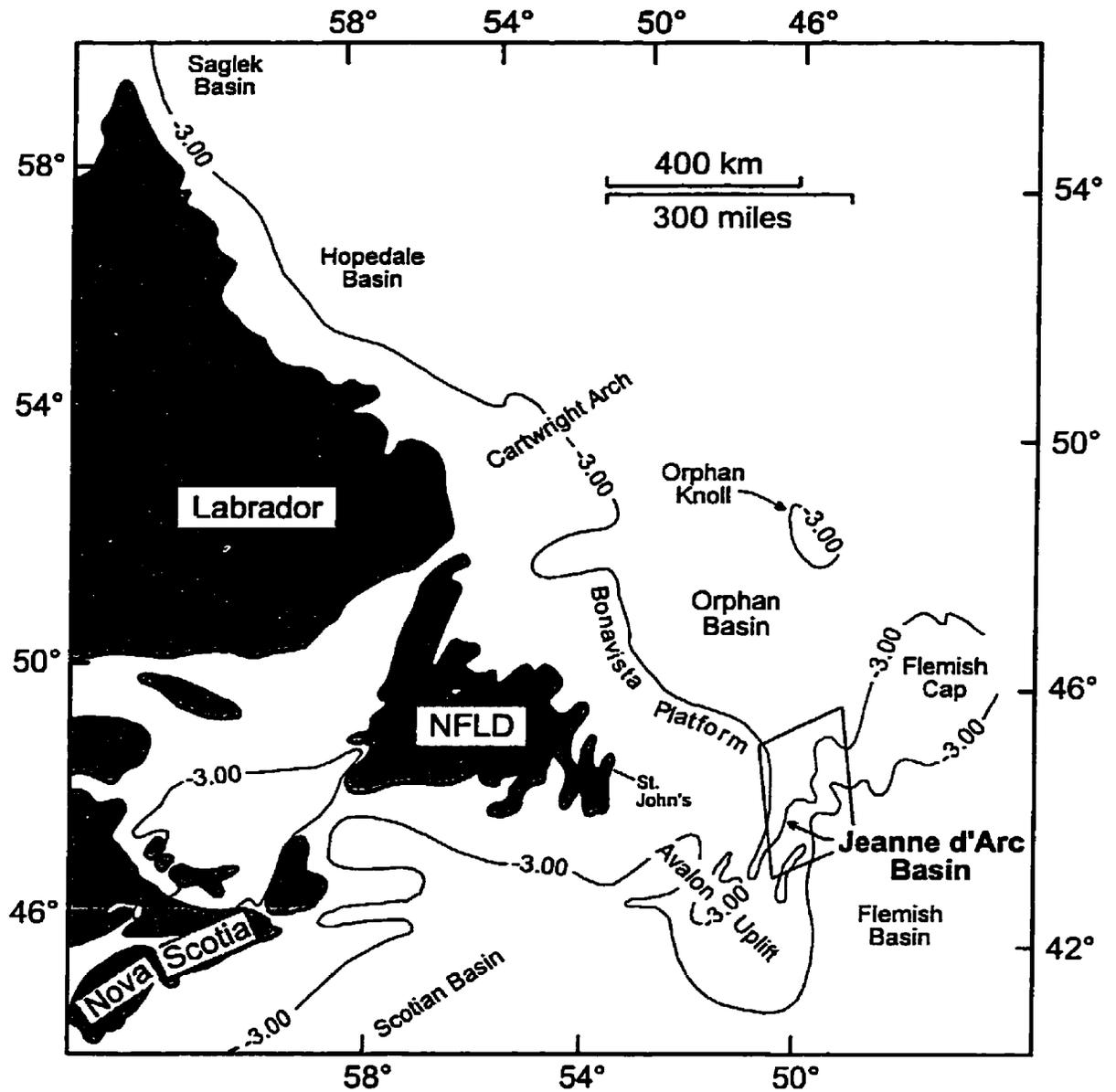
Figure 1.1. Map showing the location of the Jeanne d'Arc Basin. The 3km contour shows the depth to the basement. Note the Avalon uplift to the South. Modified from Arthur et al., 1982.

vitrinite reflectance data from well files (archived at Canada-Newfoundland Offshore Petroleum Board, C-NOPB) and open files (Geological Survey, Canada) with the compositional variations of I/S in order to evaluate the utility of I/S as a "geothermometer" in the Jeanne d'Arc Basin. The application of I/S "geothermometry" has never reached its full potential since several secondary factors including pore-fluid composition, porosity and permeability, fluid/rock ratio, time and nature of the starting material can significantly control the I/S composition. Therefore, each basin needs a careful investigation of the secondary factors to evaluate whether I/S can be used as a "geothermometer".

The third objective is to use the oxygen-isotopic composition of I/S rich clay-fractions to evaluate I/S compositional trends with increasing burial depths, and to understand the isotopic evolution of basinal fluids (Yeh and Savin, 1977; Suchecki and Land, 1983; Primmer and Shaw, 1991).

1.2 OVERVIEW OF PREVIOUS WORK, JEANNE D'ARC BASIN

The first detailed geological history of the offshore eastern Canada was published by Sherwin (1973). Stratigraphic nomenclature of the Scotian Shelf (McIver, 1972) was extended with little modification to the Grand Banks by Amoco and Imperial (1973), and Jansa and Wade (1975). Sinclair (1988) and McAlpine (1990) further refined the stratigraphic

3

nomenclature of the Jeanne d'Arc Basin (although some disagreement between them still exists). General depositional environments of various formations have been discussed by numerous workers (Sinclair, 1988; Brown et al., 1989; Harding, 1988; Hiscott et al., 1990; McAlpine, 1990; and Sinclair, 1993). The role of tectonism on depositional sequences was addressed by Tankard and Welsink (1987, 1988), Sinclair (1993), and Soliman (1995). The structural and geodynamic evolution of the Grand Banks basins was reviewed by Keen and Barrett (1981), Royden and Keen (1990), Keen et al., (1987), Keen and Beaumont (1990), Enachescu (1992), and others.

Results of earlier organic-matter studies indicated that Kimmeridgian shales of the Grand Banks are locally rich enough to generate hydrocarbons (Bujak et al., 1977a, b; Purcell et al., 1979, and Swift and Williams, 1980). Following the discovery of the Hibernia oil field several workers constructed present day maturation maps for the Kimmeridgian source rock (Egret Member) in the Jeanne d'Arc Basin (Avery et al., 1986; Creaney and Allison, 1987; Von der Dick et al., 1989; and Williamson, 1992). Correia et al. (1990) used corrected Bottom Hole Temperatures (BHT) to calculate geothermal gradients for several wells. Studies of the diagenesis of reservoir sandstones have been undertaken locally in the Hibernia oil field by Hutcheon et al. (1985), Abid (1988), and Abid and Hesse (1988).

4

This short summary of previous work reveals that many geological aspects of the Jeanne d'Arc Basin have been studied systematically in the past except for clastic diagenesis. Only a couple of papers address the sandstone diagenesis. No data are presently available in the literature regarding the distribution of clay minerals and possible depth/temperature dependent mixed-layer illite/smectite diagenesis from the Jeanne d'Arc Basin, which is the primary objective of this study.

1.3 STRUCTURES OF ILLITE, SMECTITE AND MIXED-LAYER ILLITE/SMECTITE

Both illite and the minerals of the smectite group are three-layer clays, consisting of a central layer of octahedrally coordinated metal ions sandwiched between two layers of silica tetrahedra. These tetrahedral-octahedral-tetrahedral layer packages are separated by interlayer sites. In illite these interlayer sites are occupied by K^+, resulting in a 10 angstroms ($\mathring{A}$) thick unit cell. In the smectite group minerals, the interlayer sites may be occupied by any of a number of hydrated metal ions, such as Ca^{2+} and Na^+. These interlayer cations are usually exchangeable, resulting in a unit cell with a variable thickness.

Another group of important clay minerals results from the interstratification of illite and smectite unit cells. If

5

interstratification is random, then the probability that an illite-layer (I-layer) will follow a smectite layer is controlled only by the proportion of illite layers in the crystal. Conversely, interstratification may be controlled by an ordering scheme. For example, an illite/smectite may exist in which any two smectite layers are always separated by at least one illite-layer.

Ordering in mixed-layer illite/smectite (I/S) can be classified according to the "Reichweite" scheme (Reynolds, 1980). In this scheme, R0 indicates random interstratification of illite and smectite layers (disordered structure), and R1 indicates ordered I/S in which each smectite layer is separated by at least one illite layer. R3 also indicates ordered I/S in which each smectite layer is separated by at least three illite layers. The criteria used to recognize different ordering patterns in I/S is discussed in section 3.4.

1.4 MIXED-LAYER ILLITE/SMECTITE DIAGENESIS

Smectite is common in fine-grained sediments at low temperatures, but during burial diagenesis, it is converted into illite through mixed-layer illite/smectite (Burst, 1969; Hower et al., 1976). The transformation of smectite into illitic material has been the focus of research among many clay mineralogists and petroleum geologists for more than

6

three decades. The transformation has been recognized in burial diagenesis (Perry and Hower, 1970), thermal alteration (Jennings and Thompson, 1986; Eberl et al., 1987), and contact metamorphic environments (Nadeau and Reynolds, 1981) and has been duplicated in laboratory experiments (Whitney and Northrop, 1988). Overall the chemical changes associated with this reaction include the uptake of potassium (K^+) and aluminum, and the expulsion of structural water, silica and other exchangeable cations (e.g. Na, Mg, Ca, Fe, etc.) from the smectite.

In Mesozoic to Lower Tertiary sediments, the I/S reaction is largely temperature dependent, provided that enough K^+ is available (Perry and Hower, 1970; Hower et al., 1976; Velde and Lijima, 1988). The I/S reaction commonly starts at about 50°/60°C and proceeds somewhat rapidly near 100°± 20°C when randomly interstratified I/S is converted into ordered I/S (Hower et al., 1976; Hoffman and Hower, 1979). Depth and temperature for random to ordered mixed-layer I/S convergence roughly overlap with the "oil window" and commonly correlate with overpressure zones (Powers, 1967; Bruce, 1984). This relationship was first observed in the U.S. Gulf Coast oil fields and it was suggested that water released from this reaction played an important role in the development of overpressure zones and for the primary migration of hydrocarbons from deeply buried source rocks (Powers, 1967;

7

Bruce 1984). Silica and other cations released during I/S diagenesis were also considered to provide material for cementation within the host shale and adjacent sandstones (Boles and Franks, 1979). Subsequently, the phenomena of illitization was reported from several other sedimentary basins worldwide (i.e. Paris Basin, Mathieu and Velde, 1989; North Sea, Pearson and Small, 1988; Niger Delta, Velde et al., 1986; California, Ramseyer and Boles, 1986 and others).

Despite general agreement on many aspects of I/S diagenesis, several aspects including the nature of the mixed-layer I/S (Nadeau et al., 1984a, b) and the reaction mechanism (Hower et al., 1976; Boles and Franks, 1979; Inoue et al., 1987; and others) remain controversial. The diversity of thoughts regarding the illitization reaction suggests that it is perhaps more complicated than previously thought and no single model can explain the illitization reaction for different areas. For example, not only do the mechanisms for I/S transformation remain problematic, but data from other sedimentary basins do not suggest a close correlation of I/S diagenesis with overpressure zones, sandstone cementation and hydrocarbon-migration from the source rocks (Colten-Bradley, 1987; Eslinger and Pevear 1988; Bloch, 1991) as previously thought. Clearly there is still no universal consensus on many issues regarding smectite illitization. Additional case studies from different sedimentary basins that examine the

8

geologic setting of the illitization reaction may increase our understanding about the illitization of smectite and its implications for basin evolution.

1.5 MATERIALS AND METHODS

Two hundred composite samples of drill-cuttings from 16 wells (Table 1.1), ranging in depth from ~1000m to more than 5000m, were collected to establish basin-wide variations in I/S mineralogy in the Jeanne d'Arc Basin. Selected stratigraphic units were also sampled from 6 additional wells (Table 1.1). Well-logs, well history reports and other available information from the C-NOPB were used to locate argillaceous zones in each of the wells. To make composite samples, drill-cuttings from about 2000 samples were combined over intervals ranging from 10m to 30m in order to obtain sufficient material and to average minor lithologic and chemical inhomogeneity. No composite sample crosses the formation boundaries. It is a common practice in mixed-layer clay studies to combine well-cuttings covering 10-30m intervals (Yeh and Savin, 1977; Pearson and Small, 1988). All samples were washed thoroughly and sieved to retain material between 2.0mm to 4.0mm. Obvious caving (Whiteside, 1932), sand/silt, and foreign materials were carefully handpicked from the samples to obtain the most homogenous argillaceous material. Approximately, 20-30 grams of clean, handpicked

9

drill-cuttings were soaked with sodium acetate-acetic acid (pH 5.0) for one night to remove carbonates followed by disaggregation with ultrasonic probe (horn-type). Organic-matter was removed using H_2O_2 (30%) following Jackson (1969). Samples were then Na-saturated and excess salt was removed by washing (4 to 5 times) with distilled water until no chloride was detected with $AgNO_3$. About 80-100mg of sodium pyrophosphate was added to the suspension to obtain better dispersion. Centrifugation according to Stokes Law was applied to separate the <0.1µm size-fraction which consists chiefly of I/S clays in the Jeanne d'Arc Basin. Suspensions of the <0.1µm fraction were concentrated using an ultracentrifuge and were oven dried at 40°C (see Appendix I).

Glass slides of oriented clay-particles (<0.1µm) were then prepared from the dried powder. For each slide, about 90mg of sample was ultrasonically dispersed in distilled water, pipetted onto a glass slide and air dried. Ethylene glycol solvation on all samples was carried out in a desiccator containing ethylene glycol at the bottom. The desiccator was kept at 60°C for >30hrs which is considered to be an adequate period to obtain a maximum glycol-layer thickness for these samples. Samples were kept in an air-tight desiccator until subjected to X-ray diffraction (XRD). Selected samples were subjected to heat-treatment at 375°C and 550°C for an hour to ensure proper identification of components in mixed-layer

clays, and the distinction between chlorite and kaolinite. X-ray diffraction analyses of clay minerals were conducted with a Rigaku Ru-200 diffractometer equipped with a graphite monochrometer and rotating copper anode. The X-rays were generated at 40Kv and 70mA. Analyses were made at a scan rate of $4°2\theta$/minute using $1°$ divergence slit, $1°$ sollerslit, $0.15°$ receiving slit and $0.01°$ 2θ sampling interval. XRD analyses for all air-dried samples were made from $2.5°$ to $35°$ 2θ and for glycolated samples from $2.5°$ to $50°$ 2θ. XRD on quartz standard was frequently used to monitor the goniometer alignment which was kept under $\pm0.03°2\theta$. Most XRD reflections used to quantify I/S layer proportions and their stacking-order were repeated.

Table 1.1: Well name, locations, total depths, geothermal gradients and sample distribution. Information collected from Canada-Newfoundland Offshore Petroleum Board's Schedule of Wells (C-NOPB, 1988) and Correia et al., 1990.

Well Name	Location		Total Depth	Geothermal Gradient	No. of Sample
	Longitude	Latitude	(m)	(°C/km)	
Adolphus D-50	48°22'28.86" W	46°59'03.06" N	3686.0	30.8	25
Bonanza M-71	48°11'55.34" W	47°30'47.54" N	5294.7	32.3	11
Conquest K-09	48°15'45.08" W	47°08'34.68" N	4968.3	33.4	11
Cormorant N-83	48°58'02.07" W	46°02'45.43" N	3160.5	25.3	5
Dominion O-23	48°18'27.90" W	47°22'49.14" N	3997.8	26.4	8
Egret K-36	48°50'22.38" W	46°25'37.88" N	3352.8	23.7	7
Egret N-46	48°51'47.35" W	46°25'56.14" N	2743.2	26.9	4
Hebron I-13	48°31'45.47" W	46°32'33.95" N	4723.5	24.0	9
Nautilus C-92	48°44'20.64" W	46°51'03.55" N	5116.7	28.9	7
North Ben Nevis P-93	48°20'34.24" W	46°42'48.10" N	5282.2	28.5	13
North Dana I-43	47°36'12.62" W	47°12'43.60" N	5303.6	30.4	13
North Trinity H-71	48°25'35.52" W	46°30'23.67" N	4758.0	27.0	11
South Mara C-13	48°32'19.63" W	46°42'01.72" N	5034.1	28.5	40
South Tempest G-88	47°57'30.48" W	47°07'19.92" N	4674.8	31.6	13
West Flying Foam L-23	48°49'17.02" W	47°02'43.81" N	4553.8	29.8	12
Whiterose J-49	48°06'27.51" W	46°48'31.30" N	4561.4	31.9	11
Total: 16					200

Well Name	Location		Total Depth	Geothermal Gradient	No. of Sample
	Longitude	Latitude	(m)	(°C/km)	
Archer K-19	48°02'18.42" W	46°38'43.17" N	4299.3	N/A	4
Beothuk M-05	48°31'14.05" W	46°24'48.55" N	3779.0	24.9	2
Fortune G-57	48°08'02.21" W	46°36'18.90" N	4995.1	N/A	4
Gambo N-70	48°39'54.83" W	46°19'52.92" N	2515.0	25.7	3
Port au Port J-97	48°44'05.97" W	46°16'38.47" N	2700.0	25.5	2
Voyager J-18	48°17'00.49" W	46°27'32.50" N	3743.0	28.7	3
Total: 6					18

CHAPTER II
GEOLOGICAL SETTING, STRATIGRAPHY AND DEPOSITIONAL ENVIRONMENTS

2.1 STRUCTURAL SETTING OF THE GRAND BANKS

The continental margin of eastern Canada is underlain by a series of northeast and northwest trending Mesozoic-Cenozoic sedimentary basins separated by major uplifts (Fig. 2.1). Most of these are graben or half-graben structures initiated during different Mesozoic crustal extension and rifting episodes associated with the breakup of Pangea and the opening of the North Atlantic Ocean (McMillan, 1982; Tankard and Welsink, 1988). Proterozoic and Palaeozoic structural fabrics of the Appalachian Orogeny appear to have influenced the orientation of Mesozoic rift-grabens during the rifting of Pangea (Grant et al., 1986).

Along the east coast of Canada different rifting episodes and variable amounts of extension were accommodated by major transform faults which divide the region into different extensional terrains (Fig. 2.1). The Newfoundland and Charlie Gibbs Fracture Zones separate the Grand Banks from the Scotian Shelf in the south and the Labrador Shelf in the north (Fig. 2.1). The Grand Banks are further divided into southern (Whale, Horseshoe basins), central (Jeanne d'Arc Basin), and northeastern (Orphan Basin) zones by relatively small transfer

13
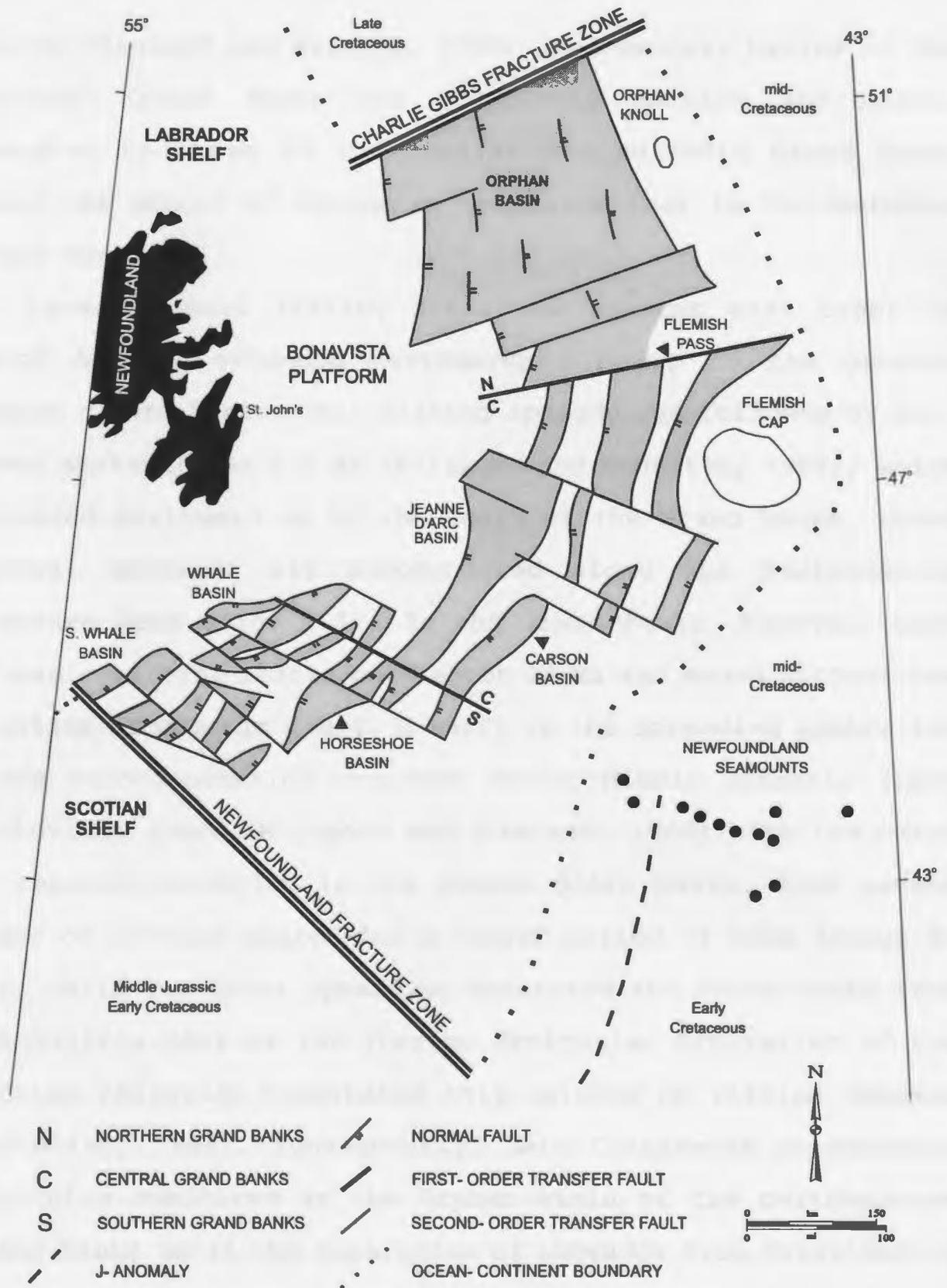
Figure 2.1. Sedimentary basins of the Grand Banks separated from the Scotian and Labrador shelves by the Newfoundland and Charlie Gibbs fracture zones respectively (from Tankard and Welsink, 1988).

faults (Tankard and Welsink, 1988). Sedimentary basins of the southern Grand Banks are relatively shallow and narrow compared to those of the central and northern Grand Banks where the amount of extension was twice that in the southern Grand Banks.

Late Triassic rifting along the present east coast of North America extended northwards only up to the present Jeanne d' Arc Basin. This rifting episode was followed by sea-floor spreading at 175 Ma (Klitgord and Schouten, 1986), which extended northward up to the south of the Grand Banks, where lateral movement was accommodated along the Newfoundland Fracture Zone (Fig. 2.1). In the Grand Banks, however, Late Triassic rifting lasted only about 25 Ma and ended without the creation of oceanic crust. A shift in the spreading centre and plate re-organization occurred during Middle Jurassic (Late Callovian) times (Klitgord and Schouten, 1986) with the onset of renewed extension in the Jeanne d'Arc Basin. This second phase of rifting lasted for a longer period of time (about 50 Ma), until sea floor spreading separated the Grand Banks from the Galicia Bank of the Iberian Peninsula. Separation of the Iberian Peninsula terminated this episode of rifting (Masson and Miles, 1984). Subsequently, Late Cretaceous extensional tectonics dominated in the Orphan Basin of the northeastern Grand Banks until the separation of Labrador from Greenland by sea-floor spreading about 80 Ma ago (Srivastava, 1978).

15

2.2 THE JEANNE D'ARC BASIN

The Jeanne d'Arc basin of the central Grand Banks is a relatively narrow, northward plunging, fault-bounded, deep trough (up to 16-20km) where all of the important hydrocarbon discoveries in eastern Canada have thus far been made (Fig. 2.2). This funnel shaped basin is ~200km long and ~90km wide in the north, and narrows to less than 40km in the south. The Jeanne d'Arc rift basin is surrounded by a stable Bonavista platform in the west (Precambrian-Cambrian basement), the Outer Ridge Complex in the east (a basement high partly covered with deformed Jurassic sediments) and an Avalon Uplift to the south (a late Jurassic to Mid-Cretaceous regional arch) (McAlpine, 1990) (Fig. 2.3). It preserves the most complete stratigraphic record and tectonic history on the Grand Banks since the Triassic period. About 70 exploration/delineation wells have been drilled in the basin. These have encountered mainly clastic sediments with minor limestone/marl and evaporite beds. The present configuration of the basin is the result of two major periods of rifting (Late Triassic and Callovian to Aptian) and post-rifting thermal subsidence.

Listric, steep normal and transfer faults are the main fault types observed in the Jeanne d'Arc Basin. The western side of the basin is marked by the northeast trending listric-type Murre fault and the eastern side by steep normal faults above the Outer Ridge Complex (Fig. 2.3). These basin-boundary

16
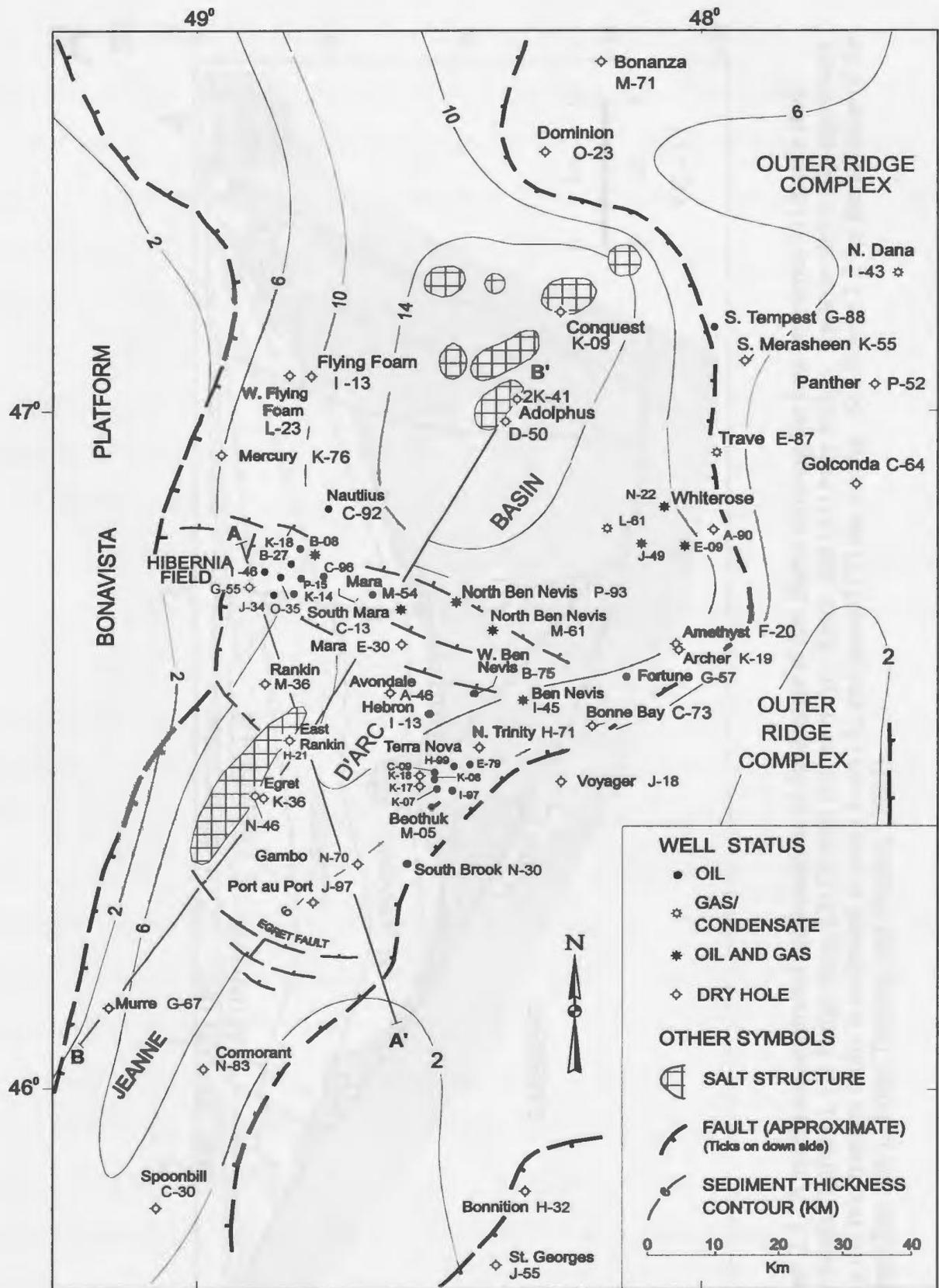
Figure 2.2. General structure and sediment-thickness map of the Jeanne d'Arc Basin. Well locations and areas of major salt-structures are also shown. Modified from Grant et al. (1986).

17
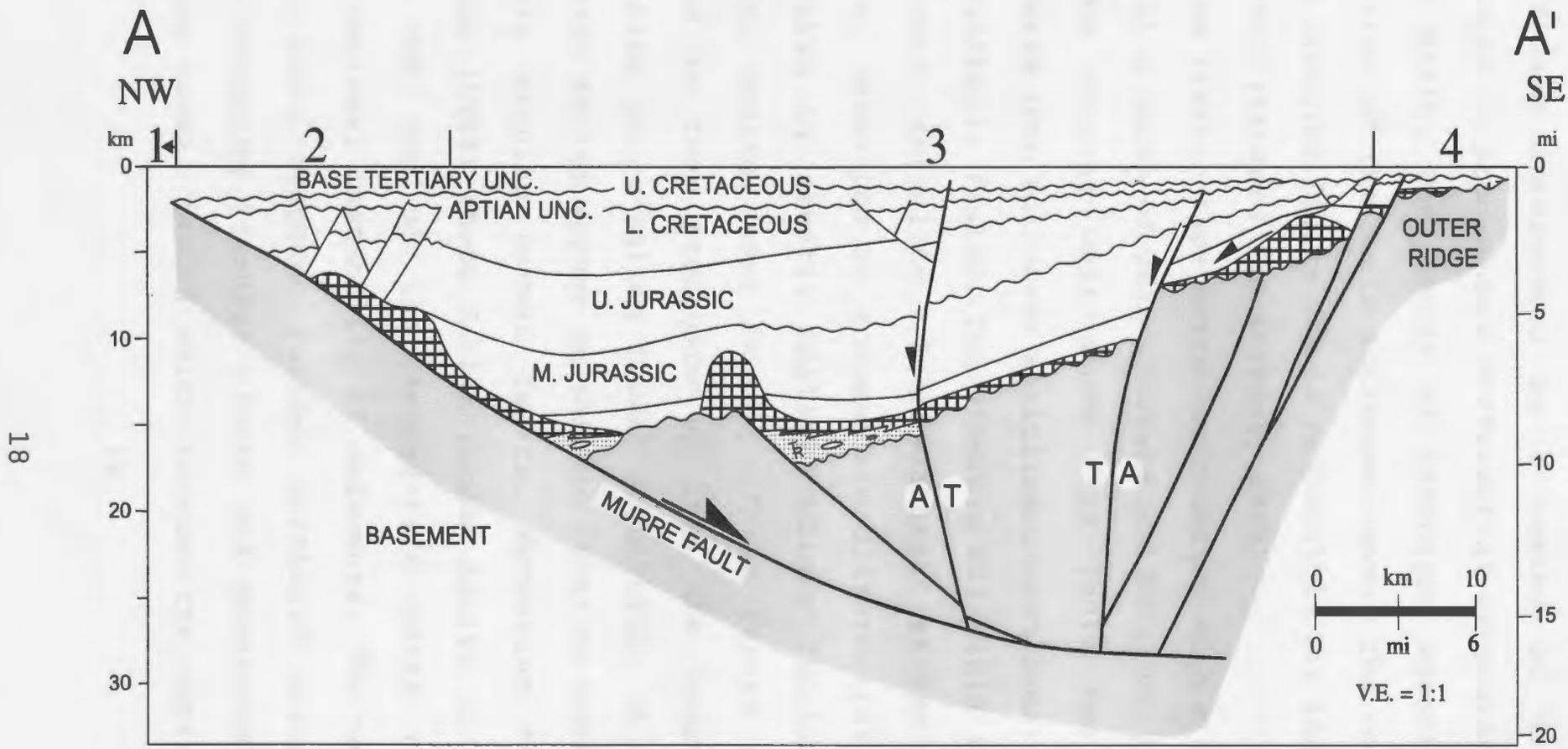
Figure 2.3. A northeast-southwest cross-section of the Jeanne d'Arc Basin showing the four segments: (1) Stable shelf (Bonavista Platform), (2) Hinge zone, (3) Central Jeanne d'Arc Basin, and (4) Outer Ridge. Relative strike-slip movement along the two transfer faults is indicated as away from (A) and toward (T) the viewer. See Figure 2.2 for the location of the section (line AA'). From Tankard and Welsink (1987).

18

faults are intersected by a series of transfer faults developed to accommodate differential extension in the Jeanne d'Arc Basin. The amount of extension associated with the formation of the basin increases toward the northeast across these transfer faults and is responsible for its funnel-shaped geometry (Tankard and Welsink, 1988).

The listric-type Murre Fault merges with a low-angle shear zone at a depth of 26km (Tankard and Welsink, 1988). Movement of the hanging wall above this fault has deformed the sediments into roll-over anticlines, synclines, and antithetic and synthetic faults. The Hibernia oil field is located on a roll-over anticline. Right-lateral strike-slip transfer faults, developed to accommodate differential extension are connected by several smaller oblique faults (i.e. Riedel shears, dogleg shape faults). These faults commonly splay upward as they propagate up into the sedimentary fills, resulting in so-called flower structures. At present, these transfer faults appear on seismic lines as moderately to very steeply dipping normal faults. According to Tankard and Welsink (1988) these faults became active in a normal sense near the end of the second-rift phase mainly due to gravitational instability of sediments. The resultant Jeanne d'Arc Basin deepened further northward across down-to-the north stepping transfer blocks and developed a new set of listric normal faults which rotated the upper parts of the

19

transfer blocks (Tankard and Welsink 1988). All these structural components of the Jeanne d'Arc Basin influenced the evolution of sedimentary facies, subsidence, formation of structural traps and migration of hydrocarbons.

2.3 STRATIGRAPHY AND DEPOSITIONAL ENVIRONMENTS

The stratigraphy of the Jeanne d'Arc Basin as described by Jansa and Wade (1975), Jansa et al. (1976), Barss et al. (1979), Sinclair, 1988), and McAlpine (1990) is summarized below. Figure 2.4 shows a simplified lithostratigraphic chart of the basin (Sinclair, 1988 and C-NOPB, 1988). The Triassic to Early Jurassic rifting (first rift phase) of Africa from the North American plate was accompanied by the accumulation of fluvial red-beds (Eurydice Formation) and evaporite (Argo Formation) deposits overlying the Precambrian and Palaeozoic basement rocks. The Early and Middle Jurassic were characterized by regional thermal subsidence and marine transgression(s). The Iroquois Formation (anhydrite, oolitic and skeletal limestones) and Downing Formation (limestone and shale) recorded this progressive change to normal open marine conditions of an epeiric sea. The Voyager and Rankin Formations (Callovian to Kimmeridgian) overlie the Downing Formation and mark the transition between the preceding epeiric-sea basin and the Lower Cretaceous flood of syn-rift (second rift phase) clastic sediments in the Jeanne d'Arc

20
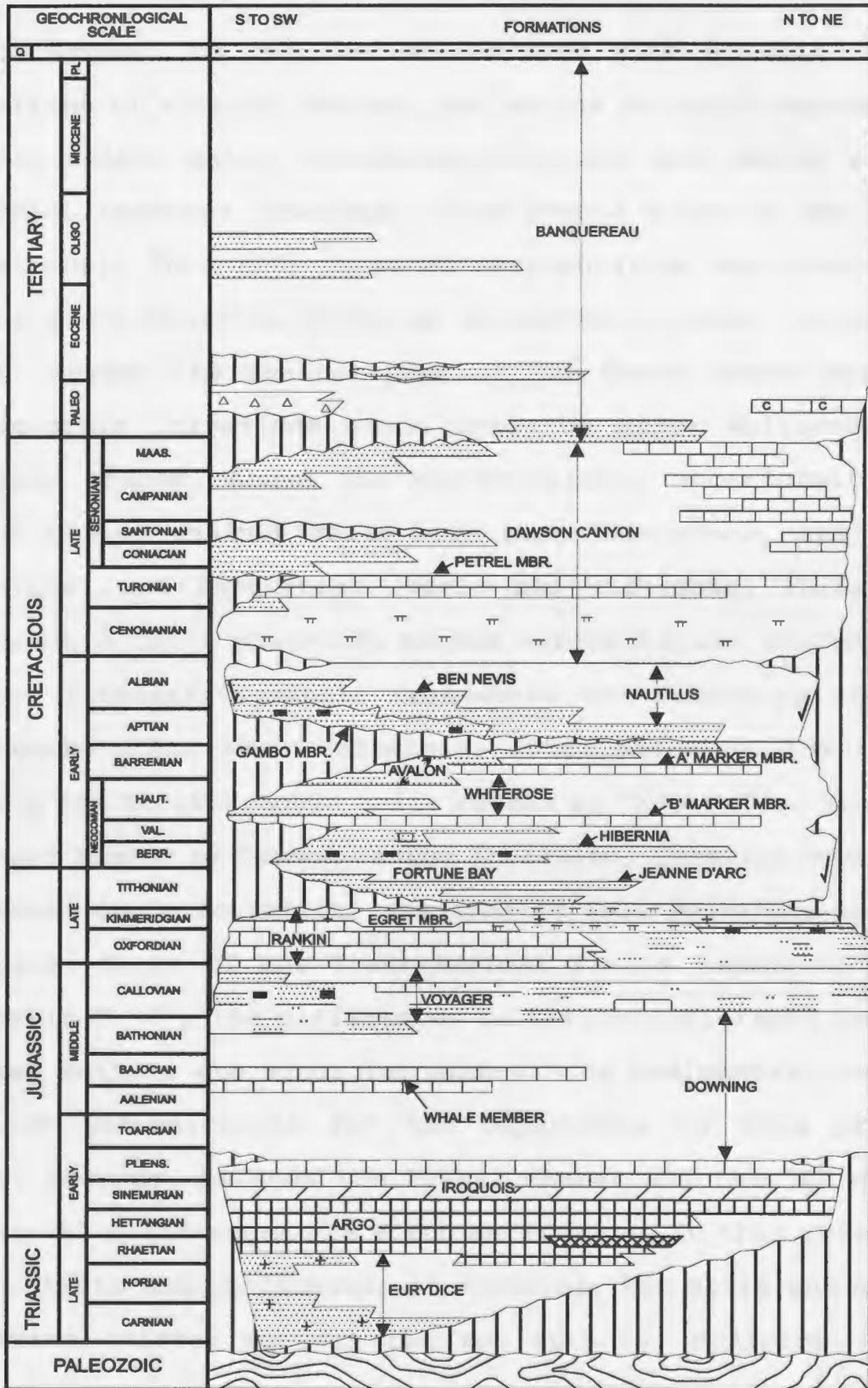
Figure 2.4. Generalized stratigraphy of the Jeanne d'Arc Basin. The white intervals represent shale/mudstone. From Sinclair (1988).

Basin. Renewal of the Iberian-Labrador Rift episode led to deposition of a thick (deltaic and marine deltaic) sequence of clastic rocks, mainly sandstone/siltstone and shales with a few thin limestone interbeds (from Jeanne d'Arc to Ben Nevis Formations). This rift phase of sedimentation was terminated by the Mid-Cretaceous break-up unconformity event (Sinclair, 1988). Toward the central part of the basin these southern coarse-grain formations grade into the thick Whiterose and Nautilus shales. Above the Mid-Cretaceous unconformity the Dawson Canyon (mainly shale with minor limestone, chalk and sandstone) and Banquereau (shale and siltstone) Formations represent a thick post-rift marine sedimentation record.

Two lithostratigraphic frameworks are presently used in the Jeanne d'Arc Basin (Sinclair, 1988; McAlpine, 1990)(Fig. 2.5). A few stratigraphic units ranked as "Member" by Sinclair (Wyandot Member of Dawson Canyon Formation, Catalina Member of Whiterose Shale Formation) are granted full formation name by McAlpine. South of the Trans-Basinal Faults (south of North Ben Nevis P-93), the differences in lithostratigraphy between the two authors are minor for much of the sedimentary section and are insignificant for the objectives of this present study. However, between the Petrel Member and the "A" Marker Member the differences are worth monitoring. In this interval, the contacts and thicknesses of Nautilus, Ben Nevis and Avalon Formations differ between the two authors. McAlpine (1990)

22

Figure 2.5: A cross-section passing roughly through the basin-axis showing the main stratigraphic units in the Jeanne d'Arc Basin. Two stratigraphic frameworks presently in use are shown for the comparison: (A) after Sinclair (1988) and C-NOPB (1988), (B) after McAlpine (1990) (see text for description). Main Formations: B=Banquereau, W=Wyandot, D=Dawson Canyon, E=Eider, N=Nautilus, BN=Ben Nevis, A=Avalon, ES=Eastern Shoals, WR=Whiterose, C=Catalina Member, H=Hibernia, F=Fortune Bay, 'F'=Fortune Bay, undifferentiated Tithonian to Barremian, J=Jeanne d'Arc, R=Rankin, and V=Voyager.
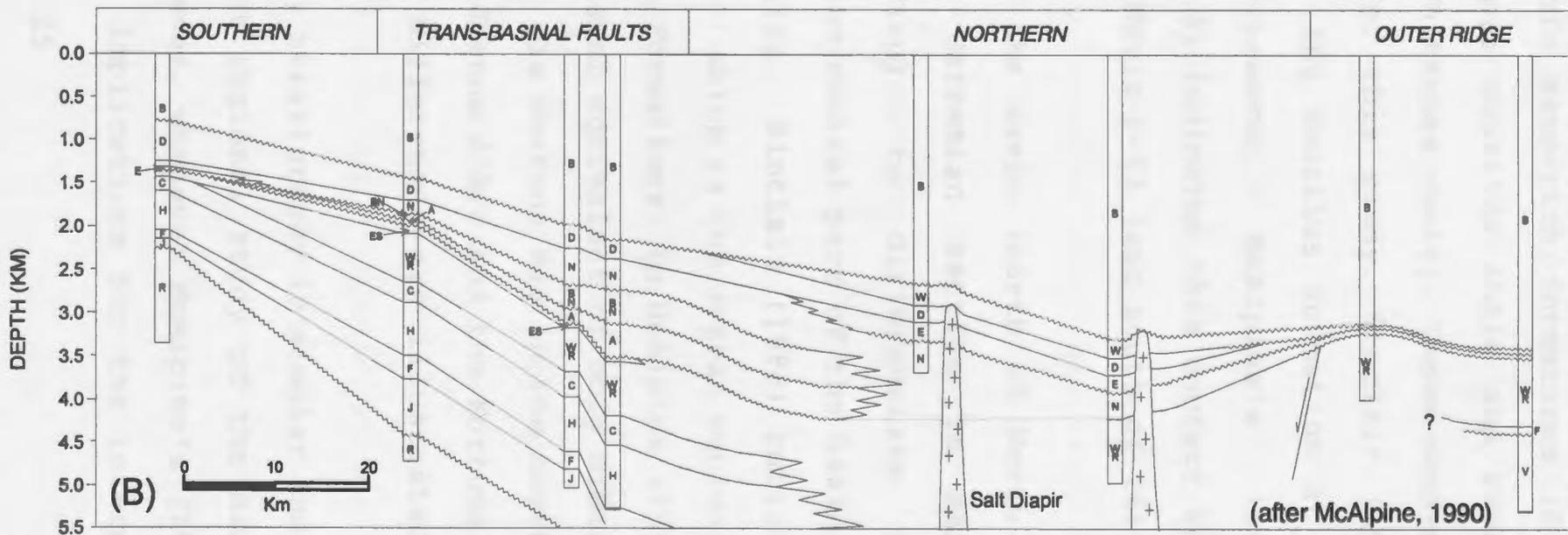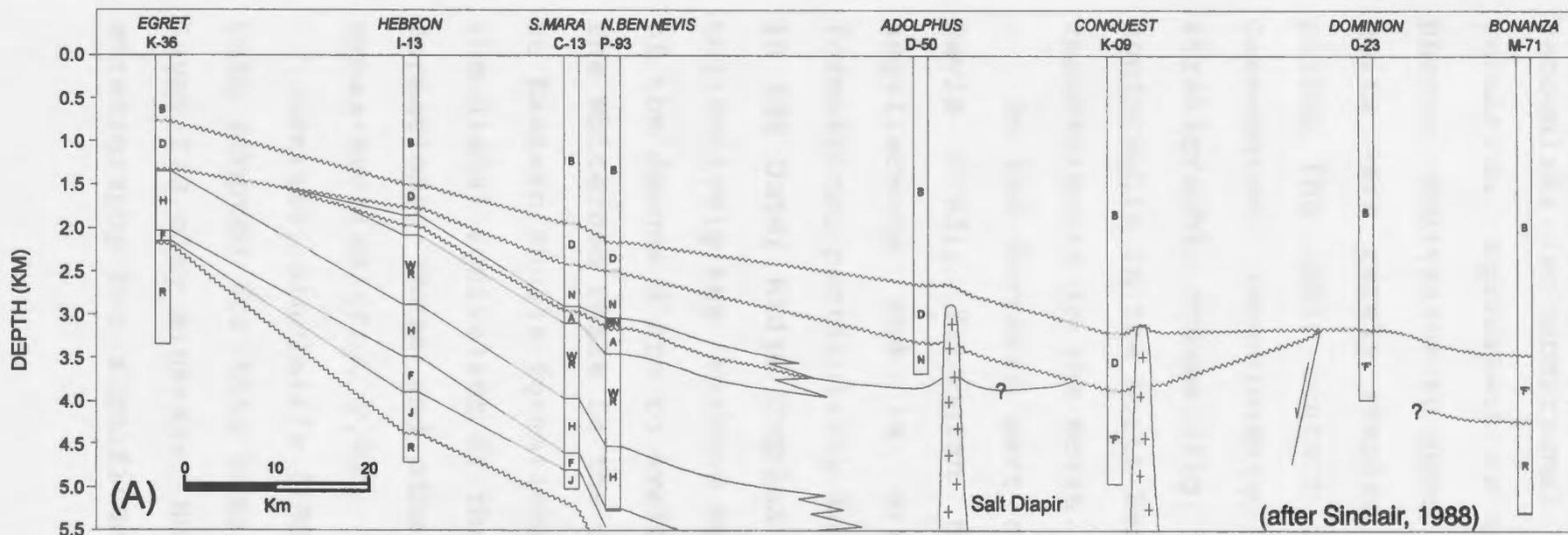
recognizes two additional thin sand-rich formations (Eider Formation, equivalent to upper Nautilus shale and Eastern Shores, equivalent to upper Whiterose shale). These sand-rich units were rarely sampled for this study. Sinclair (1988) places the upper contact of the Nautilus Formation at the Cenomanian unconformity, however, McAlpine's litho-stratigraphic scheme (Fig. 2.5) indicates this contact to be conformable in the North Ben Nevis P-93 (and south of it) but unconformable in the North.

In the Northern part of the basin (north of North Ben Nevis P-93), Tithonian to Barremian section is mainly argillaceous and is difficult to differentiate into formations, particularly in the central part of the basin and in the Outer Ridge Complex area. Sinclair (1988) called it collectively the 'Fortune Bay' which is the distal equivalent of the Jeanne d'Arc to Avalon Formations. In McAlpine (1990), the Whiterose Shale is the distal equivalent of only Hibernia to Eastern Shoals formations. His Fortune Bay in the north is the distal equivalent of the Jeanne d'Arc and the Fortune Bay formations. These and other differences are illustrated on cross-section (Fig. 2.5).

Overall, Sinclair's (1988) stratigraphy is simpler and has been adopted for this present regional study of the mixed-layer I/S clay minerals. However, whenever McAlpine's (1990) stratigraphy has significant implications for the interpre-

tation of illite/smectite data in this study, it is discussed in the text. No attempt is made in this study to resolve differences in their lithostratigraphy of the Jeanne d'Arc Basin.

2.4 SUBSIDENCE HISTORY OF THE JEANNE D'ARC BASIN

The total subsidence in the Jeanne d'Arc Basin is the result of lithospheric thinning, thermal cooling and sediment (including water) loading associated with at least two episodes of extensional and post extensional tectonics (Keen and Barrett, 1981; Tankard and Welsink, 1988). The amounts and rates of subsidence vary in different parts of the basin and generally coincide with the major tectonic events of the Grand Banks (Fig. 2.6A to 2.6D).

In the main part of the basin (north of Egret K-36 well, Fig. 2.2) subsidence was more or less continuous since Late Triassic (Williamson, 1992) (Fig. 2.6A). The Late Triassic rifting episode (which lasted for about 20 MY) was followed by a rapid post-rift regional thermal subsidence during the Early and Middle Jurassic (Argo to Voyager Formations). Rapid subsidence continued during the second rifting episode from Late Callovian to Aptian/Albian time. Crustal extension during the rifting episodes was accommodated by movement along listric and planar normal faults which created significant subsidence and also contributed coarser sediments into the

26
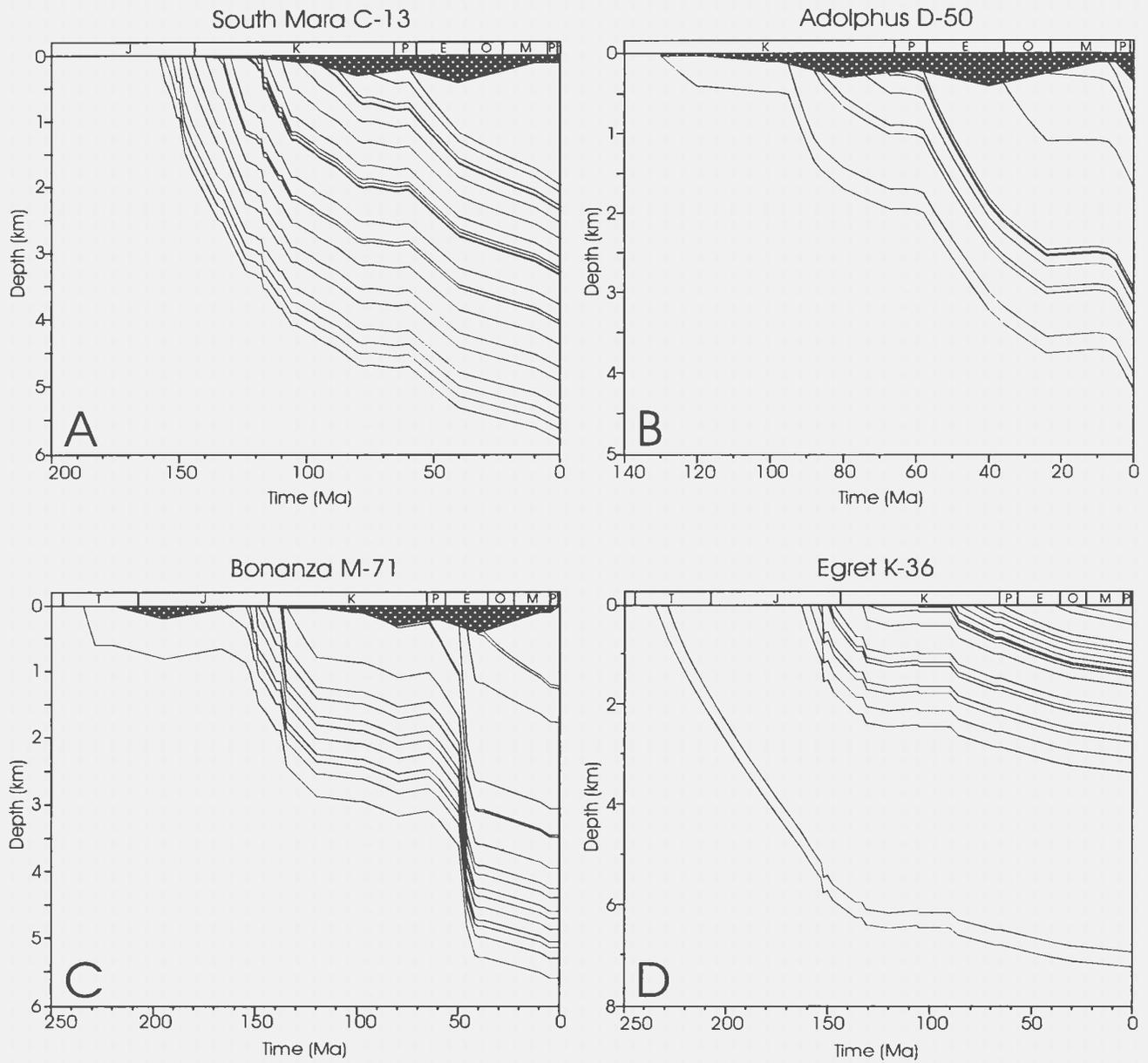
Figure 2.6. Burial history (compaction corrected) for the South Mara C-13, Adolphus D-50, Bonanza M-71 and Egret K-36 wells, which represent four different areas of the Jeanne d'Arc Basin. Significant uplift and erosion is not involved. (From Williamson, unpublished data).

27

basin. The subsidence rate increased towards the north across transfer faults which were reactivated in the normal sense at approximately Aptian time (Tankard and Welsink, 1988). High sedimentation rates kept pace with fast subsidence with the result that thick Lower Cretaceous sediments accumulated in the Jeanne d'Arc Basin. Separation of the Grand Banks and Iberian margins in Aptian time marks a significant change in the overall subsidence history of the Basin. Post break-up thermal subsidence was generally slow (except for a few rapid events) and regional in extent, indicating the combined effects of thermal contraction and flexural response of the lithosphere (Sleep, 1971; McKenzie, 1978; Keen et al., 1987).

The Southern part of the Jeanne d'Arc Basin and the Outer Ridge Complex do not show continuous subsidence (Fig. 2.6D). In these areas, rapid early subsidence (Triassic to Jurassic and minor Early Cretaceous) was followed by a long period of erosion and/or non-deposition during much of the Cretaceous. This erosion and non-deposition was probably related to large scale uplifting followed by thermal subsidence due to extensional tectonics and rifting (Keen et al., 1987). Tertiary thermal subsidence was relatively faster over the Central and the Outer Ridge Complex areas (Fig. 2.6B and 2.6C) than in the Southern part of the Jeanne d'Arc Basin (Fig. 2.6D).

28

2.5 OVERPRESSURE ZONES

Overpressure, defined as any pressure above normal hydrostatic pressure at a given depth, has been reported from several wells in the Jeanne d'Arc Basin (Fig. 2.7), (Grant and McAlpine, 1990). Details about the origin, timing, and possible relationship of overpressure zones to structural elements in the Jeanne d'Arc Basin were discussed by Williamson et al., (1993) and Rogers and Yassir (1993). The tops of the overpressured zones are generally observed at or near the top of the Fortune Bay Formations (Grant and McAlpine, 1990). Sediments within the overpressured zones generally show higher porosity and lower density indicating less compaction or compaction disequilibrium (see Magara, 1976) due primarily to the higher sedimentation rate during the Late Jurassic and Early Cretaceous (Grant and McAlpine, 1990). It is important to note that most of the known hydrocarbon accumulations are presently pooled in the hydrostatic pressure regime while the mature source rocks are in the overpressured regimes. These overpressured zones may have played a significant role in the expulsion and migration of hydrocarbons from the source intervals to the porous reservoir rocks (McAlpine, 1990).

29
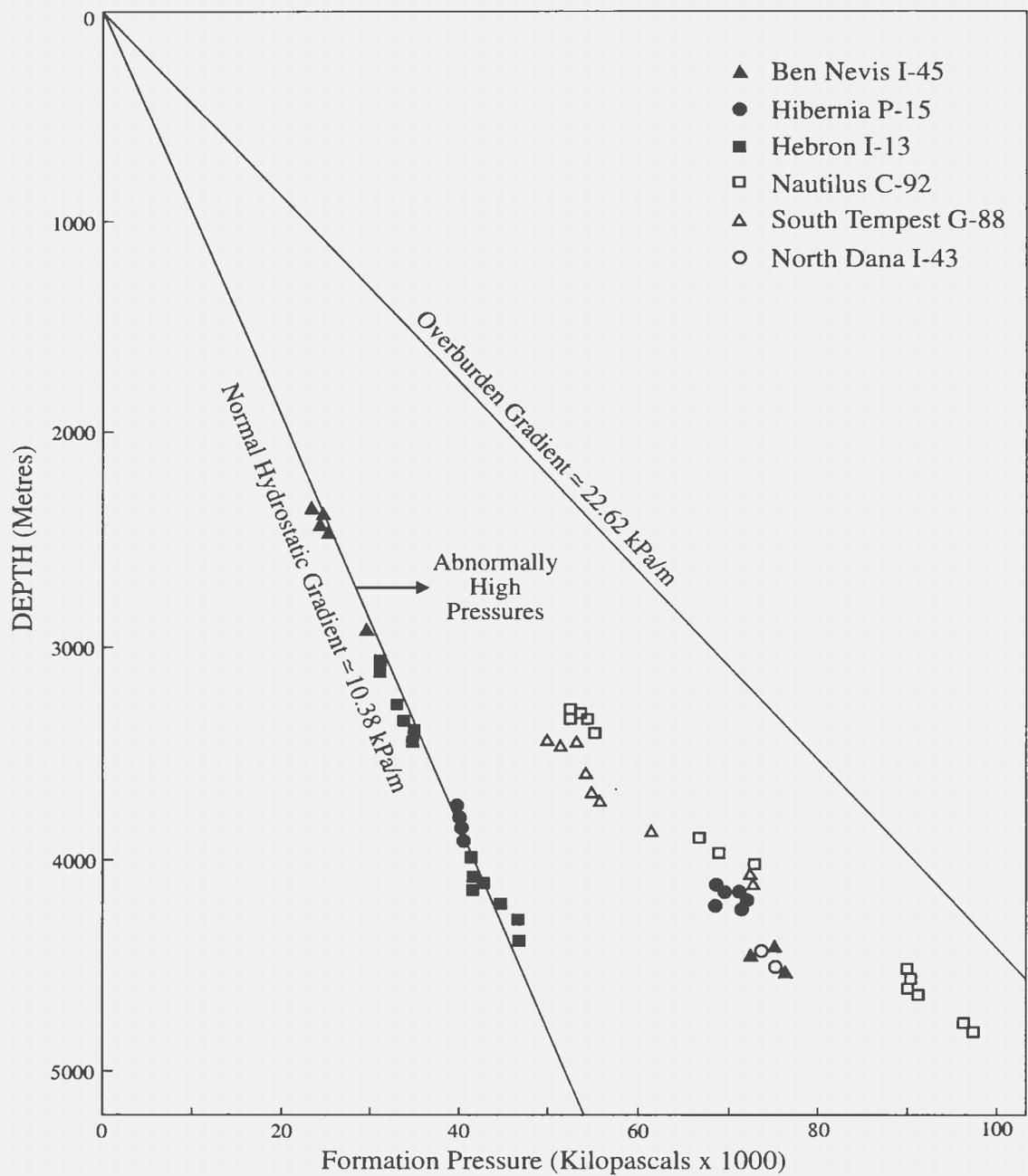
Figure 2.7. Measured pressure versus depth for six discovery wells in the Jeanne d'Arc Basin (after Grant and McAlpine, 1990).

2.6 SALT STRUCTURES

Triassic to Early Jurassic rifting of Africa from the North American plate was accompanied by the accumulation of fluvial red beds and evaporite deposits overlying the Palaeozoic basement rocks in the Jeanne d'Arc Basin. The Argo Formation evaporites have been encountered in several wells (Cormorant N-83, Spoonbill C-30, and Adolphus 2K-41) and are believed to be widespread in the Jeanne d'Arc Basin. Differential gravity loading of younger sediments due to variable extension and rotation of fault blocks initiated salt flowage in the Jeanne d'Arc Basin. Several large salt diapirs, piercing as much as 9km of overlying sedimentary rocks (Adolphus D-50 and Conquest K-09 wells), together with numerous smaller salt pillow or salt-cored structures, have been observed. Flowage of salt in the central part of the basin may have accentuated the movement of high-angle normal faults towards the eastern side of the basin (Grant and McAlpine, 1990). The major salt movement is believed to have occurred during Cretaceous times (Jansa and Wade, 1975). Many of these salt diapiric structures were early targets in the search for hydrocarbons in the Jeanne d'Arc Basin.

2.7 GEOTHERMAL GRADIENT

Correia et al. (1990) calculated geothermal gradients for 41 wells using corrected Bottom Hole Temperatures in the

31

Jeanne d'Arc Basin. The average geothermal gradient is 27°C/km with a range in different wells from 21° to 33°C/km. North of the Trans-Basin Faults, the basin shows a higher geothermal gradient (30°-33°C/km) than in the Southern part (21°-29°C/km). Wells drilled close to the salt structures give the highest values (33°C/km), probably due to higher heat flow along the salt bodies. Grant and McAlpine (1990) also constructed a geothermal gradient map for the Jeanne d'Arc Basin but did not report the source of the temperature data. Their values are generally 2°-3°C/km higher than those of Correia et al. (1990).

2.8 DEPOSITION AND MATURATION OF SOURCE ROCKS

The Egret Member (Kimmeridgian) of the Rankin Formation is considered to be the main source rock for all hydrocarbons discovered so far in the Jeanne d'Arc Basin (Swift and Williams, 1980; Creaney and Allison, 1987; Von der Dick et al., 1989). The contribution from other rocks (Jeanne d'Arc and Banquereau Formations) seems insignificant (Snowdon and Krouse, 1986). The Egret Member is 75-100m thick and consists mainly of calcareous shales together with minor amounts of marl and fine-grained sandstones, and is widely distributed in the basin (Grant and McAlpine, 1990). The organic-matter is mainly marine amorphogen (Type II, I) and has, on average, a Total Organic Carbon content of 3% (maximum of up to 8%). The

32

Egret Member was deposited in restricted, low energy marine or silled basins developed during the early stage of the second rifting (Powell, 1985). By Late Kimmeridgian times, influx of coarser sediments ended deposition of oil-prone source rocks in most parts of the basin.

The present burial depth of the Egret Member increases from 1850m in the south (Port au Port J-97) to about 10,000m in the Northern part of the basin (Adolphus D-50). Egret rocks are thermally immature in the south, become mature further north and are overmature in the central part of the basin (Creaney and Allison, 1987; Von der Dick et al., 1989; Williamson, 1992) (Fig. 2.8). This maturity trend shows a simple linear relationship with burial depths that correspond with basin geometry (Von der Dick et al., 1989). Time-temperature modelling indicates that hydrocarbon generation first started in the central part of the basin in Barremian times (122-116Ma) and progressed towards the basin periphery (Von der Dick et al., 1989; and Williamson, 1992). In the Trans-Basinal Fault area where almost all important hydrocarbon discoveries have been made, oil generation started in the Late Albian (100Ma). Peak oil generation was reached in Tertiary time (60-50Ma, Von der Dick et al., 1989; and McAlpine, 1990). Various structural traps (rollover anticlines, tilted fault blocks, salt structures etc.) which developed prior to Tertiary time provided an ideal opportunity

33
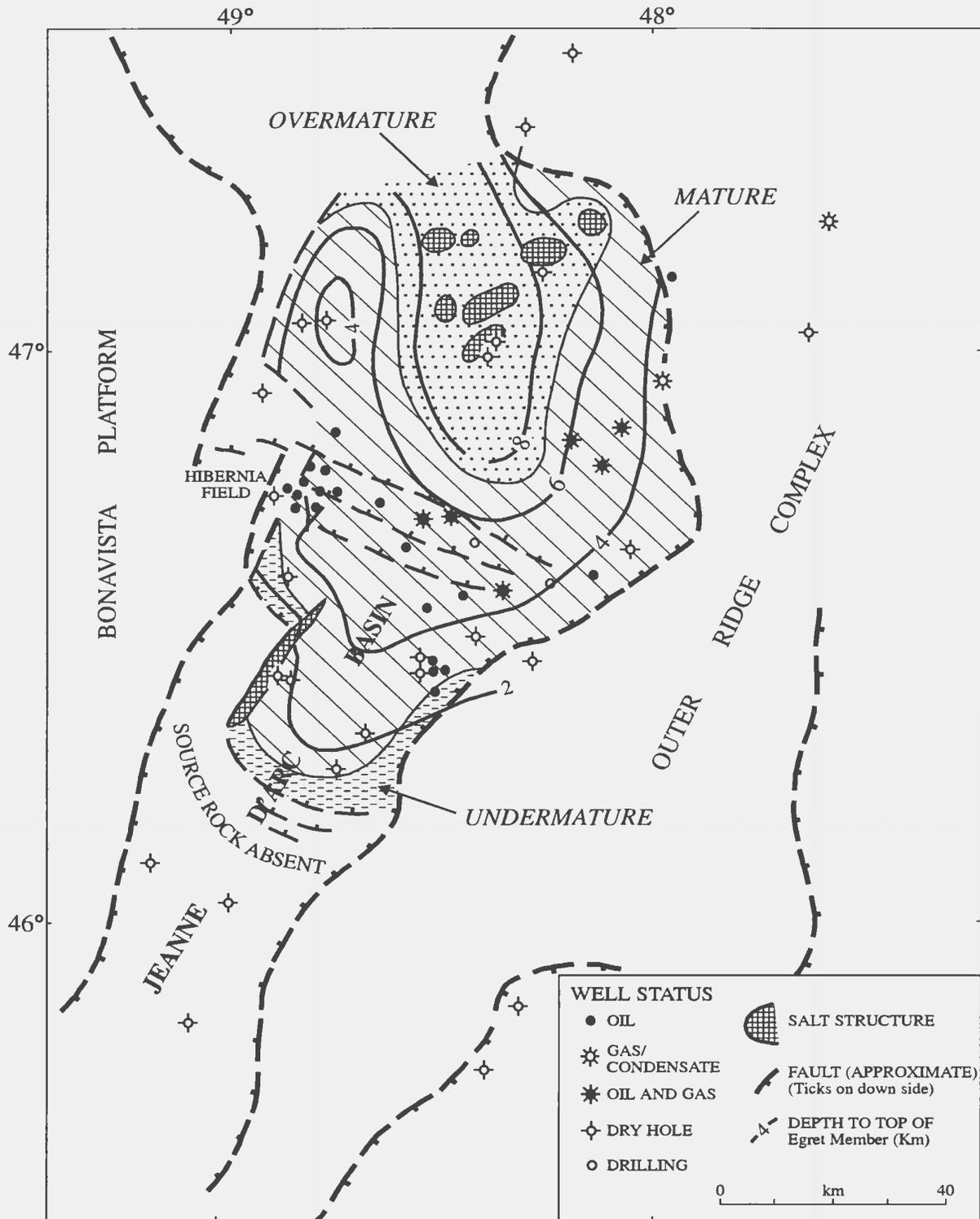
Figure 2.8. Regional distribution of the Egret Member source rock and its present maturity obtained from vitrinite reflectance and pyrolysis temperature data for 35 wells across the basin (modified from Grant and McAlpine, 1990).

34

to retain these hydrocarbons.

2.9 MIGRATION AND ENTRAPMENT OF HYDROCARBONS

Geochemical data from discovered oils and Kimmeridgian source rocks (Egret Member), together with several geological observations (see below), indicate that oil in the Jeanne d'Arc Basin has moved several kilometres, primarily in a vertical direction (Von der Dick et al., 1989; McAlpine, 1990). These hydrocarbons are presently stacked in several younger reservoirs (Jeanne d'Arc to the Ben Nevis Formations) ranging from Tithonian to Albian age, over a vertical distance of as much as 2500m above the Egret Member. This upward migration occurred primarily along faults and fractures which are common in pre-Aptian Albian sediments. These faults may have repeatedly opened during the overpressure build-up and may have served as conduits for deep basinal fluids (Meneley, 1986). Fault control upward migration of hydrocarbons are evident from the distribution of oil fields in the basin (Fig. 2.9). The fields are closely related to deep trans-basinal faults and, also, to the faulted eastern flank of the basin.

Migration of hydrocarbons occurred during the Tertiary (50-30 Ma) as a result of periodic leakage of fluids along fault zones which opened repeatedly to release the build-up of overpressures (Von der Dick et al., 1989; Grant and McAlpine, 1990).

35

JEANNE D'ARC BASIN OILFIELDS

S. TEMPEST

47°

NAUTILUS

WHITEROSE

HIBERNIA

MARA

HEBRON

BEN
NEVIS

TERRA
NOVA

0 10 20 30

km

46°

49°

48°
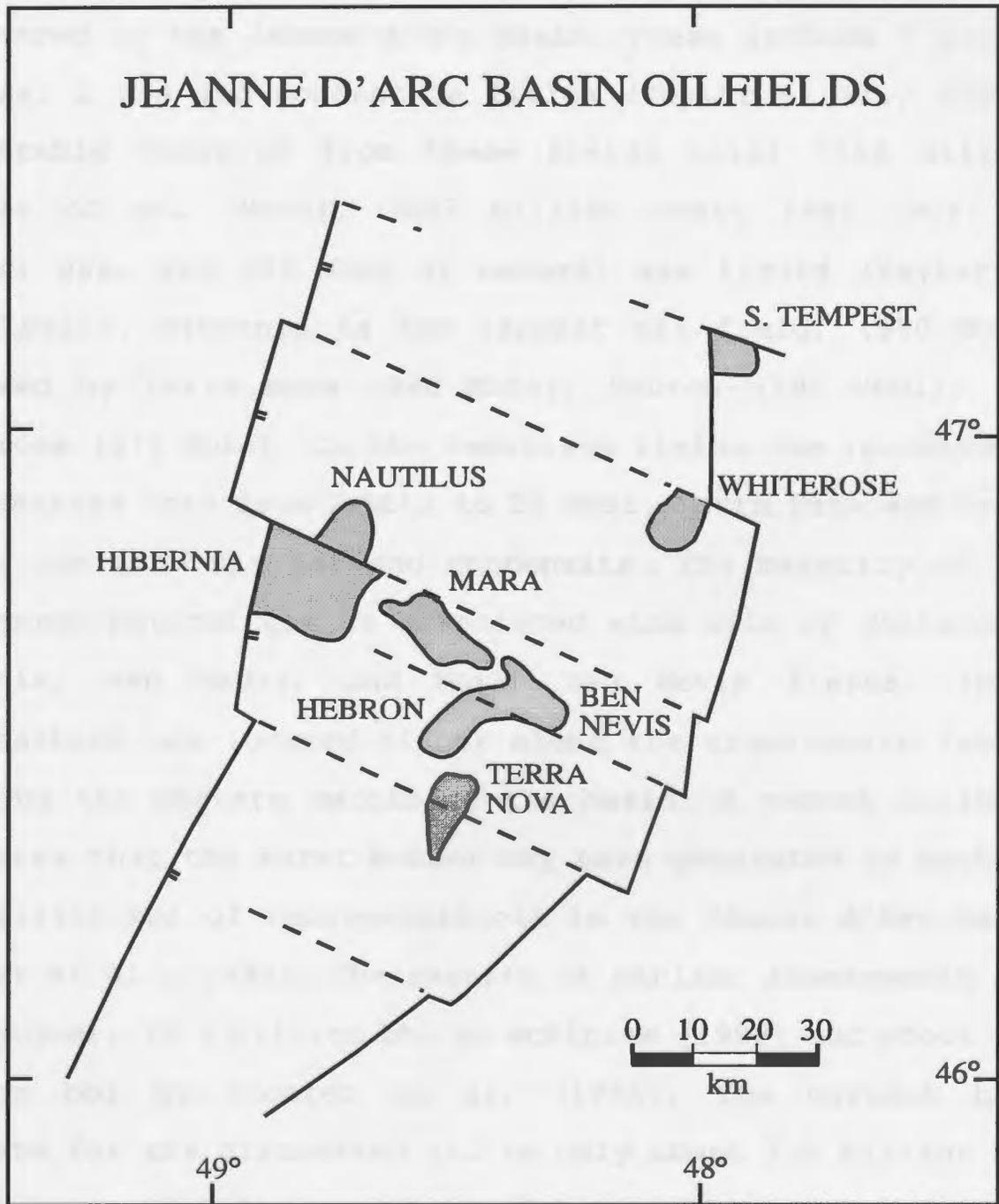
Figure 2.9. In the Jeanne d'Arc Basin, the location of oil fields are closely associated with transfer-faults. These faults appear to be an important controlling factor for hydrocarbon migration and accumulation (from Tankard and Welsink, 1988).

2.10 HYDROCARBON POTENTIAL OF THE JEANNE D'ARC BASIN

Fourteen significant oil and gas fields have been discovered in the Jeanne d'Arc Basin. These include 7 oil, 5 oil/gas, 2 gas and condensate fields (Taylor et al., 1992). Recoverable reserves from these fields total 1506 million barrels of oil (Mbbl), 3597 billion cubic feet (BCF) of natural gas, and 109 Mbbl of natural gas liquid (Taylor et al., 1992)). Hibernia is the largest oil field, (670 Mbbl) followed by Terra Nova (340 Mbbl), Hebron (191 Mbbl), and Whiterose (174 Mbbl). In the remaining fields the recoverable oil reserves vary from 2 Mbbl to 25 Mbbl. North Dana and Trave fields contain only gas and condensate. The majority of the discovered natural gas is associated with oils of Whiterose, Hibernia, Ben Nevis, and North Ben Nevis fields. These hydrocarbons are located either along the trans-basin faults or along the eastern margin of the basin. A recent estimate indicates that the Egret Member may have generated as much as 4.7 billion bbl of recoverable oil in the Jeanne d'Arc Basin (Taylor et al., 1992). The results of earlier assessments are even higher; 12.3 billion bbl by McAlpine (1990) and about 8.0 billion bbl by Procter et al. (1984). The current best estimate for the discovered oil is only about 1.5 billion bbl and it seems that large amounts of hydrocarbons are yet to be discovered in the Jeanne d'Arc Basin.

CHAPTER III

MIXED-LAYER ILLITE/SMECTITE MINERALOGY OF THE
JEANNE D'ARC BASIN

3.1 INTRODUCTION

Information on the burial and thermal history of sedimentary rocks can be obtained from clay minerals, especially mixed-layered illite/smectite (I/S), which is useful in the exploration, evaluation, and production of hydrocarbons. Illite/smectite is the finest-grained component of an argillaceous rock (Środoń, 1981). However, I/S is usually mixed with other clay minerals (e.g. discrete illite) that interfere with XRD peaks of I/S and this makes the interpretation of XRD patterns of I/S very difficult. In the Jeanne d'Arc Basin, the XRD of <2.0μm grain-size fractions are dominated by discrete illite and kaolinite particularly in the deeper samples and investigation of mixed-layer I/S is therefore difficult. To overcome this problem, I/S clays are concentrated by separating fine-grained clay fractions. For this study, the <0.1μm grain-size fraction was isolated from argillaceous sediments of the Jeanne d'Arc Basin because this clay fraction is the most sensitive monitor of burial diagenesis (Środoń, 1981).

In this chapter, I/S mineralogy from 16 wells with increasing burial depths (vertical profiles) is presented. The

38

clay data are then described in the context of individual stratigraphic units. I/S data from 18 samples from 6 additional wells are also presented. The last part of this chapter covers the discussion and interpretation of the I/S data.

3.2 XRD CHARACTERISTICS OF <0.1μm FRACTION OF ARGILLACEOUS SEDIMENTS

Figure 3.1 shows characteristic XRD patterns of <0.1μm fine-grained clay fractions from the Jeanne d'Arc Basin. Mixed-layer illite/smectite is the most common component in all of these samples. Pure I/S is not common. Small to trace amounts of kaolinite (7.1 Å) are present in most samples whereas traces of chlorite are observed only in the deeper samples. Variable amounts of discrete illite are always present and these interfere with several XRD reflections of the mixed-layer I/S. Illite (001) and (002) XRD reflections usually occur as a shoulder on the high-angle side of the I/S reflections. The (003) XRD reflection of illite and $(003)_{10}/(005)_{17}$ reflection of the I/S are close to each other and give a single combined reflection between 26°-27° 2θ.

Discrete smectite, quartz, feldspar, calcite and other minerals were not detected in these fine-grained clay separates. The XRD patterns of these samples show broad reflections due to the fine grain-size and the mixed-layer

39

Figure 3.1: X-ray diffraction patterns of oriented illite/smectite-rich clays (<0.1μm fractions) from the Jeanne d'Arc Basin showing random (A), weakly-ordered (B), R1-ordered (C), and R3-ordered illite/smectite (D). All diffraction patterns were analyzed before and after ethylene glycol solvation. Arrows (<4.02°2θ region) in (B) and (C) indicate the presence of superlattice structures (001)$_{27}$. All peaks on glycolated samples are labelled in °2θ and proportion of illite-layers in illite/smectite are also indicated. Sample numbers, indicating present depth in meters, are listed on the right side of the x-ray diffraction patterns. K=Kaolinite. CuK$_a$ radiation. SM=South Mara C-13; AD=Adolphus D-50; CON=Conquest K-09; DOM=Dominion O-23. For description, see text.

Random I/S

A

5.16

← Ethylene Glycol
    Solvated

← Air-dried

31.50

26.30

10.16

15.72   15% I-layers

SM 2170

5.16

31.46

26.38

9.82

15.98   35% I-layers

SM 2395

5.16

31.42

26.42

9.52

16.28   55% I-layers

SM 2520

Intensity

°2Θ

2.5   5   10   15   20   25   30   35   40

Weakly Ordered R1 I/S

B

26.42

31.64

~3.34   5.40

9.72

16.28   53% I-layers

AD 2884

5.52

31.94

26.38

9.42

16.34   55% I-layers

CON 2420

3.16

6.03

32.75

26.42

ND

K

16.54   58% I-layers

DOM 3110

Intensity

°2Θ

2.5   5   10   15   20   25   30   35   40

41

nature of the sediments. The thickness of the glycol-smectite layer complex varies between 16.80 to 17.26Å for smectite-rich I/S and about 17.0Å for illite-rich I/S as inferred from methods of Środoń (1980, 1981, 1984).

3.3 METHODS TO ESTIMATE ILLITE/SMECTITE COMPOSITION

Several methods have been developed to measure the proportion of I-layers in I/S (Reynolds and Hower, 1970; Reynolds, 1980; Środoń, 1980; Watanabe, 1981; Reynolds, 1985; Tomita et al., 1988). Most of these methods are based on computer modelling or pure I/S samples from bentonite. Thus, for pure I/S, %I-layers can be determined accurately by applying several of these methods. Mixed-layer I/S from shale/mudstone almost always contains variable amounts of discrete illite, even in very fine-grained material. This discrete illite can influence the results of the above mentioned methods resulting in large errors. Środoń (1981, 1984) published several diagrams to avoid this problem. A preliminary examination of glycolated XRD patterns from 2.5° to 50°2θ indicated that two of his methods, one for random I/S, and the other one for ordered I/S, can be applied on most of the Jeanne d'Arc Basin samples. No single method can be used for the whole range of mixed-layer I/S, and different methods are required to quantify random and ordered I/S (Środoń, 1981).

43

For random I/S, the Środoń (1981) method requires accurate positioning of two XRD reflections at 15.5°-16.6° and 31°-32°2θ. These two reflections were present in almost all of the random I/S samples from the Jeanne d'Arc Basin. This method has two advantages over the Reynolds and Hower (1970) and Reynolds (1980) methods. It takes into account the variable thickness of a smectite-glycol layer complex which can vary from 16.6 to 17.2Å and result in up to 30% error (Środoń, 1981). Secondly, even small amounts of discrete illite can displace the $[(002)_{10}/(003)_{17}]$ reflection of I/S toward the nearby (002) illite reflection, thus causing overestimation of I-layers (Reynolds and Hower, 1970). Środoń's (1981) method includes a correction-factor for this interference from illite reflections. The error in the estimation of the proportion of I-layers in I/S using this method is approximately less than 5% (Środoń, 1981).

For ordered I/S, a reflection between 33° to 35°2θ has been used to estimate the proportion of I-layers in I/S following the Środoń (1984) method. He constructed an empirical working curve by plotting the 33°-35°2θ reflection position versus percent illite for pure I/S samples of various ages. For these pure I/S samples, two reflections at 16.6°-17.7° and 26°-27°2θ were used precisely to measure the percent I-layers in I/S. The data show a ±4% error for samples containing greater than 60 percent I-layers. The objective of

44

this empirical curve was that if discrete illite affects the 16.6°-17.7°2θ or other reflections of I/S, then the 33°-35°2θ reflection which is not influenced by discrete illite (Środoń, 1984) or small crystallite size (Reynolds and Hower, 1970) can be used to estimate percent illite in I/S. The 33°-35°2θ reflection is sensitive to ordering type and to the thickness of the smectite-glycol complex (Środoń, 1984). The type of ordering changes with increasing I-layers in I/S and with smectite-glycol complex thickness does not change very much in ordered I/S. These factors, therefore, will not significantly affect the quantification by this method (Środoń, 1984). For a few samples for which the above mentioned methods cannot be applied, XRD patterns were compared with computer calculated patterns in order to estimate the percent illite in I/S (Reynolds and Hower, 1970; Reynolds, 1980; Hower, 1981). Repeated XRD analyses of the same sample indicates that the reproducibility error is on the order of <5% I-layers.

3.4 TYPES OF MIXED-LAYER ILLITE/SMECTITE IN THE JEANNE D'ARC BASIN

Mixed-layer I/S of the Jeanne d'Arc Basin can be grouped into four main types of interstratification (Fig. 3.1) by using the criteria of Reynolds and Hower (1970), Reynolds (1980), Bethke et al., (1986) and Środoń (1984). These include: (1) random I/S (R0), (2) weakly ordered I/S (WR1),

45

(3) short-range ordered I/S (R1 or IS) and (4) long-range ordered I/S (R3 or ISII).

3.4.1 RANDOM ILLITE/SMECTITE

Random I/S (Fig. 3.1A) shows a strong reflection between 7.1 and $8.0°2\theta$ at room humidity (45 ± 10). Upon glycolation the reflection fully expands to about 17.1Å ($5.16°2\theta$). Non-integral, higher-order reflections indicate randomly interstratified illite/smectite (I/S). The relative intensity and sharpness of the higher-order I/S peaks also increases upon glycolation. Almost all glycolated random I/S samples give measurable reflections at about $5.16°$ $[(001)_{10}/(001)_{17}]$, $15.75-16.70°$ $[(002)_{10}/(003)_{17}]$, $26.00-27.00°$ $[(003)_{10}/(005)_{17}]$, and $31.00-32.00°$ $[(004)_{10}/(006)_{17}]$. The second-order I/S reflection $[(001)_{10}/(002)_{17}]$ gives a peak or shoulder or plateau toward the higher-angle side of the $[(001)_{10}/(001)_{17}]$ I/S reflection in most of the samples. Two I/S peaks between $43.0°$ and $48.0°2\theta$ are either weak or suffer interference from discrete illite (005) reflections and cannot be measured precisely. These two peaks were measurable only in a few samples.

In random I/S, increasing amounts of I-layers produce significant changes in the XRD patterns. As the I-layers increase, the lower-angle background of the first order $[(001)_{10}/(001)_{17}]$ reflection also increases; however, the

46

position of this peak does not migrate from its position at about 5.16°2θ. Conversely, the [(002)$_{10}$/(003)$_{17}$] peak moves toward the (002) illite peak as the degree of illitization increases. The [(003)$_{10}$/(005)$_{17}$] reflection remains essentially fixed in position because the smectite (005) and the illite (003) are very close to each other at about 3.33Å. The intensity of higher order reflections also increases as the percentage of I-layers increases in the random I/S. At about 60% I-layers in I/S, the first-order reflection at about 5.16°2θ changes into a shoulder and the [(004)$_{10}$/(006)$_{17}$] reflection becomes so broad and diffuse that its precise position cannot be measured.

3.4.2 WEAKLY-ORDERED ILLITE/SMECTITE

The second-order XRD reflection for ordered I/S usually occurs at 6.1° (14.5Å) or higher °2θ values (Bethke et al., 1986) compared to the first-order reflection for the random I/S which occurs at about 5.16°2θ (17Å) and does not move with increasing I-layers (see Fig. 3.1B for an example of weakly ordered XRD patterns). In the Jeanne d'Arc Basin, several samples show a reflection between 5.3° (16.6Å) and 6.0°2θ (14.7Å) with a low-angle (<4.0°2θ) superlattice reflection or a very high low-angle (<4.0°2θ) background. For these samples, the reflection between 31°-32°2θ becomes weak and diffuse and moves towards 33.0°2θ as the [(001)$_{10}$/(002)$_{27}$] reflection

47

shifts closer to 6.0°2θ. Such samples occur in a transition zone between the random and ordered I/S zones in about half of the wells examined in this study and are considered to be weakly ordered I/S.

The proportion of I-layers in these samples ranges from about 46% to 60% I. Środoń (1984) and Bethke et al. (1986) suggest that the transition from random to ordered I/S is a continuous process, rather than being a distinct phase change. These weakly-ordered samples appear to represent a transition from random to ordered restructuring of I/S. Whitney and Northrop (1988) reported the presence of both 17Å and (001)$_{27}$ superlattice reflections in a few samples during their hydrothermal experiments and considered them a mixture of random and ordered I/S. In the Jeanne d'Arc Basin, the 17Å reflection of random I/S has clearly moved toward 6.0°2θ. Whether some of these samples represent a mixture of random and ordered I/S is not clear.

3.4.3 R1-ORDERED ILLITE/SMECTITE

Upon glycolation, all ordered (R1) samples from the Jeanne d'Arc Basin show a characteristic reflection between 6.1° and 7.6°2θ (Fig. 3.1C). This reflection represents a higher-order reflection from a superlattice structure (10Å + 17Å = 27Å) and indicates the presence of ordering of the mixed-layer I/S in illite and smectite layers (Reynolds, 1980; Bethke et al.,

48

1986; Środoń, 1984). This reflection represents a dominant component of a second-order superlattice reflection and is called [(001)$_{10}$/(002)$_{27}$]. Samples showing a reflection between 6.1° and 7.6°2θ also show a reflection between 33°-35°2θ or close to 33.0°2θ. According to Środoń (1984), this reflection is a characteristic feature of ordering in I/S and does not exist in randomly-ordered samples. A reflection between 31°-32°2θ, present in random I/S samples, is absent from ordered I/S. Both 6.1°-7.6° and 33°-35°2θ reflection move toward higher 2θ values as the percent of I-layers in I/S increases. The first-order reflection of superlattice structure (001)$_{27}$ occurs only in a few samples with 60-70% I-layers in this present study. As the percent of I-layers increases, the presence of (001)$_{27}$ reflection is indicated by either a low-angle (<4.0°2θ) convexity or by a change in the slope of low-angle background. The [(001)$_{10}$/(003)$_{27}$] reflection is usually weak or makes a shoulder toward the higher-angle side of the [(001)$_{10}$/(002)$_{27}$] reflection. The [(002)$_{10}$/(005)$_{27}$] reflection is influenced by the (002) illite reflection and cannot be exploited for the determination of layer proportion. Two I/S reflections between 43°-48°2θ are clear only in few samples with <70% I-layers.

R1-ordered I/S generally shows 58-80% and rarely up to 85% I-layers. As I-layers in I/S increase, the relative intensity of [(001)$_{10}$/(002)$_{27}$] reflection decreases to a shoulder. R1-

ordering occurs deeper in the wells than random I/S, usually below 2500m depths, and may be observed down to 5000m in a few wells. A distinction between short-range (R1) and long-range (R3) ordering is based on two parameters, BB1[1] and BB2[1], as defined by Środoń (1984). For all R1 ordered I/S, both BB1 and BB2 values are larger than 4.0.

3.4.4 R3-ORDERED ILLITE/SMECTITE

With increasing illite-layers in R1-ordered I/S, the $[(001)_{10}/(002)_{27}]$ reflection moves toward higher-angle values and indicates the evolution of long-range ordering (Fig. 3.1D). The presence of long-range ordering (R3-ordered I/S) is indicated by the presence of a small shoulder or a peak between 7.6 and $8.0°2\theta$ and is confirmed by BB1 and BB2 values which are less than four. Small amounts of chlorite are often present in R3-ordered I/S samples which can increase the BB1 value above 4.0; however BB2 is not affected by the presence of chlorite. This highly illitic I/S, with 80-92% I-layer, is less common and usually occurs in the deepest part of the wells (below 4000m) in the Jeanne d'Arc Basin.

---

[1]"BB1: the joint breadth of (001) illite and adjacent I/S reflections, measured in $2°\theta$ from where the tails of the reflection join the X-ray background. BB2: the joint breadth of (004) illite and adjacent I/S reflections measured like BB1."

3.5 ILLITE/SMECTITE COMPOSITION WITH INCREASING BURIAL DEPTHS

In this section, down-hole profiles of I/S composition from 16 wells are reported. Based on their geographic location in the basin, these wells are divided into four groups having different stratigraphies and structural configuration (for details see sections 3.5.1, 3.5.2, 3.5.3, and 3.5.4). These four groups and the wells occurring in them are (Fig. 3.2):

1). **The Trans-Basinal Fault area (TBF)**

   (South Mara C-13, North Ben Nevis P-93, Nautilus C-92, Hebron I-13, North Trinity H-71)

2). **The Northern part of the Basin (NPB)**

   (Adolphus D-50, Conquest K-09, Whiterose J-49, West Flying Foam L-23)

3). **The Outer Ridge Complex (ORC)**

   (Dominion O-23, Bonanza M-71, South Tempest G-88, North Dana I-43)

4). **The Southern part of the Basin (SPB)**

   (Egret K-36, Egret N-46, Cormorant N-83)

Profiles of depth versus I/S composition for individual wells have been divided into three zones for the purposes of description and discussion of the I/S data. Zone I contains only random (R0) I/S with usually more than 65% expandability (<35%I). Zone II is characterized by a significant (often rapid) increase in proportion of I-layers and contains both random and ordered I/S. Zone III represents mainly ordered I/S

51
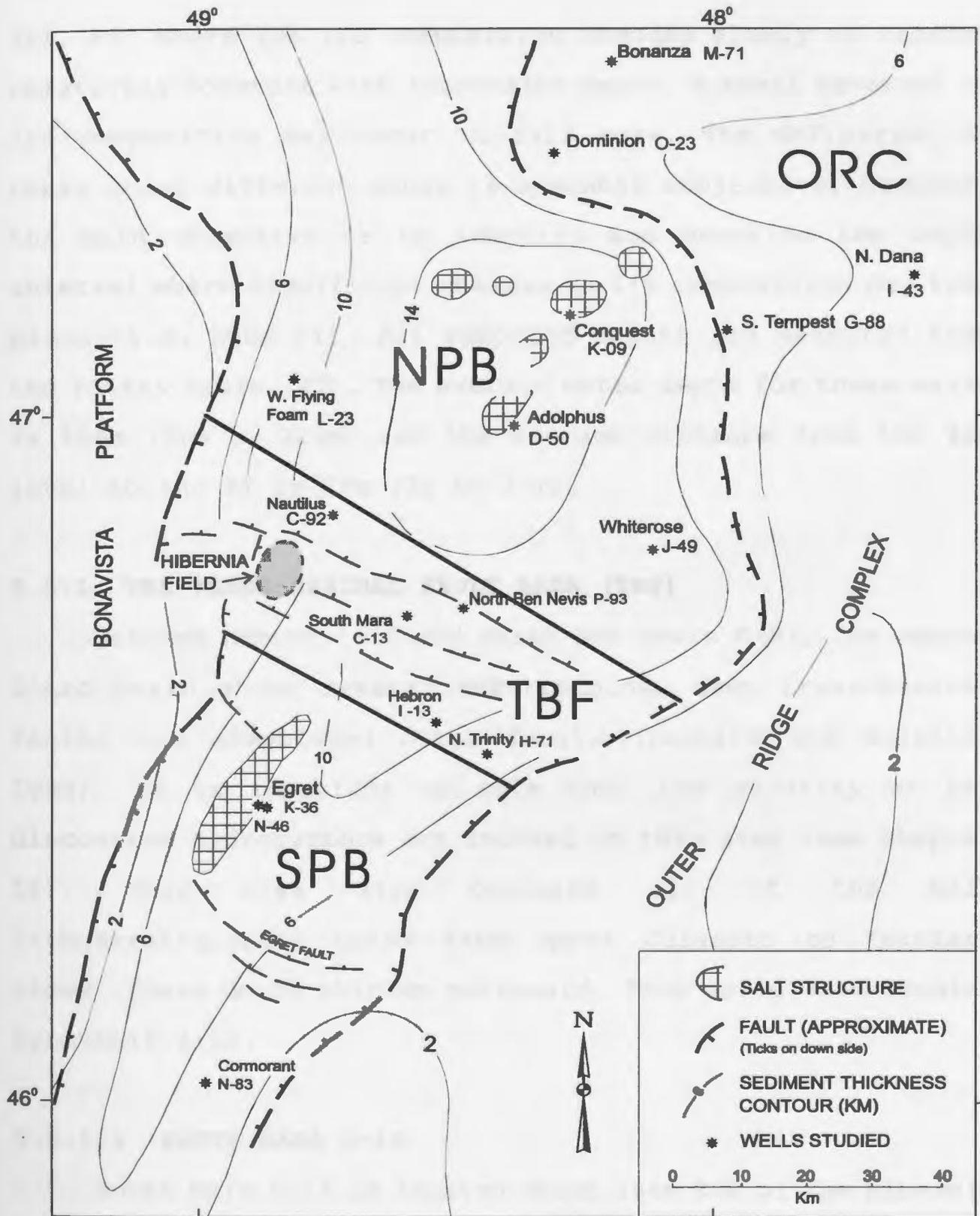
Figure 3.2. Basemap showing the Jeanne d'Arc Basin divided into four areas including the location of the wells studied for this project. Wells studied for selected intervals are not shown in this figure. SPB=Southern part of the basin; TBF= Trans-Basinal Fault; NPB=Northern part of the basin; ORC=Outer Ridge Complex. Modified from Grant et al. (1986).

52

(R1, R3) where the I/S composition changes slowly or remains relatively constant with increasing depth. A small reversal in I/S composition may occur in this zone. The definition of these three different zones is somewhat subjective, however, the main objective is to identify and describe the depth interval where significant changes in I/S composition may take place (i.e. Zone II). All reported depths are measured from the rotary table (RT). The average water depth for these wells is 116m (66m to 221m) and the average distance from the sea level to the RT is 26m (22 to 30m).

3.5.1 THE TRANS-BASINAL FAULT AREA (TBF)

Between Hebron I-13 and North Ben Nevis P-93, the Jeanne d'Arc Basin shows several WNW-trending, deep trans-basinal faults and associated other faults (Tankard and Welsink, 1988). It is important to note that the majority of the discovered hydrocarbons are located in this area (see Chapter II). This area also contains all of the main lithostratigraphic units from upper Jurassic to Tertiary times. These units thicken northward. Five wells were studied from this area.

3.5.1.1 SOUTH MARA C-13

South Mara C-13 is located about 16km ESE of the Hibernia field (Fig. 3.2). It was drilled to a depth of 5034.1m (RT)

and intersected all of the main formations from the Jeanne d'Arc Formation (Tithonian) to the Banquereau Formation (Tertiary). The South Mara field is located on a northeast dipping fault block which is bounded to the southwest by an antithetic fault. Both gas (2926-2932m) and oil (2952-2958m) were discovered from the Avalon and Ben Nevis Formations (Sinclair et al., 1992).

South Mara C-13, located in the middle of the basin, was selected as one of the main wells to characterize the I/S composition in the Jeanne d'Arc Basin. A total of 40 drill-cutting samples were studied ranging from a depth of 1225m to 5010m, covering a 3780m interval. The clay mineralogy of the <0.1μm grain-size fraction indicates that I/S is the main component, however, minor amounts of kaolinite and discrete illite (~<5%) are present in most samples. In samples with random I/S, chlorite was not detected. Trace to minor amounts of chlorite are present below 2815m, particularly in samples containing greater than 80% I-layers.

Overall, the South Mara C-13 well shows a continuous trend of compositional change in I/S with increasing burial depths (Fig. 3.3). The I/S compositions range from 15% to 85% I-layers. All samples above 2640m depth show randomly interstratified I/S for which the I/S compositions varies from 15% to 60%I. R1-ordered I/S with 65% I-layers first appears at 2640m at a present temperature of about 80°C. Below this

54

Figure 3.3: Proportion of illite-layers (%I) in mixed-layers illite/smectite (I/S) versus present burial depths from South Mara C-13. XRD analyses were carried out on fine-grained (<0.1μm) oriented clay particles after saturation with ethylene glycol by using Copper K_a radiation. Methods used to calculate the I/S composition are discussed in section 3.3. The location of Zone I, II, III are shown (see text). Note a rapid increase of illite-layers in I/S within a narrow depth interval (shaded area). Random to R1-ordered I/S change occurs at 2640m where the present temperature is 80°C. The gamma(γ)-ray log shows the basic lithology in clastic dominant sediments. Higher γ-ray values (left side) indicate the presence of argillaceous sediments. Solid spikes on the left side of the γ-ray log indicate casing depths (for depths see Appendix II). The ordering in the brackets (R3) indicates a rare occurrence. The STG column represents the main stratigraphic units encountered in South Mara C-13: J=Jeanne d'Arc Formation, F=Fortune Bay Formation, H=Hibernia Formation, W=Whiterose Formation, B=Banquereau Formation, D=Dawson Canyon Formation, TD=Total depth. Stratigraphic data from C-NOPB's Schedule of Wells (1988).

Trans-Basinal Fault Area

SOUTH MARA C-13

STG. GAMMA RAY

DEPTH (km)

1

B

2

D

N

BN

3

A

W

C

4

H

F

J

5

TD

I

II

III

R0

R1 (R3)

0   20   40   60   80   100

%ILLITE IN I/S
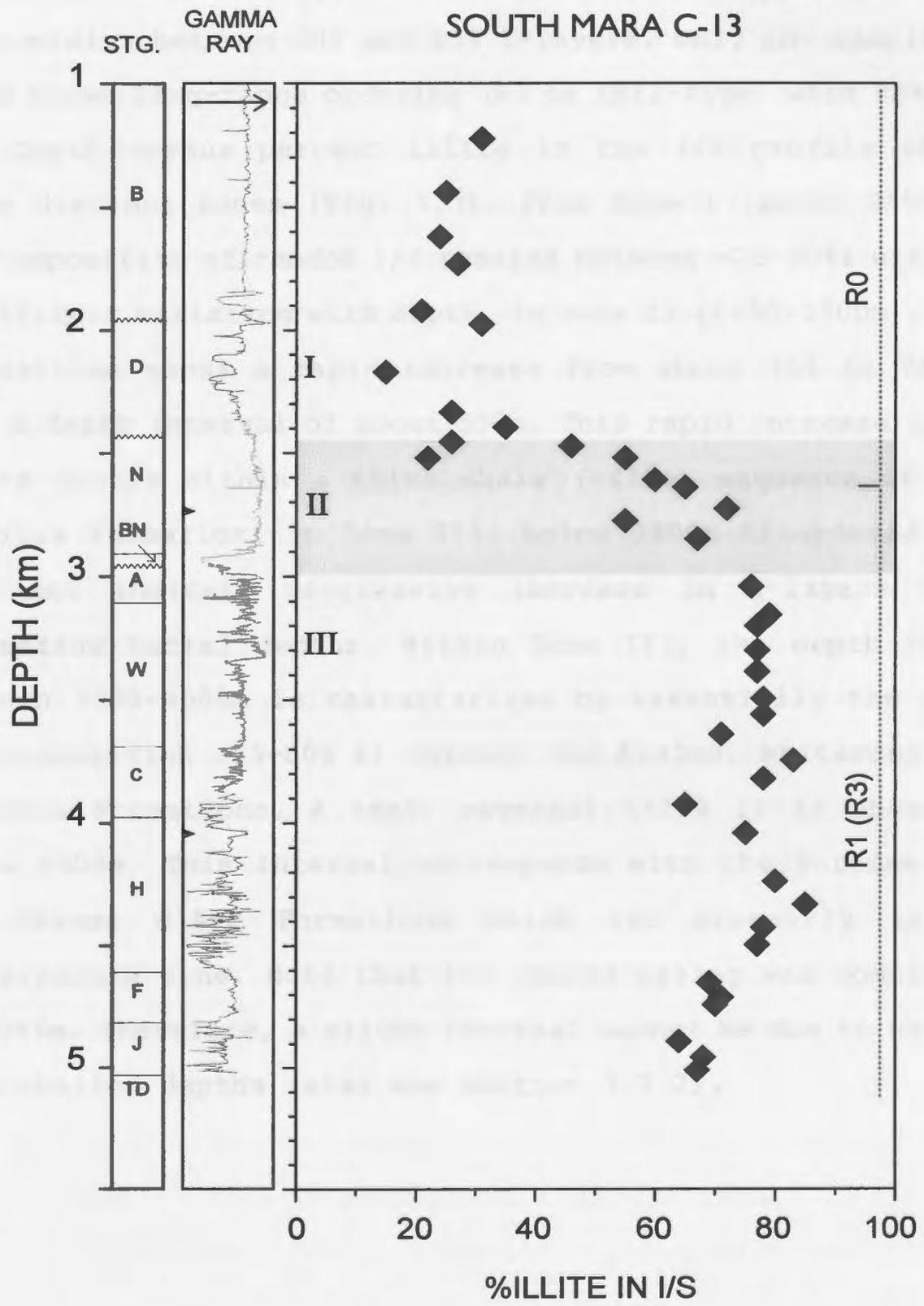
depth, only ordered I/S is encountered. From 2640m to 5010m (>2.5km), ordering is predominantly R1 (or IS-type), and the I/S contains between 63% and 83% I-layers. Only one sample at 4330m shows long-range ordering (R3 or ISII-type) with 85% I.

Depth versus percent illite in the I/S profile shows three distinct zones (Fig. 3.3). From Zone I (above 2450m), the composition of random I/S remains between ~20-30%I with no significant variation with depth. In Zone II (2450-3000m), I/S composition shows a rapid increase from about 35% to 75% I over a depth interval of about 550m. This rapid increase in I-layers occurs within a thick shale (~475m) sequence of the Nautilus Formation. In Zone III, below 3000m R1-ordered I/S does not indicate progressive increase in I-layers with increasing burial depths. Within Zone III, the depth range between 3000-4500m is characterized by essentially the same I/S composition (75-80% I) through the Avalon, Whiterose and Hibernia Formations. A small reversal (~10% I) is observed below 4500m. This interval corresponds with the Fortune Bay and Jeanne d'Arc Formations which are presently in an overpressure zone. Note that the second casing was completed at 4046m. Therefore, a slight reversal cannot be due to caving from shallow depths (also see section 3.7.2).

3.5.1.2 NORTH BEN NEVIS P-93

North Ben Nevis P-93 is located in the Trans-Basinal Fault (TBF) area, about 5km east of South Mara C-13 well (Fig. 3.2). The well is 5282.2m deep. It was drilled on a north-east dipping fault block which is truncated by a southwest dipping normal fault (Gibbons, 1990). This fault ends below the Upper Cretaceous sediments. A corrected geothermal gradient of 28.5°C/km is reported from this well (Correia et al., 1990). Thirteen samples analyzed from this well cover a depth interval of about 3100m (1565-4125m). Fine-grained clay samples (<0.1μm) consist mainly of I/S. Minor amounts to traces of kaolinite and illite are present in many samples, however, chlorite is detected only from very illitic samples (i.e. 2915m).

The vertical profile of I/S composition from North Ben Nevis P-93 resembles the profile for South Mara C-13 (Fig. 3.4A). The composition of I/S varies from 25% to 90% I. Random I/S persists up to 2600m and contains 25% to 43% I-layers. Weak-ordering appears at 2625m at a present formation temperature of about 80°C. Below 2670m depth all samples are R1 or R3-ordered I/S. The random to ordered transition occurs within the Nautilus Formation.

In Zone I, the composition of I/S remains between 25-36% I. In Zone II, the proportion of illite-layers, as was the case in South Mara C-13, increases rapidly from 36% to 90%

58

Figure 3.4: Estimated proportion of illite-layers in illite/smectite versus present burial depth, stratigraphy and γ-ray log for four wells located in the Trans-Basinal Fault area. Note a rapid increase of illite-layers in illite/smectite within a narrow depth interval (shaded area). Depth-illite/smectite composition profile is divided into three zones as described in section 3.5. For abbreviations see figure 3.3.

Trans-Basinal Fault Area

Figure showing four depth vs. %Illite in I/S plots: A) NORTH BEN NEVIS P-93, B) NAUTILUS C-92, C) HEBRON I-13, D) NORTH TRINITY H-71
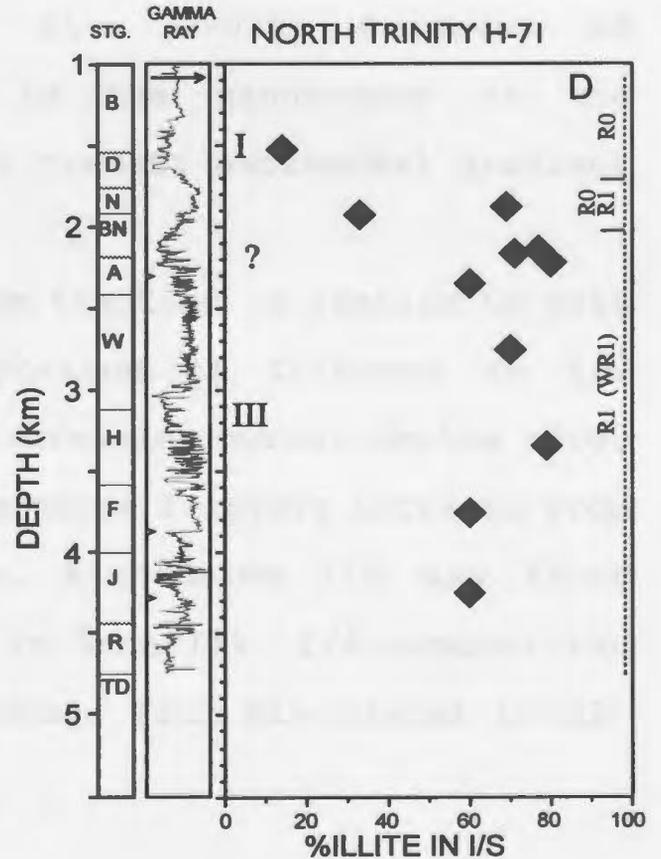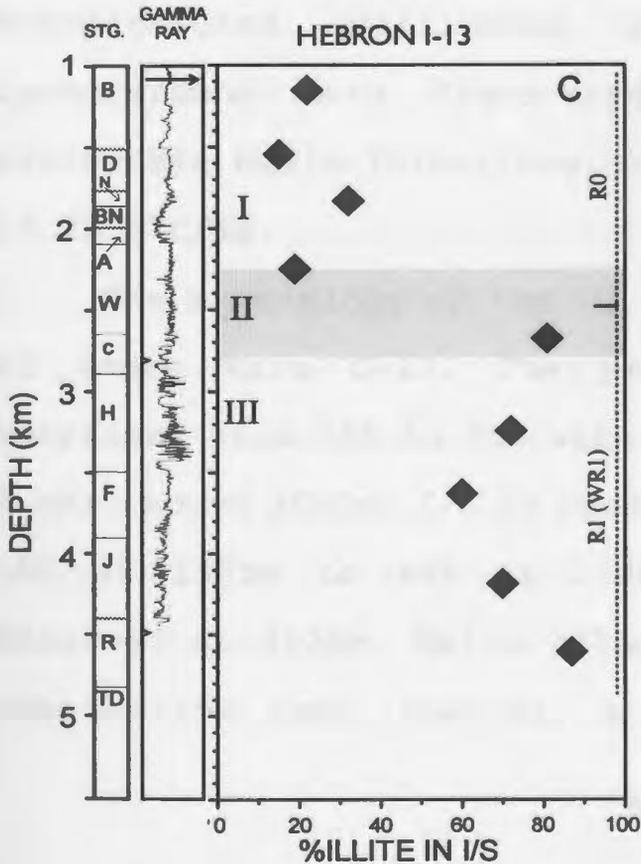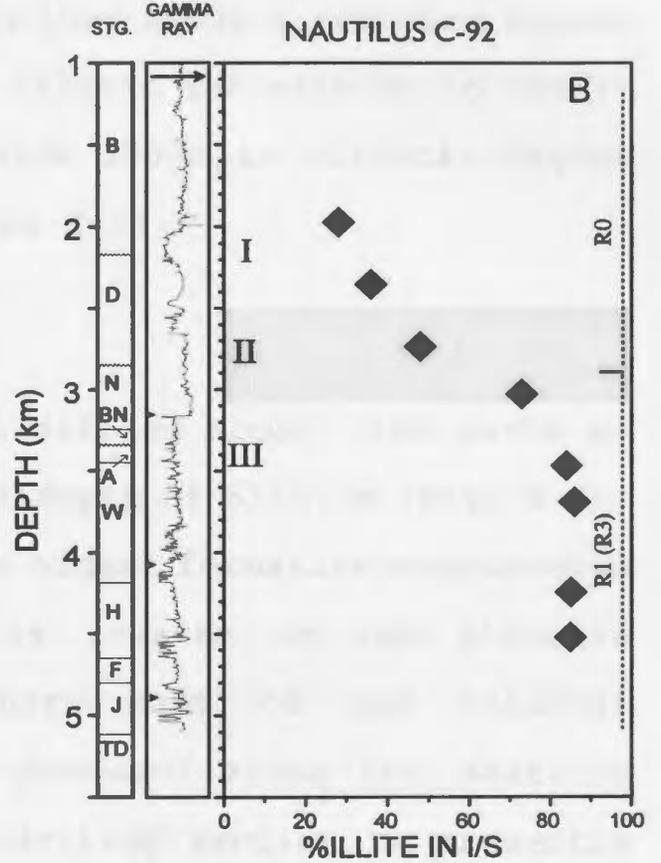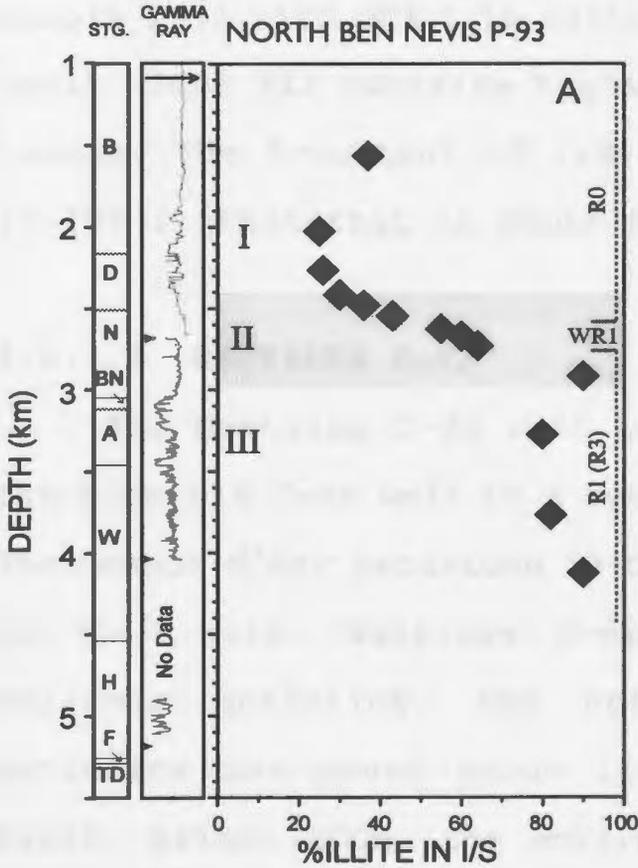
over a 600m depth interval. It is important to note that sample 2915 with 90% I is sitting just above a reported normal fault. Zone III contains highly illitic I/S with 80 to 90% I-layers. The I-content of I/S below 3000m is slightly higher (5-10% I) than that in South Mara C-13.

3.5.1.3 NAUTILUS C-92

The Nautilus C-92 well was drilled about 10km north of the Hibernia C-96 well to a total depth of 5116.7m (Fig. 3.2). The Jeanne d'Arc sandstone is the oldest formation encountered in this well. Nautilus C-92 is located on the Hibernia rollover anticline. The northern part of the rollover anticline has moved about 1km downward along the Nautilus Fault. Below 3300m, the entire drilled section is presently overpressured (Williamson et al., 1993). Reserves of hydrocarbons were discovered in the sandstones of the Avalon/Ben Nevis Formations. The present geothermal gradient is 28.9°C/km.

The mineralogy of the <0.1µm fraction is similar to that of South Mara C-13. The proportion of I-layers in I/S increases from 28% to 85% with increasing burial depths (Fig. 3.4B). Above 3000m, I/S is random where I-layers increase from 28% at 1975m to 48% at 2740m. R1-ordered I/S was first observed at 3030m. Below 3400m in Zone III, I/S composition remains the same, however, a change from R1-ordered to R3-

ordered was observed in the deepest sample. Similar to both South Mara C-13 and North Ben Nevis P-93, R1-ordered I/S first appears in the Nautilus Formation at a present formation temperature of about 90°C. Zone II is almost the same as in South Mara C-13 and North Ben Nevis P-93.

3.5.1.4 HEBRON I-13

The Hebron I-13 is located about 10km north of Terra Nova K-08 with a total drilled-depth of 4723.5m in the Rankin Formation (Fig. 3.2). The well was drilled on a horst/graben structural complex associated with the trans-basinal faults (Gibbons, 1990). The well intersects a fault near 2650m. Reserves of hydrocarbons were discovered from the Jeanne d'Arc, Hibernia, and Ben Nevis Formations.

Nine samples ranging from 1155m to 4605m were analyzed from the Hebron I-13 well (Fig. 3.4C). Clay mineralogy of the <0.1µm grain-size fraction is similar to that of South Mara C-13. I/S composition ranges from 15% to 87% I with a somewhat variable vertical depth profile. The random I/S persists up to 2250m (Zone I). The I/S composition varies from 15% to 32%I and does not increase with depth. From 2250m to 2675m, a rapid increase (from 19% to 81%I) in I-layers is observed. Unfortunately, no sample was available between 2250m and 2675m and therefore the nature of this transitional interval (Zone II) between random and ordered I/S is not clear. R1-ordered

I/S with 81%I was first observed close to a fault at 2675m (Catalina Member of Whiterose Formation) where the present formation temperature is about 70°C. All samples below 2700m are in Zone III and have ordered I/S. In Zone III, one sample from the Fortune Bay Formation at 3630m shows weak-ordering with only 60% I-layers. It is important to note that the Nautilus Formation in this well is intersected several hundred meters shallower than in the South Mara C-13 and it shows random I/S.

3.5.1.5 NORTH TRINITY H-71

North Trinity H-71 was drilled as a delineation well to determine the extent of the Hebron hydrocarbon structural complex, about 7km south-east of the Hebron discovery (Fig. 3.2). It is 4758m deep and encountered all of the main stratigraphic units between the Rankin and the Banquereau Formations. Only minor amounts of hydrocarbons were recovered from the Hibernia Formation so this well is classified a dry hole.

Eleven samples were analyzed from the 1520m to 4250m interval (Fig. 3.4D). Clay mineralogy of the <0.1μm grain-size is similar to other wells of this group. The proportion of I-layers in I/S varies from 14% to 80%. I/S above 1925m is mainly randomly interstratified. However, one sample from the Nautilus Formation at (1875)m depth, showed ordered I/S with

63

69% I-layers. This situation, where ordered I/S is present above the random I/S, is not observed in any other well studied for this project. Below 2145m, all samples have ordered I/S with generally 70-80% I-layers. Two samples below 3750m show weak-ordering with only 60% I-layers. These samples are from the Fortune Bay and Jeanne d'Arc Formations. A change from random to ordered I/S occurs over a short interval (220m) where expandability decreases from 60% to 24%. Ordered I/S (1875m) first appears at a much lower present temperature (55°C) than in other wells.

3.5.1.6 SUMMARY

Most wells in the TBF area show smectite-rich random I/S above 2600m. With the exception of North Trinity H-71, ordered I/S first appears between 2640m to 3030m at present formation temperatures of about 80° to 90°C. In North Trinity H-71, however, ordering occurs at relatively shallow depth (1875m) and low present formation temperature (56°C). Random to ordered I/S transition in the TBF area usually occurs rapidly over a 600m to 550m depth interval. In several wells (South Mara C-13, North Ben Nevis P-93, Nautilus C-92, and North Trinity H-71) this transition occurs within the shales of the Nautilus Formation. In Hebron I-13, it occurs at the top of the Catalina Member of the Whiterose Formation. Several wells show a small reversal (10-20% I) in percent I-layers at

64

greater depths corresponding with the Fortune Bay and Jeanne d'Arc Formations. R3-ordered I/S only occurs in a few samples below 4000m.

3.5.2 THE NORTHERN PART OF THE BASIN (NPB)

The Northern part of the Jeanne d'Arc Basin (north of North Ben Nevis P-93 and Nautilus C-92 wells) is relatively wide and deep, preserving up to 20km of sediments (McAlpine, 1990). The following wells in this area were studied; Adolphus D-50, Conquest K-09, Whiterose J-49, and West Flying Foam L-23. This distal part of the basin is rich in argillaceous sediments and lacks abundant faulting, particularly in its centre (Adolphus D-50 and Conquest K-09). The Egret Member source rocks are overmature in much of this area (McAlpine, 1990). The central part of the northern area is characterized by several salt diapirs that pierce up to several kilometres into younger sediments and elevate the geothermal gradient (i.e. 33°C/km). Adolphus D-50 and Conquest K-09 were drilled close to these salt structures (Fig. 3.2).

3.5.2.1 ADOLPHUS D-50

Adolphus D-50 was drilled to a depth of 3686m on the flank of a salt dome (Fig. 3.2). This well penetrated a thick shale sequence of Nautilus, Dawson Canyon, and Banquereau Formations. Adolphus D-50 is a dry-hole with a relatively high

65

geothermal gradient (30.8°C/km). Twenty five samples, from the 1565 to 3660m interval, were studied. These samples (<0.1μm) contain relatively less kaolinite and discrete illite than was the case in Trans-Basinal Fault area. XRD patterns from this well suggest that several samples are probably close to pure I/S.

Adolphus D-50 was selected as one of the main wells to characterize I/S composition in a shale dominated, less faulted area. In Adolphus D-50, I/S shows a whole spectrum of X-ray diffraction patterns of random, weakly-ordered and R1-ordered structures (Fig. 3.5A). With increasing burial depths, I-layers in I/S increase more or less continuously from 29% to 76% I (Fig. 3.5A). Random I/S persists down to a depth of 2580m spanning the entire Banquereau Formation, for which the composition ranges from 29% to 47% I. From 2665m to 3135m (Dawson Canyon Formation), I/S is weakly-ordered. In this 470m interval, temperatures range from about 87° to 101°C. For weakly-ordered I/S, compositions vary from 49% to 60% I. Ordered I/S first appears within the Dawson Canyon Formation at a depth of 3135m around 101°C. Below this depth only R1-ordered I/S is found for which the composition ranges from 60% to 76% I. Most weakly-ordered and R1-ordered I/S samples show a first-order superlattice reflection between 30-27Å.

In Zone I, the proportion of illite-layers remains between 29-35% illite independent of depth. In Zone II (2300-

66

Figure 3.5: Estimated proportion of illite-layers in illite/smectite versus present burial depth, stratigraphy and γ-ray log for four Northern wells. Note a gradual increase of illite-layers in illite/smectite with depth and as a result zone II is thicker than for wells located in the Trans-Basinal Fault area. 'F'=Fortune Bay Formation, undifferentiated Tithonian to Barremian. For abbreviations, see figure 3.3.

Northern Part of the Basin
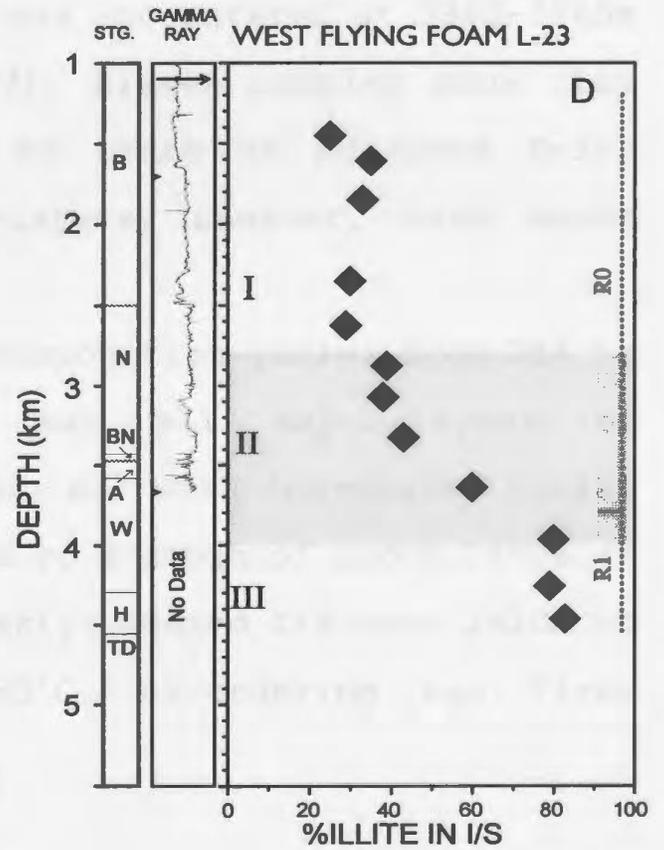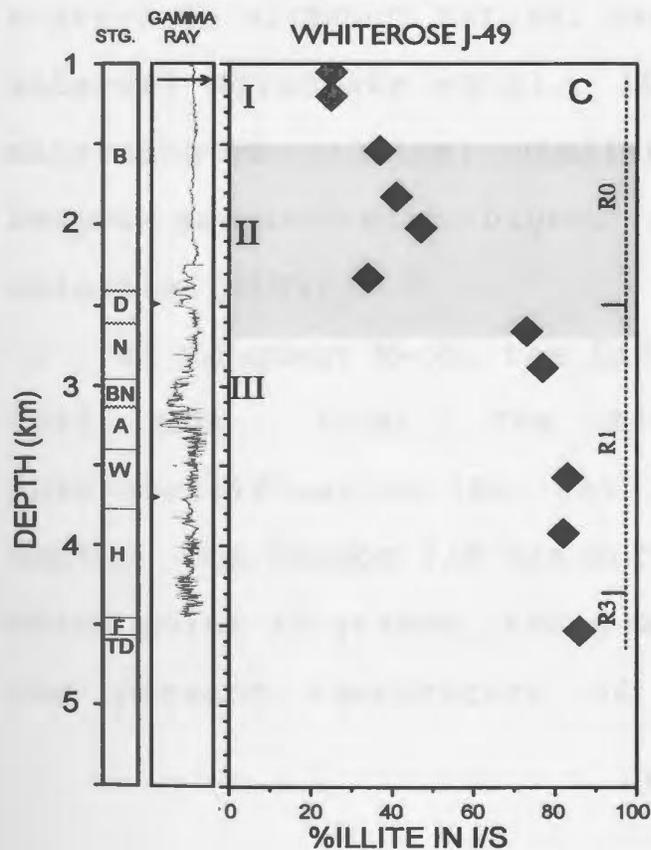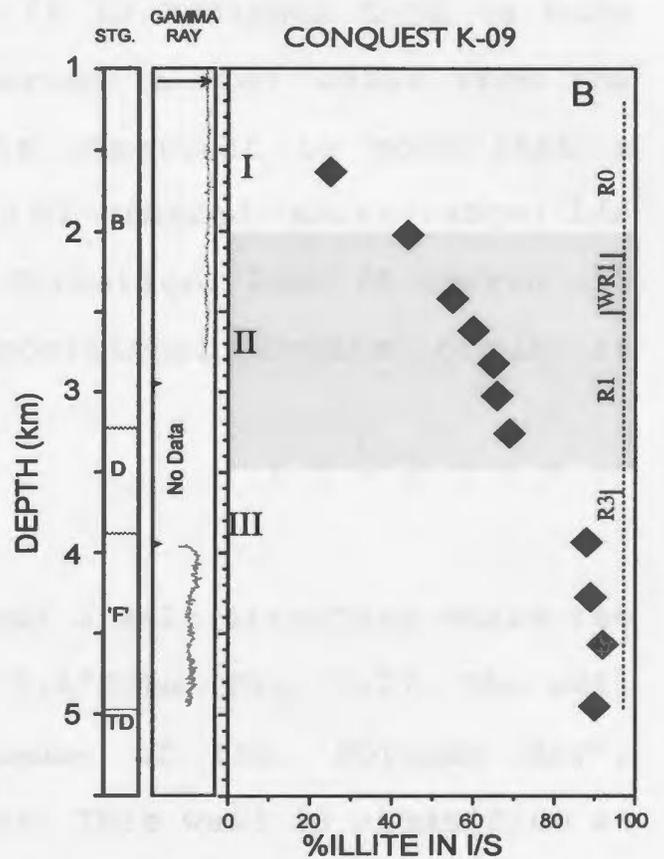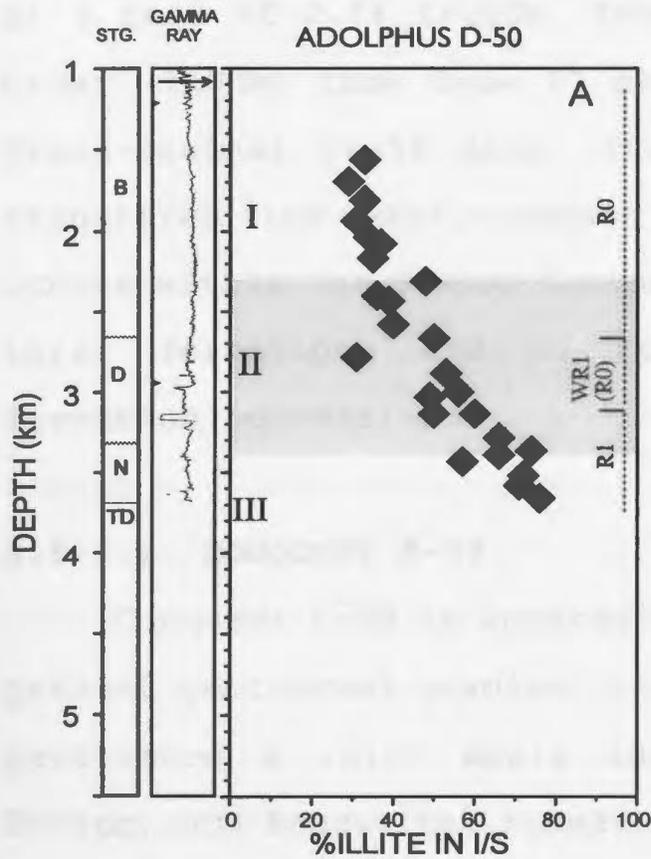
3400m), I-layers progressively increase from about 35% to 75% at a rate of 2.7% I/100m. Zone II in Adolphus D-50 is much wider (1100m) than Zone II observed in most wells from the Trans-Basinal Fault area. It is important to note that a transition from weakly-ordered to R1-ordered (short-range) I/S occurs within the Dawson Canyon Formation. Zone II covers all three formations and no compositional breaks occur at formation boundaries.

3.5.2.2 CONQUEST K-09

Conquest K-09 is located near a salt structure where the present geothermal gradient is 33.4°C/km (Fig. 3.2). The well penetrated a thick shale sequence of the 'Fortune Bay', Dawson, and Banquereau Formations. This well is classified as a dry-hole although natural gas was encountered at 3940-3965m interval (Sinclair et al., 1992). Eleven samples show clay mineralogies (<0.1μm) similar to those of Adolphus D-50. Deeper samples with higher I-layers, however, have minor chlorite (~10%).

In Conquest K-09, the I/S composition varies from 25% to 92%I (Fig. 3.5B). The I/S has all major types of interstratification (R0, WR1, R1, R3) with increasing burial depths. The random I/S was noted to a depth of about 2400m at which point it grades into a weakly ordered I/S near 2420m at the present temperature of 85°C. R1-ordering was first

69

recognized within the Banquereau Formation at 2620m with 60% I-layers where the present formation temperature is near 90°C. R1-ordered I/S continues to exist to at least 3220m (69% I) at the top of the Dawson Canyon Formation. No samples were analyzed between 3260m to 3935m. All samples below 3900m show long-range ordering (R3) for which the I/S composition remains at 88-92% I-layers and the temperature is above 140°C. Only one sample falls in Zone I. In Zone II, the proportion of I-layers increases continuously with depth at about 2% I-layers per 100m; which is slower than in South Mara C-13. In Zone III (~3500m), the composition of I/S remains nearly constant (~90%I). It is important to note that in Conquest K-09, ordering appears within the Banquereau Formation whereas in Adolphus D-50, it appears in the Dawson Canyon Formation.

3.5.2.3 WHITEROSE J-49

Whiterose J-49, a delineation well for the Whiterose structure, is situated on the eastern flank of the northern Jeanne d'Arc Basin (Fig. 3.2). It is 4561.4m deep and intersects all of the main stratigraphic units from the Banquereau to Fortune Bay Formations. Oil and gas reserves have been found in the Avalon/Ben Nevis Formations. The present geothermal gradient is 31.9°C/km. Eleven samples studied from this well have clay mineralogies (<0.1μm) similar to that of South Mara C-13.

In Whiterose J-49, the I/S composition varies from 25% to 86%I as interstratification changes from random to R3-ordered I/S with increasing burial depths (Fig. 3.5C). In Zone I, I/S compositions remain below 30%I. In Zone II, I-layers appear to increase slightly (37% to 47%I) but the nature of the transition from random to ordered I/S is not clear due to the insufficiency of samples available between 2020m and 2655m. In fact, one sample (2325m) in this interval suggests a possible reversal in the trend. The apparent change from random to R1-ordered I/S probably occurs near 2655m in the Nautilus Formation, at a present formation temperature of about 90°C. In Zone III, I-layers increase slowly (0.64% I/100m) from 77% to 86%I over an 1875m depth interval. R1-I/S ordering changes into R3-I/S below 4500m at a present temperature of about 150°C.

3.5.2.4 WEST FLYING FOAM L-23

West Flying Foam L-23, situated about 27km north of Hibernia K-18, penetrated to a depth of 4553.8m (Fig. 3.2). All of the main stratigraphic units from the Hibernia to Banquereau Formations were encountered, with the exception of the Dawson Canyon Formation which is either missing (Sinclair, 1988) or very thin (~20m, McAlpine, 1990). In this dry-hole, the present geothermal gradient is about 30°C/km. Twelve samples were analyzed from this well.

71

The I-content of I/S increases with depth from 25% at 1450m to 83% I at 4460m (Fig. 3.5D). Random I/S persists down to 3640m (115°C), more than 1000m deeper than that observed in South Mara I-13. For random I/S, the composition remains at about 25-30% I up to 2625m and, below this depth I-content increases slightly to 43% I near 3325m depth. At 3640m, the random I/S reaches the maximum I-content of about 60% I in the Whiterose Shale. R1-ordered I/S was first encountered at 3965m in the Catalina Member of the Whiterose Formation where the present temperature is around 125°C. Below this depth ordering remains R1 with a maximum composition of 83% I. In this well the proportion of I-layers increases rapidly from 43% to 80% I in the interval from 3325m to 3965m.

3.5.2.5 SUMMARY

With the exception of West Flying Foam L-23, random to R1-ordered I/S transition occurs between depths of 2620m to 3135m and at 90°-100°C present temperatures. In the West Flying Foam L-23, the random I/S persists, with minor modifications, at greater depths than any other well discussed so far. In the Northern part of the basin, I-layers in I/S generally increase slowly, instead of showing a rapid increase with depth commonly observed in the Trans-Basinal Fault area. This fact is most obvious from the Adolphus D-50 and Conquest K-09 profiles and probably for the Whiterose J-49 well. Furthermore, ordering in each well first appears in different

72

formations in contrast to the Trans-Basinal Fault area where it occurs mostly in the Nautilus Formation. This demonstrates that the mixed-layer I/S versus depth trends are not detrital in origin, rather the I/S trends reflect the conversion of smectite-rich I/S during burial diagenesis within the basin. R3-ordered I/S is observed only below 3920m depth in Conquest K-09 and Whiterose J-49.

3.5.3 THE OUTER RIDGE COMPLEX (ORC)

The Outer Ridge Complex is a basement high partly covered with deformed Jurassic sediments and bounds the Jeanne d'Arc Basin from the east and northeast sides (McAlpine, 1990). The Tertiary sediments are thicker (2700-3500m) than those of the Early Cretaceous (500-700m), whereas the Late Cretaceous sediments are generally missing (Sinclair, 1988). Four wells (Dominion O-23, Bonanza M-71, South Tempest G-88, North Dana I-43) from the Northern part of the ridge were studied (Fig. 3.2).

3.5.3.1 DOMINION O-23

Dominion O-23 is located on the northern part of the Outer Ridge Complex (Fig. 3.2). The well encountered a thick shale package of the 'Fortune Bay' (Whiterose of McAlpine, 1990) and Banquereau Formations. Sediments representing Aptian to Companian age are either missing (Sinclair, 1988) or are very thin in this section (McAlpine, 1990). Eight samples were

studied from this dry-hole where the present geothermal gradient is around 26.4°C/km.

In Dominion O-23, the I-content of mixed-layer I/S continuously increases from 34% to 79% (2.7% I/100m) with increasing burial depths (2275m to 3700m)(Fig. 3.6A). All I/S samples above 3110m are randomly interstratified (Fig. 3.6A). Weak-ordering with 58% I-layers first appears in the Banquereau Formation near 3110m depth where the present temperature is about 85°C. The R1-ordered I/S with 60% I-layers is first encountered around 3235m depth ('Fortune Bay' Formation, Tithonian to Aptian) and at a present temperature of about 91°C. It is important to note a linear trend of I/S composition across the unconformity, although a significant hiatus (Aptian to Campanian) is present in the section.

3.5.3.2 BONANZA M-71

Bonanza M-71 was drilled 15km northeast of Dominion O-23 (Fig. 3.2). The section contains a sequence of Upper Jurassic (Rankin Formation), Lower Cretaceous ('Fortune Bay' of Sinclair, 1988 or Whiterose of McAlpine, 1990) and Tertiary sediments. Aptian to base Tertiary sediments are absent (Sinclair, 1988) or very thin (McAlpine, 1990). Eleven samples were analyzed. The clay mineralogy of the <0.1μm fraction is similar to that observed in other wells. The present geothermal gradient is 32.3°C/km.

The I/S composition ranges from 21% to 85% I (Fig. 3.6B).

Figure 3.6: Estimated proportion of illite-layers in illite/smectite versus present burial depth, stratigraphy and γ-ray log for four Outer Ridge Complex area wells. With the exception of Bonanza M-71, most samples suggest a gradual increase of illite-layers compared to wells located in the Trans-Basinal Fault area. Bonanza M-71 shows a rapid jump of 35% illite-layers near 3500m. In South Tempest G-88, a small reversal near 2700m corresponds to an unnamed limestone interval. 'F'=Fortune Bay Formation, undifferentiated Tithonian to Barremian. For abbreviations, see figure 3.3.

Outer Ridge Complex Area
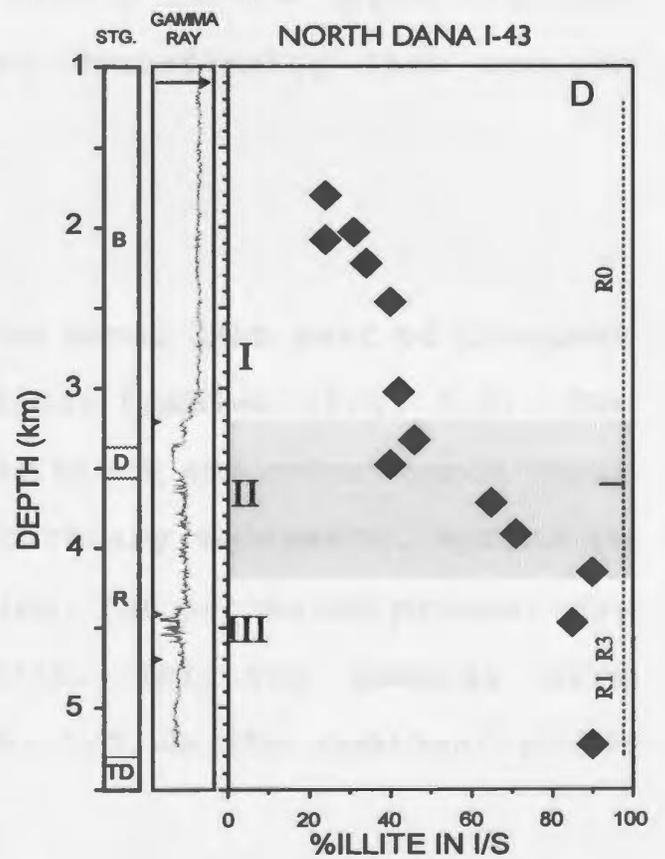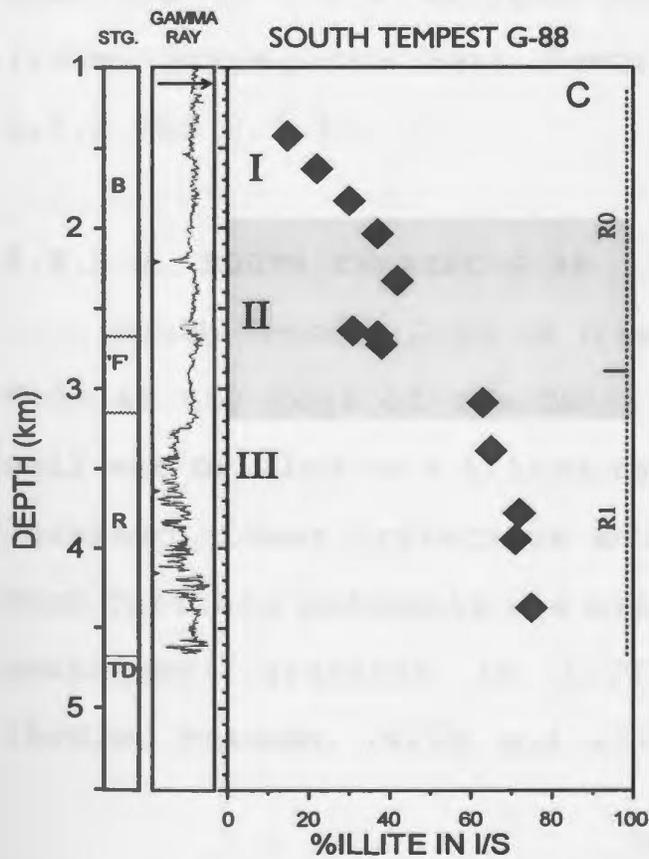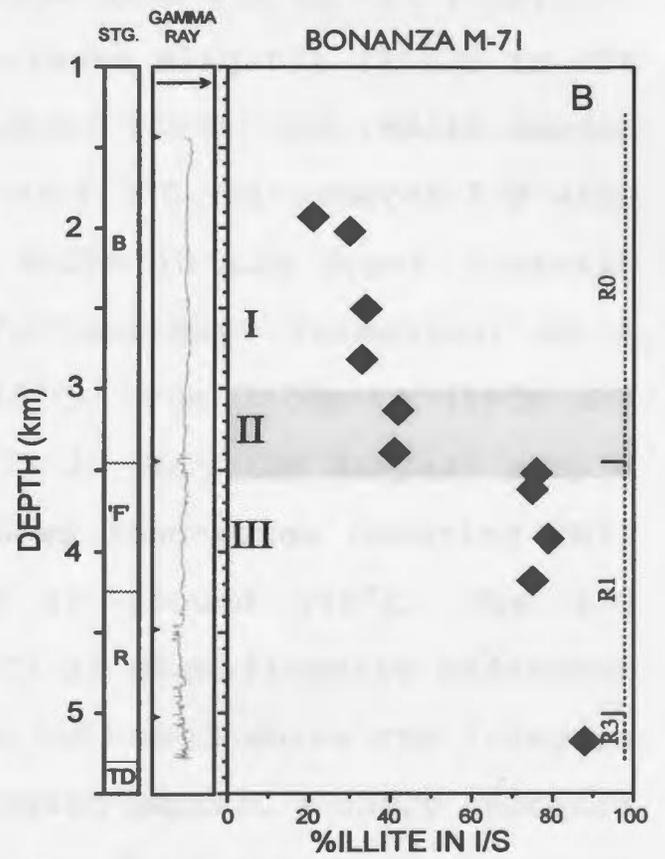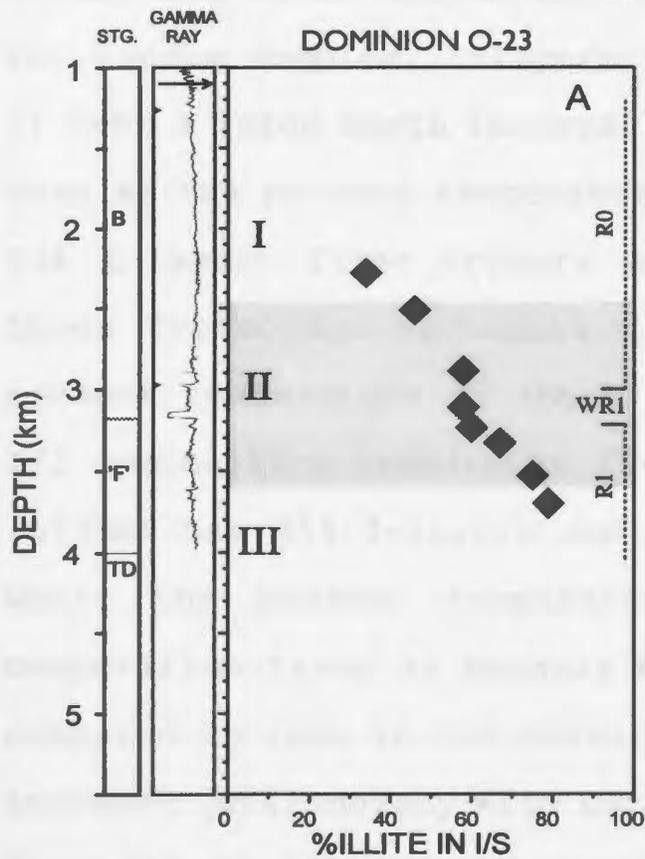
All of the I/S shallower than 3400m (Banquereau Formation) are random and their composition varies from 21% to 41% I-layers. For random samples, I-layers increase slightly (20/30 to 40% I) over a large depth interval (about 1500m) and remain random even at the present temperature of 115°C. R1-ordered I/S with 76% I-layers first appears at 3520m in the Upper Jurassic Lower Cretaceous sediments ('Fortune Bay' Formation) at a present temperature of about 118°C. From 3520m to 4180m the I/S composition remains at 75-77% I. Only the deepest sample (5175m) has 85% I-layers and shows long-range ordering (R3) where the present temperature is around 170°C. The I/S composition trend in Bonanza M-71 is significantly different compared to that in the Dominion O-23 well where the I-layers increase continuously with increasing depths. A sharp increase from 41% to 75% I is observed over a narrow depth interval (130m) across the Base Tertiary Unconformity (see section 3.7.2 and 3.7.3).

3.5.3.3 SOUTH TEMPEST G-88

South Tempest G-88 is located about 22km east of Conquest K-09 at the edge of the Outer Ridge Complex (Fig. 3.2). The well was drilled on a tilted fault block and encountered Upper Jurassic, Lower Cretaceous and Tertiary sediments. Aptian to base Tertiary sediments are missing. The estimated present-day geothermal gradient is 31.6°C/km. Thirteen samples were studied between 1425m and 4370m. I/S is the dominant phase

present in all of the <0.1μm grain-size fractions. Kaolinite and illite are present only in trace amounts. Chlorite was not detected in these samples.

With the exception of a few samples at 2640-2670m, XRD data show a progressive increase of I-layers with increasing burial depths (Fig. 3.6C). The I/S from the Banquereau and the Upper part of the 'Fortune Bay' Formations are randomly interstratified, for which the compositions vary between 15-42% I. R1-ordered I/S with 63% I-layers was first observed at 3085m within the 'Fortune Bay' Formation. The present temperature at this depth is 102°C. Below 3085m, the I-content in I/S increases slowly up to 75% where the present temperature is around 142°C. It is important to note that the random to R1-ordered transition occurs rapidly (a 25% increase in I-layers over 360m interval) within the Upper Jurassic Lower Cretaceous 'Fortune Bay' Formation.

3.5.3.4 NORTH DANA I-43

The North Dana I-43 well is also located on the Outer Ridge Complex (Fig. 3.2). It penetrated to a depth of 5303.6m over a tilted fault-block consisting of Jurassic sediments overlain by Late Cretaceous (Dawson) and Tertiary (Banquereau) sediments. Lower Cretaceous sediments are missing in this area. The structure contains about 470 BCF of natural gas reserves (Taylor et al., 1992). Thirteen clay samples were analyzed from the well which had a similar mineralogy to that

78

of South Mara C-13.

In North Dana I-43, the proportion of I-layers increase from 24% at 1800m to 90% at 5230m (Fig. 3.6D). The I/S composition versus depth profile is not linear and shows significant variation with increasing burial depths. The I/S is random down to 3500m depth (110°C) which includes Tertiary and Upper Cretaceous sediments of the Banquereau and Dawson Formations. The R1-ordered I/S is first encountered at 3720m in the Rankin Formation where the present temperature is around 118°C. Below 4155m, the I-content remains at 85-90% I with R1 or R3-ordering.

The upper part of the well that has random I/S shows a small gradual increase of I-content (24% to 40% I). Between 2465m and 3500m, the composition of random I/S remains around 40-46%. From 3500m to 4155m, the I-content increases rapidly (40% to 90% I) as random I/S changes first into R1-ordered, followed by R3-ordered I/S. Note the occurrence of ordering at greater depths (3720m) in this well compared to that in the Trans-Basinal Fault area (~2650m).

3.5.3.5 SUMMARY

Overall, the I/S profiles of Dominion O-23 and South Tempest G-88 wells look similar and show a progressive increase of I-layers. The random to R1-ordering occurs near 3150m (±100m) at 90°-100°C present temperatures. In Bonanza M-71 and North Dana I-43, R1-ordering occurs at greater depths

79

(3520-3720m) and higher temperatures (118°C) when the Lower Cretaceous or older sediments are encountered. In the latter two wells, the rate of increase of illite layers is very slow through a thick Tertiary section. The I/S versus depth profiles of Dominion O-23 and Bonanza M-71 are significantly different although their stratigraphy and lithology are quite similar. Only a few samples below 4155m depth show R3-ordered I/S.

3.5.4 THE SOUTHERN PART OF THE BASIN (SPB)

The Southern part of the Jeanne d'Arc Basin is uplifted where much of the Lower Cretaceous and older sediments are either missing or comparatively thin (Sinclair, 1988; McAlpine, 1990). Wells in this area intersect the oldest rocks of the basin (Triassic red beds and salt). Three wells from this area were studied (Egret K-36, Egret K-46 and Cormorant N-83) (Fig. 3.2).

3.5.4.1 EGRET WELLS (K-36 AND N-46)

Egret K-36 and N-46 were drilled near a salt structure about 30km south of the Hibernia K-14 well (Fig. 3.2). Above the Hibernia Formation, much of the Lower Cretaceous sediments are missing due to erosion (McAlpine, 1990), and the Upper Cretaceous and Tertiary sediments are relatively thin (~1300m). The present-day geothermal gradient in Egret K-46 is higher (26.9°C/km) than in Egret K-36 (23.7°C/km). Seven

80

samples from Egret K-36 and 4 samples from Egret N-46 were analyzed. Fine-grained clay fractions (<0.1µm) from both wells are rich in I/S with minor kaolinite and illite (<5%). Chlorite was not detected on XRD patterns.

In Egret K-36, fine-grained clay samples from about the 1500m interval indicate a progressive increase of I-layers in I/S with increasing burial depths (Fig. 3.7A). Illite-content increases from 22% at 1625m in the Hibernia Formation to 69% at 2935m in the Rankin Formation. A change from random to R1-ordered I/S occurs at 2420m within the Rankin Formation where the present drill-hole temperature is around 62°C. There is a higher expandability for the clays from the Hibernia and Fortune Bay Formations at relatively shallow burial depths in this well compared to wells further north.

Egret K-46 also shows an increase of I-layers in I/S from 44% to 75% with increasing depth (Fig. 3.7B). Two samples from the Jeanne d'Arc Formation are randomly interstratified (44% and 60% I) and 2 samples from the Rankin Formation show ordered I/S (72% and 75% I). Ordering in Egret N-46 occurs at about 400m shallower than in Egret K-36.

3.5.4.2 CORMORANT N-83

Cormorant N-83, the most southerly well studied for this project, is located about 45km southwest of the Egret wells (Fig. 3.2). The well intersected the Argo, Iroquois and Downing Formations (Early to Middle Jurassic), followed by

81

Figure 3.7: Estimated proportion of illite-layers in illite/smectite versus present burial depth, stratigraphy and γ-ray log for three Southern wells. No γ-ray log data were available from Cormorant N-83. Note relatively shallow depths for R1-ordered illite/smectite compared to other wells. Do=Downing Formation, Ir=Iroquois Formation, Ar=Argo Formation. For remaining abbreviations, see figure 3.3.

Southern Part of the Basin
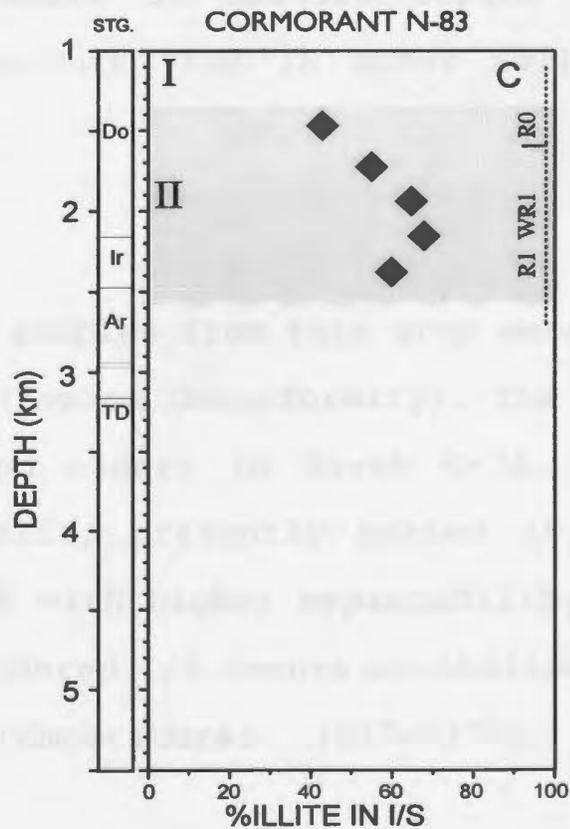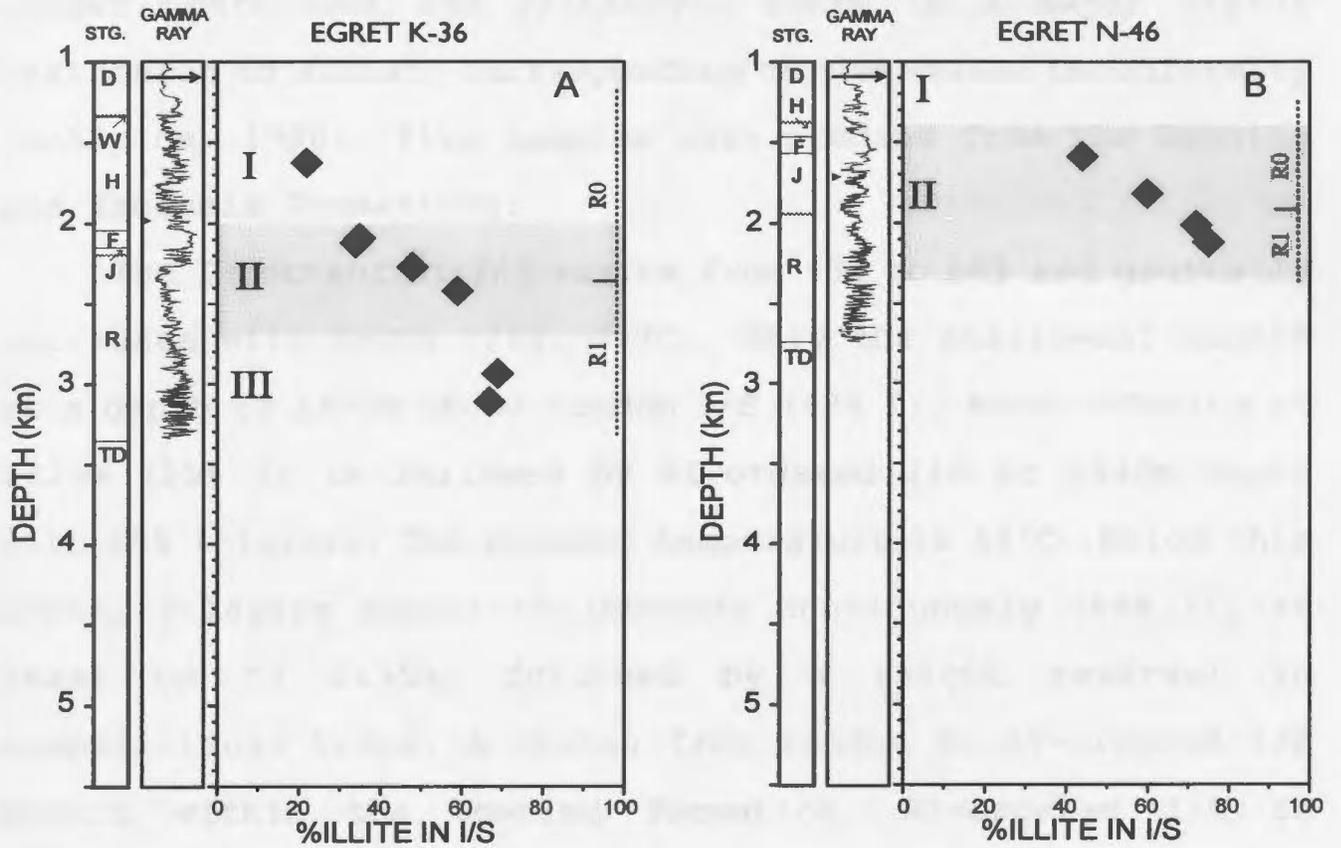
relatively thin (~830m) Dawson and Banquereau Formations (Upper Cretaceous and Tertiary). There is a major hiatus (Bathonian to Albian) corresponding to the Avalon Unconformity (McAlpine, 1990). Five samples were studied from the Downing and Iroquois Formations.

The I-content of I/S varies from 43% to 68% and generally increases with depth (Fig. 3.7C). Only the shallowest sample at a depth of 1470m shows random I/S (43% I). Weak ordering at 1725m (55% I) is followed by R1-ordered I/S at 1940m depth with 65% I-layers. The present temperature is 54°C. Below this depth, I-layers appear to increase continuously (68% I), at least up to 2155m, followed by a slight reversal in compositional trend. A change from random to R1-ordered I/S occurs within the Downing Formation. R1-ordered I/S in Cormorant N-83 occurs at shallow depths and at a lower present-day temperature than in other wells of the Jeanne d'Arc Basin.

3.5.4.3 SUMMARY

All the clay samples from this area were collected below the major hiatus (Avalon Unconformity). The older formations (i.e. Hibernia and older) in Egret K-36, Egret N-46, and Cormorant N-83 wells, presently buried at shallow depths, contain random I/S with higher expandability. The transition of random to R1-ordered I/S occurs at shallower depths (1940-2420m), lower temperatures (54°-62°C), and in older

84

stratigraphic units compared to other areas of the Jeanne d'Arc Basin. Grant and McAlpine (1990) have reported a relatively shallow "oil window" from this area.

3.6 ILLITE/SMECTITE COMPOSITION OF MAIN STRATIGRAPHIC UNITS WITH INCREASING BURIAL DEPTHS

In the previous section, vertical profiles of I/S composition from 16 wells intersecting several stratigraphic units (Oxfordian to Eocene) were summarized. In order to interpret I/S profiles it is important to first establish the original composition of detrital I/S in these sediments. For example, if only ordered I/S with high illite-content had been deposited in the basin, this would lead to a false interpretation if such clays were considered diagenetic in origin. By analyzing clays from cross-sections of individual stratigraphic units buried at different subsurface depths in the basin, detrital illitic material can be distinguished from diagenetic clays. For this purpose, I/S samples from each stratigraphic unit are summarized below (Fig. 3.8).

3.6.1 BANQUEREAU FORMATION

The Banquereau Formation predominantly consists of marine shale/mudstone with minor sandstone, siltstone, silicious mudstone and chalk (McAlpine, 1990). These basin-wide fine-grained sediments were deposited during several transgressive and regressive episodes (Gradstein and Williamson, 1981) and

Figure 3.8: Percent illite-layers in illite/smectite versus depth for individual stratigraphic units. Only limited samples were available from the Ben Nevis Formation which is the lateral coarse-grained equivalent of the Nautilus Formation. These two formations were combined (C). Note smectite-rich (random) illite/smectite at shallow depths for the majority of the formations. The Jeanne d'Arc and Rankin Formations show relatively less change in their illite/smectite composition with depth. Illite/smectite from which few specific formations were sampled are indicated by letters inside the box. A=Archer K-18, B=Beothuk M-05, F=Fortune G-57, G=Gambo N-70, P=Port au Port J-97, V=Voyager J-18, 'Fortune Bay Formation'=undifferentiated Tithonian to Barremian (also see section 2.3).

BANQUEREAU FORMATION

DAWSON FORMATION

NAUTILUS FORMATION
(+ B. NEVIS FORMATION)

AVALON FORMATION

WHITEROSE FORMATION

LEGEND FOR WELLS

TBF
- + S. Mara C-13
- ◇ N. Ben Nevis P-93
- ✳ Nautilus C-92
- ○ Hebron I-13
- ✶ N. Trinity H-71

NPB
- ✕ Adolphus D-50
- ● Conquest K-09
- □ W. F. Foam L-23
- ■ Whiterose J-49

ORC
- ✶ Dominion O-23
- ◆ Bonanza M-71
- ● S. Tempest G-88
- ■ N. Dana I-43

SPB
- ◆ Egret K-36
- ■ Egret N-46

87

HIBERNIA FORMATION

FORTUNE BAY FORMATION (S)

'FORTUNE BAY FORMATION' (N)

JEANNE D'ARC FORMATION

RANKIN FORMATION

LEGEND FOR WELLS

TBF
- ┼ S. Mara C-13
- ◇ N. Ben Nevis P-93
- ✳ Nautilus C-92
- ○ Hebron I-13
- ✶ N. Trinity H-71

NPB
- ✕ Adolphus D-50
- ● Conquest K-09
- □ W. F. Foam L-23
- ■ Whiterose J-49

ORC
- ✶ Dominion O-23
- ◆ Bonanza M-71
- ● S. Tempest G-88
- ■ N. Dana I-43

SPB
- ◆ Egret K-36
- ■ Egret N-46

88

during thermal subsidence of the continental margin following breakup of the Grand Banks from Europe (Kean et al., 1987). Its thickness increases from 450m in the south (Cormorant N-83) to more than 3400m in the north (Bonanza M-71). A total of 63 samples from 13 wells were studied from the 1050m to 3390m depth interval.

The I/S composition of the <0.1μm fraction from the Banquereau Formation varies from 14% to 66%I, with the majority of the samples falling between 30% and 40%I (Fig. 3.8A). With the exception of the Conquest K-09 and Dominion O-23 wells all samples are randomly interstratified, even those at 3400m subsurface depths with present temperatures above 100°C. For the Trans-Basinal Fault area (South Mara C-13, North Ben Nevis P-93, Hebron I-13, Nautilus C-92, North Trinity H-71) the I/S composition of Banquereau Formation generally remains between 20-35% I and does not increase with depth. For these samples, maximum present day temperature remains below 60°C and burial depths <2000m. The Banquereau Formation in the West Flying Foam L-23 well is thicker (2500m) but still does not show an increase in I-content with depth. In the Adolphus D-50 and Whiterose K-09 wells, the I-content of mixed-layer I/S slowly increases from about 25% to 48% but remains random even at a depth of 2580m at about 80°C temperature. In Conquest K-09, the rate of increase of I-layers in I/S is faster than in other wells. In this well, the composition varies from 25% to 66% as random I/S first changes

into weakly-ordered I/S, followed by R1-ordered structure that appears around 2620m (90°C). In the Outer Ridge Complex area (South Tempest G-88, North Dana I-43, and Bonanza M-71), the I-layers increase slowly from about 15-25% to 40-47%. Even at a depth of 3400m and a temperature greater than 110°C, the composition of I/S remains less than 50% I and random. Only in the Dominion O-23 well, does weak-ordering (58% I) occur at the bottom of the Banquereau Formation (3110m and 85°C).

In summary, most samples from the Banquereau Formation above 2000m are highly expandable (<30-35%I). Between 2000-3000m, I-layers increase slightly to about 30-40%. Samples below 3000m usually show more than 40% I-layers. Conquest K-09 and Dominion O-23 wells however, show a somewhat more rapid rate of increase of I-layers.

3.6.2 DAWSON CANYON FORMATION

The Late Cretaceous Dawson Canyon Formation consists mainly of shales and limestones (i.e. Petrel Limestone) with minor siltstone and sandstone. Basinward time-equivalent sediments include chalks and limestones of the Wyandot Member (Grant et al., 1986). These sediments were deposited in shallow shelf seas (Tankard and Welsink, 1987) and are relatively undeformed with a few faults extending into them. The formation becomes thicker (220m to >600m) and deeper (1540m to >3800m) northward in the basin. A total of 20 Dawson Canyon Formation samples were studied from the 1500m to 3500m

90

depth interval in 7 different wells.

The I-content of I/S varies between 15% to 69% and generally increases with increasing depth (Fig. 3.8B). In the Trans-Basinal Fault area, the I-content increases from 15% to 48% and remains random. The deepest sample (2800m) from this area shows a present temperature of about 80°C. In the northern part of the basin (Adolphus D-50 and Conquest K-09), the I-content varies from 49% to 69% and shows random, weakly-ordered and R1-ordered I/S. R1-ordered I/S first occurs at about 105°-110°C present temperature. The formation is missing from much of the Outer Ridge Complex area (Sinclair, 1988).

3.6.3 NAUTILUS AND BEN NEVIS FORMATIONS

The Nautilus and Ben Nevis Formations of Aptian/Albian age are the main units between the Aptian and Cenomanian unconformities/disconformities. The Ben Nevis Formation overlies the Aptian unconformity/disconformity and consists of fine-grained sandstone with minor interbedded shales. The Nautilus Formation is composed mainly of shale/mudstone with minor sandstone/siltstone characteristic of low energy, open-marine shelf environments (McAlpine, 1990). The total thickness (215-587m) and depth (1770m to >3300m) of these formations generally increases northward in the basin. These formations are generally missing from the Outer Ridge Complex area.

Thirty-two samples from 8 wells, ranging from 1830m to

>3300m depths, were analyzed. Three samples from the North Trinity H-71 well represent the sandstone-rich Ben Nevis Formation. The I/S composition of the Nautilus/Ben Nevis Formations varies from 22% to 90% I (Fig. 3.8C). The data suggest considerable scattering having no clear trend with depth. North Trinity H-71 and West Flying Foam L-23 exhibit trends which are common to the other associated wells but are different from the general trend. These wells illustrate the need to recognize geographic differences of well locations in the basin. The remaining 6 wells plot in a relatively narrow zone and show progressive increase of I-layers with increasing burial depths. Above 2500m, I/S is generally random with 20-30% I. From 2500m to 2800m, the I-content increases rapidly to about 70-80%I. Below this depth, the I-content remains more or less the same. The random to R1-ordered transition occurs at or above 80°C. Samples from North Trinity H-71 and West Flying Foam L-23 wells do not follow this trend. Three samples from North Trinity H-71 show higher I-content (69-77%) at relatively shallow depths (1875-2165m). Four samples from West Flying Foam L-23 (2625-3325m) show higher expandability (29-43% I) and fall below the above-mentioned trend.

3.6.4 AVALON FORMATION

The Avalon Formation (Barremian/Early Aptian) is represented by fine to medium-grained coarsening-upward sandstone interbedded with shales. The Formation contains a

92

thin limestone/calcareous sandstone unit which has been used as a seismic-marker ("A"-Marker Member) in much of the basin. The Formation grades into more fine-grained sediments basinward. These sediments were deposited in marine to marginal-marine and lagoonal complex depositional environments (Sinclair, 1993).

For this sand-rich interval, only 4 samples between 2220-3275m depths from three wells (South Mara C-13, North Ben Nevis P-93, North Trinity H-71) were analyzed. I-content varies from 60-80% and shows weakly ordered to R1-ordered I/S (Fig. 3.8D). The present temperature for these samples varies from 64°-95°C. I/S with 80% I-layers is observed at 64°C (2220m) in North Trinity H-71 and at 95°C (3275m) in North Ben Nevis P-93. Although only a few samples were available from this formation, the lower three samples suggest an increase of I-layers with depth.

3.6.5 WHITEROSE FORMATION

The Whiterose Shale (Middle Valanginian to Early Barremian) is sandwiched between the Hibernia and Avalon Formations. This formation contains a thin limestone unit at the base ("B" Marker Member) followed by calcareous sandstone, siltstone, shale and minor limestone of the Catalina Member (Catalina Formation of McAlpine, 1990). The Catalina Member grades laterally and vertically into a shale. These sediments were deposited in marine and marginally-marine environments

(McAlpine, 1990).

Twenty-one samples from 7 wells were studied from this formation. Present burial depths and temperatures for these samples vary from 2250m (59°C) to 4255m (128°C). The I/S composition varies from 19% to 90% I (Fig. 3.8E). One sample at 2250m (Hebron I-13) shows random I/S. The majority of the samples below 2600m show ordered I/S. Due to the lack of sample material between 2250-2675m, the transition from random to ordered I/S is not clear. Most of the ordered I/S samples are from more than 3100m depth and show close to 80% (±5%) I-layers where the present temperature is >95°C. Only 3 samples below 3100m indicate 60-70% I-layers.

3.6.6 HIBERNIA FORMATION

The Hibernia Formation (Berriasian to Valanginian) is one of the main reservoir intervals for hydrocarbons in the Jeanne d'Arc Basin. The lower part of the formation is represented by thick-bedded, medium-to-coarse-grained sandstone interbedded with relatively thin sandstone bodies interbedded with thick shales. The formation passes laterally northward into basinal shale. These sediments were deposited in a prograding deltaic system (Brown et al., 1989). The formation depth increases northward from about 1600m in Egret K-36 to >4400m in the North Ben Nevis P-93 well.

Fifteen samples were analyzed from 12 wells between 1625-4495m depth interval. Mixed-layer I/S composition from the

94

Hibernia Formation varies from 13% to 85% I (Fig. 3.8F). Proportions of I-layers increase with depth. Only two samples above 2000m show random I/S with 13-22% I-layers at <60°C present temperature. All samples below 2500m are ordered I/S. Their composition vary from 62% to 85% I and present temperatures from 72° to 130°C. R3-ordering (ISII-type) occurs below 4200m depth. It is important to note that ordered I/S clays from different wells plot in a relatively narrow zone and show a progressive increase of I-layers at a rate of about 1.0%I/100m (Fig. 3.8F). The random to ordered transition, however, is not clear since no sample material was available between 1845-2530m depth interval.

3.6.7 FORTUNE BAY (SOUTH OF ADOLPHUS D-50)

South of the Adolphus D-50 well, the Fortune Bay of Late Tithonian to Early Berriasian age (Sinclair, 1988) occurs between the Hibernia and Jeanne d'Arc Formations. It consists predominantly of shales with minor siltstone and sandstone. These sediments were deposited in marginal marine to shallow neritic depositional environments during a transgressive event (Sinclair, 1988 and McAlpine, 1990).

Ten samples from 7 wells between 2090-4740m depth interval were studied from this unit. Mixed-layer I/S compositions vary from 33% to 86% I as their layer ordering evolves from random (R0) to weakly-ordered, R1-ordered and R3-ordered I/S with increasing burial depths (Fig. 3.8G1). Shallow samples above

95

2200m from three different wells show random I/S with higher expandability (33-36% I). The present temperature for these samples is <60°C. No sample material was available between 2120-3630m. Weakly-ordered I/S at 3600-3700m contains 60% I-layers at about 100°C. Samples below 4500m show ordered I/S (R1 or R3-ordered) with higher I-content (>68%) and above 137°C present temperatures. Although the deeper samples of this formation show somewhat less I-content, overall the I-layers in I/S show a progressive increase with increasing burial depths.

3.6.8 'FORTUNE BAY' (UNDIFFERENTIATED, TITHONIAN TO BARREMIAN)

North of the Adolphus D-50 well, the term 'Fortune Bay' represents undifferentiated shale-rich sediments ranging in age from Tithonian to Barremian. Stratigraphically, these sediments are distal equivalents of several sandstone-rich southern formations (south of Adolphus D-50) from the Jeanne d'Arc to Avalon Formations (Sinclair, 1988). These undifferentiated sediments, equivalents of Hibernia to Eastern Shales Formations in this area, are called Whiterose Shale by McAlpine (1990). This stratigraphic unit is relatively thin (<800m) on the northern part of the Outer Ridge Complex and is missing from the North Dana I-43 well.

Fourteen samples from 4 wells (Conquest K-09, Dominion I-23, Bonanza M-71, South Tempest G-88) between 2725-4950m depth

96

interval were analyzed. The I/S composition ranges from 38% to 92% I (Fig. 3.8G2). Only one sample at 2725m (South Tempest G-88) shows random I/S (38%I). All remaining samples are presently buried below 3000m showing R1 or R3-ordered I/S. Between 3000-4000m, I-layers in I/S increases with depth from about 60% to 79% and the ordering remains predominantly R1. The present temperature for this interval in these wells increases from 90°C to about 130°C. Below 4000m, R3-ordered is the most common I/S for which I-layers vary from 88-90% with 136°C to 170°C present temperature. Overall, the I-layers in I/S from 2725 to 4000m increases with increasing burial depths. Below this, the I-content remains between 88-92%.

3.6.9 JEANNE D'ARC FORMATION

The Jeanne d'Arc Formation consists mainly of sandstones, shales and minor conglomerates along the basin margin and grades into fine-grain sediments basinward. These sediments were deposited in a sandy fan-delta complex along the basin margin while basinal facies were deposited in a weak marine environments (Tankard and Welsink, 1988; McAlpine, 1990). The formation is either missing (Sinclair, 1988) or is difficult to differentiate (McAlpine, 1990) over much of the northern Outer Ridge Complex area.

Seven samples were available from the Jeanne d'Arc Formation. The I-content for these samples varies from 44% to 70% (Fig. 3.8H). However, most of the samples show 60-70% I.

97

Above 2000m, two samples show random I/S with 48-60% I-layers at present-day temperatures of <60°C. No sample was available between the 1820m and 4185m depth interval. Below 4100m, I/S generally shows R1-ordered I/S with 60-70% I-content where the present temperature is above 100°C (105°-148°C). The majority of the samples from other stratigraphic units (Hibernia and Whiterose Formations) presently buried below 4000m show higher I-content (75-90% I) compared to the Jeanne d'Arc Formation buried at equivalent depths.

3.6.10 RANKIN FORMATION

The Rankin Formation (Oxfordian-Kimmeridgian) shows variable lithology across the basin. Thick massive limestones with interbedded shales and sandstones are predominant in the southern part of the basin. Toward the basin centre and on the Outer Ridge Complex, the formation consists mainly of shales with minor sandstones and limestones (Sinclair, 1988; McAlpine, 1990). Organic-matter rich calcareous shale (Egret Member) represents the upper part of the formation.

Twenty-eight samples of the Rankin Formation from 12 wells were analyzed. Out of these, 11 samples came from wells located near the basin margin and in the Southern part of the basin from which only specific stratigraphic units were sampled. The remaining samples came from the Outer Ridge Complex area and the Egret wells. Present depths and temperatures of these samples range from 1865-5230m and 52°-

165°C respectively.

The I-content of the Rankin Formation varies from 48% to 90% (Fig. 3.8I). The shallowest sample above 2000m shows a random I/S with 58% I. Within the 2000-2415m interval both random and R1-ordered I/S are encountered where the present temperature remains below 70°C. Random I/S in this interval contains a higher I-content (48-60% I) than the I/S of the Banquereau and Dawson Formations at comparable depths. Two samples from Egret N-46 with relatively higher I-content (72-75% I) were sampled above a salt dome. Between 2415m and 4000m, the I-content remains between 60-75%. Below 4000m, the majority of samples contain close to 80% or higher I-content at greater than 120°C present temperature. Few samples in this zone show R3-ordered I/S. With the exception of four samples from Egret N-46 and Fortune G-57 wells, there seems to be an overall increase of I-layers from approximately 50-60% to more than 80% with increasing burial depth, although the I/S composition remains near 70% for a considerable depth interval (2500-4000m).

3.6.11 SUMMARY OF INDIVIDUAL STRATIGRAPHIC UNITS

The Banquereau, Dawson Canyon, Hibernia, and Fortune Bay Formations show a clear increase of I-layers in I/S with increasing burial depths, although the rate of increase of I-layers decreases once the ordering is achieved in the I/S layers (Fig. 3.8). The Whiterose and Avalon Formations also

show a transition of random or weakly-ordered I/S into R1 or R3-ordered I/S with depth.

The increase of I-layers with depth in the Jeanne d'Arc and Rankin Formations is relatively small, partly because samples from shallow depths contain higher I-layers. Some of these shallow samples are from wells located close to salt structures, and as a result may have been subjected to higher temperatures.

Nautilus and Ben Nevis Formations show the most scattered values of I/S composition, reflecting different geographic positions of wells within the basin. For example, samples from the West Flying Foam L-23 well (western margin) show the lowest I-layers compared to the North Trinity H-71 well (eastern margin) having the highest values. The remaining samples from the Nautilus Formation show a fairly clear trend of increasing I-layers with depth. Some of the scattering in the data may be the result of variable lithology and differing geothermal gradients (also see Chapter VI).

3.7 DISCUSSION AND INTERPRETATION OF ILLITE/SMECTITE DATA

Interpretation of downhole I/S compositional profiles must consider factors such as (1) the availability of smectite-rich clays, (2) uplift and erosion of sediments, (3) contamination by caving, (4) burial diagenesis, and/or (5) combination of the above factors. Each of these factors are discussed below.

Mixed-layer I/S clays from 218 argillaceous samples

representing different parts of the Jeanne d'Arc Basin have been described in this chapter. The results show that clay mineralogies (<0.1μm) consist dominantly of mixed-layer I/S with small amounts of kaolinite and illite. Chlorite is rarely present. The proportion of I-layers and the degree of ordering in I/S generally increases with increasing burial depths in all the wells studied.

3.7.1 THE AVAILABILITY OF SMECTITE-RICH CLAYS

In order to evaluate the role of burial diagenesis on clay minerals in a sedimentary section, it is important to establish that smectite and/or smectite-rich random I/S were originally present during deposition, and prior to deep burial.

The Rankin to Avalon Formations presently buried at shallow depths (≤2000m) in the south and towards the basin margins are smectite-rich random I/S. For example the Hibernia Formation, in the Voyager J-18 and Egret K-36 wells, contains <22% illite-layers. The Fortune Formation in the Port au Port J-97, Gambo N-70, and Egret K-36 wells, contains <36% illite-layers. The Jeanne d'Arc Formation in the Egret N-46 contains <44% illite-layers. Similarly the Rankin Formation in the Port au Port J-97, Gambo N-70, and Egret K-36 wells contains random I/S with <50% illite-layers. The Nautilus Formation in the Hebron I-13 and the West Flying Foam L-23 wells is smectite-rich and randomly ordered. The upper part of the Whiterose

Formation in the Hebron I-13 well is also highly expandable. In the Cormorant N-83 (the most southern) well, even the Middle Jurassic sediments contain random I/S (43% I). The consistently low content of I-layers in all of the wells suggests that the ordered I/S in the deeply buried rift and transitional sediments (i.e. South Mara C-13) were not illite-rich or ordered at the time of deposition and that smectite-rich clays were available from the source area during sedimentation.

The regions of the Grand Banks and the eastern part of the island of Newfoundland (Avalon Zone) most likely provided much of the clastic sediments in the Jeanne d'Arc Basin. The Grand Banks are the offshore extension of the Avalon Zone which consists mainly of Precambrian felsic and mafic volcanics, marine and non-marine volcaniclastics and feldspathic sandstone overlain partly by early to mid-Paleozoic marine and terrestrial sediments locally rich in feldspar and mica (Haworth and Lefort, 1979; O'Brien et al., 1983; King et al., 1986; and King, 1990).

Chemical weathering of these volcanic-rich rocks could have provided smectite and/or random I/S in the rift sediments of the Jeanne d'Arc Basin. In addition, volcanic activity in the Southern part of the Grand Banks during Early Cretaceous time (Sinclair, 1988) may have provided additional smectite-rich clays into the basin. Formation of smectite is favoured by low-relief and warm climate with seasonal humidity (Weaver,

1989). During the Upper Jurassic and Early Cretaceous times, the Grand Banks were closer to the equator (~35° latitude) and would have experienced warmer climate compared to the present temperatures (Chamley, 1979; Kanasewich et al., 1981).

Deep burial of Precambrian and Paleozoic sedimentary rocks of the Grand Banks prior to erosion would have subjected them to extensive illitization. However, it can be expected that smectite-rich clays would have resulted also from chemical weathering of mica, illite, feldspar, and other minerals (Weaver, 1989). For example, Loughnan et al. (1962) described weathering of illite into smectite in Triassic shales of New South Wales. Similarly, Droste et al. (1960) reported the weathering of illite and chlorite into smectite in till and loess deposits of the State of Indiana. McKeague and Brydon (1970) also reported the formation of smectite in soils developed over illite and chlorite rich Paleozoic rocks in the Atlantic provinces of Canada.

Consideration of the preceding basin-wide I/S data and regional geology of the area leads to the conclusion that smectite and/or smectite-rich I/S clays were deposited throughout the sedimentary section studied.

3.7.2 CAVING AND MIXING

Contamination of deeper drill-cuttings by caving of shallow sediments can potentially affect I/S-depth profiles by mixing of diagenetically less evolved I/S into the deeper

103

samples. Once casing has been positioned down to a given depth, caving can no longer occur from shallow depths.

A comparison of casing depths (indicated on figures 3.3 to 3.7, also see Appendix II) with I/S profiles indicates that mixing due to caving is not the cause of the observed trends of I/S in the Jeanne d'Arc Basin, nor has it caused a significant effect on the I/S depth profiles. With the exception of Bonanza M-71, all I/S trends are independent of casing depths. For instance, in several wells (Adolphus D-50, Conquest K-09, Dominion O-23, North Ben Nevis P-93, West Flying Foam L-23, South Tempest G-88 and North Dana I-43), I/S trends are continuous across the casing depths. No abrupt change in I/S composition was noted below the casing depths in the above-mentioned wells. In other wells (South Tempest G-88 and North Dana I-43) random to ordered I/S transition occurs below the casing depths where shallow smectite-rich I/S could not have mixed with deeper cuttings. In Hebron I-13 and North Trinity H-71 wells, a rapid increase in I/S composition with depth occurs above the casing depths instead of below it. Furthermore, in several wells both weakly ordered and R1-ordered I/S first appears above the casing depths (South Mara C-13, North Ben Nevis P-93). Thus, contamination and mixing due to caving has no significant effect on I/S profiles or the depths where the ordering in I/S is first observed.

In Bonanza M-71, a significant increase (35%I) in I-layers occurs abruptly across the casing depth (3455m, Fig. 3.6B).

Ordered I/S first appears just below the casing depth (3520m).
An unconformity is reported by Canada-Newfoundland Offshore
Petroleum Board (1988) at about the same depth (3460m). In
view of all other wells, caving of smectite-rich shallow
sediments up to the casing depth is considered less likely an
explanation for this abrupt increase of I-layers in Bonanza M-
71. In this well, the unconformity coincides with the break
and may account for the abrupt increase in I-layers.

3.7.3 UPLIFT AND EROSION OF SEDIMENTS

Uplift and erosion of significant amounts of sedimentary
section can also affect I/S well-profiles. For example, uplift
and erosion of sediments followed by renewed subsidence and
deposition of younger sediments may give an abrupt change in
the I/S composition.

North of Egret K-36, the main part of the basin contains
the most complete sediment record (see section 2.4). Hiatuses
along several unconformities (Kimmeridgian, Aptian,
Cenomanian) are small (McAlpine, 1990; Sinclair, 1988;
Driscoll et al., 1995). This part of the basin has experienced
a more or less continuous subsidence at a variable rate since
the Triassic/Jurassic times (Williamson, 1992; Brown et al.,
1989). Minor uplift and erosion is associated with tilted
fault blocks during rifting and relative changes of sea level.
Vitrinite reflectance trends in several wells (see Chapter IV)
lack offset, thereby suggesting that large amounts of uplift

and erosion probably did not occur. Thus, uplift and erosion are not considered to have had significant impact on I/S profiles in the main part (Trans-Basinal Fault and Northern areas) of the Jeanne d'Arc Basin.

Large amounts of uplift and erosion in the south and over the Outer Ridge Complex may have occurred. In the Southern part of the basin (Spoonbill C-30, Cormorant N-83, Egret K-36 and Egret N-46 wells), much of the Lower Cretaceous and Jurassic sediments are missing. In the northern Outer Ridge Complex area (Bonanza M-71, Dominion O-23, and South Tempest G-88), the late Early Cretaceous and Late Cretaceous record is missing (Sinclair, 1988, McAlpine, 1990). An abrupt increase in I-layers in the Bonanza M-71 well across the unconformity (~3460m) may suggest a large amount of erosion prior to the deposition of Tertiary sediments although the vitrinite reflectance data do not support large amount of erosion (see sections 4.4.3.2 and 6.7.3).

In Egret K-36, Egret N-46 and Cormorant N-83 wells, no samples above the major hiatuses (Avalon unconformity) are available. The occurrence of R1-ordered I/S at relatively shallow depths in Egret N-46 (2015m) and Cormorant N-83 (1940m) wells may indicate 500m to 1500m uplift and erosion of sediments. This rough estimate is based, assuming no change in the geothermal gradient, on the range of depths where R-1 ordered I/S first appears in most of the wells in the Jeanne d'Arc Basin (also see Chapter VI).

In summary, the main part of the basin has not experienced a large amount of uplift and erosion. Uplift and erosion in the basin flank area may be a significant factor which affected the well-profiles of I/S (i.e. in Egret N-46 and Cormorant N-83 and in the Bonanza M-71 wells).

3.7.4 BURIAL DIAGENESIS

The above discussion indicates that smectite and/or smectite-rich I/S along with other clays were deposited throughout the sedimentary section in the Jeanne d'Arc Basin. At present, however, smectite-rich I/S clays occur only in shallow samples, irrespective of their geologic age. The proportion of I-layers, as well as their ordering, generally increases with increasing burial depths. The random to R1-ordered transition first appears in different stratigraphic units ranging from the Rankin to the Banquereau Formations and crosses several stratigraphic boundaries (Fig. 3.9 and 3.10). In addition, illite-layering within individual stratigraphic units increases with depth and changes from random to R1-ordered I/S or R3-ordered I/S. Some scattering is present due to different geographic locations of the wells and samples (i.e. Nautilus Formation). All of these observations clearly indicate that smectite-rich I/S clays have been illitized due to an increase in the degree of burial diagenesis with increasing depths and temperatures within the Jeanne d'Arc Basin. Burst (1969) first observed similar changes in the U.S.

107
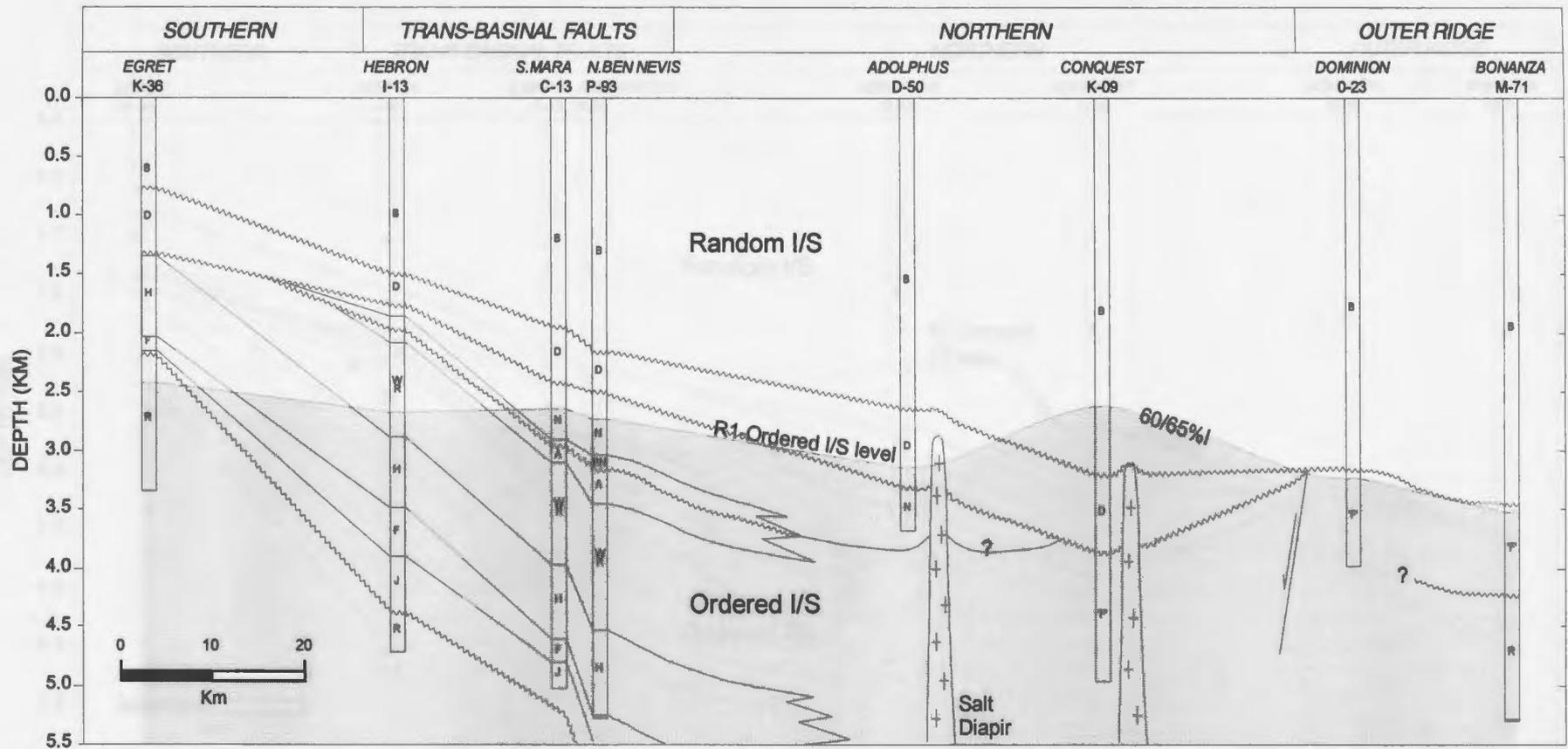
Figure 3.9. Depths where R1-ordered I/S is first observed in several wells are plotted on a cross-section which passes roughly through the basin axis. The R1-ordering level crosses several stratigraphic boundaries representing different geologic ages. Stratigraphy from C-NOPB (1988).
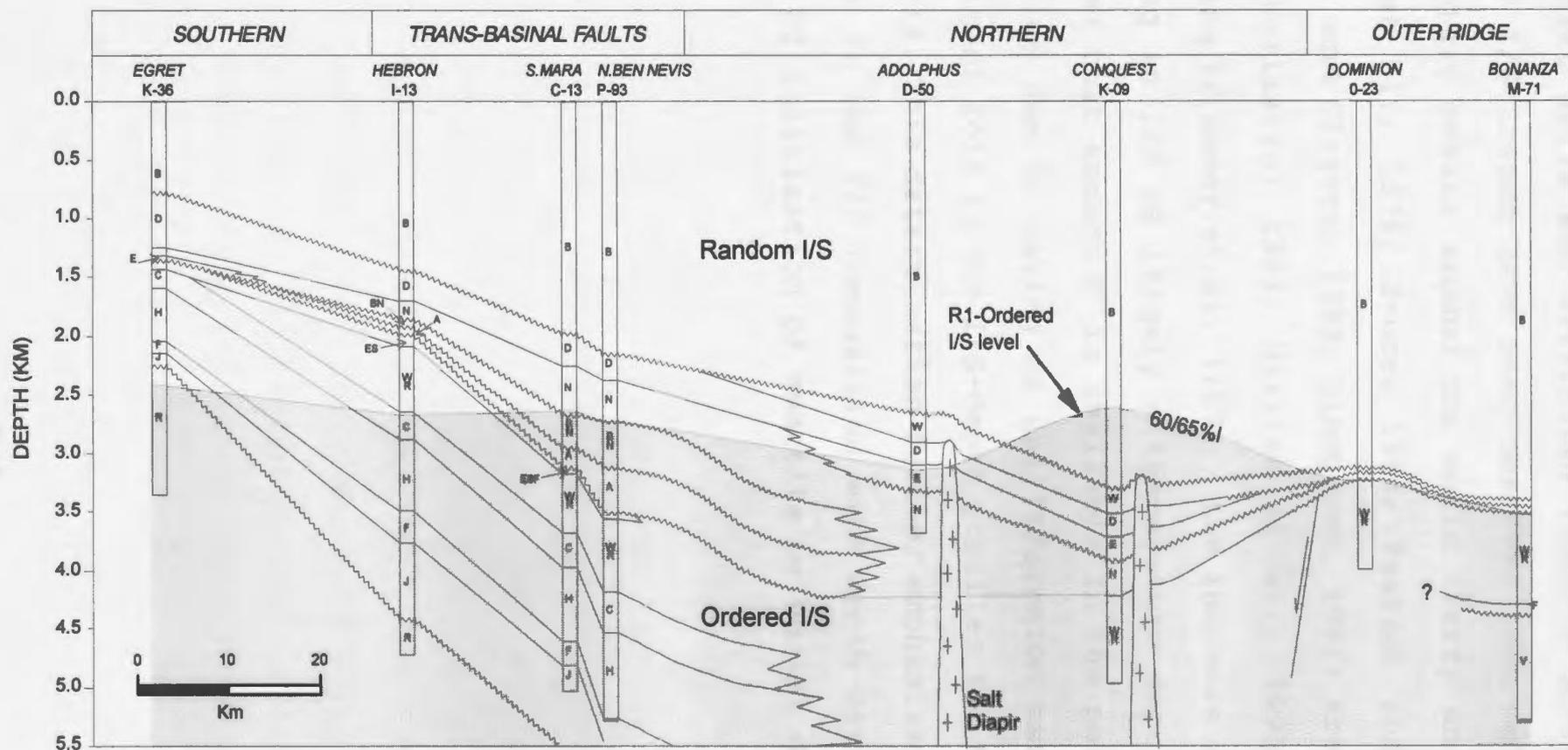
Figure 3.10. Depths where R1-ordered I/S is first observed in several wells are plotted on a cross-section which passes roughly through the basin axis. The R1-ordering level crosses several stratigraphic boundaries representing different geologic ages. Stratigraphy from McAlpine (1990).

Gulf Coast wells and attributed them to burial diagenesis. Similar I/S trends have been observed from wells in several sedimentary basins around the world (Perry and Hower, 1970; Hower et al., 1976; Bruce, 1984; Pearson and Small, 1988; Hillier and Clayton, 1989; Lindgreen, 1991; Arostegui et al., 1991; Pollastro, 1993; Hillier et al., 1995 and others). According to Hower et al. (1976), the increase of I-layers and ordering in I/S is largely a temperature dependent reaction provided that enough K^+ is available in the pore-fluid.

Mixing due to caving or uplift/erosion has not played a significant role in the I/S-depth profiles for the majority of the wells. This determination further emphasizes the fact that changes in the I/S composition with depth are primarily the result of illitization of smectite or burial diagenesis.

CHAPTER IV

COMPARISON OF MIXED-LAYER ILLITE/SMECTITE COMPOSITION AND ORDERING WITH THE MATURITY OF ORGANIC-MATTER

4.1 INTRODUCTION

The temperature dependence of I/S composition prompted several workers to use the mixed-layer I/S as a "geothermometer" in several sedimentary basins (Hoffman and Hower, 1979; Pollastro, 1993 and others). The percentage of light reflected from vitrinite is a widely accepted indicator to study the thermal maturation of sedimentary rocks. However only a few studies have attempted to correlate vitrinite reflectance data with I/S composition at shallow to intermediate levels of burial diagenesis (Pearson et al., 1983; Hillier et al., 1995; Pearson and Small, 1988).

The objective of this chapter is to document the correlation of I/S composition with vitrinite reflectance in order to evaluate the utility of I/S as an indicator of diagenetic grade in the Jeanne d'Arc Basin. This correlation will provide the first data on I/S "geothermometry" in the Jeanne d'Arc Basin. These data may be useful in other Canadian east coast frontier-basins where vitrinite reflectance or other organic-maturity indicators may not be available.

4.2 VITRINITE REFLECTANCE

Organic matter in sedimentary rock consists mainly of kerogen (insoluble) with minor amounts of bitumen (soluble in organic solvents). The kerogen (high molecular weight) is made up of three major organic constituents: (1) vitrinite/huminite (woody tissue, bark, and stem derived from higher plants), (2) liptinite (plant and animal lipid) and (3) inertinite (oxidized vitrinite or liptinite) (Tissot and Welte, 1978). With increasing temperature in a subsiding sedimentary basin, the organic particles of kerogen progressively lose their oxygen, hydrogen, water and other volatile components. By this process, the larger organic molecules of kerogen are thermally cracked into smaller molecules (hydrocarbon generation) and as a result the remaining kerogen becomes progressively poorer in oxygen and hydrogen, richer in carbon, darker in colour, and more dense. The amount of light reflected from kerogen particles increases with the increase of density and carbon content (Teichmüller, 1987). Specifically, in the case of vitrinite particles the amount of light reflected demonstrates a linear relationship to increasing thermal maturity. Liptinite and inertinite lack such a relationship (Smith and Cook, 1980). Therefore, vitrinite is the organic matter most widely used to evaluate the thermal history of sedimentary basins (Hood et al., 1975; Dow, 1977; Bostick et al., 1978; Teichmüller, 1979).

112

4.3 NATURE AND SOURCE OF THE VITRINITE REFLECTANCE DATA

Vitrinite reflectance data on more than 300 samples from 13 wells (out of 16 wells studied for I/S) are available in the public domain from the industry well files archived at the Canada-Newfoundland Offshore Petroleum Board, St. John's, Newfoundland and from the Geological Survey of Canada, Halifax. For 10 wells, the samples were analyzed by Geochemical Laboratories in Calgary between 1981 and 1986. For three wells (Hebron I-13, Dominion O-23, Egret N-46), the samples were analyzed by Avery (1985, 1993) and Harrison (1984) at the Geological Survey of Canada. The vitrinite reflectance analyses were performed on randomly dispersed polished organic-matter using conventional microscopic methods. For the majority of the samples, 10-30 measurements were made on each sample. Samples with fewer measurements generally fall within the main vitrinite reflectance trends. Mean random vitrinite reflectance values ($\%R_o$) were calculated after excluding the reworked and caved population. For more than 90% of the samples, the vitrinite reflectance measurements have <0.25% range in R_o values and a standard deviation of <0.1. For the majority of the wells, samples were collected at a 100-150m depth interval (average 37 samples per well). For Whiterose J-49, Conquest K-09, Adolphus D-50, and North Ben Nevis P-93, an average of 11 samples per well were available (300m to 500m depth intervals). This large amount of

113

data provides an adequate sampling for assessing the present thermal maturity in these wells.

4.4 COMPARISON OF ILLITE/SMECTITE COMPOSITION AND VITRINITE REFLECTANCE TRENDS

Thirteen wells are divided into 4 groups representing different parts of the Jeanne d'Arc Basin, as outlined in the previous chapter. They include: 1) Trans Basinal Fault area, 2) Northern part of the basin, 3) Outer Ridge Complex area, and 4) Southern part of the basin. Mean $\%R_o$ values (percent reflectance in oil) are plotted on a logarithmic scale and burial depths on linear scales. Vitrinite reflectance is plotted on a log scale because commonly there is a linear relationship between log vitrinite reflectance and burial depths or temperatures. A least squares best-fit line calculated through R_o values gives the maturation gradient for each well (Table 4.1). The level of maturity (vitrinite reflectance value) at any given depth is taken from the best-fit line (Dow, 1977).

4.4.1 THE TRANS-BASINAL FAULT AREA

Vitrinite reflectance data from 4 wells (South Mara C-13, North Ben Nevis P-93, Nautilus C-92, and Hebron I-13) located in this area are compared with the mixed-layer I/S trends (Fig. 4.1 and 4.2). The mean vitrinite reflectance ($\%R_o$)

114

values in these wells increase from 0.25% in the Tertiary (Banquereau Formation) to about 1.0% in the Upper Jurassic sediments due to increasing burial depths and temperatures. The average thermal maturation gradient for these wells is 0.107 log %R_o/km and does not show a significant variation (0.128-0.08 log %R_o/km). A majority of the data fit along a linear regression line with a high correlation coefficient (>0.80).

4.4.1.1 SOUTH MARA C-13: In the South Mara C-13 well, ordered I/S first appears at 0.59% R_o in the Nautilus Formation (2640m). A rapid increase of illite-layers (I-layers) in I/S (~30-75%) occurs between 2500-3000m depth interval where vitrinite reflectance value increases from 0.57% to 0.63% (Fig. 4.1A). Between 3000-4500m interval, vitrinite reflectance continues to increase from 0.63% to 0.83% R_o, however, I-layers in I/S for a majority of the samples remain between 75-85%. Below 4500m, reflectance continues to increase from 0.83% to 0.91%, but I/S shows a small reversal (65-75%) corresponding mainly to the Fortune Bay Formation.

4.4.1.2 NORTH BEN NEVIS P-13: In North Ben Nevis P-93, R1-ordering in I/S occurs in the Nautilus Formation close to 0.47% R_o (2730m) (Fig. 4.1B). Above 2500m, thermally immature

115

Figure 4.1. Comparison of mean vitrinite reflectance and I/S composition (%I-layers) profiles plotted with respect to burial depths for South Mara C-13 (A) and North Ben Nevis P-93 (B) wells. The stratigraphic units with gamma-ray logs are indicated on the left-side (for abbreviations see Fig. 3.3). Calculated geothermal gradients are shown in the upper right corner (see Table 1.1).

sediments ($\%R_o$ < 0.47) contain only random I/S (<40% I). A rapid increase in I-layers in I/S (40% to 90%) corresponds with 0.45% to 0.52% R_o values. Below 3000m, R_o increase up to 1.0%, but I-layers content remains between 80-90%I. Long-range ordering (R3) appears at 0.72% R_o values (4125m).

4.4.1.3 NAUTILUS C-92: In Nautilus C-92, ordered I/S first occurs at 0.53%R_o (3030m) (Fig. 4.2A). Vitrinite reflectance values between 2500-3250m increase from 0.46% to 0.55% where I-layers in I/S increase rapidly (40-80%). Below 3250m, R_o increases up to about 0.9%, but %I remains near 85%I. Long range ordering (R3) occurs at 4245m depth where R_o is 0.73%.

4.4.1.4 HEBRON I-13: R1-ordered I/S in the Hebron I-13 well was first observed at 2675m depth, just above the Catalina Member of the Whiterose Formation where the maturity data indicate 0.52% R_o (Fig. 4.2B). The thermally immature section above the 2675m depth contains only random I/S. I-layers in I/S show a rapid increase from 20% to 80% over a narrow depth interval (~500m) where no I/S sample was available. A normal fault intersects the well at about the same depth where R1-ordered I/S is first observed (Gibbons, 1990) The vitrinite reflectance values indicate no obvious dislocation in the profile possibly suggesting only a minor

117

TRANS-BASINAL FAULT AREA
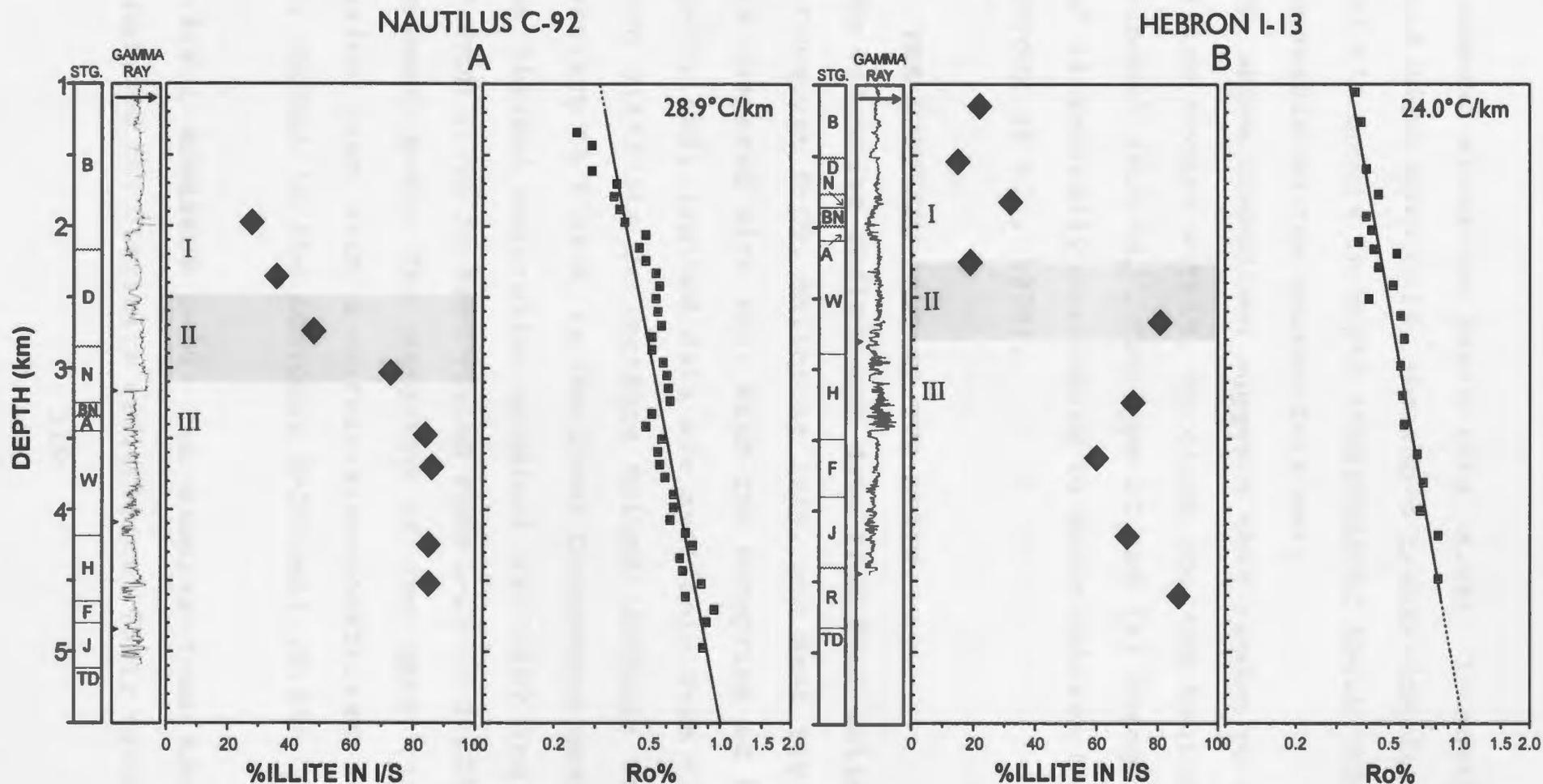
Figure 4.2. Comparison of mean vitrinite reflectance and I/S composition (%I-layers) profiles plotted with respect to burial depths for Nautilus C-92 (A) and Hebron I-13 (B) wells. The stratigraphic units with gamma-ray logs are indicated on the left-side (for abbreviations see Fig. 3.3). Calculated geothermal gradients are shown in the upper right corner (see Table 1.1)

118

displacement along the fault (Fig. 4.2B). In North Ben Nevis P-93 and South Mara C-13, the rapid transition from random to ordered I/S occurs in depth intervals of about 500-600m which is comparable to the Hebron I-13 well.

The above comparison suggests that random to ordered I/S transition occurs within, or close to, the beginning of the "oil window" (0.5 %R_o). For type II and III kerogen, the "oil window" is generally considered to occur between 0.5% and 1.35 %R_o (Héroux et al., 1979).

4.4.2 THE NORTHERN PART OF THE BASIN

The vitrinite reflectance data from four wells (Adolphus D-50, Conquest K-09, Whiterose J-49, and West Flying Foam L-23) are compared with I/S. With the exception of West Flying Foam L-23, only limited data are available from these wells. The mean vitrinite reflectance values increase from 0.34 in the Tertiary to 1.8% R_o in the Lower Cretaceous sediments. The average thermal maturation gradient is 0.152 log %R_o/km and varies from 0.099 in West Flying Foam L-23 to 0.224 log %R_o/km in Conquest K-09. The majority of the data fit a linear regression line with a correlation-coefficient of 0.90 or better, except in the Adolphus D-50 well (0.67).

4.4.2.1 ADOLPHUS D-50: Ten samples from Adolphus D-50 were analyzed for vitrinite reflectance. Their values increase

119

with depth from 0.46% to 0.83% R_o (Fig. 4.3A). Down to 2300m depth, sediments are thermally immature (<0.5% R_o) and the I-layer content in I/S remains below 40%. I-layer content increases slightly but ordering remains random as sediments enter the "oil window". Weakly-ordered I/S appears only between 2665-3035m where the R_o values range from 0.56% to 0.64% and R1-ordered I/S first appears at 0.66% R_o (3135m). Down to the bottom of the drill-hole (3660m), I-layers increase to 76% at 0.78% R_o. It is important to note that both weakly-ordered and R1-ordered I/S first appear in the Dawson Canyon Formation which supports a diagenetic origin for these clays. Below the Cenomanian unconformity (3321m), a small "jump" in the R_o values cannot be evaluated due to limited data. However, I/S data across the unconformity show no significant change.

4.4.2.2 CONQUEST K-09: In Conquest K-09, 8 samples (3820-4962m) for vitrinite reflectance give a regression line with a high correlation coefficient (0.91). However, the line may change in slope as more data become available, particularly from the shallow depths. The present data show one of the highest thermal maturity gradients in this basin (0.224 log %R_o/km).

Above 2400m, in the thermally immature section (<0.5% R_o), the proportion of I-layers increases slightly (25% to 45%) but
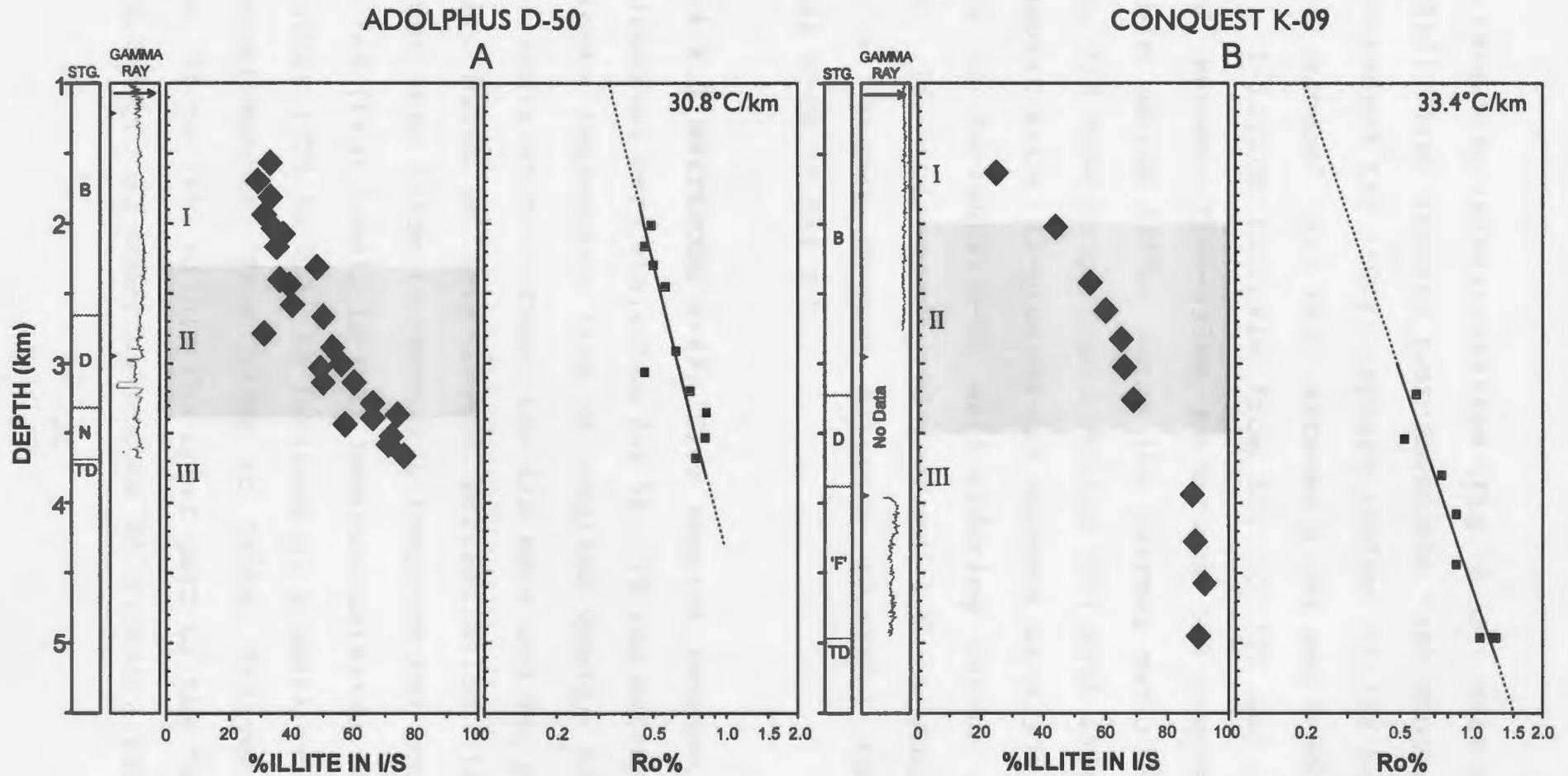
Figure 4.3. Comparison of mean vitrinite reflectance and I/S composition (%I-layers) profiles plotted with respect to burial depths for Adolphus D-50 (A) and Conquest K-09 (B) wells. The stratigraphic units with gamma-ray logs are indicated on the left-side (for abbreviations see Fig. 3.3). Calculated geothermal gradients are shown in the upper right corner (see Table 1.1).

remain random by interstratified (Fig. 4.3B). Weak-ordering in I/S (55%I) first appears just above the "oil window" at 2420m and R1-ordered I/S (60%I) appears (2620m) at the beginning of the "oil window" (0.5 %R_o). Between 0.50% and 0.69 %R_o (2620-3260m), I-layers increase from 60% to 70% and remain R1-ordered. Between 3260-3935m, no data on I/S composition were available. Below 3935m, where the thermal maturity is above 0.95%R_o, I/S show long-range ordering (R3) with ≥85% I-layers. In Conquest K-09, R1-ordered I/S appears at 0.50% R_o (2620m) whereas in Adolphus D-50 weak-ordering begins at 0.58%R_o (2665m). In other words, R1-ordered I/S in Adolphus D-50 occurs at higher thermal maturity (0.66%R_o) than in the Conquest K-09 (0.50% R_o).

4.4.2.3 WHITEROSE J-49: Five samples between the 3700-4550m interval were available for %R_o. If the extrapolation of the linear regression line to shallow depths is valid, a general correlation between the I/S data and %R_o profile can be made. Based on this linear extrapolation, the section shallower than 2355m is thermally immature and contains only random I/S (Fig. 4.4A). In this immature interval, an increase in I-layers (25% to 45%) is followed by a small reversal near the Petrel Member. From 2355m to 2655m, I-layers increase rapidly (34 to 74%) within the upper part of the "oil window" (0.50-0.60%R_o). R1-ordering occurs at 0.56%R_o. For the 300m

122
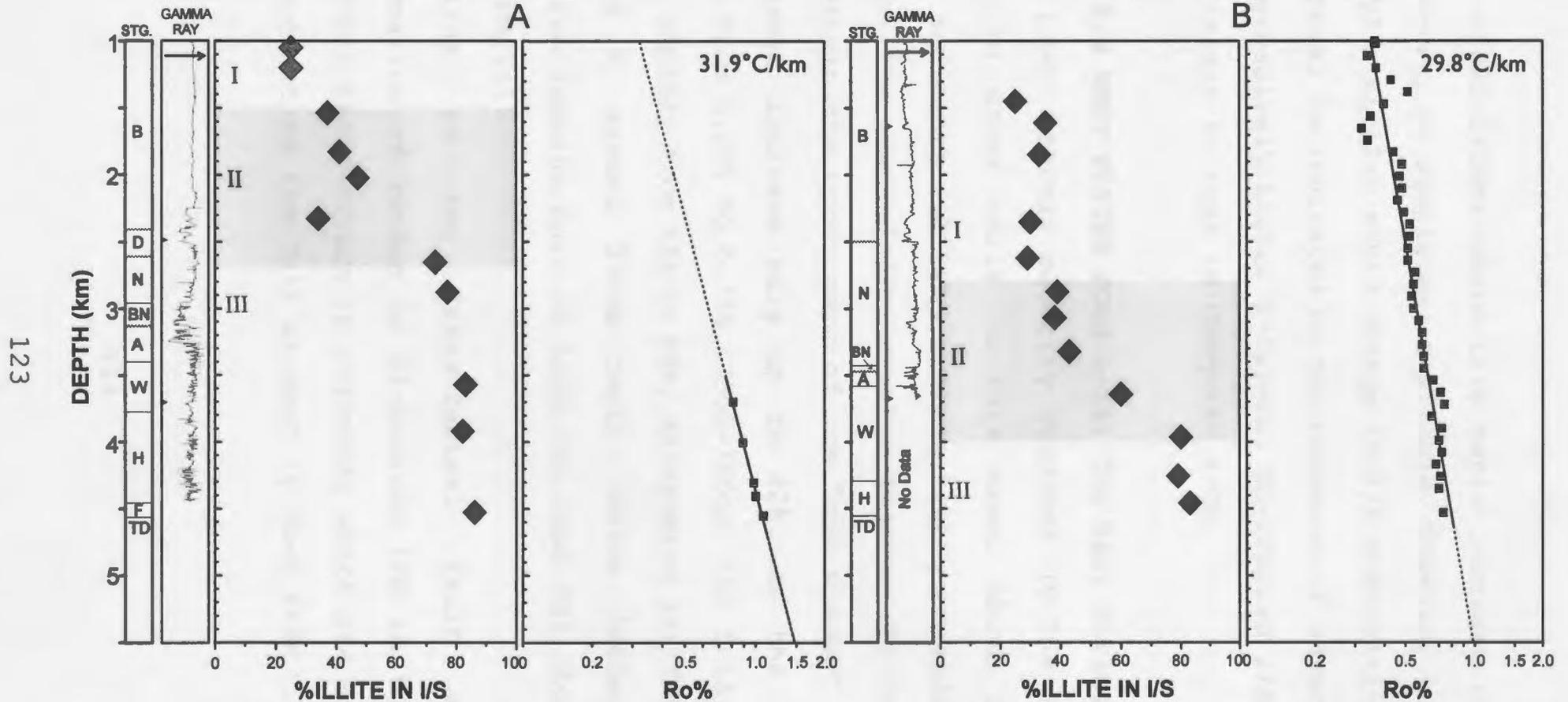
Figure 4.4. Comparison of mean vitrinite reflectance and I/S composition (%I-layers) profiles plotted with respect to burial depths for Whiterose J-49 (A) and West Flying Foam L-23 (B) wells. The stratigraphic units with gamma-ray logs are indicated on the left-side (for abbreviations see Fig. 3.3). Calculated geothermal gradients are shown in the upper right corner (see Table 1.1).

interval (2355-2655m) where this rapid increase of I-layers in I/S occurs, no sample was available. However, in North Ben Nevis P-93 a similar rapid change in I/S composition within a 300m interval is indicated by the presence of several samples with progressively higher I-layers. R3-ordered I/S occurs at 1.1% R_o similar to that in Conquest K-09.

4.4.2.4 WEST FLYING FOAM L-23: The West Flying Foam well shows a lower thermal maturity gradient (0.099 log %R_o/km) compared to other wells in this area. Above 2600m, the immature sediments (<0.5%R_o) contain highly expandable random I/S where the composition remains between 25-35% I (Fig. 4.4B). Within the upper part of the "oil window" (0.5-0.60% R_o) I-layers increase only up to 42%. As the %R_o values increase from 0.60% to 0.70% (3300-3965m) the I-layers in I/S increase rapidly from 42% to 80%. R1-ordered I/S first appears at 0.66% R_o around 3700m depth. Below 3965m, the I/S composition remains more or less the same for about 500m of further burial.

Similar to the Trans-Basinal Fault area, the transformation of random to R1-ordered I/S in the northern Jeanne d'Arc Basin occurs in sediments which are either at or near the onset of the "oil window" (0.50-0.66%R_o).

124

4.4.3 THE OUTER RIDGE COMPLEX AREA

Vitrinite reflectance values in four wells (Dominion O-23, Bonanza M-71, South Tempest G-88, North Dana I-43) vary from 0.25% to 0.96% with increasing burial depths. Linear regression lines calculated through R_o values give an excellent correlation coefficient for Dominion O-23 and Bonanza M-71 wells, 0.93% and 0.94% respectively. Correlation coefficients for the South Tempest G-88 (0.84%) and the North Dana I-43 (0.83%) wells are slightly lower due to small scattering in R_o values. The average thermal maturity gradient is 0.11 log%R_o/km. In the Dominion O-23 and Bonanza M-71 wells, the thermal maturity gradient is higher (0.142 and 0.127 log%R_o/km) compared to the South Tempest G-88 and North Dana I-43 wells (0.86 and 0.087%log R_o/km).

4.4.3.1 DOMINION O-23: In thermally immature sediments (<0.50%R_o), the random I/S contains <35% I-layers (Fig. 4.5A). I-layer content increases up to 58% in the upper part of the "oil window" (0.50-0.60%R_o) but the ordering remains random. Weak-ordering (58% I) is first observed at the base of the Banquereau Formation (3110m) at 0.62%R_o. R1-ordered I/S (60% I) first occurs in the Upper Cretaceous-age sediments (3235m) below the unconformity at a maturity level of 0.65%R_o. As maturity increases from 0.65% to 0.75% R_o, the I-layer content increases from 60% to 79% and remains R1-ordered I/S.

125

OUTER RIDGE COMPLEX
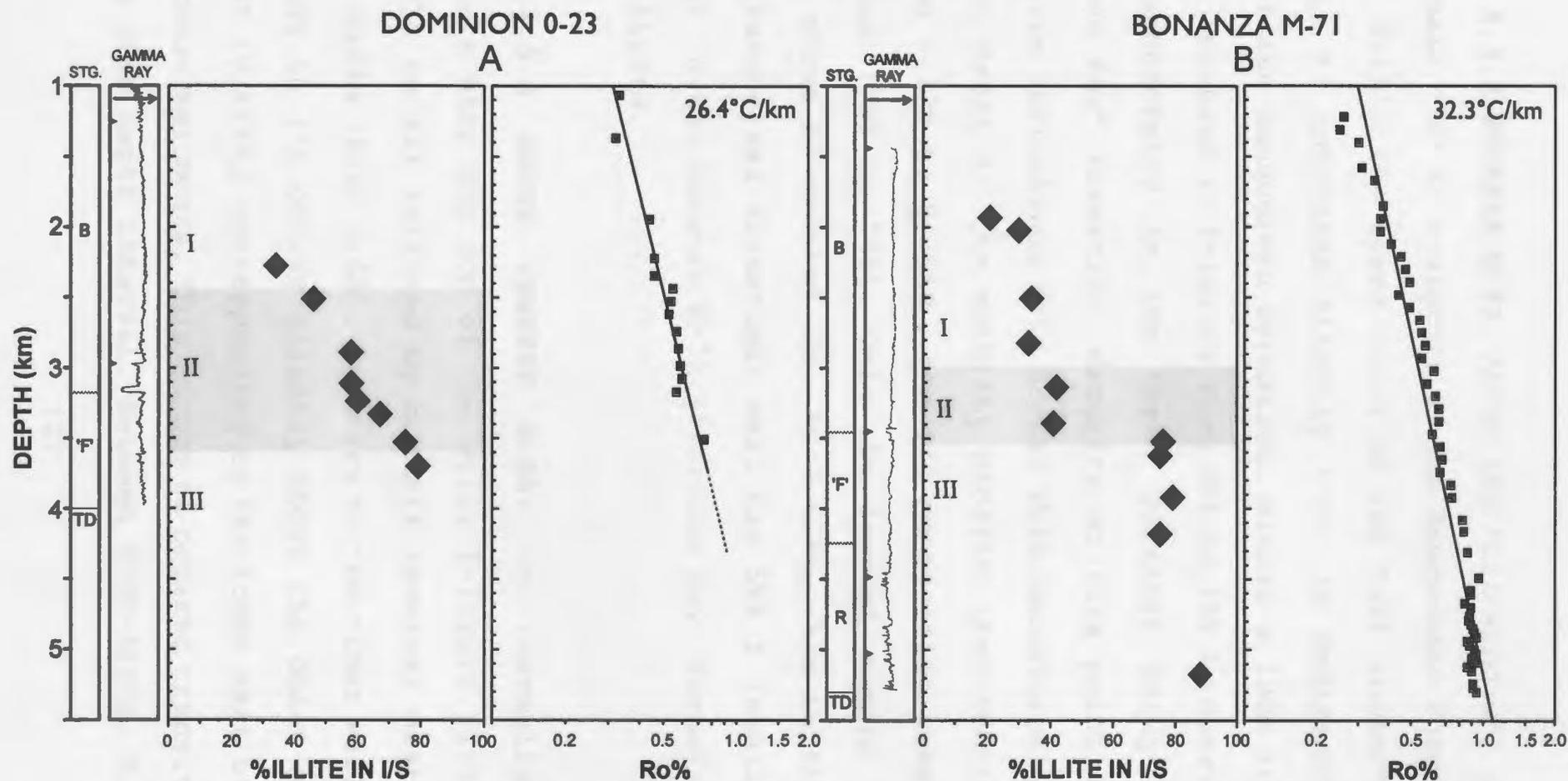
Figure 4.5. Comparison of mean vitrinite reflectance and I/S composition (%I-layers) profiles plotted with respect to burial depths for Dominion O-23 (A) and Bonanza M-71 (B) wells. The stratigraphic units with gamma-ray logs are indicated on the left-side (for abbreviations see Fig. 3.3). Calculated geothermal gradients are shown in the upper right corner (see Table 1.1).

4.4.3.2 BONANZA M-71: Above the "oil window", I-layers in I/S remain <35% in sediments of the Banquereau Formation (Fig. 4.5B). Within the upper level of the "oil window" (0.50% to 0.60%R_o) %I increases slightly (~40) in sediments near the base of the Banquereau Formation. Within a 130m interval, an abrupt increase in I-layers from 40% to 75% is observed across the unconformity in the Upper Jurassic Early Cretaceous 'Fortune Bay' Formation. Maturity at this point is 0.62%R_o. Vitrinite reflectance data across this unconformity, however, show no break in the maturity profile (see section 6.7.3). Between 0.62% to 0.75%R_o, the I/S composition remains almost the same (75% to 77%). Only the deepest sample (5175m) at 1.0%R_o shows R3-ordered I/S. At 0.62%R_o, I/S in the Dominion O-23 (Banquereau Formation) well has 58% I (weakly-ordered) whereas in the Bonanza M-71 ('Fortune Bay' Formation) it has 76% I-layers.

4.4.3.3 SOUTH TEMPEST G-88: In thermally immature sediments near the top of the well, I-layers first increase from 15% to 42% followed by a small reversal near the 2640-2725m depths (Fig. 4.6A). Contrary to the other wells studied, ordering in I/S occurs slightly above the onset of the "oil window" (0.47%R_o) corresponding to the lower part of the Lower Cretaceous sediments. This random to ordered transition occurs over a 360m depth interval. Between 3085-4400m, R_o increases

127
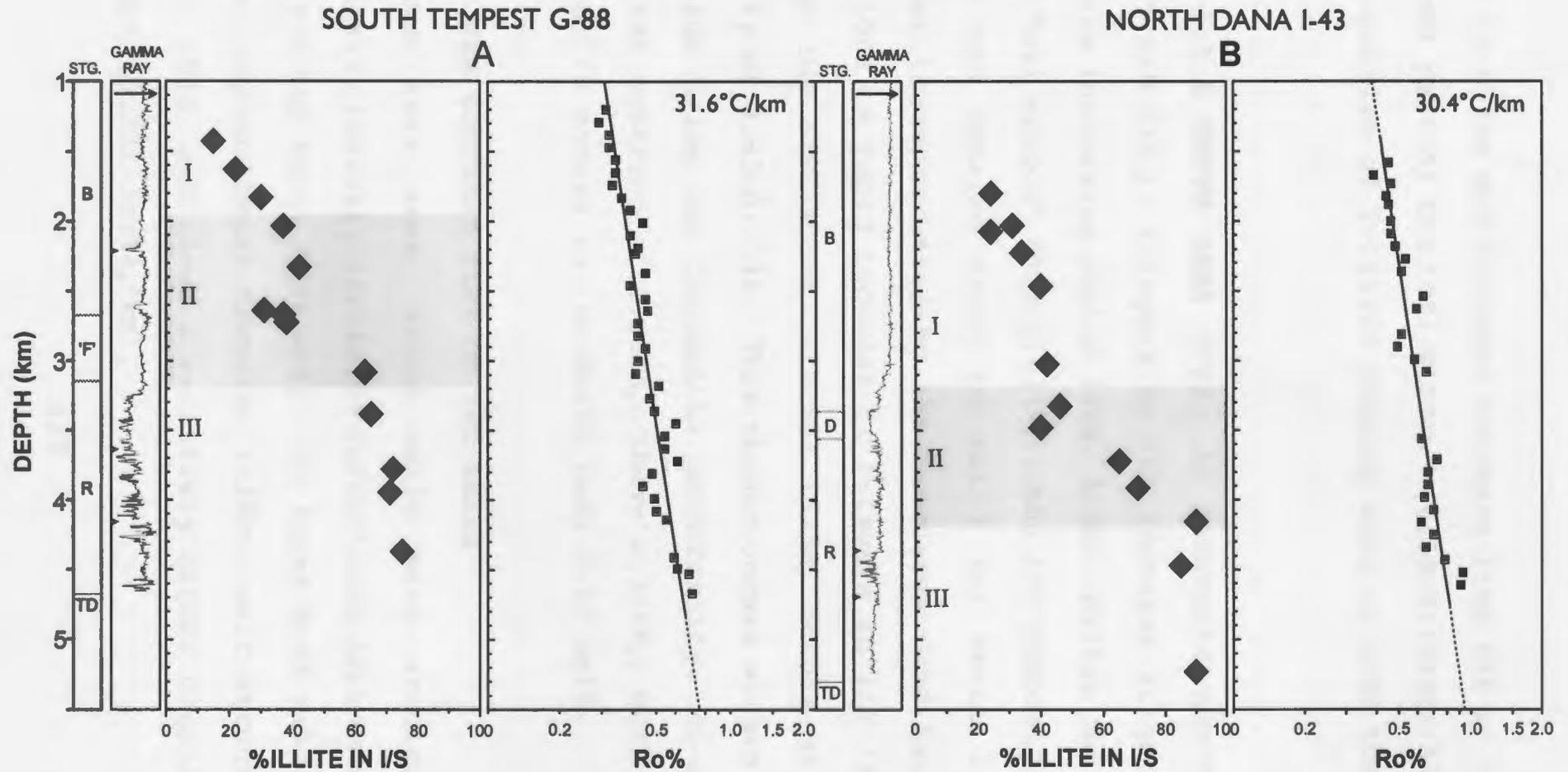
Figure 4.6. Comparison of mean vitrinite reflectance and I/S composition (%I-layers) profiles plotted with respect to burial depths for South Tempest G-88 (A) and North Dana I-43 (B) wells. The stratigraphic units with gamma-ray logs are indicated on the left-side (for abbreviations see Fig. 3.3). Calculated geothermal gradients are shown in the upper right corner (see Table 1.1).

128

from 0.47-0.60% and I-layers increase from 63% to 75%. Within the upper part of the "oil window" (0.50-0.60%R_o; 3500-4000m), the proportion of I-layers remains more or less the same (71-75% I).

4.4.3.4 NORTH DANA I-43: In sediments above the "oil window" (<0.5%R_o), I-layers in I/S increase slightly (24% to 35%) with increasing depths (Fig. 4.6B). Within the upper part of the "oil window" (0.5-0.63%R_o), the I/S composition changes little and remains close to 40% I for about 1000m. This interval is represented by the Banquereau and Dawson Canyon Formations. A rapid increase of I-layers in I/S (40% to 90%) between the 3480-4155m interval (675m) occurs at a thermal maturity of 0.63-0.72%R_o. This change occurs within the Rankin Formation below the Cenomanian unconformity. R1-ordered I/S was first observed at 0.66%R_o. Above 0.72%R_o, both R1 and R3-ordered I/S occurs in the North Dana I-43 well.

4.4.4 THE SOUTHERN PART OF THE BASIN

From this area, three wells were studied for I/S diagenesis, however, vitrinite reflectance data were available only from the Egret N-46 well. The Egret N-46 well is located over a long northeast trending (~30km) salt structure (Grant et al., 1986) and shows a relatively higher organic maturity gradient (0.222 log%R_o/km).

129

4.4.4.1 EGRET N-46: The "oil window" $(0.5\%R_o)$ in the Egret N-46 well starts at about 1500m present depth. Above 1500m, no clay samples were studied from the thermally immature sediments $(<0.5\%R_o)$. Within the upper part of the "oil window" $(0.50-0.60\%R_o)$, I-layers in I/S increase from 44% to 60% but ordering remains random (Fig. 4.7). Samples below 2000m in the Rankin Formation show ordered I/S (72-75% I-layers) at 0.65% or higher $\%R_o$ values. Ordering in I/S commenced between sample 1820m and 2015m at about 1920m depth with $0.65\%R_o$.

4.5 SUMMARY AND DISCUSSION OF THE COMPARISON

4.5.1 SUMMARY

There is no simple linear relationship between $\%R_o$ values and I/S composition in the Jeanne d'Arc Basin. Nevertheless, several important observations can be outlined about their co-variations. In figure 4.8, R_o values derived from the best-fit line, as suggested by Dow (1977), are plotted versus I/S composition for three areas from which most of the wells are studied. The majority of the samples below $0.50\%R_o$ are highly expandable and show random ordering in I/S. The only exceptions are from the South Tempest G-88 and North Ben Nevis P-93 wells where R1-ordered I/S first appears at 0.47 and $0.48\%R_o$, respectively, which is close to the on set of the "oil window" $(0.50\%R_o)$. All of the samples above $0.66\%R_o$ are either R1 or R3-ordered I/S with a high percentage of
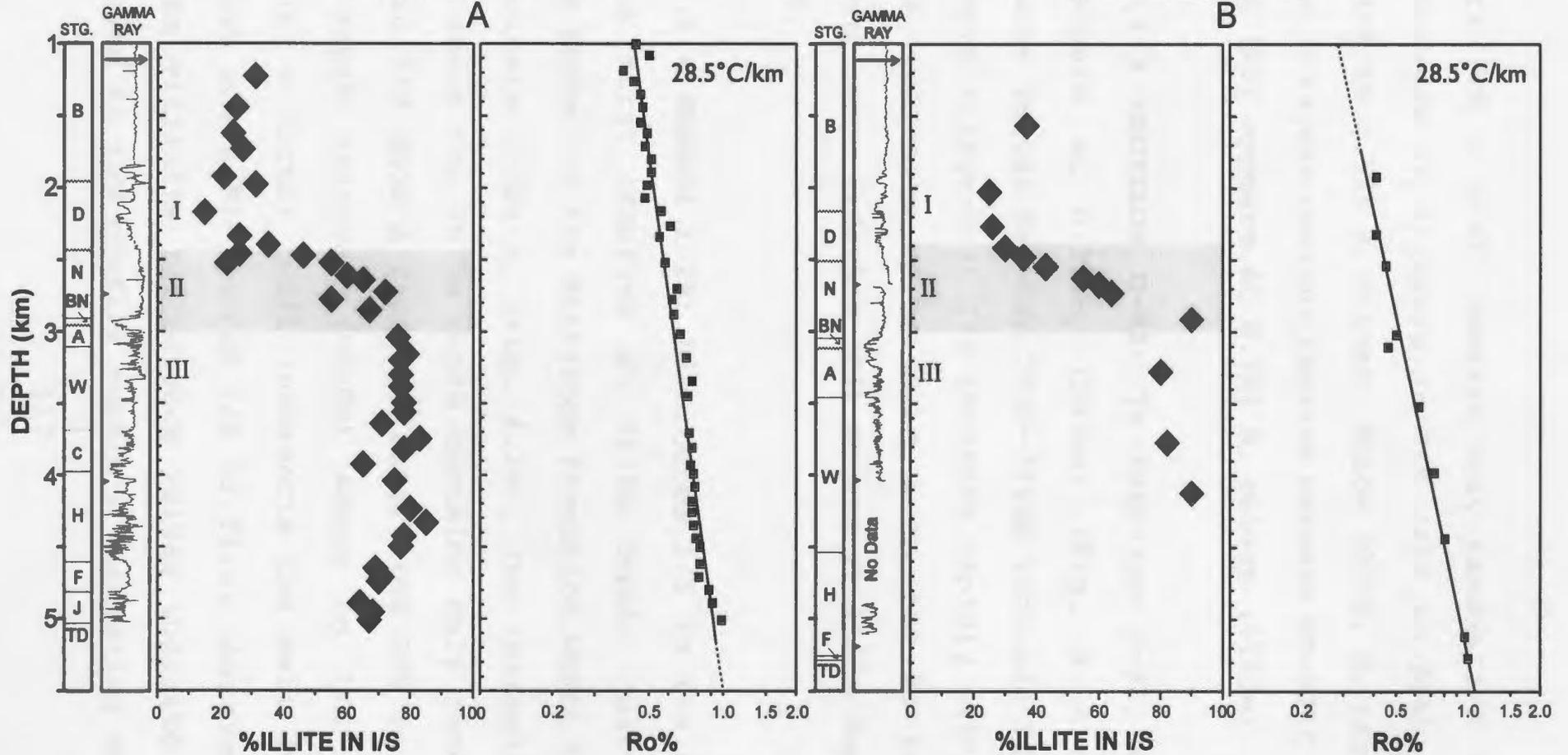
130

SOUTHERN PART OF THE BASIN
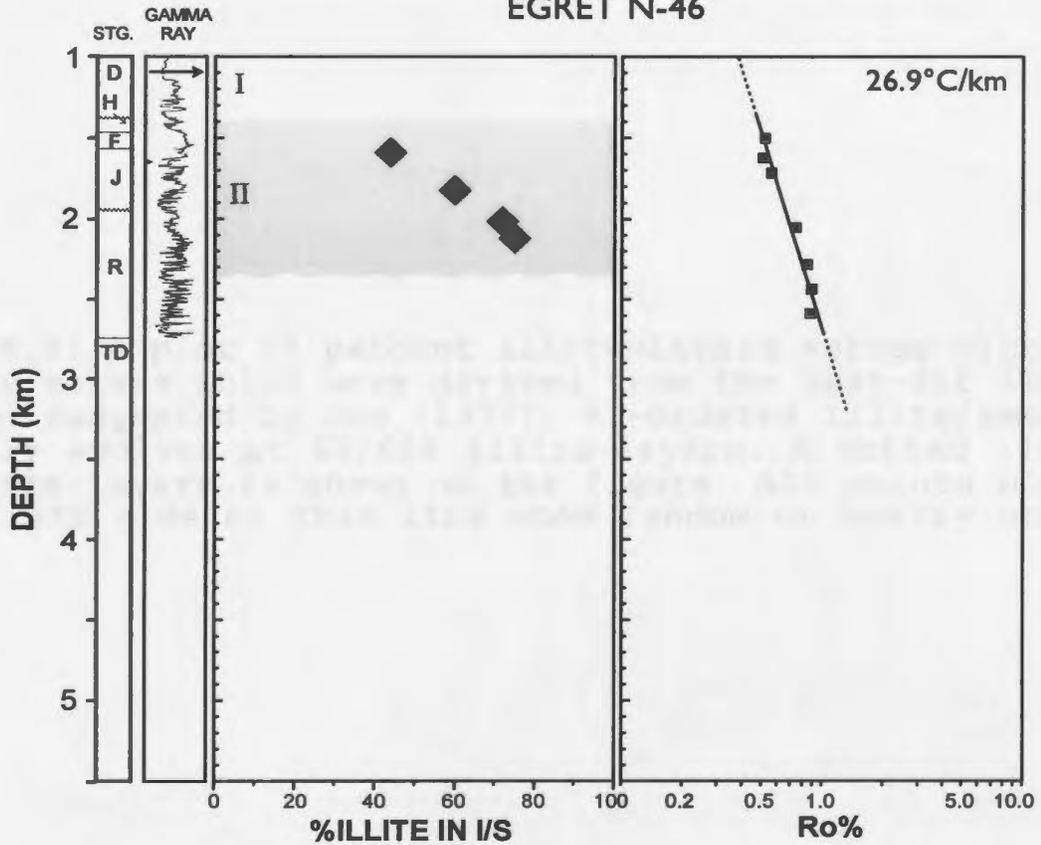
EGRET N-46

Figure 4.7. Comparison of mean vitrinite reflectance and I/S composition (%I-layers) profiles plotted with respect to burial depths for the Egret N-46 well. The stratigraphic units with gamma-ray logs are indicated on the left-side (for abbreviations see Fig. 3.3). Calculated geothermal gradient is shown in the upper right corner (see Table 1.1).

Figure 4.8: A plot of percent illite-layers versus vitrinite maturity values which were derived from the best-fit line as has been suggested by Dow (1977). R1-ordered illite/smectite generally evolves at 60/65% illite-layers. A dotted line at 60% illite-layers is shown on the figure. All points plotted on the left side of this line show random or weakly ordered I/S.

TRANS-BASINAL FAULT AREA

SOUTH MARA C-13 — A

N. BEN NEVIS P-93 — B

NAUTILUS C-92 — C

HEBRON I-13 — D

NORTHERN PART OF THE BASIN

ADOLPHUS D-50 — E

CONQUEST K-09 — F

W. FLYING FOAM L-23 — G

WHITEROSE J-49 — H

OUTER RIDGE COMPLEX

DOMINION O-23 — I

BONANZA M-71 — J

NORTH DANA I-43 — K

S. TEMPEST G-88 — L

133
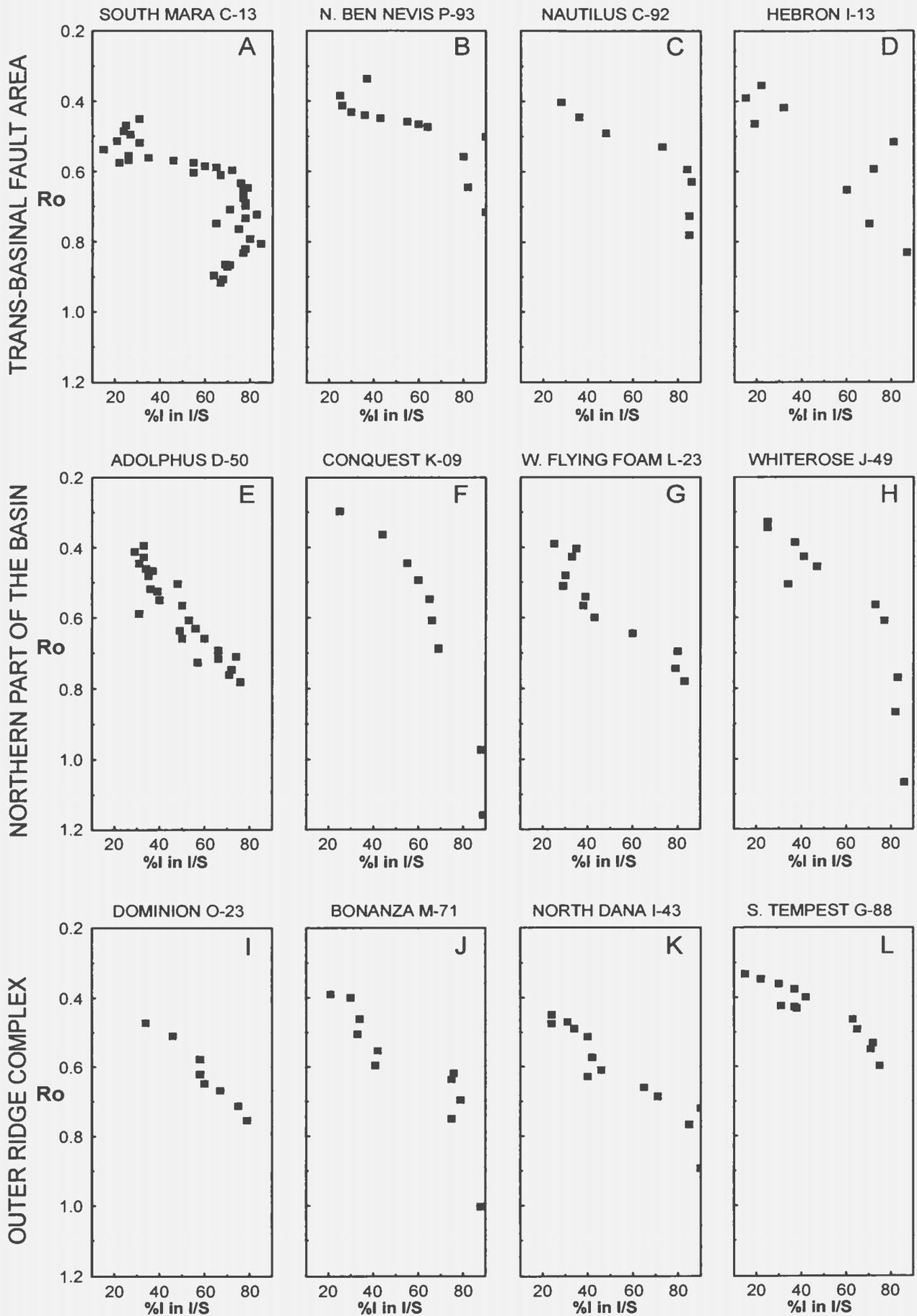
I-layers. Between 0.50-0.66% R_o both random and R1-ordered I/S with a considerable variation in I/S composition are observed. Table 4.1 and figure 4.9 summarize R_o and present temperatures for random to R1-ordering transition and Table 4.2 summarizes the data about the R1 to R3-ordering change in I/S. Figures 4.9A and 4.9B show proposed contours for vitrinite reflectance and present temperatures where the random to R1-ordered I/S is first observed in the Jeanne d'Arc Basin. Regarding the comparison of I/S and R_o, important points for three areas are summarized below.

THE TRANS-BASINAL FAULT AREA: This area is characterized by a rapid increase of I-layers in I/S as a function of depth near 0.50 R_o (0.59 R_o for South Mara C-13). At <0.45%R_o, I-layers remains <40%. Between 0.45-0.53%R_o a rapid increase of I-layers is observed in North Ben Nevis P-93, Nautilus C-92 and Hebron I-43 wells where R1-ordered I/S first appears in the Nautilus or older formations (Fig. 4.8). However in South Mara C-13, the Dawson Formation with 0.57%R_o maturity level still contains random I/S with <40% I-layers. Illite-layers, however, increase rapidly within the Nautilus Formation near 0.60%R_o value. The Nautilus Formation in the Hebron I-13 well, however, is presently at a lower maturity level (<0.45%R_o) and remains random with less than 40%I. Below 0.60%R_o most samples contain >70% I-layers. The above data suggest a rapid increase

134

Figure 4.9: Maps showing (A) vitrinite reflectance values and (B) present formation temperatures where the R1-ordered illite/smectite is first observed in different wells of the Jeanne d'Arc Basin. Suggested contours may modify with the availability of additional data. AD=Adolphus D-50; BO=Bonanza M-71; CON=Conquest K-09; DO=Dominion O-23; EG=Egret N-46; HB=Hebron I-13; NAT=Nautilus C-92; NBN=North Ben Nevis P-93; ND=North Dana I-43; SM=South Mara C-13; ST=South Tempest G-88; WFF=West Flying Foam L-23; and WR=Whiterose J-49.

A

Vitrinite Reflectance for Random to R1-Ordering

BO ✳ 0.62
DO ✳ 0.65
ND ✳ 0.66
0.65   0.6
COMPLEX
CON ✳ 0.50
ST ✳ 0.48
WFF ✳ 0.66
0.5
AD ✳ 0.66
47°
PLATFORM
NORTHERN PART OF BASIN
RIDGE
NAT ✳ 0.53
WR ✳ 0.56
0.65
0.59
BONAVISTA
NBN ✳
SM 0.47
TRANS-BASINAL FAULT AREA
OUTER
0.52
HB ✳
N
0.6
0.65 ✳ EG   0.5
SOUTHERN PART OF BASIN
0   km   40
49°   48°

B

Present Temperatures for Random to R1-Ordering

BO ✳ 118
DO ✳ 91   110
100
COMPLEX
ND ✳ 118
?
CON ✳ 92   100
ST ✳ 102
WFF ✳ 115   110
100
101 ✳ AD
47°
PLATFORM
NORTHERN PART OF BASIN
RIDGE
NAT ✳ 92
90
WR ✳ 89
BONAVISTA
SM   NBN ✳ 83
80
80
TRANS-BASINAL FAULT AREA
OUTER
69 ✳ HB   70
N
59 ✳ EG   60
SOUTHERN PART OF BASIN
0   km   40

in I-layers within the Nautilus Formation above 0.45% R_o, however, at <0.45% R_o I-layers do not increase rapidly within the Nautilus Formation (i.e. Hebron I-13).

THE NORTHERN PART OF THE BASIN: With the exception of Whiterose J-49, I-layers increase progressively in this area. On average, R1-ordering appears at slightly higher R_o values (0.59%) than in the Trans-Basinal Fault area (0.53%) (Table 4.1). At <0.5%R_o, %I in I/S slightly increases and remains random in the Banquereau Formation except in the Conquest well. Between 0.5-0.6%R_o, %I slightly increases in the Nautilus Formation of the West Flying Foam L-23 (<40%I) but rapidly increases in the Nautilus Formation of the Whiterose J-49 well. In Adolphus D-50, I/S changes from random to weakly ordered (40-50%I) at the top of the Dawson Canyon Formation. Between 0.60-0.70%R_o, weak-ordering changes into R1-ordered within the Dawson Canyon Formation of the Adolphus D-50 well while in the West Flying Foam L-23, random I/S is converted into R1-ordered I/S as the profile enters into the Whiterose Formation. Below 0.7%R_o most of the samples contain ≥70% I-layers. In Whiterose J-49 the rapid increase of I-layers in the Nautilus Formation at 0.50-0.56% R_o resembles the Trans-Basinal Fault area, however, West Flying Foam L-23 show no such trend in the Nautilus Formation.

137

THE OUTER RIDGE COMPLEX AREA: Both rapid and gradual increase in I-layers with increasing organic maturity are observed in this area (Fig. 4.8). On average, R1-ordering appears at 0.60% R_o. At <0.50% R_o in South Tempest G-88, I-layers in I/S increase up to 63% and becomes R1-ordered in the 'Fortune Bay' Formation. In the other three wells, it remains <40% in the Banquereau Formation. The Banquereau Formation continues, between 0.50-0.60% R_o, in the Dominion O-23, Bonanza M-71, and North Dana I-13 wells. Here the composition does not change in Bonanza M-71 and North Dana I-43 wells and remains near 40%I, however, in Dominion O-23 it increases up to 58% I and remains random (Fig. 4.8). Between 0.60-0.70% R_o, I-layers increases rapidly in Bonanza M-71 and North Dana I-43 wells when entering into the 'Fortune Bay' or Rankin Formations respectively. In Dominion O-23, I-layers increase progressively and weakly-ordered I/S change into R1-ordered I/S in the Upper Cretaceous sediments. Above 0.7% R_o, only R1 or R3-ordered I/S with >70% I-layers are observed. Higher vitrinite reflectance values (average 0.60%) for random to R1-ordered I/S change are probably due to a thick Banquereau Formation (see Fig. 4.5 and 4.6) in which I-layers increase slowly especially in Bonanza M-71 and North Dana I-13 wells.

4.5.2 DISCUSSION

The above summary suggests that I/S composition is less evolved and shows higher expandability in Banquereau and Dawson Canyon Formations than in the Nautilus or older formations at a given R_o maturity level. The only exceptions are Conquest K-09 and Adolphus D-50 (close to a salt domes), and West Flying Foam L-23 (close to the western margin of the basin). These observations suggest that if Nautilus and older formations occur at shallow depths then, I-layers in I/S may increase rapidly and become R1-ordered around 0.50% R_o. If Nautilus and older rocks are buried at greater depths beneath thick Banquereau and Dawson Canyon Formations, then the random to R1-ordered transition seems to occur at a higher maturity level ($\sim$0.65%R_o) because the I/S diagenesis is slow in these sediments (Banquereau and Dawson Formations). The lack of internal K^+ source and/or lack of faults and sandy intervals to facilitate the external K^+ supply in the Banquereau and Dawson Formations may have been responsible for slower I/S diagenesis (also see Chapter VI). This factor must be remembered if I/S "geothermometry" is to be used in the Jeanne d'Arc and possibly associated East Coast basins. Conquest K-09 and Adolphus D-50 are the only wells where a significant increase of I-layers and R1-ordering occurs within the Banquereau and Dawson Canyon Formations, possibly due to the presence of salt domes.

139

The vitrinite reflectance values for R1-ordering generally increase from the east to the west (Fig. 4.9A) whereas the present temperature generally increases northward (Fig. 4.9B). The slightly lower R_o values observed for R1-ordering along the eastern side of the basin (including part of the TBF area), may suggest the movement of deep basinal fluids upward along numerous faults and the westward dipping sedimentary strata. The increase in temperature for R1-ordering toward the north may, in part, reflect the thickening of the post-rift sediments where the illitization reaction is slower than the rift sediments (see Chapter VI).

Table 4.3 summarizes $\%R_o$ and present temperature where R1 and R3-ordered I/S first appears in sedimentary rocks ranging in age from Carboniferous to Tertiary. It shows that R1-ordering in different basins appears within the upper "oil window" level of organic maturity (0.50-0.70$\%R_o$) at about 100 $\pm15°C$ present temperature. Using T_{max} data, Burtner and Warner (1986) also demonstrated that convergence of random to R1-ordered I/S occurs within the "oil window" in the Cretaceous shales of North Dakota. They found that samples with less than 437 T_{max} contain only random I/S. Results of this study also show that the random to R1-ordering generally occurs within the upper "oil window" level (0.50-0.66$\%R_o$) and substantiate earlier findings by other workers (see Table 4.3). The R1 to R3-ordered I/S change occurs at 0.72-1.10$\%R_o$. These values are

also comparable with reported data from other sedimentary basins (Środoń, 1979; Glasmann et al., 1989; and Connolly, 1989) (see section 6.2.2 for further discussion).

Although R1-ordering of I/S first appears within the "oil window", the presence of R1-ordered I/S, however, cannot be used to correlate a specific level of organic maturity in sedimentary rocks, as Table 4.3 shows. There is a wide range in vitrinite reflectance values where this change occurs. Although both reactions (R_o and I/S) are mainly temperature dependent, the relationship breaks down where other factors such as pore-water composition and bulk-rock composition vary from basin to basin or within a basin thus causing either retardation or advancement of the illitization reaction (Scotchman, 1987; see Chapter VI). Once the I/S reaction begins, it goes to completion or near completion over a narrow temperature range when the chemical environment is favourable (Ramseyer and Boles, 1986). This explains the wide range of temperature over which illitization has been reported in the literature.

Although the R1-ordering temperature in Table 4.3 is close to 100±15°C, a wide range (72° to 140°C) is reported in the literature (Heling, 1974; Dunoyer de Segonzac, 1970). For the random to R1-ordered transition, the lower temperature reported in the literature (i.e. 72°C in the Rhine Graben by Heling, 1974, 1978) may not reflect the actual temperature

141

where this change occurred. For example, in the Jeanne d'Arc Basin, the Egret N-46 well shows only 57°C present temperature where ordering is first observed. Vitrinite reflectance at the same depth, however, is about 0.65% R_o indicating that temperature in the past may have been at least 40°C higher at the ordering depth. In such cases the temperature could have been higher in the past due to either: (1) higher geothermal gradient, (2) movement of hot fluids from the deeper part of the basin (3) or due to uplifting and erosion of large amounts of sediments (also see sections 6.2.1 and 6.7.3). These observations stress the importance of integrating different maturity parameters to understand anomalous I/S cases.

Table 4.1. Depth, vitrinite reflectance, %I-layers in I/S, formation/age, maturation gradient and present formation temperature for various wells where random to R1-ordering first appears in I/S (see figure 4.9 for map of the data).

Well Name	Depth (m)	%R_o	%I in I/S	Maturation Gradient[*]	Present Temp.°C	Formation/ Age[+]
Trans-Basinal Fault Area:						
South Mara C-13[1]	2640	0.59	65	0.080	80	Nautilus/Early Cretaceous
N. Ben Nevis P-93[1]	2730	0.47	64	0.128	83	Nautilus/Early Cretaceous
Nautilus C-92[1]	3030	0.53	73	0.113	92	Nautilus/Early Cretaceous
Hebron I-13[2]	2675	0.52	81	0.107	69	Whiterose/Early Cretaceous
Average:		0.53		0.107	81	
Northern Part of the Basin:						
Adolphus D-50[2]	3135	0.66	60	0.141	101	Dawson Canyon/Late Cretaceous
Conquest K-09[1]	2620	0.50	60	0.224	92	Banquereau/Tertiary
W. Flying Foam L-23[1]	3700	0.66	65	0.099	115	Whiterose/Early Cretaceous
Whiterose J-49[1]	2655	0.56	74	0.147	89	Nautilus/Early Cretaceous
Average:		0.59		0.152	99	
Outer Ridge Complex:						
Dominion O-23[2]	3235	0.65	60	0.142	91	'Fortune'/L.Jurassic/E.Cretaceous
Bonanza M-71[1]	3520	0.62	76	0.127	118	'Fortune'/L.Jurassic/E.Cretaceous
South Tempest G-88[1]	3085	0.48	63	0.086	102	'Fortune'/L.Jurassic/E.Cretaceous
North Dana I-43[1]	3720	0.66	65	0.087	118	Rankin/Late Jurassic
Average:		0.60		0.110	107	
Southern Part of the Basin:						
Egret N-46[2]	2015	0.65	65	0.222	59	Rankin/Late Jurassic
Total Average:	**2975**	**0.58**	**67**	**0.131**	**93**	

[1] Vitrinite reflectance data (%R_o) of C-NOPB, analyzed by Geochem Lab, Calgary, Alberta
[2] Vitrinite reflectance data (%R_o) from the Geological Survey of Canada (Avery 1985, 1993 and Harrison 1984)
[*] Log R_o/km, derived from the best fit line (see text)
[+] Stratigraphy and age from Sinclair (1988)

143

Table 4.2. Depth, vitrinite reflectance, %I-layers in I/S, stratigraphic unit, maturation gradient and present formation temperature for various wells where R1 to R3-ordering first appears in I/S.

Well Name	Depth (m)	%R$_o$	%I in I/S	Maturation Gradient[*]	Present Temp.°C	Formation[+]
Trans-Basinal Fault Area:						
South Mara C-13	4330	0.80	85	0.080	128	Hibernia Formation
Nautilus C-92	4245	0.73	85	0.113	128	Hibernia Formation
North Ben Nevis P-93	2915	0.50	90	0.128	88	Nautilus Formation
Northern Part of the Basin:						
Conquest K-09	3935	0.85	88	0.224	136	'Fortune' Formation
Whiterose J-49	4530	1.10	86	0.147	150	Fortune Formation
Outer Ridge Complex:						
Bonanza M-71	5175	1.00	88	0.127	170	Rankin Formation
North Dana I-43	4155	0.72	90	0.087	131	Rankin Formation
Total Average:	**4184**	**0.81**	**87**	**0.130**	**133**	

[*] Log R$_o$/km, derived from the best fit line (see text)
[+] Stratigraphy from Sinclair (1988)

Table 4.3. Vitrinite reflectance, present temperature and age of sedimentary rocks where R1 or R3-ordered I/S first appears in different sedimentary basins.

Sedimentary Basins	Ordering	%R$_o$	Temp.°C[*]	Age	Reference
1. Viking Graben and Moray Firth North Sea	R1	0.64 (0.54-0.72)	93 (87-100)	Quarternary-Triassic	Pearson and Small, 1988
2. Central Trough North Sea	R1	0.63	(90-115)	Upper Jurassic	Lindgreen, 1991
3. Sverdrup Basin N. West Canada	R1	0.50	NA	Jurassic-Tertiary	Powell et al., 1978
4. Gulf Coast Basin	R1	NA	95	Oligocene	Hower et al., 1976
5. Pannonian Basin	R1	0.60	NA	Tertiary	Hillier et al., 1995
6. Jeanne d'Arc Basin	R1	0.58 (0.47-0.66)	93 (57-118)	Tertiary-Upper Jurassic	**This study**
7. Bergen High North Sea	R3	(>0.70-0.80)	(150-160)	Mesozoic-Tertiary	Glasmann et al., 1989
8. Upper Silesian Basin Poland	R3	(0.85-0.90)	NA	Carboniferous	Środoń, 1979
9. Northwest Alberta	R3	1.06	171	Early Cretaceous	Connolly, 1989
10. Jeanne d'Arc Basin	R3	(0.72-1.10)	(128-170)	Tertiary-Upper Jurassic	**This study**

[*] Present formation temperature

CHAPTER V

OXYGEN-ISOTOPE COMPOSITION OF MIXED-LAYER ILLITE/SMECTITE

5.1 INTRODUCTION

The mineralogy of fine-grained mixed-layer I/S from the Jeanne d'Arc Basin has been discussed in Chapter III. Here, the oxygen-isotope data on mixed-layer I/S from 3 wells are discussed. Oxygen-isotope studies of clay minerals can provide valuable information about the source area and the diagenetic history of sedimentary rocks (Yeh and Savin, 1977; Suchecki and Land, 1983; Eslinger and Yeh, 1981; Tribble and Yeh, 1994).

Clay minerals produced during weathering are enriched in ^{18}O relative to the water from which they form owing to the large oxygen-isotope fractionation factors at low temperature in the near surface environment (Urey, 1947; Savin and Epstein, 1970 a, b; Lawrence and Taylor, 1971). Land-derived, ^{18}O-rich detrital clay minerals do not exchange oxygen isotopes during transportation and deposition in meteoric or marine waters (Yeh and Eslinger, 1986) except when they are subjected to higher temperatures and/or undergo mineralogical and chemical alterations (Yeh and Savin, 1976). Diagenetic clays that form as a result of the alteration of detrital minerals such as feldspar have $\delta^{18}O$ values that reflect the oxygen-isotope composition of the diagenetic fluid and the

146

temperature of formation. In a diagenetic system where smectite layers in I/S are progressively illitized, the chemical changes in their crystal structure (i.e. increase of Al and decrease of Si) are accompanied by isotopic exchange between I/S clays and the subsurface pore-fluids. Laboratory experiments show that the extent of oxygen-isotope exchange between I/S and water increases with increasing degree of illitization (Whitney and Northrop, 1988). Thus a comparison of I/S composition with their isotopic ratios can provide valuable information about I/S diagenesis as well as the evolution of pore-fluids assuming that the isotopic equilibrium between I/S clays (<0.1μm) and the coexisting pore-fluids was achieved (Yeh and Savin, 1977).

Though many oxygen-isotope studies of clay minerals have been presented in the literature (see review by Longstaffe, 1989), only a few workers have studied the oxygen-isotopic composition of I/S clays covering several kilometre-thick sedimentary sequences in relation to changes in I/S composition (Yeh and Savin, 1977; Eslinger et al., 1979; Suchecki and Land, 1983). Results of these studies indicate that in most cases the $\delta^{18}O$ values of I/S progressively decrease and at the same time $\delta^{18}O$ values of pore-water in equilibrium with I/S (<0.1μm) increase with increasing burial depth. The isotopic results have been interpreted to indicate that no large-scale vertical movement of basinal fluids has

147

occurred in the Gulf Coast Basin (Yeh and Savin, 1977).

The objective of this chapter is to investigate the relationships between the oxygen-isotopic compositions of I/S as a function of changes in I/S composition with increasing burial depth. The data constrain the nature of the I/S burial diagenesis and the evolution of pore-fluid in the Jeanne d'Arc Basin.

5.2 SAMPLING AND ANALYTICAL PROCEDURE

Three wells from near the centre of the basin were selected for oxygen-isotope analyses. From the Southern part of the Jeanne d'Arc Basin the Egret K-36 well was selected because here the random to Rl-ordered I/S clay transition occurs in relatively older rocks. From the Trans-Basinal Fault area South Mara C-13 well was selected to see the effect of faults on the processes of illitization and the oxygen-isotopes. The Adolphus D-50 well from the Northern area was chosen to represent shale-rich distal sediments of a structurally less disturbed area.

Fine-grained clay fractions (<0.1µm) from 42 samples were analyzed, representing Upper Jurassic to Tertiary sediments ranging in depth from 1440m to 4955m. The method used to separate the fine-grained clay fractions is described in Chapter I and in the Appendix I. The chemical techniques applied to separate the clays (Jackson, 1969) have been shown

148

not to significantly alter the $\delta^{18}O$ values (Yeh and Savin, 1977).

The XRD mineralogy of the <0.1μm clay fractions described in Chapter III indicates that they are predominantly composed of an I/S phase (>95%) with minor to trace amounts of kaolinite and illite. Chlorite is rarely present. The presence of these other minerals does not show any trend with depth and at <5% abundance are not considered to have a significant influence on the isotopic data collected (Yeh and Savin, 1977; Primmer and Shaw, 1991).

Oxygen-isotope analyses were conducted in the Department of Geology, University of Western Ontario under the supervision of Dr. F. J. Longstaffe. Samples were pretreated at 200°C for 2 hours to remove absorbed and interlayer water. Oxygen was extracted by BrF_5 according to the technique described by Clayton and Mayeda (1963), and converted to CO_2 for mass spectrometry. All results are reported in the familiar δ-notation in units of permill (parts per thousand or ‰) relative to standard mean ocean water (SMOW, Craig, 1961). For the NBS-28 quartz standard, the laboratory reports a mean $\delta^{18}O$ value of 11.55‰.

The isotopic composition of pore-waters in the Jeanne d'Arc Basin, assumed to be equilibrated with fine-grained I/S clays, were calculated using the I/S-H_2O oxygen isotope

fractionation factors of Savin and Lee (1988):

$$1000 \ln \alpha (I/S - H_2O) = [(2.58 - 0.19 \times I) \times 10^6 T^{-2}] - 4.19$$

Where I=%illite in I/S and T=temperature in degrees Kelvin. Maximum burial temperatures for the pore-water calculations were derived from vitrinite reflectance profiles using $T(^\circ C) = 104(\ln R_o) + 148$ correlation of Barker (1988). Unfortunately, vitrinite reflectance data were not available from the Egret K-36 well to derive burial temperatures needed to calculate the isotopic composition of pore-waters.

5.3 ISOTOPIC RESULTS

The oxygen-isotope results for the I/S samples are listed in Table 5.1 along with information regarding stratigraphy, I/S composition, and present formation temperatures. In the Jeanne d'Arc Basin, $\delta^{18}O$ values for I/S range from 25.8‰ to 17.8‰ (SMOW) and are similar to those reported by Yeh and Savin (1977) for I/S from the U.S. Gulf Coast Basin (CWRW well #6). Depth versus $\delta^{18}O$ trends from the Jeanne d'Arc Basin, however, show both similarities and differences compared to the well documented I/S clays from the U.S. Gulf Coast Basin. The data from individual wells are described below.

5.3.1 SOUTH MARA C-13: Compared to the Adolphus D-50 and Egret K-36 well, the South Mara C-13 well was drilled to a

Table 5.1: Oxygen isotopic composition of I/S clays (<0.1μm) and relevant data for South Mara C-13, Adolphus D-50, and Egret wells of the Jeanne d'Arc Basin.

South Mara C-13

Depth (m)	Age	Formation	%I	Ordering	Present* Temp. °C	δ¹⁸O
1440	Tertiary	Banquereau	25	R0	46	21.2
1730	Tertiary	Banquereau	27	R0	54	20.8
1975	L. Cretaceous	Dawson	31	R0	61	23.2
2170	L. Cretaceous	Dawson	15	R0	67	25.8
2395	L. Cretaceous	Dawson	35	R0	73	22.7
2395	L. Cretaceous	Dawson	35	R0	73	23.3
2470	E. Cretaceous	Nautilus	46	R0	75	22.8
2470	E. Cretaceous	Nautilus	46	R0	75	22.8
2520	E. Cretaceous	Nautilus	55	R0	77	23.3
2640	E. Cretaceous	Nautilus	65	R1	80	20.8
2725	E. Cretaceous	Nautilus	72	R1	82	20.7
2850	E. Cretaceous	Nautilus	67	R1	86	19.1
3040	E. Cretaceous	Avalon	76	R1	91	19.4
3155	E. Cretaceous	Whiterose	79	R1	95	17.8
3200	E. Cretaceous	Whiterose	77	R1	96	18.2
3300	E. Cretaceous	Whiterose	77	R1	99	18.0
3385	E. Cretaceous	Whiterose	77	R1	101	18.4
3495	E. Cretaceous	Whiterose	78	R1	104	19.6
3640	E. Cretaceous	Whiterose	71	R1	108	19.1
3925	E. Cretaceous	Whiterose	65	R1	116	19.5
4425	E. Cretaceous	Hibernia	78	R1	131	19.7
4710	L. Jurassic	Fortune	71	R1	139	17.9
4955	L. Jurassic	Jeanne d'Arc	68	R1	146	21.8
4955	L. Jurassic	Jeanne d'Arc	68	R1	148	22.3

*   Present formation temperature from corrected Bottom Hole Temperature data

R0   Random I/S

R1   Ordered I/S

151

Table 5.1 Continued.

Adolphus D-50

Depth (m)	Age	Formation	%I	Ordering	Present* Temp.°C	$\delta^{18}O$
1565	Tertiary	Banquereau	33	R0	53	21.3
1810	Tertiary	Banquereau	33	R0	60	21.1
2035	Tertiary	Banquereau	34	R0	67	21.4
2310	Tertiary	Banquereau	48	R0	76	21.8
2580	Tertiary	Banquereau	40	R0	84	21.6
2665	Tertiary	Banquereau	50	WR1	87	21.4
2785	L. Cretaceous	Dawson	31	R0	91	23.1
2884	L. Cretaceous	Dawson	53	WR1	94	21.7
3000	L. Cretaceous	Dawson	56	WR1	97	22.4
3032	L. Cretaceous	Dawson	49	WR1	98	22.3
3135	L. Cretaceous	Dawson	50	WR1	101	21.9
3285	L. Cretaceous	Dawson	66	R1	106	22.3
3390	E. Cretaceous	Nautilus	66	R1	109	21.9
3520	E. Cretaceous	Nautilus	72	R1	114	20.9
3660	E. Cretaceous	Nautilus	76	R1	117	20.2

Egret K-36

Depth (m)	Age	Formation	%I	Ordering	Present* Temp.°C	$\delta^{18}O$
1625	E. Cretaceous	Hibernia	22	R0	43	25.7
2090	L. Jurassic	Fortune	35	R0	54	24.6
2120	L. Jurassic	Fortune	34	R0	55	25.1
2265	L. Jurassic	Rankin	48	R0	58	24.5
2420	L. Jurassic	Rankin	59	R1	62	23.3
2935	L. Jurassic	Rankin	69	R1	74	21.9

*	Present formation temperature from corrected Bottom Hole Temperature data
R0	Random I/S
WR1	Weekly ordered I/S
R1	Ordered I/S

152

greater depth (5034m) so that all of the main stratigraphic units down to the Jeanne d'Arc Formation were intersected. A total of 21 samples, covering a 3515m depth interval (1440-4955m), were analyzed. Oxygen-isotope values range from 25.8 to 17.8‰ with depth (Fig. 5.1). The $\delta^{18}O$ profile can be divided into three main segments. Down to 2170m, $\delta^{18}O$ values increase from about 21.0 to 25.8‰. The sample at 2170m with the highest $\delta^{18}O$ value (25.8‰) has the lowest I-layer content in I/S (15% I). Between the 2170m to 3300m interval, the $\delta^{18}O$ values rapidly decrease (25.80‰ to 18.0‰) in a linear fashion (0.7‰/100m). Within the same depth interval, the I/S shows a significant increase in I-layers (15% to 77%I) and is accompanied by the first appearance of R1-ordering. From 3155m to 4710m, the $\delta^{18}O$ values remain within a relatively narrow range (17.8-19.7‰) and the I/S composition also remains more or less the same. The deepest sample (4955m) is from an overpressure zone (C-NOPB, unpublished data) and it shows a reversal of 4.1‰ (17.9 to 22.0‰) from the overall normal trend .

In the U.S. Gulf Coast, the $\delta^{18}O$ values of fine clay fractions (<0.1μm) in CWRU well #6 decrease more or less continuously (22.4 to 17.6‰) with increasing burial depths and are in sharp contrast to those from South Mara C-13 (for

153

Figure 5.1: The proportion of illite-layers in illite/smectite (A), $\delta^{18}O$ of illite/smectite clays (B), and calculated isotopic composition of pore-water (C), versus depth for South Mara C-13. Pore-water isotopic composition was calculated according to Savin and Lee (1988). All $\delta^{18}O$ values in SMOW. For abbreviations, see figure 3.3.

SOUTH MARA C-13
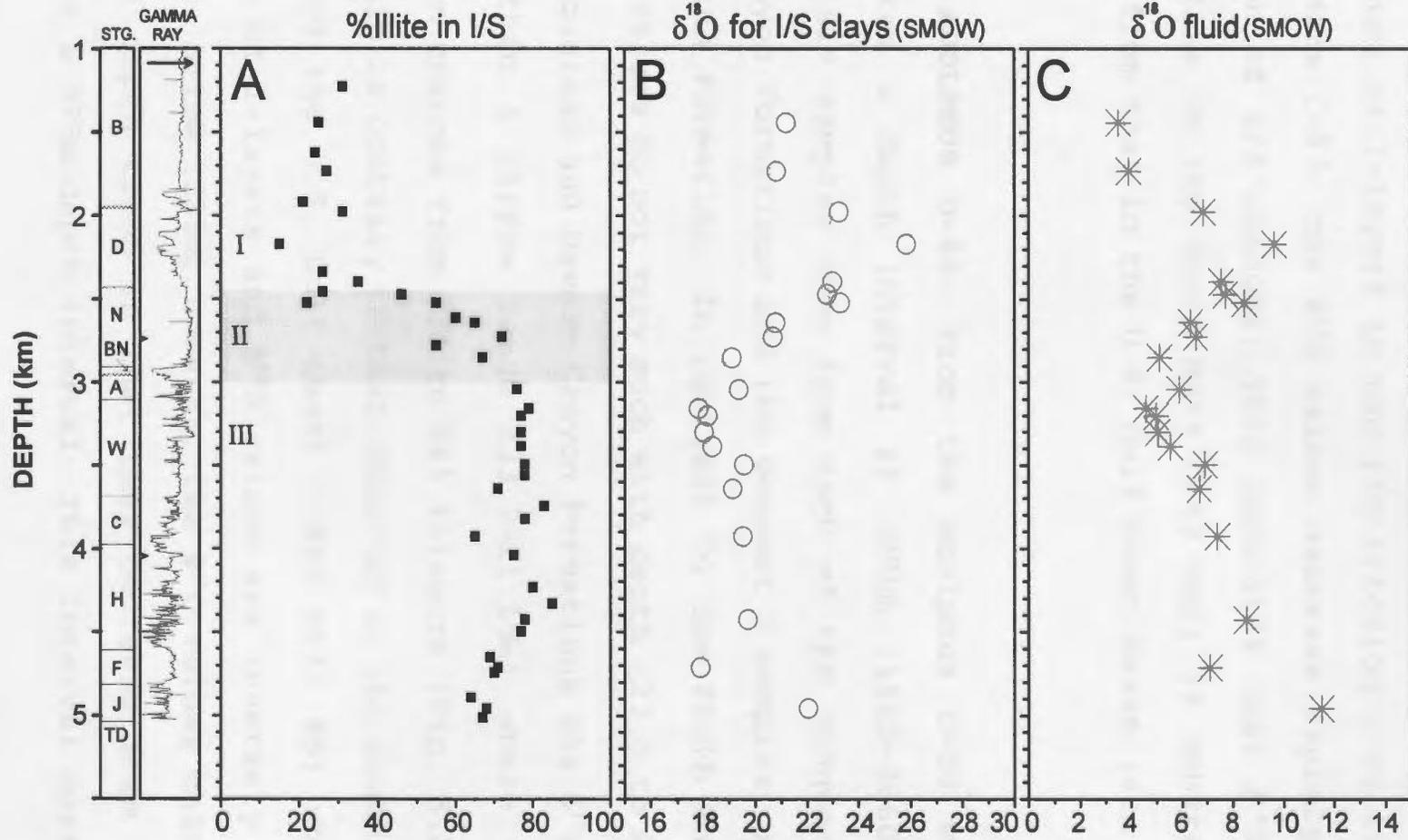
comparison see Fig. 5.1 this study and Yeh and Savin, 1977).

The $\delta^{18}O$ trend in the U.S. Gulf Coast is largely independent of the amount of I-layers in the I/S fraction (~40 to ~80%), in South Mara C-13, the $\delta^{18}O$ values decrease rapidly as the composition of I/S changes. This indicates that $\delta^{18}O$ versus depth profile in the South Mara C-13 well is substantially different from that in the U.S. Gulf Coast Basin (see section 5.4).

5.3.2 ADOLPHUS D-50: From the Adolphus D-50 well, 15 samples from a depth interval of 2095m (1565-3660m) were analyzed. Six samples came from each of the Banquereau and Dawson Canyon Formations and the deepest 3 samples came from the Nautilus Formation. In contrast to the South Mara C-13 well, $\delta^{18}O$ values do not vary much with depth (23.0 to 20.2‰). In the Banquereau and Dawson Canyon Formations the $\delta^{18}O$ values remain within a narrow range (23.0-21.1‰) where the I/S composition changes from 33% to 66% I-layers (Fig. 5.2). This relationship is contrary to that observed in the South Mara C-13 well and the U.S. Gulf Coast (CWRU well #6) where the percentage of I-layers and $\delta^{18}O$ values are inversely related with depth. Below 3285m, however, the $\delta^{18}O$ values change from the normal depth trend in that they decrease from 22.3 to 20.2‰ over a 375m depth interval. This interval corresponds

156

Figure 5.2: The proportion of illite-layers in illite/smectite (A), $\delta^{18}O$ of illite/smectite clays (B), and calculated isotopic composition of pore-water (C), versus depth for Adolphus D-50. Pore-water isotopic composition was calculated according to Savin and Lee (1988). All $\delta^{18}O$ values in SMOW. For abbreviations, see figure 3.3.

ADOLPHUS D-50
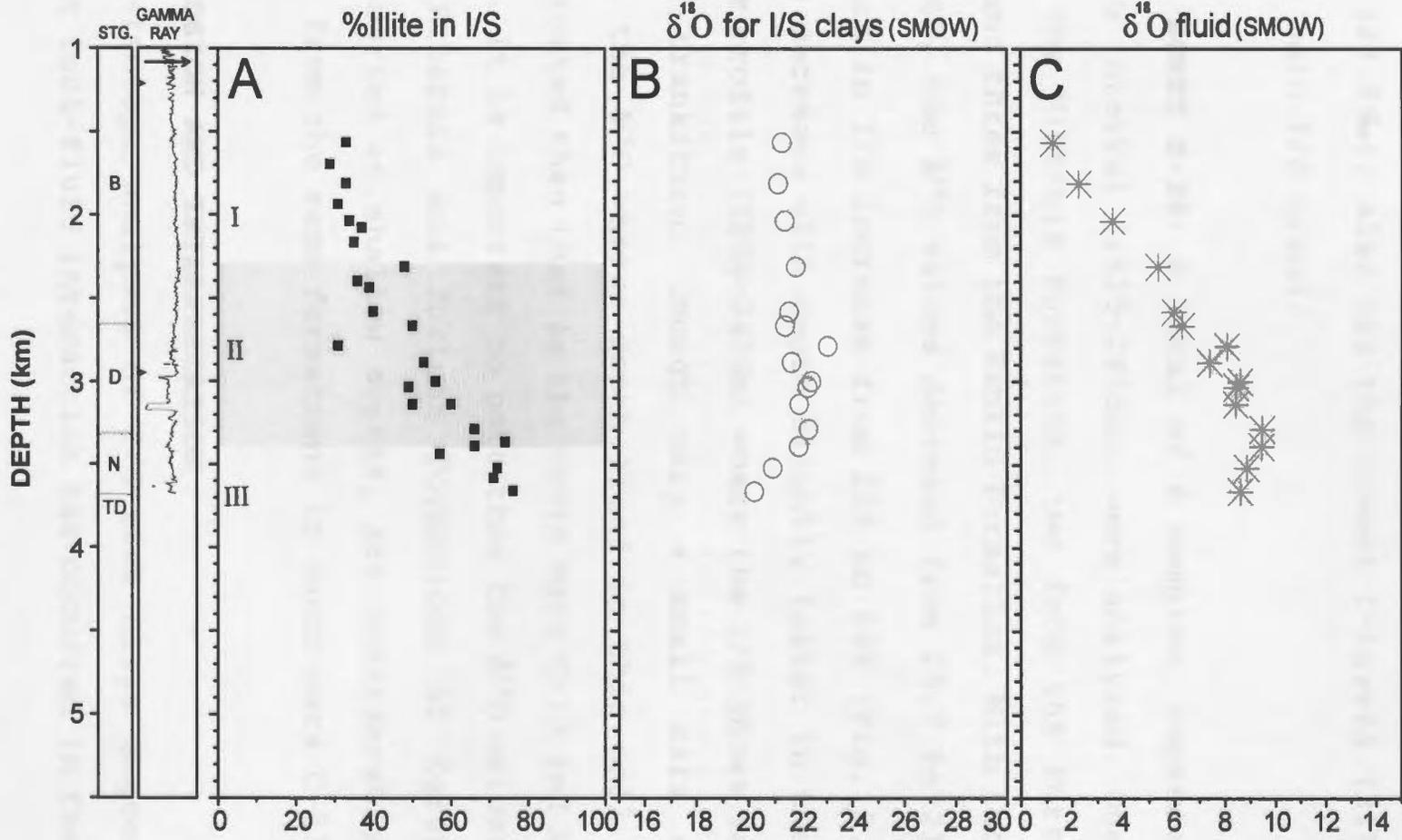
to the R1-ordered zone where I-layers increase up to 76%. It is important to note that sample 2785m, which has the highest $\delta^{18}O$ value (23.0‰), also has the lowest I-layers (31% I) and is off the main I/S trend.

5.3.3 EGRET K-36: A total of 6 samples, representing a 1310m depth interval (1625-2935m), were analyzed. One sample came from the Hibernia Formation, two from the Fortune Bay Formation and three from the Rankin Formation. With increasing burial depth, the $\delta^{18}O$ values decrease from 25.7 to 21.9‰ as the I-layers in I/S increase from 22% to 69% (Fig. 5.3). The $\delta^{18}O$ values decrease with depth slightly faster in the middle part of the profile (2100-2400m) where the I/S shows random to R1-ordered transition. Though only a small data set was collected, the $\delta^{18}O$ versus depth trend in this well appears less complicated than that in the South Mara C-13 and Adolphus D-50 wells. It is important to note that the $\delta^{18}O$ values of I/S from the Hibernia and Fortune Formations of Egret K-36, presently buried at shallow depths, are considerably higher than those from the same formations in South Mara C-13 well.

5.4 DISCUSSION AND INTERPRETATION

Oxygen-isotope analyses of I/S-rich clays suggest that significant rock-fluid interaction has occurred in the Jeanne

Figure 5.3: The proportion of illite-layers in illite/smectite (A) and $\delta^{18}O$ of illite/smectite clays (B) versus depth for Egret K-36. All $\delta^{18}O$ values in SMOW. For abbreviations, see figure 3.3.

EGRET K-36

| STG. | GAMMA RAY | %Illite in I/S | $\delta^{18}O$ for I/S clays (SMOW) |

A

B

DEPTH (km)

D
W
H
F
J
R
TD

I

II

III

0 20 40 60 80 100

16 18 20 22 24 26 28 30
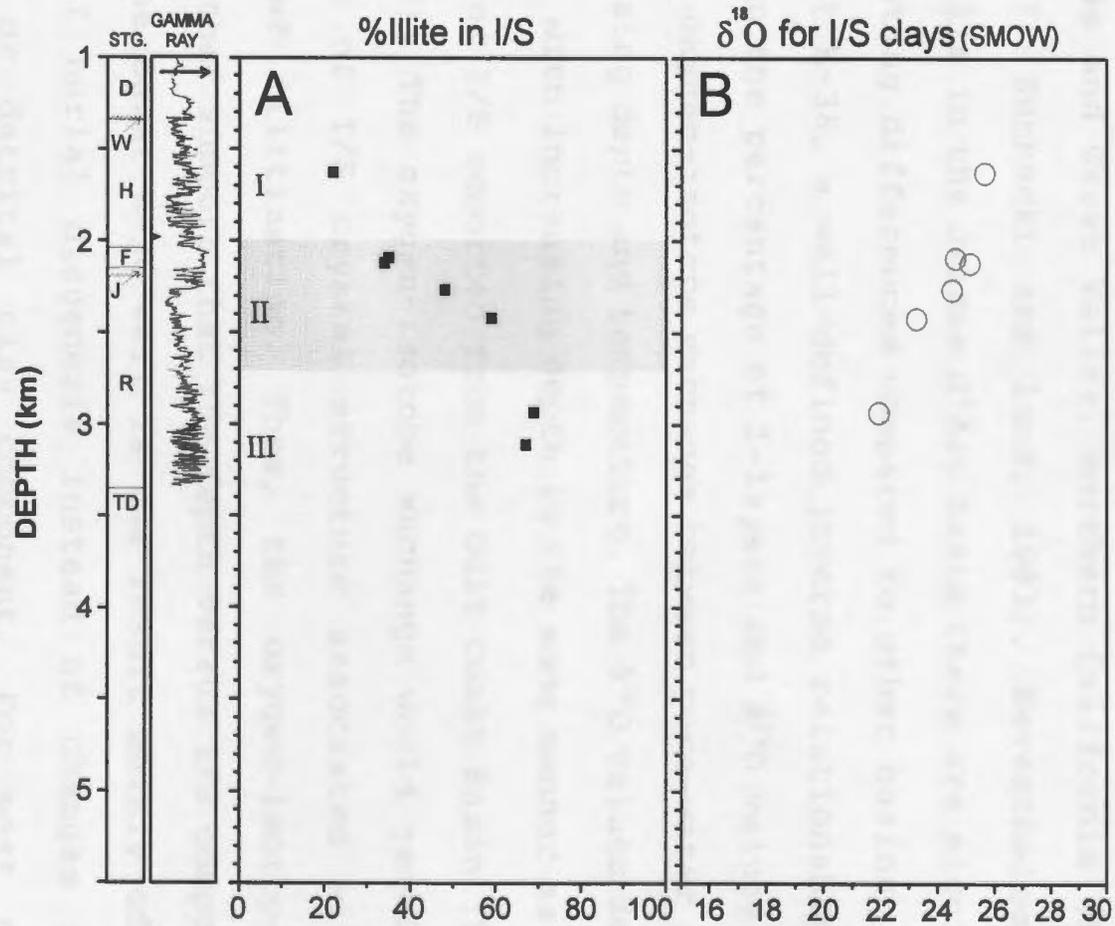
d'Arc Basin. As a result, the $\delta^{18}O$ values of I/S clays generally decrease and calculated $\delta^{18}O$ values of the pore-fluid, believed to be in equilibrium with fine clays, generally increase with increasing %illite in I/S. Overall, these results are similar to those reported for the Gulf Coast, Texas and Great Valley, northern California (Yeh and Savin, 1977; Suchecki and Land, 1983). Nevertheless, for specific wells in the Jeanne d'Arc Basin there are significant and interesting differences compared to other basins.

In Egret K-36, a well-defined inverse relationship (Fig. 5.3) between the percentage of I-layers and $\delta^{18}O$ values of I/S suggests an oxygen-isotope exchange between pore-water and I/S with increasing depth and temperature. The $\delta^{18}O$ values decrease about 3.7‰ with increasing depth in the same manner as do the $\delta^{18}O$ values of I/S reported from the Gulf Coast Basin (Yeh and Savin, 1977). The oxygen-isotope exchange would require re-structuring of I/S crystal structure associated with the processes of illitization. Thus, the oxygen-isotope data provide further support that the depth versus I/S composition trend in the Egret K-36 well is the result mainly of post-depositional burial diagenesis instead of changes in the provenance or detrital clay component. For most of the Adolphus D-50 well (down to 3300m), both I-layer content (31% to 66%I-layers) and $\delta^{18}O$ values of I/S (i.e. 1 permill) increase with depth (Fig. 5.2). This change in $\delta^{18}O$, though

162

small, is opposite to what is observed in the Egret K-36 well of the Jeanne d'Arc Basin and CWRU well #6 of the U.S. Gulf Coast (Yeh and Savin, 1977). However, the Gulf Coast study does report $\delta^{18}O$ values from 2 other wells (CWRU well #9 and #10; which are virtually ignored in the literature) in which the $\delta^{18}O$ values for I/S either remain constant with depth or increase about 3‰. The small increase in $\delta^{18}O$ in the Adolphus D-50 well could reflect an inheritance of oxygen-isotopes from a detrital component, but this is unlikely because no significant change in isotopic composition or I/S composition occurs across the stratigraphic boundaries. A preferred interpretation for the slight increase in $\delta^{18}O$ values with depth is that the pore-fluids in this well were slightly more enriched in ^{18}O compared to fluids in the Egret K-36 or Gulf Coast #6 cases. Such a slightly ^{18}O-enriched fluid would reflect an upward migration of deeper basinal fluids to shallower depths in the sediment column compared to the Egret or Gulf Coast #6 wells.

The ^{18}O values in the Adolphus D-50 well, however, decrease below 3300m (about 2‰) as I/S becomes R1-ordered (Fig. 5.2). Ordering of I/S probably involves a complete dissolution and re-precipitation of I/S and would be associated with a complete exchange of oxygen with pore-water, compared to partial exchange in reactions with random I/S (up to 65%;

163

Whitney and Northrop, 1988).

The ^{18}O of pore-water in sedimentary basins generally increases with time and temperature due to isotopic exchange associated with water-rock interaction, provided that the sediments are isolated from any influx of meteoric waters. The ^{18}O of pore-fluid in a sedimentary basin can increase to values of more than 10‰ (Sheppard, 1986; Wilkinson et al., 1992; Fig. 5.4). For example, pore fluids from the Gulf Coast basin have measured $\delta^{18}O$ values ranging from -1 to 10 permill with increasing depth (Fig. 5.4).

The results for two wells from the Jeanne d'Arc Basin show that $\delta^{18}O$ values calculated for the pore-water vary from 1.5 to 11.6 permill (Table 5.2). In the Adolphus D-50 wells, the $\delta^{18}O$ values of water increase progressively with depth and increasing burial temperatures, as would be expected for a typical, subsiding sedimentary basin (Fig. 5.5). The calculated oxygen isotopic composition of pore-waters from the Adolphus D-50 well overlaps quite closely with those of the Gulf Coast basin (Fig. 5.5). The absence of any pore-fluids with $\delta^{18}O$ values less than zero permill suggest that either the original pore-fluid was mainly of marine origin or that the isotopic composition of any meteoric water has been significantly modified by water-rock interaction. The regular variation with depth of the pore-fluid compositions for Adolphus D-50 indicates a lack of significant vertical

164

Figure 5.4: (A) Depth versus oxygen isotopic composition of pore-waters within mud dominated sediments in Bengal Fan (Boulegue and Bariac, 1990) and U.S Gulf Coast (Land, L.S., unpublished data). (B) Temperature versus oxygen isotopic composition of pore-water in U.S. Gulf Coast calculated from $\delta^{18}O$ of illite/smectite clays (Yeh and Savin, 1977).

ADOLPHUS D-50

Figure 5.5. Comparison of calculated oxygen isotopic composition of pore
-waters from Adolphus D-50 with three U.S. Gulf Coast wells.

Table 5.2: Data (Temperature, %I in I/S, and $\delta^{18}O$ I/S) used to calculate the isotopic composition of pore-water according to Savin and Lee (1988). Temperature values were calculated from vitrinite reflectance data according to Barker (1988).

Well Name	Depth (m)	R_o	T°C	T^2K	%I in I/S	$\delta^{18}O$ Clay	$\delta^{18}O$ Water
South Mara C-13	1440	0.470	69	116964	25	21.18	3.72
	1730	0.496	75	121104	27	20.81	4.12
	1975	0.519	79	123904	31	23.23	7.07
	2170	0.538	83	126736	15	25.83	9.89
	2395	0.561	87	129600	35	22.99	7.79
	2470	0.569	89	131044	46	22.78	7.95
	2520	0.575	90	131769	55	23.29	8.69
	2640	0.588	92	133225	65	20.78	6.53
	2725	0.597	94	134689	72	20.67	6.72
	2850	0.611	96	136161	67	19.10	5.28
	3040	0.634	100	139129	76	19.37	6.05
	3155	0.647	102	140625	79	17.82	4.73
	3200	0.653	103	141376	77	18.17	5.15
	3300	0.665	105	142884	77	18.03	5.19
	3385	0.676	107	144400	77	18.35	5.69
	3495	0.690	109	145924	78	19.55	7.08
	3640	0.709	112	148225	71	19.14	6.83
	3925	0.748	117	152100	65	19.52	7.56
	4425	0.821	127	160000	78	19.70	8.69
	4710	0.866	133	164836	71	17.89	7.25
	4955	0.907	137	168100	68	22.04	11.65
Adolphus D-50	1565	0.395	51	104976	33	21.28	1.49
	1810	0.428	59	110224	33	21.14	2.49
	2035	0.461	67	115600	34	21.39	3.82
	2310	0.504	76	121801	48	21.82	5.58
	2580	0.550	85	128164	40	21.56	6.21
	2665	0.565	88	130321	50	21.41	6.53
	2785	0.588	92	133225	31	23.06	8.33
	2884	0.607	96	136161	53	21.65	7.63
	3000	0.631	100	139129	56	22.43	8.84
	3032	0.637	101	139876	49	22.27	8.68
	3135	0.659	104	142129	50	21.94	8.65
	3285	0.692	109	145924	66	22.31	9.68
	3390	0.716	113	148996	66	21.93	9.65
	3520	0.747	117	152100	72	20.92	9.05
	3660	0.781	122	156025	76	20.21	8.79

movement of deep, ^{18}O-rich basinal fluids, though minor movement is inferred in the Adolphus D-50 well (see earlier discussion in this section).

The I/S clays from the South Mara C-13 well can be discussed as sub-groups defined in terms of their geologic setting and δ^{18}O values (Fig. 5.1). The <u>first sub-group</u> includes the two uppermost samples in the well with δ^{18}O values near 21‰ (Table 5.2 and Fig. 5.1). These samples are from the Banquereau Formation and have the same isotopic composition and almost similar I/S content as samples from the Banquereau Formation in the Adolphus D-50 well (Fig. 5.2). The similarities between the two wells suggest that the clays from this formation in both wells have a similar origin.

The <u>second sub-group</u> from the South Mara C-13 well includes clays from a depth of 1975m to 2520m having δ^{18}O values near 23-25‰ (Table 5.2 and Fig. 5.2). These clays are considered here to occur in an "anomalous zone" because they have higher calculated pore-fluid compositions than those observed in Adolphus D-50 at an equivalent depth, and there is a rapid and large increase in I/S composition from 30%I to 55%I. The elevated δ^{18}O values are not a direct result of the rapid increase in I/S composition. In Egret K-36 and Adolphus D-50 wells, the increase in I-layers in I/S (22% to 50%I) are not associated with any distinct increases in the δ^{18}O values.

169

It is noteworthy that the vitrinite temperatures for the "anomalous zone" in the South Mara C-13 well are approximately 10 degrees warmer than those for an equivalent depth interval from the Adolphus D-50 well. The interpretation for the isotopic data for the "anomalous zone" is that the $\delta^{18}O$ values of the clays reflect alteration/formation from a deeper, warm, ^{18}O-rich basinal fluid. This interpretation requires upward movement of fluids from a deeper part of the basin, a process which is supported by the presence of deep, trans-basinal faults and associated normal faults that typify the Trans-Basinal Fault area. Furthermore, the down-hole gamma-ray log for South Mara C-13 shows that the top of the "anomalous zone" corresponds to the top of a sand-body that defines the Dawson Formation (Fig. 5.1). The sand-rich nature of the sediments should be associated with increased permeability which would facilitate local migration of the deeper fluid. The presence of the deeper warmer fluid in the sand-body, presumably rich in cations such as K^+, could account for the 'step-like' and variable I/S compositions in this relatively narrow depth interval of South Mara C-13 compared to that in Egret K-36 and Adolphus D-50 (also see section 6.7).

Potassium-rich fluids have been reported as accelerating the transformation of I/S to illite-rich clays at temperatures above 60°C (Perry and Hower, 1970). This model involving the upward movement of deep basinal fluid along faults is also

supported by various studies tracing the source of hydrocarbons and maturation of source rock in the Jeanne d'Arc Basin (Creaney and Allison, 1987; Von der Dick et al., 1989). Results of these tracer studies indicate that the deeply buried, organic-matter rich Kimmeridgian shale is the main source rock for all important hydrocarbon discoveries in the Jeanne d'Arc Basin implying upward migration of hydrocarbons (as much as 2-3km) into the overlying Aptian/Albian reservoir rocks.

Below the "anomalous zone" in the South Mara C-13 well, the third sub-group includes I/S clays from a depth of 2640m to 4710m. Determining the actual boundary between the "anomalous zone" and this third sub-group is somewhat problematic. The change is herein linked to the sharp decrease below 2520m in the $\delta^{18}O$ value of the clay from values of above 23 permill to less than 21 permill (Table 5.2). This break also corresponds to a decrease below 5 permill for the $\delta^{18}O$ value calculated for pore-fluids. However, in detail, from a depth of 2640 to 3040m, the $\delta^{18}O$ values of the clays and the pore-fluids are intermediate between those associated with the "anomalous zone" and those below 3155m (a so-called "normal zone"). The preferred interpretation of these intermediate isotopic values is that this zone reflects a mixing of fluids from the overlying "anomalous zone" and the underlying "normal zone" (below 3155m). The gamma-ray logs indicate the presence

171

of sandy intervals in the Avalon-Ben Nevis Formations, which would facilitate any mixing process.

Other noteworthy observations from the South Mara C-13 well include the fact that there is no significant change in the $\delta^{18}O$ values of the clays across the Nautilus-Avalon stratigraphic boundary thereby reinforcing the earlier interpretation that sediment provenance is not a factor and that the isotopic results reflect diagenetic events. The $\delta^{18}O$ values of the I/S clays in South Mara C-13 are generally 2-3 permill lower than those from the Adolphus D-50 well, and up to 5 permill lower than those from the Egret K-36 well. One possible interpretation for the decreased $\delta^{18}O$ values in South Mara C-13 could involve the influx of meteoric water to the area, however this is viewed as unlikely. The Egret K-36 well is the closest to the source area of the sediment. If meteoric water were important, the Egret K-36 well should have clays with lower $\delta^{18}O$ values than the South Mara C-13 well.

The changes in calculated oxygen isotopic compositions with depth of pore-fluid in the South Mara C-13 well differ appreciably compared to the "normal" trends as defined by the Adolphus D-50 and Gulf Coast wells (Fig. 5.6). The presence of a component of ^{18}O-rich fluids over a wide depth interval of 1975m to 3040m reflects the vertical movement of deep basinal brines along faults and sandy intervals.

172
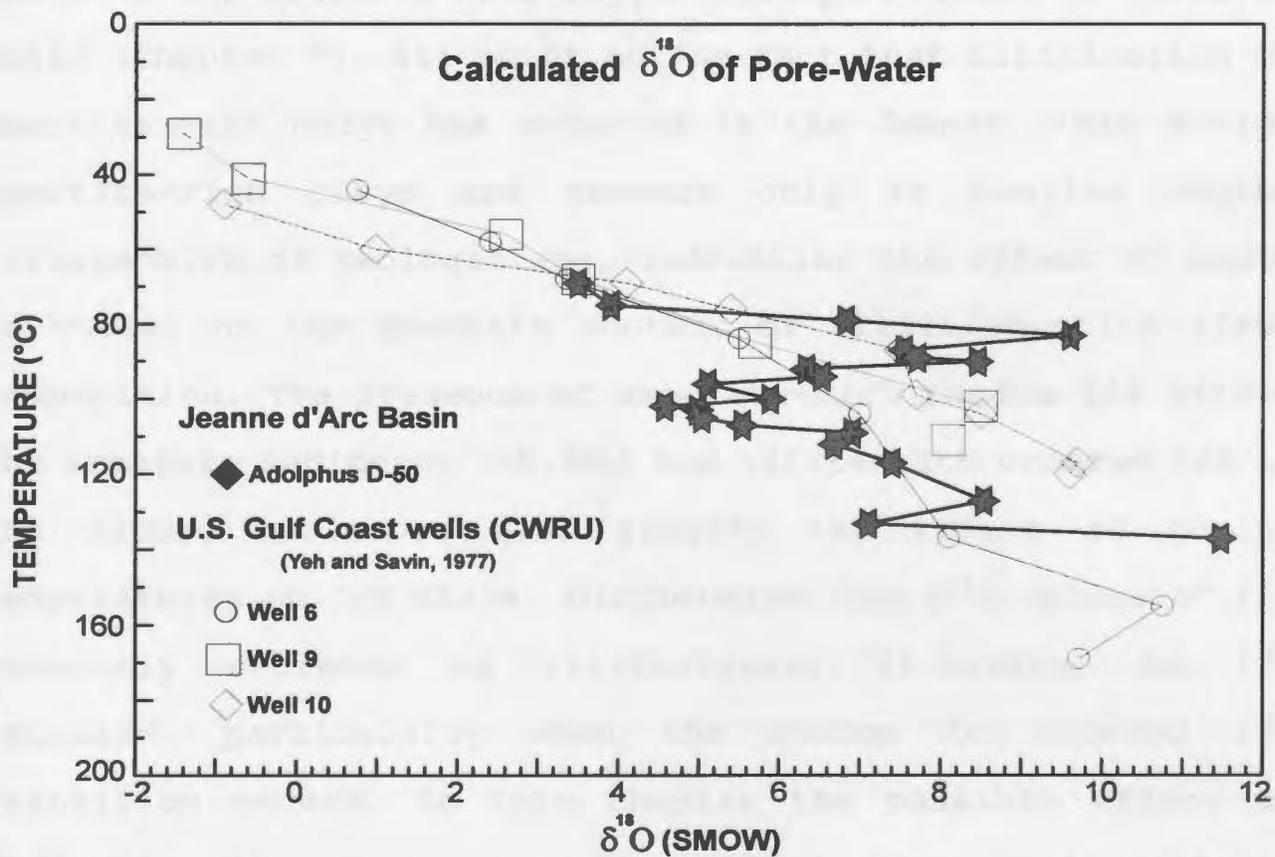
Figure 5.6. Comparison of calculated oxygen isotopic composition of pore-waters from South Mara C-13 with three U.S. Gulf Coast wells.

CHAPTER VI

DISCUSSION AND INTERPRETATION

6.1 INTRODUCTION

Basin-wide XRD study of fine-grained clays (Chapter III) and their comparison with vitrinite reflectance (R_o) data (Chapter IV) together with oxygen-isotope studies on selected wells (Chapter V), all point to the fact that illitization of smectite-rich clays has occurred in the Jeanne d'Arc Basin. Smectite-rich clays are present only at shallow depths irrespective of geologic age, indicating the effect of depth of burial on the smectite content of illite/smectite (I/S) composition. The presence of smectite-rich random I/S within the immature sediments (<0.5R_o) and illite-rich ordered I/S in the mature sediments also suggest the effect of burial temperatures on I/S clays. Furthermore, the $\delta^{18}O$ values of I/S generally decrease as illite-layers (I-layers) in I/S increase, particularly when the random to ordered I/S transition occurs. In this chapter the possible effect of different parameters on the illitization and regional variations of I/S diagenesis are discussed. The final part of the chapter deals with the implications of the I/S data in the Jeanne d'Arc Basin.

174

6.2 TEMPERATURE OF ILLITIZATION

Several parameters are considered to influence the I/S reactions. Among these, temperature and the availability of K^+ are by far the most important parameters (Hower et al., 1976; Bruce, 1984; Pollastro, 1993 and others). According to several workers, illitization of smectite layers in I/S for sediments older than 5MY begins at about 50°C, the random to R1-ordered transition occurs near 100±20°C, and long-range R3-ordering emerges at 175±5°C (for a literature review see Hoffman and Hower, 1979; Jennings and Thompson, 1986; Lindgreen, 1991). Thus, two changes in I/S layer-structures at two threshold temperature zones (100±20°C and 175±5°C) are considered important in studying the thermal maturity of sedimentary rocks since much of the oil and gas are generated between 80°-175°C temperature zone(Pollastro, 1993).

Other factors such as bulk-rock composition, pore-water composition, heating time, porosity/permeability (rock/water ratio) are considered secondary (Pollastro, 1993) but may play a significant role under special geologic circumstances (Jennings and Thompson, 1986; Ramseyer and Boles, 1986; Schoonmaker et al., 1986; Howard, 1987; Abercrombie et al., 1994).

6.2.1 TEMPERATURE AND R1-ORDERING OF ILLITE/SMECTITE

Regarding present day temperatures where the random to R1-ordered I/S transition is first observed in the Jeanne d'Arc Basin, the wells can be grouped into two classes based on temperature: (1) 100±20°C group and (2) <70°C group.

6.2.1.1 (1) 100±20°C GROUP: R1-ordering in the majority of the wells (11 out of 16) begins at about 100±20°C (Table 4.1). This R1-ordering temperature agrees well with those reported from several other sedimentary basins, such as the U.S. Gulf Coast (Perry and Hower, 1970; Hower et al., 1976; Freed and Peacore, 1989), North Sea (Pearson and Small, 1988), offshore Brazil (Chang et al., 1986); and Niger Delta (Velde et al., 1986). These basins (like the Jeanne d'Arc Basin) are presently active and their temperatures are considered close to the maximum temperatures to which these sediments were ever subjected. This similarity in R1-ordering temperatures confirms the fact that temperature is one of the most important controlling factors for R1-ordering of I/S layers. Furthermore, the temperature values recorded in these wells seem currently close to their maximum temperatures. Some variation of ordering temperature (80°-118°C) may, in part, be due to the availability of K^+ or bulk rock composition (see below).

176

6.2.1.2 (2) <70°C GROUP: Five wells (Hebron I-13, North Trinity H-71, Egret K-36, Egret N-46, and Cormorant N-83) fall in the second group where R1-ordering first appears at less than 70°C (69°-54°C) present temperatures. These temperatures are lower than would be normally expected for a random to R1-ordered I/S change. The possibility that the I/S clays were originally illite-rich and ordered derived from a detrital source for these wells at the time of deposition has been eliminated in earlier discussion (see section 3.7).

The present temperature may not reflect the temperature of the illitization in Egret K-36, Egret N-46, North Trinity H-71, Hebron I-13 and Cormorant N-83 wells. Based on the fact that significant amounts of the sedimentary section are missing in the south (Egret K-36, Egret N-46, and Cormorant N-83) along the Avalon Unconformity (McAlpine, 1990), it is probable that prior to the uplift and erosion the Southern part of the Jeanne d'Arc Basin was either buried deeply enough to cause ordering at higher temperatures or that the geothermal gradient was initially higher for these wells.

An independent control on temperature from vitrinite reflectance data provides support for this interpretation. In Egret N-46, R1-ordering occurs at 0.65% R_o value which is close to several other wells in the main part of the Jeanne d'Arc Basin. Using the correlation of Barker (1988), a vitrinite reflectance value of 0.65 corresponds to a maximum

paleotemperature of about 103°C. This temperature value is close to that inferred for R1-ordering in several other wells of the Jeanne d'Arc Basin, where significant amounts of uplift did not occur (see section 6.2.1.1). Thus, R1-ordering temperature in Egret N-46 must be near ~100°C instead of the present day low temperature (59°C). A similar scenario can be envisioned for Egret K-36, Cormorant N-83, and North Trinity H-71 wells, although an independent temperature control from these wells is presently not available.

Heling (1974) reported a present temperature of only 72°C for the R1-ordering (disappearance of the 17Å peak) from the Rhine Graben. He did not, however, study R_o or any other maturity parameters to confirm whether illitization occurred at present temperature or if in the past the sediments were subjected to higher temperatures. For this reason his conclusion is noted cautiously.

6.2.2 TEMPERATURE AND R3-ORDERING OF ILLITE/SMECTITE

A change from R1 to R3-ordering in I/S with 85-92% I-layers was observed in only twelve samples (from seven wells) which are usually buried below 4000m (Table 4.2). This R3-ordering occurs in wells where the geothermal gradient is slightly higher (30.6°C/km) compared to the average value of the Jeanne d'Arc Basin (27.5°C/km) as reported by Correia et al. (1990).

Except for the North Ben Nevis P-93 well, the present temperatures for the conversion of R1-ordered to R3-ordered I/S vary from 128°-170°C (average 140°C) and R_o values vary from 0.72 to 1.10 (Table 4.2). These present temperatures are lower (up to 45°C) than reported from other sedimentary basins (175±5°C; Hoffman and Hower, 1979; Jennings and Thompson, 1986; Velde et al., 1986; Pollastro, 1993). The argument that the low temperature R3-ordered I/S observed in this study could have been detritus derived from older deeply buried (≥175°C) rocks is not supported if basin-wide I/S data are considered (see section 3.7). The equivalent stratigraphic units in the south (close to the source area) at shallow depths show smectite-rich random and R1-ordered I/S (see Chapter III). In addition, $\delta^{18}O$ of I/S clays generally decreases with increasing I-layers (South Mara C-13 and Egret K-36) suggesting the effect of post-depositional burial diagenesis instead of changes in the provenance or detrital clay component. An alternate explanation may be that in the past temperatures at these sample locations were higher (up to 45°C) compared to the present values, either due to a higher paleogeothermal gradient or to upward movement of hot deep basinal fluids, possibly along faults. Large amounts of uplift/erosion in these areas did not occur.

Depth versus vitrinite reflectance profiles for several wells suggest that the paleogeothermal gradient in the deeper

179

sediments (>4000m) was not significantly higher than in post-rift sediments (see Chapter IV). If the paleogeothermal gradient in the older sediments was higher, then a normal burial temperature of $175\pm5°C$ would require vitrinite reflectance values to be near ~1.3% (Barker, 1988). In this study, the R3-ordered I/S occurs at vitrinite reflectance values lower than 1.3 and indicate that higher temperatures ($175\pm5°C$) did not occur unless the reflectance values from the vitrinite particles were suppressed by oil staining. Thus, either R3-ordered I/S containing sediments were never subjected to higher temperatures or vitrinite particles failed to respond to such higher temperature anomalies. The possibility that oil staining has suppressed reflectance values from vitrinite particles cannot be completely excluded.

It is interesting to note that other workers (Środoń, 1979; Glasmann et al., 1989) have also reported the occurrence of R3-ordered I/S at 0.72-1.06% R_o, which is in agreement with the present study (Table 4.3). Środoń (1979) did not give present temperature data from either of the two wells he studied nor did he give any tentative temperature values for 0.85-0.90% R_o values where the R1 to R3 changes occur. Glasmann et al. (1989) reported the occurrence of R3-ordered I/S at >0.72-0.80% R_o at $150°-160°C$ present temperatures. In fact their data suggest even lower temperatures (~$140°C$). They suggested that deeper warm fluid rich in K^+ associated with

180

hydrocarbon migration may have moved upward prior to deep burial of sediments.

In North Ben Nevis P-93, the R3-ordered I/S occurs at an apparently lower present temperature (88°C) and an apparently lower vitrinite reflectance value (0.50) than expected (see Table 4.2). This anomaly may be due to the fact that there are no vitrinite sample coincident with the clay sample. Only radiogenic isotopic dating can provide an answer to this anomalous sample. If the radiogenic isotopic age is younger than the stratigraphic age, it would indicate the diagenetic origin for R3-ordered I/S.

6.3 R3-ORDERED ILLITE/SMECTITE AND KAOLINITE

Conflicting results have been reported in the literature regarding the R3-ordered I/S and kaolinite. Earlier workers have observed that kaolinite in shales is lost before the appearance of R3-ordered I/S (Steiner, 1968; Dunoyer de Segonzac, 1970; Weaver and Beck, 1971; and Velde et al., 1986). Results of this Jeanne d'Arc project show that kaolinite persists into R3-ordered I/S zone, although its abundance appears to decrease. A similar relationship was observed by Glasmann et al. (1989) in the North Sea, and by Jennings and Thompson (1986) in the Colorado River Delta.

6.4 POSSIBLE SOURCE OF POTASSIUM

The conversion of smectite layers into illite requires an input of K^+ ions. Dissolution of K-feldspar is considered the most important source of K^+ for a smectite to illite reaction (Hower et al., 1976; Boles and Franks, 1979; Heling, 1978; Pearson and Small, 1988). A lack of K^+ source has been shown to slow down the I/S diagenesis (Pearce et al., 1991; Altaner et al., 1984; Pearson et al., 1983, Arostegui et al., 1991).

K-feldspar was not detected by XRD in either rift or post-rift bulk-shale samples of the South Mara C-13. The possibility that K-feldspar was originally available from the source area for the rift sediments (of South Mara C-13), whereas it was not available for the post-rift sediments, would imply that a significant change in the source area had occurred. However, bulk chemical analyses of South Mara C-13 rocks show no significant changes with depth, suggesting that K-feldspar was probably not available for either the rift or the post-rift sediments.

Detrital mica and illite have also been suggested as possible sources of K^+ for illitization (Perry and Hower, 1970, Hower et al., 1976; Eslinger and Sellars, 1981; Freed, 1981; Lindgreen, 1991; Awwiller, 1993). Rift and transitional sediments (Nautilus and Ben Nevis Formations) appear to contain more micaceous clay minerals in coarser clay fractions, as indicated by a strong 10Å peak. In the absence

182

of K-feldspar, assuming no external source for K$^+$, the breakdown of detrital illite and mica may have provided K$^+$ for illitization. In several wells (i.e. South Mara C-13, North Ben Nevis P-93, North Trinity H-71, Whiterose J-49, Bonanza M-71) an increase in I-layers and ordering occurs in transitional and rift sediments which contain more 10Å micaceous material.

Lindgreen (1991) documented illitization in the Central Trough, North Sea, and the Norwegian Danish Basin where bulk-shale contains no K-feldspar. He suggested that detrital illite may have provided some of the required K$^+$. Eslinger and Sellars (1981) also suggest that K$^+$ can be derived from the breakdown of detrital mica when insufficient K-feldspar is present for the I/S reaction. However, Heling(1978) and Pearce et al. (1991) did not believe in simultaneous decomposition of muscovite and illite, and formation of authigenic illite. If the dissolution of the least stable illitic phase or mica is not possible (Heling, 1978; Pearce et al., 1991), then in the absence of K-feldspar, K$^+$ may have been supplied from deeper levels and a distant source by pore-water possibly moving along the faults and permeable sandy intervals. In South Mara C-13 the high $\delta^{18}O$ values for calculated pore-fluid compositions, between 1975-3040m, indicate upward migration of deeper ^{18}O-rich fluids (see Chapter V).

In the Northern area and the Outer Ridge Complex area

where the post-rift sediments are thick, the record shows a relatively slower rate of illitization compared to the rift and the transitional sediments probably because of a lack of K^+ (also see section 6.7).

6.5 THE ROLE OF GEOLOGIC TIME IN ILLITIZATION

In addition to temperature and the availability of K^+ in the pore-water, the age of sediments and duration of heating are considered important factors for the advancement of the illitization reaction (Eberl and Hower, 1976; Roberson and Lahann, 1981; Pytte and Reynolds, 1989). For example, sediments younger than the Mid-Tertiary require higher temperatures for the illitization reaction (Bruce, 1984; Jennings and Thompson, 1986). Similarly, sediments heated by a short-lived event (<3MY) either due to very rapid burial at the critical reaction temperature (~120°-140°C) (Ramseyer and Boles, 1986) or due to igneous intrusion (Smart and Clayton, 1985) are known to show less advanced stage of I/S diagenesis compared to a long-term burial diagenetic setting. In a long-term burial diagenetic setting (i.e. Jeanne d'Arc Basin) with a longer duration of heating (>5MY) the effect of time on I/S diagenesis is less important than temperature, particularly for Mid-Tertiary to Cretaceous or even Mississippian-age sediments (Weaver, 1978; Hoffman and Hower, 1979; Pollastro, 1993; Pollastro and Schmoker, 1989; Deng et al., 1996). The

184

above review on previous work suggests that the influence of time on I/S diagenesis must be considered when Miocene or younger sediments, or a sedimentary sequence subjected to short-lived thermal pulse is compared with a long-term (>25MY) burial diagenetic setting.

About 90 percent of the samples used in this study represent Mid-Tertiary to Lower Cretaceous age and the remaining samples are mainly from the Upper Jurassic. None of the wells studied here have encountered igneous rocks or the presence of igneous activity below the total drilled-depths (probably excluding Bonanza M-71 well). The Jeanne d'Arc Basin is characterized by a long burial history. All samples used in this study have experienced longer duration of heating. Considering the results of previous workers (Weaver, 1978; Hoffman and Hower, 1979; Pollastro, 1993; Pollastro and Schmoker, 1989), geologic time may not have played a significant role on I/S diagenesis in the Jeanne d'Arc Basin.

If geologic time was a significant factor, then the I/S reaction must have been at a more advanced stage in older Jurassic/Lower Cretaceous rocks compared to Mid-Tertiary sediments. This, however, is not the case because in several wells (Egret K-36 and Egret N-46, Gambo N-70, Port au Port J-97, and Voyager J-18) Jurassic/Lower Cretaceous sediments at less than 2000m depths still show random I/S with a higher percentage of smectite layers. Furthermore, the R1-ordered I/S

in the Jurassic rocks of Egret N-46 emerged at $0.65R_o$ value instead of occurring at lower organic maturity, if time was a factor to enhance the illitization reaction. Thus, geologic time has not played a significant role in I/S diagenesis for samples used in this project.

6.6 EFFECTS OF LITHOLOGY AND INHIBITING CATIONS ON ILLITE/SMECTITE COMPOSITION

Although it appears that burial temperatures have played an important role in the smectite to illite transformation and the ordering of I/S, there are numerous small irregularities and minor reversals in the I/S composition. These could be due to local variations in lithology, porosity/permeability, and/or inhibiting cations (Mg^{2+}, Ca^{2+}, Na^+) in the pore-fluid.

Silty-shale and shales associated with sandstone-rich intervals commonly show 10-20% more I-layers compared to nearby thick homogeneous shales, particularly in the ordered I/S series. For example, I/S from the sand-rich Hibernia Formation in South Mara C-13, North Trinity H-71, and Hebron I-13 wells contains 10-20% higher I-layers compared to the nearby Fortune Bay Formation. The Catalina Member and the upper part of the Whiterose Formation in South Mara C-13, which contain more silt and sand, also show slightly more I-layers, as do the sand-rich Avalon/Ben Nevis Formations of the North Trinity H-71.

186

These silty/sandy zones probably provided easy pathways for the migration of pore-fluids carrying K^+ and other cations due to higher porosity/permeability thus causing a greater rate of illitization. It is important to note that the Trans-Basinal Fault area is characterized by numerous faults which rarely extend into post-rift sediments (Dawson and Banquereau Formations). These faults may have provided access for deep basinal K^+-rich fluids into the sandy/silty intervals for I/S diagenesis. The oxygen isotopic data from South Mara C-13 discussed in section 5.4 also suggest vertical migration of deep basinal fluids in the Trans-Basinal Fault area. Hydrothermal experiments by Whitney (1990) show that higher water/rock ratio can increase the processes of illitization.

While I/S from sandy/silty zones generally show higher I-layers in I/S, it is interesting to note that most of the reversals in I/S composition correspond to thin limestone beds (Petrel Limestone "A" Marker Member, "B" Marker Member). Other reversals occur in the Fortune Bay Formation (South Mara C-13, Hebron I-13, North Trinity H-71) and less commonly in the Jeanne d'Arc Formation. This reversal in I-layers can be explained either due to higher concentration of inhibiting cations in the pore-fluids (Mg^{2+}, Ca^{2+}) or due to reduction of porosity/ permeability by cementation. Pore-water rich in Mg^{2+}, Ca^{2+}, Na^+ has been suggested by laboratory experiments to slow down the illitization reaction by inhibiting K^+ fixation

187

(Eberl, 1978; Roberson and Lahann, 1981).

Not all I/S samples close to the limestone beds show an impeded I/S reaction (e.g. "B" Marker Member in Whiterose J-49, "A" and "B" Marker Members in Nautilus C-92). More recently, experimental work by Huang et al. (1993) shows that the effect of inhibiting cations is significantly less than previously thought and that their effect is important only at the early stages of I/S reaction in random I/S series. Reversal in random I/S were observed in several samples of Whiterose J-49, South Tempest G-88, North Dana I-43 wells.

Several reversals occur in the ordered I/S series where the I-layer content is greater than or equal to approximately 60%. These shales were probably cemented after reaching the ordering stage. Further reactions may have been prevented due to lack of enough pore-fluids and reacting cations (K^+ and Al^{3+}). The occurrence of such reversals in the Fortune Bay Formation (South Mara C-13, Hebron I-13, North Trinity H-71) supports this interpretation since this formation is believed to act as a seal for overpressures in much of the basin (McAlpine, 1990).

Nadeau and Reynolds (1981) found that the amount of I-layers in I/S was lower in calcareous than in non-calcareous rocks. Ramseyer and Boles (1986) also noticed that cemented sandstones in San Joaquin Basin, California contain fewer I-layers in I/S compared to uncemented sandstone. These studies

188

suggest that some of the reversals in I/S composition (less I-layers) observed in this study could be due to cementation. Future petrographic studies should be pursued when samples become available.

6.7 REGIONAL VARIATION OF ILLITE/SMECTITE DIAGENESIS IN THE JEANNE D'ARC BASIN

The drill-holes studied in the Jeanne d'Arc Basin have been grouped into four areas as described in Chapter III and IV. In Fig. 6.1, various I/S composition-depth profiles for each area are combined. It is clear that in each area I/S composition-depth profiles show characteristic similarities, although within each area some differences are present.

6.7.1 TRANS-BASINAL FAULT AREA: All wells in the Trans-Basinal Fault area show a relatively rapid ('step-like') increase (from 25/30% to ≥75%) of I-layers in I/S (Fig. 6.1A). With the exception of North Trinity H-71, the rapid increase occurs over a 550-600m depth interval between 60°-95°C present temperatures. R1-ordering generally occurs at 80°-90°C and 0.53 mean R_o value. A systematic trend observed in 40 samples from the South Mara C-13 supports the validity of the trends from other wells of the Trans-Basinal Fault area where the sample density is lower.

This rapid increase in I-content occurs in the Nautilus

Figure 6.1: Percent illite-layers versus depth for the (A) Trans-Basinal Fault, (B) Northern, (C) Outer Ridge, and (D) Southern areas of the Jeanne d'Arc Basin. Note a rapid increase of illite-layers (2500-3000m) in Trans-Basinal Fault area compared to Northern and Ridge areas. In the Southern area, illite-rich illite/smectite occurs at relatively shallower depths than the areas to the north. For some irregularities in the illite/smectite composition, see section 6.6 and 6.7. F=Fortune Bay Formation, J=Jeanne d'Arc Formation. For location of wells, see figure 2.2.

Trans-Basinal Fault Area

A

Hebron I-13
N. Trinity H-71
S. Mara C-13
Nautilus C-92
N. B. Nevis P-93

Northern Part of the Basin

B

Whiterose J-49
Adolphus D-50
W. F. Foam L-23
Conquest K-09

Outer Ridge Complex

C

Slow I/S
Diagenesis

N. Dana I-43
Bonanza M-71
Dominion O-23
S. Tempest G-88

Southern Part of the Basin

D

Egret N-46
Cormorant N-83
Egret K-36
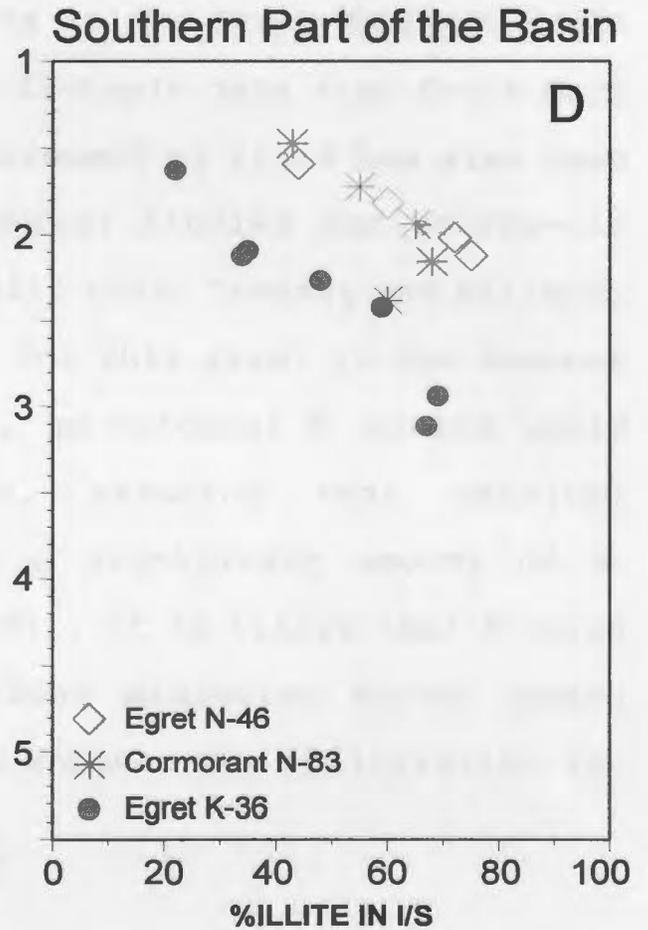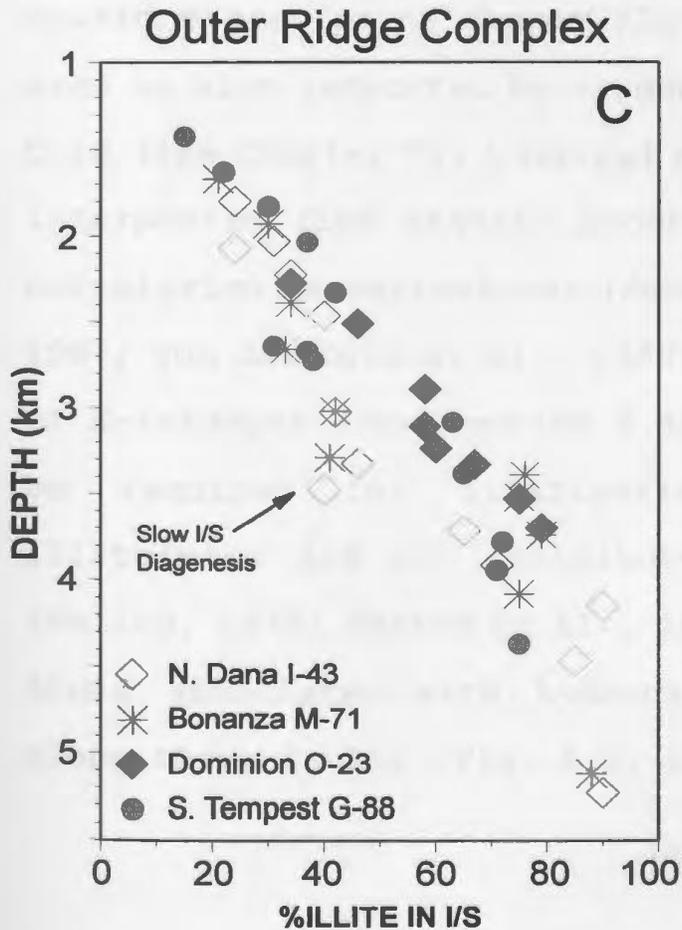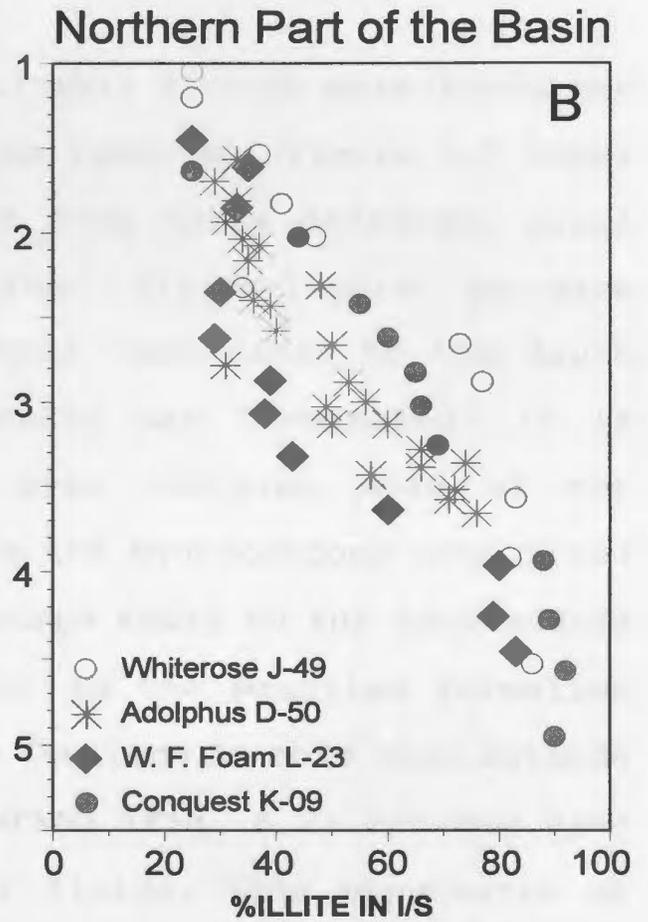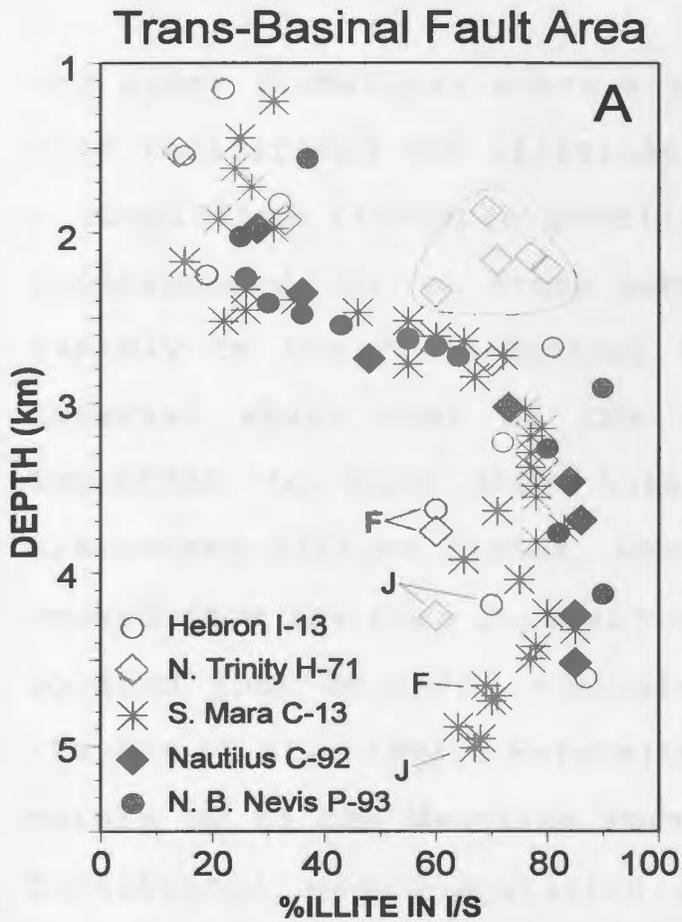
and older formations where a suitable K^+-rich pore-fluid may have facilitated the illitization reaction. Figure 6.2 shows a simplified I/S-depth profiles from three different areas superimposed on a cross-section. Illite-layers increase rapidly in the Trans-Basinal Fault area close to the depth interval where most of the faults are terminated. It is important to note that this area contains most of the discovered oil/gas fields, where the hydrocarbons have moved upward from the deep Jurassic source rocks to the sand-bodies located just below/or equivalent to the Nautilus Formation (Taylor et al., 1992). Extensive faulting in this area extends mainly up to the Nautilus Formation (Fig. 6.2) and may have facilitated upward migration of fluids. This hypothesis of upward migration of deeper fluids in the Trans-Basinal Fault area is also supported by oxygen isotopic data from South Mara C-13 (see Chapter V). Vertical movement of fluid has also been interpreted from organic geochemical studies and source-oil correlation investigations (Powell, 1985; Creaney and Allison, 1987; Von der Dick et al., 1989) for this area. In the absence of K-feldspar (see section 6.4), an external K^+ source would be required for illitization, assuming that detrital illite/mica did not contribute a significant amount of K^+ (Heling, 1978; Pearce et al., 1991). It is likely that K^+-rich fluid associated with hydrocarbons migration moved upward along these faults (Fig. 6.2) to enhance the illitization in

192
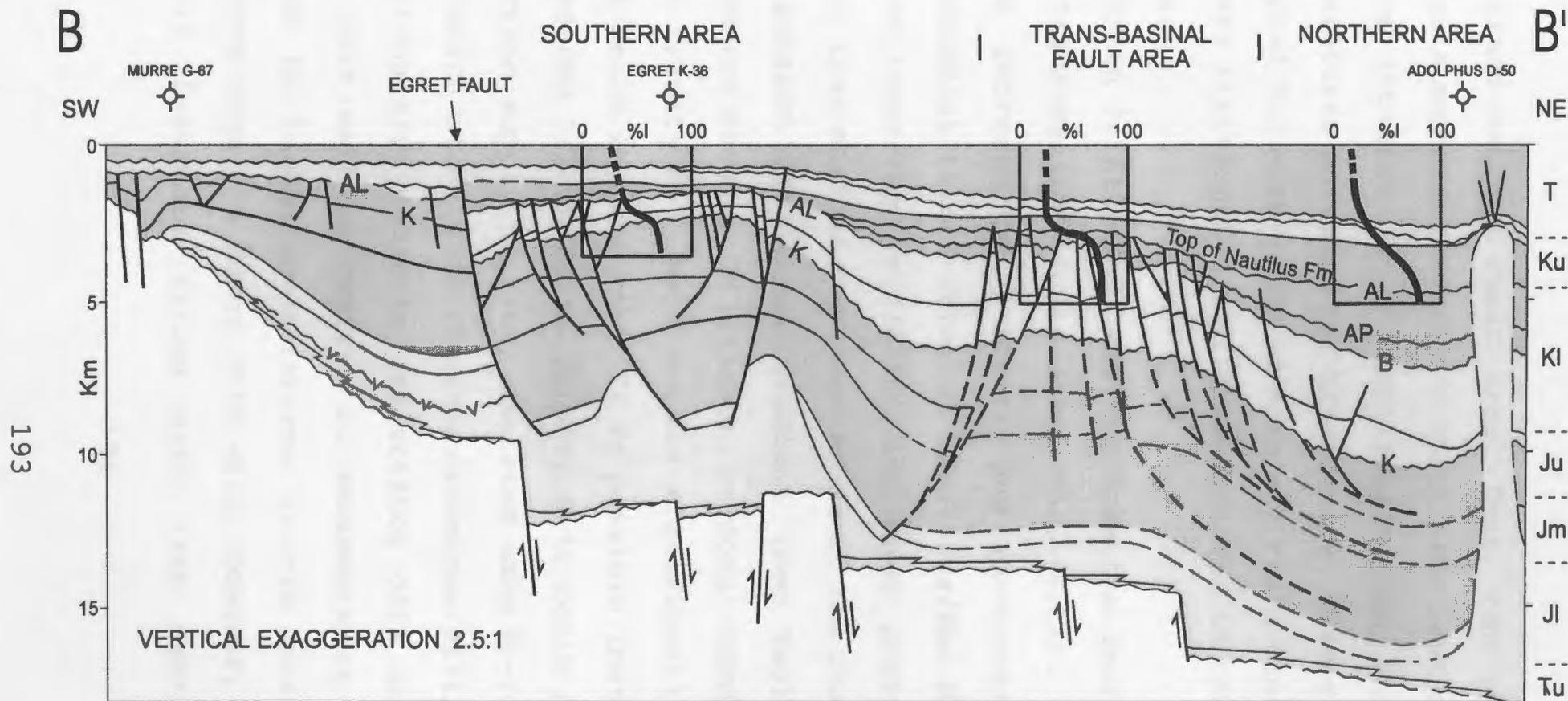
Figure 6.2. An interpreted seismic line (NF 79-112) passing approximately along the axis of the Jeanne d'Arc Basin (line BB' in Figure 2.2). Note the presence of a large number of faults which do not extend into post-Albian/Cenomanian younger sediments. Average depth versus I/S composition profiles from three different areas (Southern, Trans-Basinal Fault and Northern areas) are superimposed. Note the rapid increase in I-layers close to the faulting in the Trans-Basinal Fault Area as compared to the Northern and Southern areas. Modified from Grant and McAlpine, 1990.

the Trans-Basinal Fault area. Thus, the rapid increase in I-layers and ordering of I/S could have been controlled partly by an increase in K^+ availability in the pore-water at temperatures suitable for R1-ordering. Weaver (1979), in fact, reported the occurrence of most oil field tops at depths where intense illitization of I/S is observed in the U.S. Gulf Coast Basin.

North Trinity H-71 differs from the rest of the wells in the Trans-Basinal Fault area (Fig. 6.1A). It shows a very rapid increase of I-layers and R1-ordering in a thick sandstone/siltstone interval (Nautilus/Ben Nevis Formations) at shallower depths (1875m) and lower present temperatures (56°C) than most of the other wells of the Jeanne d'Arc Basin. The present geothermal gradient (see Table 1.1) and the subsidence history (Williamson, personal communication) of the North Trinity H-71 well are not significantly different from other wells in this area. It is possible that low temperature R1-ordered I/S in North Trinity H-71 could be the result of upsection supply of fault assisted warm K^+-rich fluid in the past which circulated through sandstone/siltstone intervals. Unfortunately vitrinite reflectance data are not available from this well to confirm if sediments at 1875-2300m were heated to higher temperatures in the past, as has been observed from the Egret N-46 well. However, the drill-cores exhibit fractures filled with late cements, suggesting

vertical fluid migration. The Fortune G-57 well located northeast (~25km) of North Trinity H-71 also shows evidence for fault controlled pore-water circulation (Rogers and Yassir, 1993) thereby supporting the interpretation of vertical fluid migration.

Several samples in the Trans-Basinal Fault area below 3500m depth record decreased I-layers in I/S. These samples are from two specific stratigraphic units (Fortune Bay and Jeanne d'Arc Formations). The retarded illitization is probably due to local variation in pore-water composition and cementation as discussed previously (see section 6.6). Whether or not the original I/S compositions of the Jeanne d'Arc and Fortune Bay Formations were different is difficult to conclude from the present data.

If a pulse(s) of upward flow of fluid associated with hydrocarbon migration has played a significant role in the smectite illitization in the Trans-Basinal Fault area, I/S dating may be helpful to determine the timing of hydrocarbon migration into the reservoir rocks. This could be helpful in the exploration for new oil/gas fields.

6.7.2 NORTHERN PART OF THE BASIN: Contrary to observations for the Trans-Basinal Fault area, most wells from the north show a gradual increase in the fraction of I-layers in I/S (Fig. 6.1B) and as a result much of the illitization reaction

195

occurs over larger depth intervals (usually >1000m). The only exception is in Whiterose J-49 where rift-related faulting extends up to ~2600m depth and I-layers increase rapidly (probably due to the related faulting and fluid flow as discussed above). The gradual increase of I-layers in this Northern area, particularly for Adolphus D-50 and Conquest K-09 wells, is considered to be due to the lack of faulting and sand/silt intervals to provide K^+-rich pore-fluids near the I/S ordering temperatures. In Adolphus D-50, the calculated $\delta^{18}O$ of pore-water increases progressively with depth and overlaps quite closely with the U.S. Gulf Coast Basin (Fig. 5.5) indicating a lack of significant vertical movement of deeper ^{18}O-rich fluids (see Chapter V).

Another noteworthy point is the separation of I/S-depth profiles (Adolphus D-50, West Flying Foam L-23, Conquest K-09) with respect to the degree of illitization between 2400-3700m depth interval (Fig. 6.1B). Among these three wells, illitization is more advanced for the Conquest K-09 and slowest in the West Flying Foam L-23 at a given depth. Data from the Adolphus D-50 falls in the middle. This separation could be partly due to small variations in the geothermal gradient and thermal maturity gradient, and partly due to the availability of K^+ in the pore-fluid. For example, West Flying Foam L-23 has a lower present geothermal gradient and lower thermal maturity (29.8°C/km, 0.099 $logR_o$/km respectively)

196

compared to Conquest K-09 (33.4°C/km, 0.222 logR$_o$/km respectively). In Adolphus D-50 these values fall between the above two wells (30.8°C/km, 0.141 logR$_o$/km respectively). The proximity of salt diapers in Adolphus D-50 and Conquest K-09 could also have provided more K$^+$ for I/S reaction and elevated temperature compared to West Flying Foam L-23.

6.7.3 OUTER RIDGE COMPLEX AREA: A majority of data from the Ridge area also shows a gradual increase in the proportion of I-layers in I/S, particularly for Dominion O-23 and South Tempest G-88 (Fig. 6.1C). For these two wells, the R1-ordering temperature (90°-100°C) is close to most of the Northern wells (Adolphus D-50, Conquest K-09 and Whiterose J-49). With the exception of Bonanza M-71, wells from the Outer Ridge Complex area also have thick depth intervals for the zone of illitization (>1000m).

A few samples (3000-3500m) from Bonanza M-71 and North Dana I-43 significantly depart from the main trend (see arrow in Fig. 6.1C). In these two wells, the Banquereau and Dawson Canyon Formations (rich in shale) make up to 3500m of the section where the rate of illitization is slower. A slower illitization rate is also observed in the West Flying Foam L-23 which contains a thick (3500m) section of mudstone/shale representing Banquereau and Nautilus Formations. Less evolved I/S in these wells is probably due to a lack of an internal K$^+$

source for illitization and a lack of easy pore-fluid circulation.

Bonanza M-71 has an abrupt increase in the I/S composition at a depth of ~3500m which appears to be due to a large amount of erosion or a local thermal anomaly prior to the deposition of Tertiary sediments. Fractures filled with quartz and chlorite, which may be due to local hydrothermal activities, were observed in a deep drill-core from the Bonanza M-71 well.

6.7.4 SOUTHERN PART OF THE BASIN: Illitization and ordering in the south occurs at shallow depths and low present day temperatures (54°-62°C). As discussed before (section 6.2.1.2), either the illitization in the south occurred at deeper levels compared to their present burial depths and temperatures or that the geothermal gradient in the past was higher (approximately 40°C/km) or a combination of these. A higher geothermal gradient in the past may be associated with a regional uplift (Avalon Unconformity) located in the south of the Jeanne d'Arc Basin. The relatively shallow "oil window" reported in the Southern part of the basin by other workers (Grant and McAlpine, 1990) also supports the above interpretations.

6.8 SIGNIFICANCE OF ILLITE/SMECTITE AND VITRINITE REFLECTANCE RELATIONSHIP IN THE JEANNE D'ARC BASIN

Random to R1-ordered I/S transition in the Jeanne d'Arc Basin generally occurs within the upper "oil window" level (Fig. 4.8). Pearson and Small (1988) also reported a similar relationship from Mesozoic shales of the North Sea where the illitization of I/S begins at $0.40\%R_o$ and becomes R1-ordered at $0.64\%R_o$. This relationship should be expected to occur in other wells of the Jeanne d'Arc Basin. Therefore, I/S study can provide an effective tool to investigate the maturity of sediments, particularly in wells where no vitrinite reflectance data are available. Furthermore, results of this investigation indicate that the processes of illitization and appearance of R1-ordering in I/S are somewhat slower (0.10% to $0.20\%R_o$) in the post-rift sediments (Banquereau and Dawson Canyon Formations) compared to rift-stage sediments of the Jeanne d'Arc Basin (Fig. 6.1C). This lag is most likely due to the lack of K^+ source and/or to different pore-fluid composition or different pore-fluid circulation history in the post-rift sediments compared to the rift sediments.

The comparison of I/S composition with $\%R_o$ can also aid in understanding whether or not burial diagenesis of I/S has occurred in a sedimentary basin under investigation. For example, the presence of highly expandable random I/S in organically immature sediments and less expandably ordered I/S

199

in organically mature sediments would argue in favour of burial diagenesis. On the other hand, the presence of only ordered I/S in both organically mature and immature sediments will suggest a detrital nature of the ordered I/S, which however is not the case in the Jeanne d'Arc Basin.

6.9 OVERPRESSURE AND ILLITE/SMECTITE DIAGENESIS

Several mechanisms have been proposed to explain overpressures including: compaction due to overburden (Dickinson, 1953; Hottman and Johnson, 1965); aquathermal pressuring, (Barker, 1972; Bradley, 1975); compaction disequilibrium (Magara, 1975 a, b); osmosis (Gretener, 1977); hydrocarbon generation (Momper, 1980; Law and Dickinson, 1985); and lateral compression (Shi and Wang, 1986). Powers (1967) and Bruce (1984) considered that I/S diagenesis is the principal mechanism for the generation of overpressures in the U.S. Gulf Coast Basin where the main zone of I/S diagenesis overlaps the zone of onset of overpressures.

Overpressure zones were encountered in several wells of the Jeanne d'Arc Basin. In many wells overpressure was encountered below the Fortune Bay Formation (≥4000m), which served as a seal over much of the basin (McAlpine, 1990). Figure 6.3 shows the zone of major I/S diagenesis (~35% to ≥75%I) and overpressure zone plotted on a basin axis cross-section. Clearly, most of the smectite content of I/S is

200

dehydrated at depths shallower than the present depths of overpressure zones (Fig. 6.3). It would appear therefore that I/S diagenesis by itself cannot be responsible for the overpressure zones of the Jeanne d'Arc Basin. Such data contradict the interpretation of Bruce (1984) for the U.S. Gulf Coast. Overpressure zones probably developed as a result of a combination of several mechanisms.

Whether or not I/S diagenesis has partly contributed toward the build-up of overpressure in this basin rests largely on the timing of overpressure development. For example, if the formation of a seal and the development of overpressure were started at shallower depths or at depths coincident with the zone of illitization (2000-3500m), smectite dehydration could have partly contributed towards the development of overpressure zones. In this case further subsidence might have led to deepening of the overpressure zones. Illitization of the subsequent overlying younger clays would have resulted in apparent separation of the observed overpressure zone ($\geq$4000m) and the observed zone of illitization (2000-3500m). If, however, the observed overpressures developed close to their present burial depths ($\geq$4000m), I/S diagenesis or clay dehydration would not have contributed significantly. At present the available data are inadequate to conclude the possible role of I/S diagenesis towards the build-up of overpressure zones in the Jeanne

201

Figure 6.3: The zone of main illite/smectite diagenesis or illitization along a cross-section passing roughly through the basin-axis. The zone of illitization (where %I in I/S increases from 30-35% to ≥75%) indicates a depth interval where maximum smectite layers are dehydrated (or converted into illite) during illite/smectite diagenesis (~35 to ≥75% illite). Present overpressure zones are generally located below 3500m whereas the zone of illitization is situated above this depth.
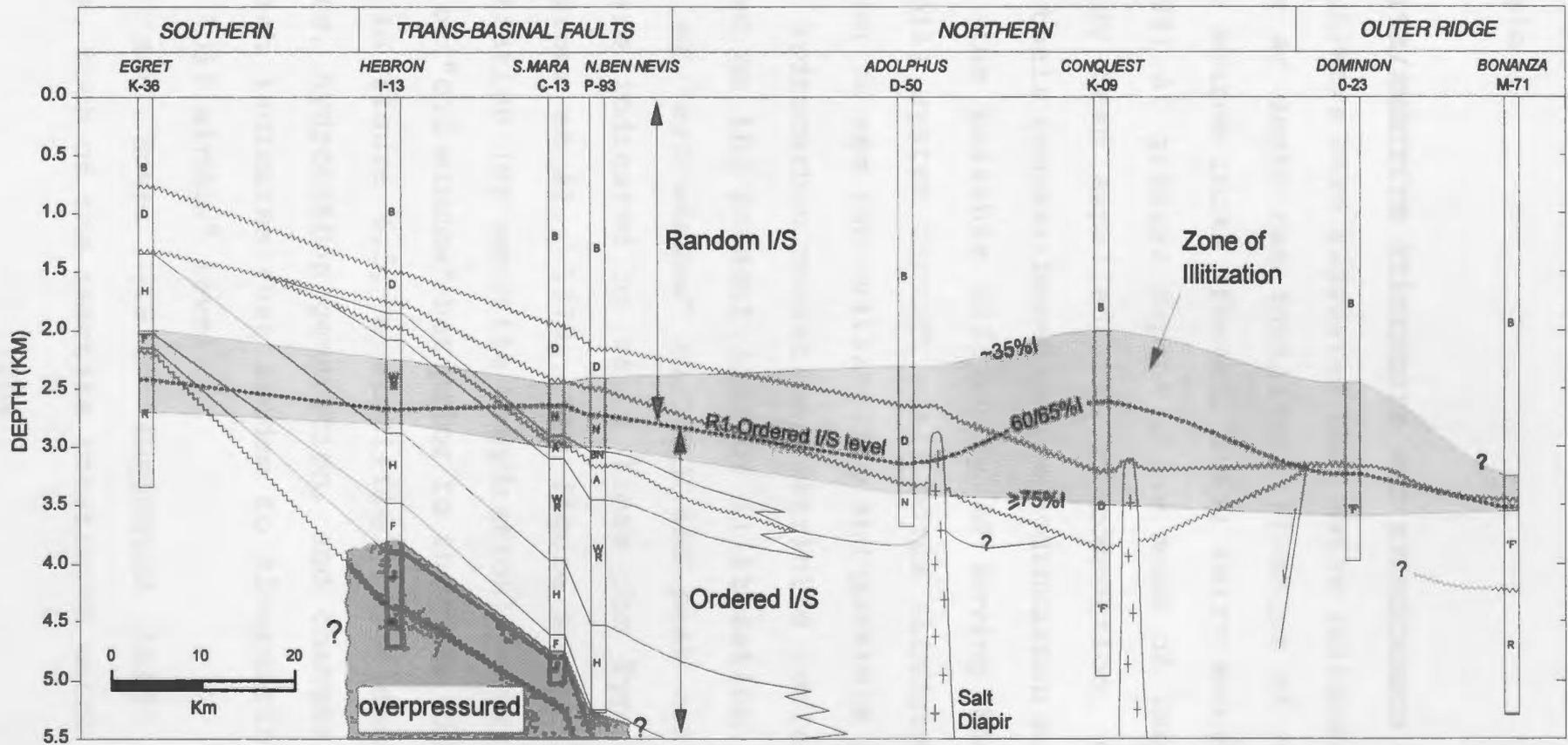
d'Arc Basin.

6.10 ILLITE/SMECTITE DIAGENESIS AND HYDROCARBON MIGRATION

Some workers have suggested that water released during I/S diagenesis at depth can facilitate flushing of hydrocarbons out of the source rocks (Powers, 1967; Perry and Hower, 1972; Bruce, 1984) at greater depths where much of the pore-water has already been expelled due to compaction. Others have expressed their concern based on low hydrocarbon solubility in water and the possible difficulty of moving the two-phase (water + oil) system through small pores (Lindgreen, 1987).

In order to see the availability and possible role of clay water for hydrocarbon migration, vitrinite reflectance data are plotted on the present zone of illitization (Fig. 6.4). The onset of "oil window" ($0.50R_o$) and peak oil generation ($0.80R_o$) are indicated by solid lines for Type II organic matter (Héroux et al., 1979). The figure shows that much of the illitization (or smectite dehydration) occurred close to the onset of "oil window" but prior to the peak oil generation ($0.80R_o$). In figure 6.5, a simplified relationship between temperature, hydrocarbon generation, and changes in I/S are shown, which indicates that random to R1-ordering occurs in the upper "oil window" level.

Perry and Hower (1972) suggested that during I/S diagenesis, much of the smectite interlayer water is released

204
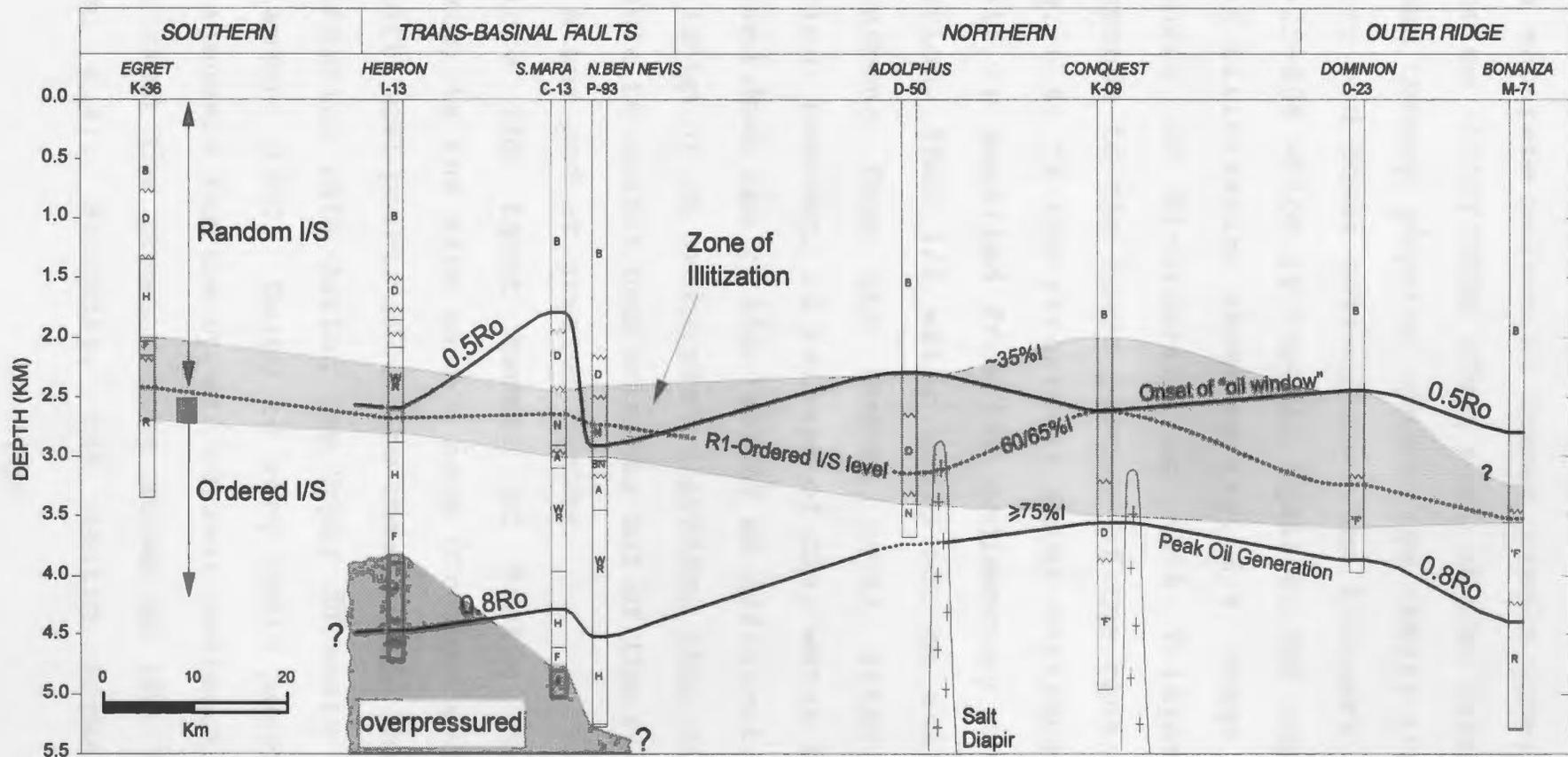
Figure 6.4. A comparison of the onset of "oil window" (0.5Ro) and the peak oil generation (0.8Ro) levels with the zone of illitization along a northeast-trending cross-section which passes roughly through the basin-axis. Note that the peak oil generation level is located below the zone of illitization.

in two separate pulses at deeper levels (their stages II and III) below ~1500/2000m after much of the interstial water is released through physical compaction (their stage I). Stage II of Perry and Hower corresponds when I-layers in I/S increase from ~25-60% which is roughly equal to the upper level of the zone of illitization shown on Fig. 6.4. Stage III starts from the onset of R1-ordering to ~80% I-layers and roughly corresponds to the lower portion of the zone of illitization in Fig. 6.4. If the structural water available from the clay minerals is expelled from the sedimentary section by normal compaction, then I/S water would not be available to carry hydrocarbons from the source rocks after the peak oil formation. However, if release of clay water from the section is slowed down due to the lack of an efficient drainage system or build-up of an overpressure system, then clay water may be available to assist hydrocarbons out of the source rocks at a later stage and at greater depths.

Since the Egret Member of Rankin Formation (Upper Jurassic) is the main source rock (Creaney and Allison, 1987) two additional points should be considered. The subsidence and sedimentation rate during the Upper Jurassic was very high (Williamson, 1992). Owing to very rapid burial, the zone of I/S diagenesis for the Upper Jurassic sediment could have been deeper than the present zone shown on the figure 6.4 (see section 6.4). Secondly, the Rankin Formation (rich in

206

Figure 6.5: A comparison between temperature, hydrocarbon generation (from Pollastro, 1993), and I/S ordering as observed in the Jeanne d'Arc Basin. The left-side of the diagram was compiled by Pollastro (1993) from Hoffman and Hower (1979), Waples (1980), Rice and Claypool (1981), and Tissot and Welte (1978). Note that random to R1—ordering occurs close to the onset of the "oil window".

208
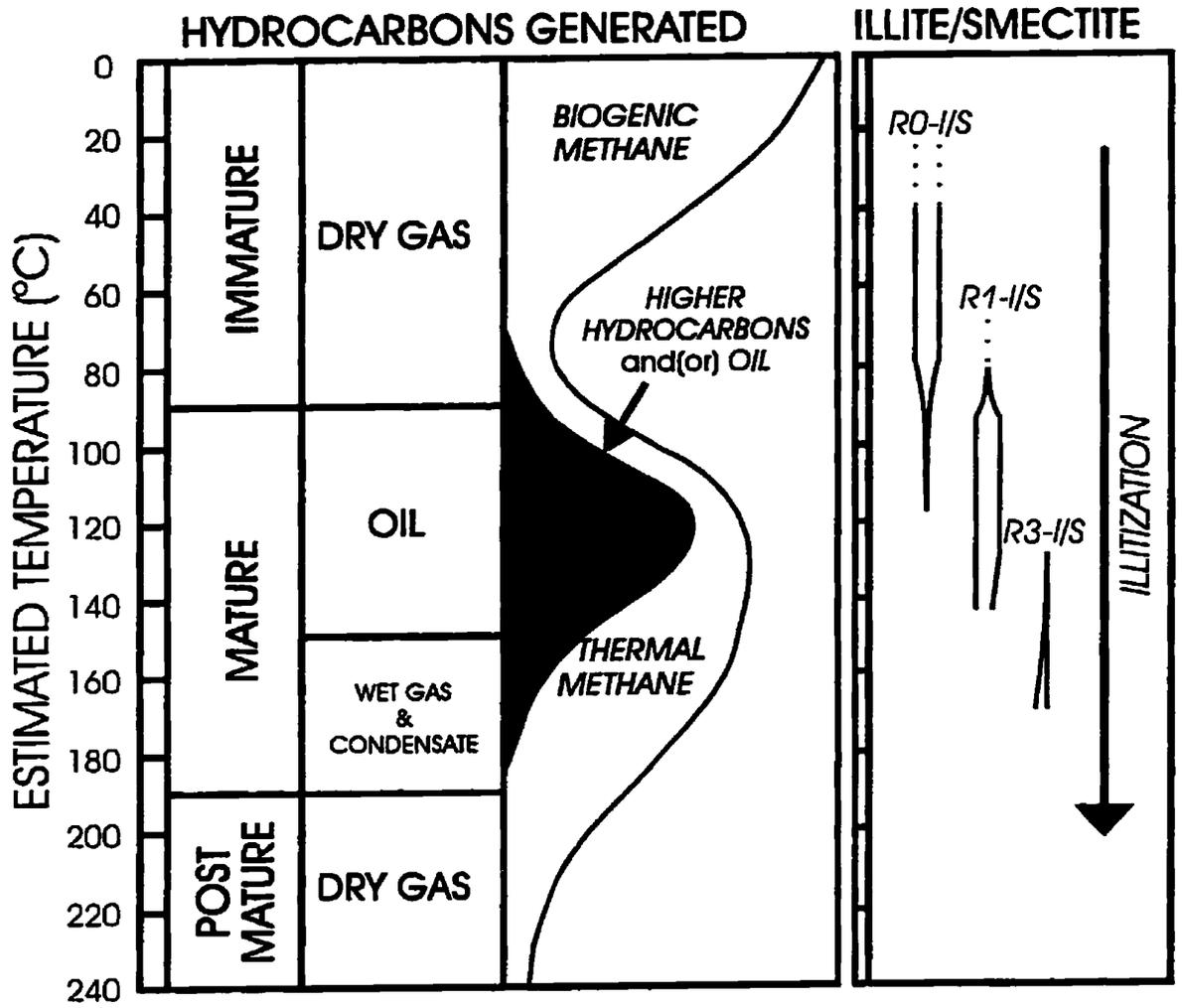
carbonates) shows a slower rate of I/S diagenesis (see Fig. 3.8I) particularly for wells located in the southern part of the basin (for reason see section 6.6) and its I/S diagenesis could have occurred at deeper levels compared to the depth zone shown on the figure 6.4. Therefore, the possible role of I/S diagenesis for hydrocarbon migration from the Egret Member of the Rankin Formation cannot be ignored simply because the present zone of illitization lies above the peak oil generation boundary.

CHAPTER VII

CONCLUSIONS AND FUTURE RESEARCH

7.1 SUMMARY AND CONCLUSIONS

The first well in the Jeanne d'Arc Basin was drilled in 1966 and the first major oil discovery was made in 1979. No one has attempted, so far, to document the effect of burial diagenesis on mixed-layer illite/smectite (I/S) clay minerals in this basin. This is the first study to document the composition of I/S clays in the Jeanne d'Arc Basin. Important conclusions of this investigation are summarized below:

(1). Mixed-layer I/S is the dominant component of fine-grained clay fractions (<0.1μm) in the Jeanne d'Arc Basin. Small to trace amounts of kaolinite and discrete illite are also present in the fine-grained clays. Chlorite was observed only in the deeper samples.

(2). Four different types of I/S were recognized using the criteria of Reynolds and Hower (1970), Bethke et al. (1986), and Środoń (1984). They include: (1) random I/S (R0), (2) weakly ordered I/S (WR1), (3) short-range ordered I/S (R1) and (4) long-range ordered I/S (R3).

(3). The results of basin-wide study of I/S clays show that smectite-rich clays were available in the basin throughout the section studied, although their relative proportion may have changed with depth. For example,

rift-related stratigraphic units in the south, buried at shallow depths contain smectite-rich I/S clays whereas their stratigraphic equivalent in the north at deeper levels have illite-rich I/S. This observation is important for the interpretation that smectite illitization has occurred from a precursor smectite or smectite-rich random I/S.

(4).   The proportion of illite-layers in I/S increases with depth in almost all the wells studied. Illite-layers in most individual stratigraphic units also increase with depth. In addition, ordering types of I/S change from random I/S to weakly-ordered I/S to R1-ordered I/S to R3-ordered I/S with increasing burial depths. All these observations suggest that smectite illitization has occurred as a result of burial diagenesis in both the rift and post-rift sediments of the Jeanne d'Arc Basin.

(5).   The observed present temperature for random to R1-ordered transition varies significantly in the basin (54°-118°C). In the majority of the wells (11 out of 16) R1-ordering begins at about 100±20°C present formation temperatures which is consistent with the expected range as reported from other sedimentary basins. The remaining five wells (Egret K-36, Egret N-46, Cormorant N-83, Hebron I-13, and North Trinity H-71), record lower present R1-ordering temperatures

($54°-70°C$). It is believed in this study that the present R1-ordering temperatures in these wells were higher in the past. This may have been due to higher paleogeothermal gradient or deep burial prior to uplift or a combination of both. The direct evidence for this conclusion comes from the Egret N-46 well, where R1-ordering occurs at $0.65R_o$ value that suggests a paleotemperature of about $100°C$ instead of $59°C$ present temperature.

The R1 to R3-ordering change is commonly believed to occur at $175±5°C$. In this present study, R3-ordered I/S occurs at lower present temperatures than expected ($130°-170°C$). Higher paleo-temperatures are not indicated by the vitrinite reflectance data ($0.72-1.10\%R_o$). It is interesting that other workers have also reported the occurrence of R3-ordered I/S at about the same vitrinite reflectance values (0.80 to $1.00\%R_o$). Thus, the possibility that R3-ordered I/S can occur at lower temperatures should be investigated in other sedimentary basins. The R3-ordering temperature may also vary in nature for the same reason as have been reported for the R1-ordered I/S.

(6). This study shows that random to R1-ordering generally occurs within the upper "oil window" level ($0.50-0.66\%R_o$). A change from R1 to R3-ordered I/S was

212

observed between 0.72-1.1%R_o. These results substantiate earlier findings by others (Powell et al., 1978; Środoń, 1979; Pearson and Small, 1988). Thus, the study of I/S can provide an effective tool to investigate the maturity of sediments (onset of "oil window"), particularly in wells where no vitrinite reflectance data are available. Due attention should be given to the fact of slower illitization in the post-rift sediments.

(7). The $\delta^{18}O$ values of I/S clays range from 25.8 to 17.9‰ (SMOW) and calculated pore-fluid compositions vary from 1.5‰ to 11.6‰. In Adolphus D-50 the calculated pore-water $\delta^{18}O$ increases progressively with depth suggesting no significant vertical migration of deep basinal fluids. However, in South Mara C-13, high $\delta^{18}O$ values of calculated pore-fluid, present at relatively shallower depths, suggest vertical migration of deep $\delta^{18}O$-rich fluid. These deeper warm fluids, probably rich in K^+, could be responsible for the rapid increase of I-layers in I/S as a function of depth as observed in the Trans-Basinal Fault area.

(8). On a regional scale, I/S composition-depth profiles show important variations geographically. Such variations are partly controlled by variable geological

213

features (i.e. temperature, faulting, lithology, etc.).
Rapid increase with depth of %illite in I/S in the
Trans-Basinal Fault area is believed to have been
controlled by upward flow of deeper fluids, rich in K^+,
along numerous faults. Most of these faults do not
extend above the rapid transition zone. The presence of
Jurassic-sourced hydrocarbons in the rapid I/S
transitional zone also suggests that fluid migration
occurred along these faults. Gradual increase in the
proportion of I-layers in the Northern and Outer Ridge
Complex areas is probably due to an insufficiency of K^+
in the pore-fluid controlled in part by a lack of
faulting and the presence of a thick shale interval.
This shale probably did not contain enough internal K^+
source. As a result, R1-ordering in these areas occurs
at slightly higher temperatures and higher R_o values
than in the Trans-Basinal Fault areas. In the Southern
area, with fewer faults than in the Trans-Basinal Fault
area, shallow depths and lower present temperatures for
R1-ordering are probably due to higher paleogeothermal
gradients, or uplift, or a combination of both.

(9). Bulk-shale XRD analyses from the South Mara C-13 well
indicate the absence of K-feldspar throughout the
section. Lacking potassium feldspar, the K^+ was supplied
either internally from detrital illite/mica or it was

214

provided externally by fluid flow from the deeper section. The rapid increase of I-layers in the Trans-Basinal Fault area together with oxygen isotopic data provide important evidence for such a deeper K^+ source. Sluggish I/S reaction in thick shale-rich Tertiary sections (West Flying Foam L-23, Bonanza M-71, and North Dana I-43) where faulting is generally absent is consistent with this model.

(10). Relatively small irregularities of I/S composition-depth profiles are probably due to local variations in lithology, porosity/permeability and inhibiting cations (Mg^{2+}, Ca^{2+}) in the pore-fluid. Silty-shale and shales from sandstone-rich intervals commonly show 10-20% more I-layers, probably due to more permeable pathways for the migration of pore-water carrying K^+ and other cations. Such observations are also consistent with a deep-section source for K^+. Existence of high water/rock ratio can increase the processes of illitization (Whitney, 1990). Small reversals (or retardation) in I/S reaction are considered to be due, based on circumstantial evidence, to either early cementation and/or inhibiting cations (Mg^{2+}, Ca^{2+}) in the pore-fluid.

(11). Upper Jurassic and Lower Cretaceous sediments buried at shallow depths do not show significantly higher illite-rich I/S compared to younger sediments at similar

215

organic maturity. Thus, time does not seem to play a significant role for the I/S diagenesis at least for samples used in this study. Most of the samples are Mid-Tertiary to Cretaceous age and are characterized by a long burial history. Hoffman and Hower (1979), and Pollastro and Schmoker (1989) also reported similar results from other sedimentary basins.

(12). Significant present day depth separation of the zone of illitization from the deeper overpressure zone in the Jeanne d'Arc Basin suggests that I/S diagenesis alone may not be able to generate overpressure zones. However, a possible contribution of I/S diagenesis towards the build-up of overpressure zones, presently located at deeper levels ($\geq$4000m), rests largely on the timing of the onset of overpressuring and the amount of smectite present at the time of sedimentation.

7.2 FUTURE RESEARCH

This study provides a first picture of I/S diagenesis on the basinal scale, which will hopefully initiate interest for future studies to investigate other issues of clay sedimentology and I/S diagenesis in the Jeanne d'Arc Basin.

Few studies have attempted to model the formation of overpressure zones, and maturation and migration of hydrocarbons in the Jeanne d'Arc Basin (Rogers and Yassir,

216

1993; Williamson et al., 1993). In these studies, the possible role of I/S diagenesis (or clay dehydration) has not been given due attention. This present study provides first-hand data on I/S diagenesis across the Jeanne d'Arc Basin which should be incorporated in the future basin modelling studies which could modify or improve the above mentioned models in the Jeanne d'Arc Basin.

If a pulse(s) of upward flow of fluid associated with hydrocarbon migration has played a significant role to cause illitization in the Trans-Basinal Fault area, I/S dating may be helpful to trace out timing of hydrocarbon migration into the reservoir rocks. This could be helpful in the exploration for new oil/gas fields.

REFERENCES

ABERCROMBIE, H.J., HUTCHEON, I.E., BLOCH, J.D., AND CARITAT, P., 1994. Silica activity and the smectite-illite reaction. Geology, **22**, 539-542.

ABID, I.A., 1988. Mineral diagenesis and porosity evolution in the Hibernia oil field, Jurassic-Cretaceous Jeanned'Arc rift graben, eastern Grand Banks of Newfoundland, Canada. Unpubl. M. Sc. thesis, McGill University, Montreal, 280pp.

ABID, I.A., AND HESSE, R., 1988. Diagenesis and porosity evolution in Hibernia oilfield, Grand Banks offshore Newfoundland (abs): Geol. Assoc. Canada Program with Abstracts, **13**, A1.

ALTANER, S.P., WHITNEY, G., ARONSON, J.L., AND HOWER, J., 1984. A model for K-bentonite formation, evidence from zoned K-bentonites in the disturbed belt, Montana. Geology, **12**, 412-415.

AMOCO CANADA PETROLEUM COMPANY LTD. AND IMPERIAL OIL LTD., 1973. Regional geology of the Grand Banks. Bull. Canadian Petrol. Geol., **21**, 479-503.

AROSTEGUI, J., ZULUAGA, M.C., VELASCO, F., ORTEGA-HUERTAS, M. AND NIETO, F., 1991. Diagenesis of the central Basque-Cantabrian Basin (Iberian Peninsula) based on illite-smectite distribution. Clay Minerals, **26**, 535-548.

ARTHUR, K.R., COLE, D.R., HENDERSON, G.G.L., AND KUSHNIR, D.W., 1982. Geology of the Hibernia discovery. In: Halbouty, M.T. (Ed.), The deliberate search for the subtle trap. Amer. Assoc. Petrol. Geol. Memoir, **32**, 181-196.

AVERY, M.P., 1985. Vitrinite reflectance (R_o) on the dispersed organics in the Mobil Gulf Dominion O-23. Geol. Surv. Canada, Open File 1200.

AVERY, M.P., 1993. Vitrinite reflectance (R_o) of dispersed organics from Mobil et al. Hebron I-13. Geol. Surv. Canada, Open File 2671.

AVERY, M.P., BELL, J.S., AND McALPINE, K.D., 1986. Vitrinite reflectance measurements and their implications for oil and gas exploration in the Jeanne d'Arc Basin. In: Current Research, Part A. Geol. Surv. Canada, Paper **86-1A**, 489-498.

218

.

AWWILLER, D.N., 1993. Illite/smectite formation and potassium mass transfer during burial diagenesis of mudrocks: A study from the Texas Gulf Coast Paleocene-Eocene. Jour. Sed. Petrol., **63**, 501-512.

BARKER, C., 1972. Aquathermal pressuring-role of temperature in development of abnormal pressure zones. Amer. Assoc. Petrol. Geol. Bull., **56**, 2068-2071.

BARKER, C.E., 1988. Geothermics of petroleum systems: implications of the stabilization of kerogen thermal maturation after a geologically brief heating duration at peak temperature, in L. B. Magoon, ed., Petroleum systems of the United States. U.S. Geol. Surv. Bull., **1870**, 26-29.

BARSS, M.S., BUJAK, J.P., AND WILLIAMS, G.L., 1979. Palynological zonation and correlation of sixty-seven wells, eastern Canada. Geol. Surv. Canada., Paper **78-24**, 118-125.

BETHKE, C.M., VERGO, N. AND ALTANER, S.P., 1986. Pathways of smectite illitization. Clays and Clay Minerals, **34**, 125-135.

BLOCH, D.J., 1991. Diagenesis and rock-fluid interaction of Cretaceous Harmon Member (Fort St. John Group) mudstones, Alberta and British Columbia. Unpubl. Ph. D. thesis, University of Calgary. 165pp.

BOLES, J. R., AND FRANKS, S. G., 1979. Clay diagenesis in Wilcox sandstones of Southwest Texas: Implication of smectite diagenesis on sandstone cementation. Jour. Sed. Petrol., **49**, 55-70.

BOSTICK, N., CASHMAN, S.M., McCULLOH, T.H., AND WADDELL, C. T., 1978. Gradients of vitrinite reflectance and present temperature in the Los Angeles and Ventura Basins, California. In: Oltz, D. F. (Ed.), Symposium in geochemistry: low temperature metamorphism of kerogen and clay minerals. Pac. Sec. Soc. Econ. Paleontologists and Mineralogists, 65-69.

BOULEGUE, J., AND BARIAC, T. 1990. Oxygen and hydrogen isotope ratios of interstitial waters from an intraplate deformation area: Bengal Fan, Leg 116. In: Cochran et al. (Eds.), Proceedings of the ODP Scientific Results, **116**, Ocean Drilling Program, College Station, 127-133.

BRADLEY, J.S., 1975. Abnormal formation pressure. Amer. Assoc. Petrol. Geol. Bull., **59**, 957-973.

BROWN, D.M., McALPINE K.D., AND YOLE, R.W., 1989. Sedimentology and sandstone diagenesis of Hibernia Formation in Hibernia Oil Field, Grand Banks of Newfoundland. Amer. Assoc. Petrol. Geol. Bull., **73**, 557-575.

BRUCE, C.H., 1984. Smectite dehydration and its relation to structural development and hydrocarbon accumulation in Northern Gulf of Mexico Basin. Amer. Assoc. Petrol. Geol. Bull., **68**, 673-683.

BUJAK, J.P., BARSS, M.S., AND WILLIAMS, G.L., 1977a. Offshore eastern Canada- Part I, Organic type and colour and hydrocarbon potential. Oil and Gas Jour., **75**, 198-202.

BUJAK, J.P., BARSS, M.S., AND WILLIAMS, G.L., 1977b. Offshore eastern Canada-Part II, Organic type and colour and hydrocarbon potential. Oil and Gas Jour., **75**, 96-100.

BURST, J.F., 1969. Diagenesis of Gulf Coast clayey sediments and its possible relation to petroleum migration. Amer. Assoc. Petrol. Geol. Bull., **53**, 73-93.

BURTNER, R.L. AND WARNER, M.A., 1986. Relationship between illite/smectite diagenesis and hydrocarbon generation in Lower Cretaceous Mowry and Skull Creek shales of the Northern Rocky Mountain area. Clays and Clay Minerals, **34**, 390-402.

CANADA-NEWFOUNDLAND OFFSHORE PETROLEUM BOARD (C-NOPB), 1988. Schedule of wells, Newfoundland Offshore Area, St. John's.

CHAMLEY, H., 1979. North Atlantic clay sedimentation and paleoenvironment since the Late Jurassic. In: Talwani, M., Hay, W., Ryan, W.B.F. (Eds.), Deep drilling results in the Atlantic Ocean: Continental margins and paleoenvironment. Maurice Ewing ser., Am. Geophys. Union, **3**, 342-361.

CHANG, H.K., MacKENZIE, F.T., AND SCHOONMAKER, J., 1986. Comparisons between the diagenesis of dioctahedral and trioctahedral smectite, Brazilian offshore basins. Clays and Clay Minerals, **34**, 407-423.

CLAYTON, R.N., AND MAYEDA, T.K., 1963. The use of bromine pentafluoride in the extraction of oxygen from oxides and silicates for isotopic analysis. Geochim. Cosmochim. Acta, **27**, 43-52.

COLTEN-BRADLEY, V.A., 1987. Role of pressure in smectite dehydration-Effects on geopressure and smectite-to-illite transformation. Amer. Assoc. Petrol. Geol. Bull., **71**, 1414-1427.

CONNOLLY, C.A., 1989. Thermal history and diagenesis of the Wilrich Member shale, Spirit River Formation, northwest Alberta. Bull. Canadian Petrol. Geol., **37**, 182-197.

CORREIA, A., JONES, F.W. AND FRICKER, A., 1990. Terrestrial heat flow density estimates for the Jeanne d'Arc Basin offshore eastern Canada. Geophysics, **59**, 1625-1633.

CRAIG, H., 1961. Standards for reporting concentrations of deuterium and oxygen-[18] in natural waters. Science, **133**, 1833-1834.

CREANEY, S., AND ALLISON, B.H., 1987. An organic geochemical model of oil generation in the Avalon/ Flemish Pass sub-basins, East Coast Canada. Bull. Canadian Petrol. Geol., **35**, 12-23.

DENG, X., SUN, Y., LEI, X., AND LU, QI., 1996. Illite/Smectite diagenesis in the NanXiang, Yitong, and North China Permian-Carboniferous Basins: Application to petroleum exploration in China. Amer. Assoc. Petrol. Geol. Bull., **80**, 157-173.

DICKINSON, G., 1953. Geological aspects of abnormal reservoir pressure in Gulf Coast Louisiana. Amer. Assoc. Petrol. Geol. Bull., **37**, 410-432.

DOW, W.G., 1977. Kerogen studies and geological interpretations. Jour. Geochem. Exploration, **7**, 79-99.

DRISCOLL, N.W., HOGG, J.R., CHRISTIE-BLICK, N., AND KARNER, G.D., 1995. Extentional tectonics in the Jeanne d'Arc Basin, offshore Newfoundland: implications for the timing of break-up between Grand Banks and Iberia. In: Stoker, R.A., Shimmield, M.S., Tudhope, A.W. (Eds.), The Tectonics, Sedimentation and Palaeoceanography of the North Atlantic Region. Geol. Soc. Special Publ., **90**, 1-28.

DROSTE, J.B., BHATTACHARYA, N. AND SUNDERMAN, J.A., 1960. Clay mineral alteration in some Indiana soils. Clays and Clay Minerals, **9**, 329-342.

DUNOYER DE SEGONZAC, G., 1970. The transformation of clay minerals during diagenesis and low-grade metamorphism: a review. Sedimentology, **15**, 281-346.

EBERL, D.D., 1978. The reaction of montmorillonite to mixed-layer clay: the effect of interlayer alkali and alkaline earth cations. Geochim. Cosmochim. Acta, **42**,1-7.

EBERL, D.D. AND HOWER, J., 1976. Kinetics of illite formation. Geol. Soc. Amer. Bull., **87**, 1326-1330.

EBERL, D.D., ŚRODOŃ, J., LEE, M., NADEAU, P.H. AND NORTHROP, H.R., 1987. Sericite from the Silveerton caldera, Colorado: Correlation among structure, composition, origin, and particle thickness. Am. Mineralogist, **72**, 913-934.

ENACHESCU, M.E., 1992. Basement extension on the Newfoundland continental margin (Canadian east coast). In: Mason, R., (Ed.), Basement Tectonics 7, Kluwer Academic, Dordrecht, 227-256.

ESLINGER, E.V., SAVIN, S.M., AND YEH, H., 1979. Oxygen isotope geothermometry of diagenetically altered shales. Soc. Econ. Paleontologists and Mineralogists. Special Publ., **26**, 113-124.

ESLINGER, E., AND SELLARS, B., 1981. Evidence for the formation of illite from smectite during burial metamorphism in the Belt Supergroup, Clark Fork, Idaho. Jour. Sed. Petrol., **51**, 203-216.

ESLINGER, E. AND PEVEAR, D., 1988. Clay Minerals for Petroleum Geologists and Engineers. Soc. Econ. Paleontologists and Mineralogists. Short Course Notes, **22**.

ESLINGER, E.V., AND YEH, H.W., 1981. Mineralogy, O^{18}/O^{16} and D/H ratios of clay-rich sediments from Deep Sea Drilling Project site 180, Aleutian Trench. Clays and Clay Minerals, **29**, 309-315.

FREED, R.L., 1981. Shale mineralogy and burial diagenesis of Frio and Vicksburg Formations in two geopressured wells, Mcallen Range area, Hidalgo Country, Texas. Trans. Gulf Coast. Assoc. Geol. Soc., **31**, 289-293.

FREED, R.L., AND PEACOR, D.R., 1989. Variability in temperature of the smectite/illite reaction in Gulf Coast sediments. Clay Minerals, **24**, 171-180.

GIBBONS, R., 1990. Hydrocarbon discoveries offshore Newfoundland and Labrador. Dept. of Mines and Energy, Govt. Newfoundland and Labrador. 44p.

GLASMANN, J.R., LARTER, S., BRIEDIS, N.A., AND LUNDEGARD, P.
A., 1989. Shale diagenesis in the Bergen High area, North
Sea. Clays and Clay Minerals, **37**, 97-112.

GRADSTEIN, F.M. AND WILLIAMSON, G.L., 1981. Stratigraphic
charts of the Labrador and Newfoundland shelves; Geological
Survey of Canada, Open File 826.

GRANT, A.C., McALPINE, K.D., AND WADE, J.A., 1986. The
continental margin of eastern Canada-geological framework
and petroleum potential. In: Halbouty, M.T. (Ed.), Future
petroleum provinces of the world. Amer. Assoc. Petrol.
Geol. Memoir, **40**, 177-205.

GRANT, A.C. AND McALPINE, K.D., 1990. The continental margin
around Newfoundland: Chapter 6. In: Keen, M.J., Williams,
G.L. (Eds.), Geology of the Continental Margin off Eastern
Canada, Geol. Surv. Canada, Geology of Canada, **No. 2**, 241-
292.

GRETENER, P.E., 1977. Pore pressure: fundamentals, general
ramifications and implications for structural geology.
Amer. Assoc. Petrol. Geol. Bull., Short Course Series, **4**,
87p.

HARDING, S., 1988. Facies interpretation of the Ben Nevis
formation in the North Ben Nevis M-61 well, Jeanne d'Arc
basin, Grand Banks, Newfoundland. In: James, D.P., and
Leckie, D.A. (Eds.), Sequences, stratigraphy,
sedimentology: surface and subsurface: Canadian Soc.
Petrol. Geol. Memoir, **15**, 291-306.

HARRISON, P.H., 1984. Vitrinite reflectance (R_o) on the
dispersed organics in the Amoco Imperial Skelly Egret N-46.
Geol. Surv. Canada, Open File 1170.

HAWORTH, R.T., AND LEFORT, J.P., 1979. Geophysical evidence
for the extent of the Avalon Zone in Atlantic Canada. Can.
Jour. Earth Sci., **16**, 552-567.

HELING, D., 1974. Diagnetic alteration of smectite in
argillaceous sediments of the Rhinegraben (SW Germany).
Sedimentology, **21**, 463-472.

HELING, D., 1978. Diagenesis in argillaceous sediments of the
Rhinegraben. Clay Minerals, **13**, 211-220.

HÉROUX, Y., CHAGNON, A., AND BERTRAND, R., 1979. Compilation
and correlation of major thermal maturation indicators.
Amer. Assoc. Petrol. Geol. Bull., **63**, 2128-2144.

HILLIER, S., AND CLAYTON, T., 1989. Illite/smectite diagenesis in Devonian lacustrine mudrocks from Northern Scotland and its relationship to organic maturity indicators. Clay Minerals, **24**, 181-196.

HILLIER, S., MÁTÁYS, J., MATTER, A., VASSEUR, G., 1995. Illite/smectite diagenesis and its variable correlation with vitrinite reflectance in the Pannonian Basin. Clays and Clay Minerals, **43**, 174-183.

HISCOTT, R.N., WILSON, R.C.L., HARDING, S.C., PUJALTE, V., AND KITSON, D., 1990. Contrasts in early Cretaceous depositional environments of marine sandbodies, Grand Banks-Iberian corridor. Bull. Canadian Petrol. Geol., **38**, 203-214.

HOFFMAN, J. AND HOWER, J. 1979. Clay mineral assemblages as low grade metamorphic geothermometers: Application to the thrust faulted Disturbed Belt of Montana, U. S. A. Soc. Econ. Paleontolgists and Mineralogists, Special Publ., **26**, 55-79.

HOOD, A., GUTJAHR, C.C.M., AND HEACOCK, R.L., 1975. Organic metamorphism and the generation of petroleum. Amer. Assoc. Petrol. Geol. Bull., **59**, 986-996.

HOTTMAN, C.E., AND JOHNSON, R.K., 1965. Estimation of formation pressures from log derived shale properties. Jour. Petrol. Tech., **17**, 717-722.

HOWARD, J.J., 1987. Influence of shale fabric on illite/smectite diagenesis in the Oligocene Frio Formation, south Texas. In: Schultz, L. G., Olphen, H. Van, and Mumpton, F. A. (Eds.), Proc. Int. Clay Conf., Denver, 1985. The Clay Minerals Society, Bloomington, Indiana, 144-150.

HOWER, J., 1981. X-ray diffraction identification of mixed-layer clay minerals: in Longstaffe, F.J., (Ed.), Clays and Resource Geologist. Mineral. Assoc. Canada, Short Course, **7**, 39-59.

HOWER, J., ESLINGER, E.V., HOWER, M.E., AND PERRY, E.A., 1976. Mechanism of burial metamorphism of argillaceous sediment: 1. Mineralogical and chemical evidence. Geol. Soc. Amer. Bull., **87**, 725-737.

HUANG, W., AND LONGO, J.M., PEVEAR, D.R., 1993. An experimentally derived kinetic model for smectite-to-illite conversion and its use as a geothermometer. Clays and Clay Minerals, **41**, 162-177.

HUTCHEON, I.E., NAHNYBIDA, C.G., AND KROUSE, H.R., 1985. The geochemistry of carbonate cements in the Avalon sand, Grand Banks of Newfoundland. Mineral. Magazine, **49**, 457-467.

INOUE, A., KOHYAMA, N., KITAGAWA, R., AND WATANABE, T., 1987. Chemical and morphological evidence for the conversion of smectite to illite. Clays and Clay Minerals, **35**, 111-120.

JACKSON, M.L., 1969. Soil Chemical Analysis-Advanced Course: 2nd Ed., Published by the author, Madison, Wisconsin, 895p.

JANSA, L.F., GRADSTEIN, F.M., HARRIS, I.M., JENKINS, W.A., AND WILLIAMS, G.L., 1976. Stratigraphy of the Amoco-IOE Murre G-67 well, Grand Banks of Newfoundland. Geol. Surv. Canada Paper **75-30**, 1-14p.

JANSA, L.F., AND WADE, J.A., 1975. Geology of the continental margin off Nova Scotia and Newfoundland. Geol. Surv. Canada Paper, **74-30**, 51-105.

JENNINGS, S., AND THOMPSON, G.R. 1986. Diagenesis of Plio-Pleistocene sediments of the Colorado River delta, southern California. Jour. Sed. Petrol., **56**, 89-98.

KANASEWICH, E.R., EVANS, M.E., AND HAVSKOV, J., 1981. Platetectonic patterns and connection in the Phanerozoic: In: O'Connell, R. J., Fyfe, W. S. (Eds.), Evolution of the Earth, Geodynamics Series, **5**, Amer. Geophy. Union, Washington, D. C., 147-166.

KEEN, C.E., AND BARRETT, D.L., 1981. Thinned and subsided continental crust on the rifted margin of eastern Canada: crustal structure, thermal evolution and subsidence history. Geophys. Jour. Royal Astronomical Soc., **65**, 443-465.

KEEN, C.E. AND BEAUMONT, C. 1990. Geodynamics of rifted continental margins, Chapter 9. Geology of the Continental Margin of Eastern Canada. In: Kenn, M.J and Williams, G.L. (Eds.), Geology of North America Series. Geol. Soc. Amer. Bull., 853p.

KEEN, C.E., BOUTILIER, R., DE VOOGD, B., MUDFORD, B.S., AND ENACHESCU, M.E., 1987. Crustal geometry and models of the evolution of the rift basins on the Grand Banks of eastern Canada: constraints from deep seismic data. In: Beaumont, C. and Tankard, A.J. (Eds.), Sedimentary Basins and Basin-Forming Mechanisms. Canadian Soc. Petrol. Geol. Memoir, **12**, 101-115.

KING, A.F., 1990. Geology of the St. John's Area. Dept. Mines and Energy, Govt. Newfoundland and Labrador., Report **90-2**, 88p.

KING, L.H., FADER, G.B.J., JENKINS, W.A.M., AND KING, E.L., 1986. Occurrence and regional geological setting of Paleozoic rocks on the Grand Banks of Newfoundland. Can. Jour. Earth Sci., **23**, 504-526.

KLITGORD, K.D., AND SCHOUTEN, H., 1986. Plate kinematics of the central Atlantic. In: Vogt, P. R. and Tucholke, B. E. (Eds.), The geology of North America, Volume M, The Western North Atlantic region. Geol. Soc. Amer. Bull., 351-378.

LAW, B., AND DICKINSON, W., 1985. Conceptual model for origin of abnormally pressured gas accumulations in low permeability reservoirs. Amer. Assoc. Petrol. Geol. Bull., **69**, 1295-1304.

LAWRENCE, J.R., AND TAYLOR, H.P., 1971. Deuterium and oxygen-18 correlation: Clay minerals and hyroxides in Quaternary soils compared to meteoric waters. Geochim. Cosmochim. Acta, **35**, 993-1003.

LINDGREEN, H., 1987. Experiments on adsorption and molecular sieving and inferences on primary migration in Upper Jurassic claystone source rocks, North Sea. Amer. Assoc. Petrol. Geol. Bull., **71**, 308-321.

LINDGREEN, H., 1991. Elemental and structural changes in illite/smectite mixed-layer clay minerals during diagenesis in Kimmeridgian-Volgian(-Ryazanian) clays in the Central Trough, North Sea and the Norwegian-Danish Basin. Bull. Geol. Soc. Denmark, **39**, 1-82.

LOUGHNAN, F.C., GRIM, R.E., AND VERNET, J., 1962. Weathering of some triasic shales in the Sydney area. Jour. Geol. Soc. Australia, **8**, 245-258.

LONGSTAFFE, F.J., 1989. Stable isotopes as tracers in clastic diagenesis. In: Hutcheon, I.E. (Ed.), Burial Diagenesis, Mineralogical Association of Canada Short Course Series, **15**, 201-277.

MAGARA, K., 1975a. Reevaluation of montmorillonite dehydration as cause of abnormal pressure and hydrocarbon migration. Amer. Assoc. Petrol. Geol. Bull., **59**, 292-302.

MAGARA, K., 1975b. Importance of aquathermal pressuring effect in Gulf Coast. Amer. Assoc. Petrol. Geol. Bull., **59**, 2037-2045.

MAGARA, K., 1976. Water expulsion from clastic sediments during compaction-directions and volumes. Amer. Assoc. Petrol. Geol. Bull., **60**, 543-553.

MASSON, D.G., AND MILES, P.R., 1984. Mesozoic sea-floor spreading between Iberia, Europe and North America. Marine Geology, **56**, 279-287.

MATHIEU, Y., AND VELDE, B., 1989. Identification of thermal anomalies using clay mineral composition. Clay Minerals, **24**, 591-602.

McALPINE, K.D., 1990. Mesozoic stratigraphy, sedimentary evolution, and petroleum potential of the Jeanne d'Arc Basin, Grand Banks of Newfoundland. Geol. Surv. Canada Paper, **89-17**, 50pp.

McIVER, N.L., 1972. Cenozoic-Mesozoic stratigraphy of the Nova Scotia shelf. Canadian Jour. Earth Sci., **9**, 54-70.

McKEAGUE, J.A., AND BRYDON, J.E., 1970. Mineralogical properties of ten reddish brown soils from the Atlantic provinces in relation to parent materials and pedogenesis. Canadian Jour. Soil. Sci., **50**, 47-55.

McKENZIE, D.P., 1978. Some remarks on the development of sedimentary basins. Earth and Planetary Science Letters, **40**, 25-32.

McMILLAN, N.J., 1982. Canada's east coast; the new super petroleum province. Jour. Petrol. Tech., **21**, 1-15.

MENELEY, R.A., 1986. Oil and gas fields in the east coast and Arctic Basins of Canada. In: Halbouty, M. T. (Ed.), Future petroleum provinces of the world. Amer. Assoc. Petrol Geol. Memoir, **40**, 143-176.

MOMPER, J.A., 1980. Generation of abnormal pressures through organic matter transformations. Amer. Assoc. Petrol. Geol. Bull., **64**, p753 (abs.).

NADEAU, P.H., AND REYNOLDS, R.C.JR., 1981. Burial and contact metamorphism in the Mancos Shale. Clays and Clay Minerals, **29**, 249-259.

NADEAU, P.H., TAIT, J.M., McHARDY, W.J., AND WILSON, M.J., 1984a. Interstratified XRD characteristics of physical mixtures of elementary clay particles. Clay Minerals, **19**, 67-76.

NADEAU, P.H., WILSON, M.J., McHARDY, W.J., AND TAIT, J.M., 1984b. Interstratified clays as fundamental particles. Science, **225**, 923-925.

O'BRIEN, S.J., WARDLE, R.J., KING, A.F., 1983. The Avalon Zone: A Pan-African terrane in the Appalachian Orogen of Canada. Geological Jour., **18**, 195-222.

PEARCE, R.B., CLAYTON, T., AND KEMP, A.E., 1991. Illitization and organic maturity in Silurian sediments from the southern uplands of Scotland. Clay Minerals, **26**, 199-210.

PEARSON, M.J., WATKINS, D., PITTION, J.L., CASTON, D., AND SMALL, J.S., 1983. Aspects of burial diagenesis, organic maturation and palaeothermal history of an area in the South Viking Graben, North Sea. Geol. Soc. London, Special Publ., **12**, 161-173.

PEARSON, M.J., AND SMALL, J.S. 1988. Illite-smectite diagenesis and paleotemperatures in northern North Sea Quarternary to Mesozoic shale sequences. Clay Minerals, **23**, 109-132.

PERRY, E.A. AND HOWER, J., 1970. Burial diagenesis in the Gulf Coast pelitic sediments. Clays and Clay Minerals, **18**, 165-177.

PERRY, E.A., AND HOWER, J., 1972. Late stage dehydration in deeply buried pelitic sediments. Amer. Assoc. Petrol. Geol. Bull., **56**, 2013-2021.

POLLASTRO, R.M., 1993. Considerations and applications of the illite/smectite geothermometer in Hydrocarbon-bearing rocks of miocene to Missisippian Age. Clays and Clay Minerals, **41**, 119-133.

POLLASTRO, R.M., AND SCHMOKER, J. 1989. Relationship of clay-mineral diagenesis to temperature, age, and hydrocarbon generation-An example from the Anadarko basin, Oklahoma. In: Johnson, K.S., (Ed.), Anadarko Basin Symposium, 1988, Oklahoma. Geol. Surv. Circular, **90**, 257-261.

POWELL, T.G., 1985. Paleogeographic implications for the distribution of Upper Jurassic source beds, Offshore Eastern Canada. Bull. Canadian Petrol. Geol., **33**, 116-119.

POWELL, T.G., FOSCOLOS, A.E., GUNTHER, P.R., AND SNOWDON, L. R. 1978. Diagenesis of organic matter and fine clay minerals: a comparative study. Geochim. Cosmochim. Acta, **42**, 1181-1197.

POWERS, M.C., 1967. Fluid release mechanisms in compacting marine mudrocks and their importance in oil exploration. Amer. Assoc. Petrol. Geol. Bull., **51**, 1240-1254.

PRIMMER, T.J., AND SHAW, H., 1991. Variations in the δD and $\delta^{18}O$ compositions of illite-smectite in a partly overpressured Tertiary sequence from an offshore well, Texas Gulf Coast, USA. Marine and Petrol. Geol., **8**, 225-231.

PROCTER, R.M., TAYLOR, G.C., AND WADE, J.A., 1984. Oil and natural gas resources of Canada-1983. Geol. Surv. Canada Paper **83-31**, 59pp.

PURCELL, L.P., RASHID, M.A., AND HARDY, I.A., 1979. Geochemical characteristics of sedimentary rocks in Scotian Basin. Amer. Assoc. Petrol. Geol. Bull., **63**, 87-105.

PYTTE, A.M. AND REYNOLDS, R.C. JR., 1989. The thermal transformation of smectite to illite. In: Naesar, N.D. and McCulloh, T.H. (Eds.), Thermal History of Sedimentary Basins, Springer-Verlag, New York, 133-140.

RAMSEYER, K., AND BOLES, J.R., 1986. Mixed-layer illite/smectite minerals in Tertiary sandstones and shales, San Joaquin Basin. California. Clays and Clay Minerals, **34**, 115-124.

REYNOLDS, R.C., 1980. Interstratified clay minerals. In: Brindley, G. W., and Brown, G. (Eds.), Crystal structures of clay minerals and their X-ray identification. Mineralogical Soc., London, 249-303.

REYNOLDS, R.C., 1985. NEWMOD, a computer program for the calculation of one-dimensional diffraction patterns of mixed-layered clays: R.C. Reynolds, Jr., Dartmouth College, Hanover, New Hampshire.

REYNOLDS, R.C., AND HOWER, J., 1970. The nature of interlaying in mixed-layer illite-montmorillonites. Clays and Clay Minerals, **18**, 25-36.

RICE, D.D., AND CLAYPOOL, G.E., 1981. Generation, accumulation, and resource potential of biogenic gas. Amer. Asoc. Petrol. Geol. Bull., **64**, 5-25.

ROBERSON, H.E., AND LAHANN, R.W., 1981. Smectite to illite conversion rates: Effects of solution chemistry. Clays and Clay Minerals, **29**, 129-135.

ROGERS, A.L., AND YASSIR, N.A., 1993. Hydrodynamics and overpressuring in the Jeanne d'Arc Basin, offshore Newfoundland, Canada: possible implications for hydrocarbon exploration. Bull. Canadian Petrol. Geol., **41**, 275-289.

ROYDEN, L., AND KEEN, C.E., 1990. Rifting process and thermal evolution of the continental margin of eastern Canada determined from subsidence curves: Earth and Planetary Science Letters, **51**, 343-361.

SAVIN, S.M., AND EPSTEIN, S., 1970a. The oxygen and hydrogen isotope geochemistry of clay minerals. Geochim. Cosmochim. Acta, **34**, 25-42.

SAVIN, S.M., AND EPSTEIN, S., 1970b. The oxygen and hydrogen isotope geochemistry of ocean sediments and shales. Geochim, Cosmochim. Acta, **34**,43-63.

SAVIN, S.M., AND LEE, M., 1988. Isotopic studies of phyllosilicates. In: Bailey, S.W. (Ed.), Hydrous Phyllosilicates, (exclusive of micas), Reviews in Mineralogy, **19**, 189-223.

SCHOONMAKER, J., MACKENZIE, F.T., AND SPEED, R.C., 1986. Tectonic implications of illite/smectite diagenesis, Barbados Accretiionary Prism. Clays and Clay Minerals, **34**, 465-472.

SCOTCHMAN, I.C., 1987. Clay diagenesis in the Kimmeridge Clay Formation, onshore UK, and its relation to organic maturation. Miner. Magazine, **51**, 535-551.

SHEPPARD, S.M.F., 1986. Characterization and isotopic variations in natural waters. In: Valley, J.W., Taylor, H.P., and O'Neil, J.R. (Eds.), Stable Isotopes in High Temperature Geological Processes. Reviews in Mineralogy, Miner. Soc. Am. Washington DC, **16**, 165-183.

SHERWIN, D.F., 1973. Scotian Shelf and Grand Banks. In: McCrossan, R. G. (Ed.), The future petroleum provinces of Canada. Canadian. Soc. Petrol. Geol., Memoir, **1**, 519-559.

SHI, Y., AND WANG, C., 1986. Pore pressure generation in sedimentary basins-overloading versus aquathermal. Jour. Geophys. Research, **91**, 2153-2162.

SINCLAIR, I.K., 1988. Evolution of Mesozoic-Cenozoic sedimentary basins in the Grand Banks area of Newfoundland and comparison with Falvey's (1974) rift model. Bull. Canada Petrol. Geol., **16**, 255-273.

SINCLAIR, I.K., 1993. Tectonism: the dominant factor in mid-Cretaceous deposition in the Jeanne d'Arc Basin, Grand Banks. Marine Petrol. Geol., **10**, 530-549.

SINCLAIR, I.K., McALPINE, K.D., SHERWIN, D.F., McMILLAN, N. J., 1992. Petroleum resources of the Jeanne d'Arc Basin and environs, Grand Banks, Newfoundland. Part 1: Geological Framework. Geol. Surv. Canada, **92-8**, 1-38.

SLEEP, N.H., 1971. Thermal effects of the formation of the Atlantic continental margins by continental breakup: Geophys. Jour. Royal Astronomical Soc., **24**, 325-350.

SMART, G., AND CLAYTON, T., 1985. The progressive illitization of interstratified illite-smectite from carboniferous sediments of Northern England and its relationship to organic maturity indicators. Clay Minerals, **20**, 455-466.

SMITH, G.C., AND COOK, A.C., 1980. Coalification paths of exinite, vitrinite and inertinite. Fuel, **59**, 641-646.

SNOWDON, L.R., AND KROUSE, H.R., 1986. The stable carbon isotope distribution of distillation fractions of three Canadian frontier crude oils. Bull. Canadian Petrol. Geol., **34**, 379-383.

SOLIMAN, O.M., 1995. Depositional facies and calcite cementation in the Avalon Formation, Hibernia oil field, Jeanne d'Arc Basin, Grand Banks of Newfoundland. Unpubl. Ph. D. thesis, Memorial University of Newfoundland, St. John's, 282pp.

SRIVASTAVA, S.P., 1978. Evolution of the Labrador Sea and its bearing on the early evolution of the North Atlantic. Geophys. Jour. Royal Astronomical Soc., **52**, 313-357.

ŚRODOŃ, J., 1979. Correlation between coal and clay diagenesis in the Carboniferous of the Upper Silesian Coal Basin. In: Mortland, M.M. and Farmer, V.C., (Eds.), Proc. Int. Clay Conf., Oxford, 1978, Dev. Sedimentology, **27**, 251-260.

ŚRODOŃ, J., 1980. Precise identification of illite/smectite interstratification by X-ray powder diffraction. Clays and Clay Minerals, **28**, 401-411.

ŚRODOŃ, J., 1981. X-ray identification randomly inter-stratified illite-smectite in mixtures with discrete illite. Clay Minerals, **16**, 297-304.

ŚRODOŃ, J., 1984. X-ray identification of illitic materials. Clay and Clay Minerals, **32**, 337-349.

STEINER, A., 1968. Clay minerals in hydrothermally altered rocks at Wairakei, New Zealand. Clays and Clay Minerals, **16**, 193-213.

SUCHECKI, R.K., AND LAND, L.S., 1983. Isotopic geochemistry of burial-metamorphosed volcanogenic sediments, Great Valley sequence, northern California. Geochim. Cosmochim. Acta, **47**, 1487-1499.

SWIFT, J.H., AND WILLIAMS, J.A., 1980. Petroleum source rocks, Grand Banks area. In: Miall, A. D. (Ed.), Facts and principles of world petroleum occurrence. Canadian. Soc. Petrol. Geol. Memoir, **6**, 167-188.

TANKARD, A.J., AND WELSINK, H.J., 1987. Extensional tectonics and stratigraphy of Hibernia oil field, Grand Banks, Newfoundland. Amer. Assoc. Petrol. Geol. Bull., **71**, 1210-1232.

TANKARD, A.J., AND WELSINK, H.J., 1988. Extensional tectonics, structural styles and stratigraphy of the Mesozoic Grand Banks of Newfoundland. In: Manspeizer, W. (Ed.), Triassic-Jurassic rifting and opening of the Atlantic Ocean, Elsevier, Amsterdam, 129-165.

TAYLOR, G.C., BEST, M.E., CAMPBELL, G.R., HEA, J.P., HENAO, D., PROCTER, R. M., 1992. Petroleum resources of the Jeanne d'Arc Basin and environs, Grand Banks, Newfoundland. Part II: Hydrocarbon Potential. Geol. Surv. Canada, **92-8**, 39-48.

TEICHMÜLLER, M., 1979. Die Diagenese der Kohligen Substanzen in den Gesteinen des Tertiars und Mesozoikums des mittleren Oberrhein-Grabens. Fortschr. Geol. Rheinl. Westfalen, **27**, 19-49.

TEICHMÜLLER, M., 1987. Recent advances in coalification studies and their application to geology. In: Scott, A.C. (Ed.), Coal and Coal-Bearing Strata: Recent Advances. Geol. Soc. London, Special Publ., **32**, 127-169.

TISSOT, B.P., AND WELTE, D.H., 1978. Petroleum Formation and Occurrence. Springer Verlag, Berlin, 538 pp.

TOMITA, K., TAKAHASHI, H., WATANABE, T., 1988. Quantification curves for mica/smectite interstratifications by X-ray powder diffraction. Clays and Clay Minerals, **36**, 258-262.

TRIBBLE, J.S., AND YEH, H.Y., 1994. Origin of smectite and illite-smectite in the Barbados accretionary complex: Oxygen isotopic evidence. Geology, **22**, 219-222.

UREY, H.C., 1947. The thermodynamic properties of istopic substances. Jour. Chemical Soc. (London), 562-581.

VELDE, B., AND LIJIMA, A., 1988. Comparison of clay and zeolite mineral occurrences in Neogene age sediments from several deep wells. Clays and Clay Mineral, **36**, 337-342.

VELDE, B., SUZUKI, T., AND NICOT, E., 1986. Pressure - temperature-composition of illite/smectite mixed-layer minerals: Niger Delta mudstones and other examples. Clays and Clay Minerals, **34**, 435-441.

Von der DICK, H., MELOCHE, J.D., DWYER, J., AND GUNTHER, P., 1989. Source-rock geochemistry and hydrocarbon generation in the Jeanne d'Arc Basin, Grand Banks, Offshore Eastern Canada. Jour. Petrol. Geol., **12**, 51-68.

WAPLES, D.W., 1980. Time and temperature in petroleum formation: Application of Lopatin's method to petroleum exploration. Amer. Assoc. Petrol. Geol. Bull., **64**, 916-926.

WATANABE, T., 1981. Identification of illite/montmorillonite interstratifications by X-ray powder diffraction. Jour. Miner. Soc. Japan, Special, **15**, 32-41.

WEAVER, C.E., 1978. Mn-Fe coatings on saprolite fracture surfaces. Jour. Sed. Petrol., **48**, 595-610.

WEAVER, C.E., 1979. Office of Nuclear Waste and Isolation Technical Report, **21**, 176p.

WEAVER, C.E., 1989. Clays, muds, and shales, Development in Sedimentology, **44**, Elsevier, New York.

WEAVER, C.E., AND BECK, K.C., 1971. Clay water diagenesis during burial, how mud becomes gneiss. Geol. Soc. Amer. Special Paper, **134**, 96pp.

WHITESIDE, R. M. 1932. Geologic interpretations from rotary well cuttings. Amer. Assoc. Petrol. Geol. Bull., **16**, 653-674.

WHITNEY, G., 1990. Role of water in the smectite-to-illite reaction. Clays and Clay Minerals, **38**, 343-350.

WHITNEY, G. AND NORTHROP, H.R., 1988. Experimental investigation of the smectite illite reaction: Dual reaction mechanisms and oxygen-isotope systematics. Am. Mineralogist, **73**, 77-90.

WILKINSON, M., CROWLEY, S.F., AND MARSHALL, J.D., 1992. Model for the evolution of oxygen isotope ratios in the pore fluids of mudrocks during burial. Marine Petrol. Geol., **9**, 98-105.

WILLIAMSON, M.A., 1992. The subsidence, compaction, thermal and maturation history of the Egret Member source rock, Jeanne d'Arc Basin, offshore Newfoundland. Bull. Canadian Petrol. Geol., **40**, 136-150.

WILLIAMSON, M.A., DESROCHES, K., AND KING, S., 1993. Overpressures and hydrocarbon migration in the Hibernia-Nautilus area of the Jeanne d'Arc Basin, offshore Newfoundland. Bull. Canadian Petrol. Geol., **41**, 389-406.

YEH, H.W., AND ESLINGER, E.V., 1986. Oxygen isotopes and the extent of diagenesis of clay minerals during sedimentation and burial in the sea. Clays and Clay Minerals, **34**, 403-406.

YEH, H.W., AND SAVIN, S.M., 1976. Mechanism of burial metamorphism of argillaceous sediments: 3. O-isotope evidence. Geol. Soc. Amer. Bull., **88**, 1321-1330.

YEH, H.W., AND SAVIN, S.M., 1977. Mechanism of burial metamorphism of argillaceous sediments: 3. O-isotope evidence. Geol. Soc. Amer. Bull., **88**, 1321-1330.

APPENDIX I

PROCEDURE FOR CLAY MINERAL SEPARATION

1. Weigh approximately 15-20g of clean handpicked drill-cuttings. Add distilled water and leave overnight.

2. To dissolve carbonate phase, remove the water and add 150ml sodium acetate-acetic acid (NaOAc) buffered at 5.0 pH. Stir and heat the sample for 1/2 hour (temperature <40°C) and leave it to react overnight at room temperature.

3. To disaggregate the clay minerals use ultrasonic probe (horn-type) for 2 minutes at 50-70 watts (use rock/water ratio of about 1:10). Repeat the above step with additional distilled water until all the drill-cuttings are disaggregated.

4. Centrifuge and discard the supernatant liquid (use International #2 centrifuge at 2000rpm for 30-60 minutes). The supernatant liquid should be crystal clear. If the sample is slightly cloudy or tinted, use a high speed centrifuge (at 15000rpm for approximately 1 hour).

5. Add 250 ml distilled water and stir slowly to disperse the sample completely and remove the water by centrifuge. Use high speed centrifuge if supernatant liquid is not clear.

6. To remove the organic matter, use Hydrogen Peroxide (30%) and follow Jackson's (1967) method.

7. Wash the sample (2-3 times) with 150 ml NaOAc of pH 5.0. Stir and leave the sample for about 15-30 (or more) minutes. This will help to remove the remaining carbonate phase, if any. Organic-matter rich samples may give a light-brownish colour after centrifugation.

8. Wash the sample with 1M NaCl for 3-5 times. Use 150ml 1M NaCl and leave for 1-2 hours before centrifugation.

9. Wash the sample 4 times with distilled water. For each run use about 200-250ml water. First use 250ml centrifuge bottles at 2000rpm (International #2 Centrifuge) for about 20-30 minutes. The water will be crystal clear and sediments will show various layers because of different grain-size. The second or third wash may give a muddy suspension and would require an ultracentrifuge (35000rpm for 20 minutes with 60Ti rotor).

10. Add 80-100mg (for 400-500ml sample) of sodium pyrophosphate as a dispersing agent and stir for a few minutes.

11. First separate <2.0μm grain-size cut from >2.0μm grain-size fraction, then separate <0.1μm grain-size fraction from <2.0μm grain-size cut. Grain-size separation should be done as soon as possible after step #10.

12. To concentrate <0.1μm grain-size fraction (if freeze-dryer is not available), flocculate the suspension with 1M NaCl (about 100ml for 500ml sample) and remove the water by vacuum suction method.

13. Wash the <0.1μm fraction 4-5 times (or more) with distilled water using low speed and ultracentrifuge.

14. Dry the sample in an oven at 40°C.

APPENDIX II
Well Casing Depths*
(meters)

Adolphus D-50:	1212.8, 2945.9
Bonanza M-71:	1438.1, 3455.0, 4488.1, 5029.9
Conquest K-09:	2949.0, 3946.6
Cormorant N-83:	2972.8
Dominion O-23:	1259.8, 2971.2
Egret K-36:	1982.1
Egret N-46:	1653.3
Hebron I-13:	2810.3, 4451.3
Nautilus C-92:	3162.9, 4087.4, 4843.0
North Ben Nevis P-93:	2673.7, 4037.4, 5196.0
North Dana I-43:	3206.5, 4368.4, 4698.2
North Trinity H-71:	2263.2, 3873.8, 4286.6
South Mara C-13:	2736.2, 4046.0
South Tempest G-88:	2208.8, 3638.7, 4162.1
West Flying Foam L-23:	1636.8, 3671.1
Whiterose J-49:	2487.5, 3702.1

* All depths from RT (Rotary Table). Data from Canada-Newfoundland Offshore Petroleum Board's Schedule of Wells (1988).

APPENDIX III

XRD Peak Positions (°2θ) and Relevant Data for Mixed-layer I/S

Sample Depth(m)	Reflections from glycolated samples (°2θCuKα radiation)					Reflections from air-dried samples		BB1	BB2	Ordering types	%I in I/S	Method (error)
Adolphus D-50												
1565	5.11	SH	15.98	26.33	31.38	7.47	27.46	-	-	R0	33	1 (<5)
1695	5.16	9.98	15.90	26.28	31.44	7.21	27.77	-	-	R0	29	1 (<5)
1810	5.16	9.98	15.94	26.30	31.38	7.42	27.77	-	-	R0	33	1 (<5)
1935	5.16	9.98	15.94	26.32	31.48	7.36	27.82	-	-	R0	31	1 (<5)
2035	5.14	9.98	15.98	26.33	31.46	7.36	27.92	-	-	R0	34	1 (<5)
2075	5.16	9.98	16.03	26.33	31.46	7.42	27.87	-	-	R0	37	1 (<5)
2165	5.18	9.86	16.03	26.33	31.56	7.36	27.87	-	-	R0	35	1 (<5)
2310	5.21	9.67	16.34	26.38	31.54	7.62	27.66	-	-	R0	48	1 (<5)
2400	5.20	9.92	16.03	26.32	31.52	7.36	27.97	-	-	R0	36	1 (<5)
2435	5.26	9.88	16.08	26.33	31.51	7.42	27.92	-	-	R0	39	1 (<5)
2580	5.26	9.83	16.08	26.33	31.46	7.47	27.97	-	-	R0	40	1 (<5)
2665	5.37	9.64	16.28	26.38	ND	7.62	27.66	-	-	WR1	50	2 (±5)
2785	5.21	9.77	15.98	26.43	31.60	7.36	28.08	-	-	R0	31	1 (<5)
2884	5.40	9.72	16.28	26.42	31.64	7.57	27.92	-	-	WR1	53	4 (<5)
3000	5.50	9.70	16.34	26.43	31.46	7.62	27.82	-	-	WR1	56	4 (<5)
3032	5.52	9.80	16.18	26.38	31.54	7.52	28.02	-	-	WR1	49	4 (<5)
3135	6.42	9.57	16.52	26.43	32.92	7.52	27.97	5.54	5.30	R1	60	4 (<5)
3135	5.52	9.77	16.18	26.38	31.56	7.83	27.66	-	-	WR1	50	4 (<5)
3285	6.70	9.47	16.64	26.49	33.30	7.88	27.61	5.34	5.52	R1	66	4 (<5)
3365	6.85	9.31	16.80	26.49	33.48	7.98	27.41	5.15	5.35	R1	74	4 (<5)
3390	6.75	9.42	16.70	26.50	33.32	7.93	27.56	5.44	5.30	R1	66	4 (<5)
3435	6.18	9.66	16.32	26.38	32.70	7.67	27.82	6.04	5.40	R1	57	4 (<5)
3520	6.75	9.40	16.70	26.48	33.36	7.98	27.51	5.29	5.23	R1	72	4 (<5)
3580	6.75	9.38	16.69	26.46	33.34	7.93	27.51	5.13	5.35	R1	71	4 (<5)
3660	6.95	9.32	16.86	26.54	33.60	8.08	27.46	5.03	5.15	R1	76	4 (<5)
Archer K-19												
2530	6.94	8.85	17.26	26.46	33.38	8.10	27.20	4.87	4.31	R1	62	3 (±4)
3220	5.26	9.52	16.49	26.28	31.70	7.67	27.31	ND	ND	R0	60	2 (±5)
3305	6.50	9.15	16.90	26.40	33.50	7.88	27.20	ND	ND	R1	65	3 (±4)
3515	6.50	8.85	16.95	26.38	33.24	7.98	27.20	5.24	4.58	R1	58	2 (±5)
Beothuk M-05												
2685	6.90	SH	17.05	26.34	33.68	8.08	27.10	4.61	4.27	R1	70	3 (±4)
3415	7.21	8.85	17.21	26.54	33.82	7.92	26.96	4.20	4.20	R1	73	3 (±4)
Bonanza M-71												
1930	5.16	10.08	15.82	26.33	31.52	7.16	27.97	-	-	R0	21	1 (<5)
2020	5.16	9.96	15.98	26.33	31.62	7.31	27.82	-	-	R0	30	1 (<5)
2505	5.26	ND	16.03	26.38	31.56	7.47	27.66	-	-	R0	34	1 (<5)
2820	5.21	9.72	16.03	26.38	31.64	7.47	27.66	-	-	R0	33	1 (<5)
3135	5.31	9.62	16.23	26.38	31.76	7.57	27.72	-	-	R0	42	1 (<5)
3390	5.37	9.76	16.22	26.49	31.84	7.62	27.82	-	-	R0	41	1 (<5)
3520	7.36	9.12	17.14	26.62	33.94	8.24	27.15	4.93	4.43	R1	76	3 (±4)
3620	7.21	9.26	17.00	26.54	33.92	8.26	27.05	4.82	4.83	R1	75	3 (±4)
3920	7.36	8.90	17.28	26.64	34.00	8.13	27.20	4.61	4.30	R1	79	3 (±4)
4180	7.22	8.85	17.16	26.59	33.88	8.03	27.25	4.90	4.45	R1	75	3 (±4)
5175	7.67	ND	17.31	26.54	34.46	8.08	27.05	3.88	ND	R3	88	3 (±4)

238

Sample Depth(m)	Reflections from glycolated samples (°2θCuKα radiation)					Reflections from air-dried samples		BB1	BB2	Ordering types	%I in I/S	Method (error)
Conquest K-09												
1635	5.16	9.86	15.84	26.38	31.42	7.26	27.82	-	-	R0	25	1 (<5)
2025	5.20	ND	16.22	26.34	31.40	7.57	27.51	-	-	R0	44	1 (<5)
2420	5.52	9.42	16.34	26.38	31.94	7.62	27.66	5.99	5.26	WR1	55	2 (±5)
2620	6.60	9.24	16.64	26.34	33.18	7.83	27.41	5.35	5.00	R1	60	2 (±5)
2825	6.54	SH	16.66	26.42	33.10	7.92	27.41	5.45	5.18	R1	65	2 (±5)
3025	6.72	9.28	16.80	26.48	33.50	7.88	27.31	5.13	4.91	R1	66	3 (±4)
3260	6.90	9.26	16.80	26.54	33.62	7.98	27.46	5.14	5.00	R1	69	3 (±4)
3935	7.82	8.80	17.48	26.64	34.68	8.29	27.10	3.78	3.82	R3	88	3 (±4)
4275	ND	8.74	17.72	26.64	34.79	8.44	26.74	3.51	3.14	R3	89	3 (±4)
4570	SH	8.65	17.56	26.58	35.10	8.24	26.79	3.77	3.37	R3	92	3 (±4)
4950	7.98	ND	17.36	26.54	34.84	8.28	27.00	3.67	3.00	R3	90	3 (±4)
Cormorant N-83												
1470	5.16	8.85	16.26	26.48	31.56	7.42	27.51	ND	ND	R0	43	1 (<5)
1725	5.88	8.75	17.28	26.48	ND	7.96	27.31	5.45	ND	WR1	55	2 (±5)
1940	6.60	8.80	17.17	26.54	33.22	8.03	27.25	5.13	ND	R1	65	2 (±5)
2155	7.16	8.75	17.46	26.58	33.60	8.19	27.20	5.03	4.22	R1	68	3 (±4)
2380	6.00	8.75	17.28	26.54	ND	8.03	27.15	5.35	ND	WR1	60	2 (±5)
Dominion O-35												
2275	5.16	ND	16.03	26.38	31.48	7.40	27.61	•	-	R0	34	1 (<5)
2510	5.21	ND	16.24	26.38	31.42	7.57	27.56	•	•	R0	46	1 (<5)
2890	5.18	9.11	16.50	26.38	31.56	7.72	27.42	-	-	R0	58	2 (±5)
3110	6.03	ND	16.54	26.42	32.75	7.72	27.51	5.84	ND	WR1	58	2 (±5)
3235	6.42	ND	16.60	26.43	32.88	7.83	27.41	5.60	5.40	R1	60	2 (±5)
3330	6.80	9.11	16.85	26.54	33.54	8.08	27.31	5.40	5.30	R1	67	3 (±4)
3530	7.26	9.06	17.00	26.54	33.80	8.03	27.25	4.71	4.71	R1	75	3 (±4)
3700	7.34	9.16	17.04	26.58	34.10	8.19	27.20	4.72	4.68	R1	79	3 (±4)
Egret K-36												
1625	5.21	ND	15.82	26.43	31.42	7.01	27.61	•	•	R0	22	1 (<5)
2090	5.16	10.18	15.98	26.22	31.32	7.31	27.62	-	•	R0	35	1 (<5)
2120	5.11	10.28	15.94	26.18	31.34	7.36	27.56	-	-	R0	34	1 (<5)
2265	5.11	SH	16.39	26.28	31.52	7.62	27.36	-	-	R0	48	1 (<5)
2420	6.68	8.80	17.16	26.54	33.28	7.98	27.12	4.72	4.64	R1	59	2 (±5)
2935	7.11	8.74	17.16	26.54	33.62	8.08	27.05	4.93	4.86	R1	69	3 (±4)
3110	6.90	8.60	17.05	26.54	33.54	8.03	27.25	4.83	4.73	R1	67	3 (±4)
Egret N-46												
1590	5.01	ND	16.23	26.13	31.38	7.42	27.30	•	-	R0	44	1 (<5)
1820	ND	ND	16.80	26.43	31.66	7.57	27.34	-	-	R0	60	2 (±5)
2015	7.14	8.80	17.22	26.38	33.78	7.83	27.00	4.93	4.55	R1	72	3 (±4)
2120	7.21	ND	17.05	26.43	33.90	8.13	27.05	4.71	4.62	R1	75	3 (±4)
Fortune G-57												
3580	7.26	9.11	17.16	26.56	33.92	8.18	27.26	4.61	4.26	R1	75	3 (±4)
3790	7.11	8.90	17.16	26.50	33.90	8.12	27.24	4.71	4.36	R1	75	3 (±4)
4175	6.20	9.52	16.55	26.30	32.90	7.77	27.36	ND	5.23	R1	60	2 (±5)
4350	6.85	SH	16.96	26.42	33.52	7.82	26.06	4.93	5.09	R1	66	3 (±4)

Sample Depth(m)	Reflections from glycolated samples (°2θCuKα radiation)					Reflections from air-dried samples		BB1	BB2	Ordering types	%I in I/S	Method (error)
Gambo N-70												
1960	5.11	10.1	15.92	26.18	31.32	7.36	27.72	ND	ND	R0	33	1 (<5)
2325	5.11	9.26	16.68	26.38	ND	7.78	27.38	ND	ND	R0	60	2 (±5)
2415	5.11	9.06	16.75	26.38	ND	7.88	27.36	ND	ND	R0	60	2 (±5)
Hebron I-13												
1155	5.21	9.98	15.82	26.28	31.46	7.16	27.60	-	-	R0	22	1 (<5)
1545	5.21	10.02	15.74	26.42	31.52	7.11	28.13	-	•	R0	15	1 (<5)
1830	5.26	9.77	15.98	26.38	31.52	7.34	27.87	-	•	R0	32	1 (<5)
2250	5.21	10.03	15.77	26.38	31.48	7.11	28.12	-	-	R0	19	1 (<5)
2675	7.32	8.80	17.26	26.59	34.28	8.19	27.10	4.40	4.18	R1	81	3 (±4)
3240	7.11	ND	17.10	26.42	33.74	8.13	27.25	5.08	4.32	R1	72	3 (±4)
3630	5.52	ND	16.90	26.28	31.52	7.83	27.31	ND	ND	WR1	60	2 (±5)
4185	6.80	ND	17.10	26.43	33.66	7.94	27.26	5.24	4.89	R1	70	3 (±4)
4605	SH	8.60	17.36	26.59	34.60	8.24	27.10	4.31	4.31	R1	87	3 (±4)
Nautilus C-92												
1975	5.26	ND	15.98	26.34	31.62	7.42	27.58	-	-	R0	28	1 (<5)
2355	5.26	ND	16.08	26.38	31.56	7.47	27.56	-	-	R0	36	1 (<5)
2740	5.16	ND	16.39	26.38	31.66	7.62	27.56	-	•	R0	48	1 (<5)
3030	7.36	8.80	17.26	26.59	33.80	8.24	27.05	4.82	ND	R1	73	3 (±4)
3470	SH	8.85	17.21	26.60	34.40	8.29	27.10	4.67	4.42	R1	84	3 (±4)
3695	7.60	8.90	17.64	26.64	34.47	8.29	27.05	4.73	4.22	R1	85	3 (±4)
4245	7.60	8.85	17.54	26.64	34.50	8.34	27.05	ND	3.95	R3	85	3 (±4)
North Ben Nevis P-93												
1565	5.21	ND	16.08	26.33	31.44	7.42	27.36	-	-	R0	37	1 (<5)
2025	5.20	9.72	15.86	26.42	31.48	7.31	27.87	-	-	R0	25	1 (<5)
2265	5.21	9.90	15.90	26.38	31.54	7.26	27.87	-	-	R0	26	1 (<5)
2415	5.21	9.88	15.98	26.44	31.66	7.32	27.92	-	-	R0	30	1 (<5)
2480	5.21	9.72	16.08	26.46	31.66	7.31	27.77	-	-	R0	36	1 (<5)
2545	5.21	9.47	16.28	26.46	31.68	7.62	27.61	-	-	R0	43	1 (<5)
2625	5.50	8.75	17.36	26.54	31.46	8.08	27.20	5.14	ND	WR1	55	2 (±5)
2670	6.19	ND	16.70	26.52	31.64	7.92	27.41	5.24	5.45	WR1	60	2 (±5)
2730	6.75	ND	16.95	26.54	33.46	8.08	27.31	5.01	4.23	R1	64	3 (±4)
2915	ND	8.75	17.72	26.68	ND	8.42	26.90	4.45	3.55	R3	90	2 (±5)
3275	7.16	8.80	17.42	26.60	ND	8.08	27.05	4.72	ND	R1	80	2 (±5)
3770	7.36	8.64	17.67	26.54	34.32	8.26	27.05	4.64	4.16	R1	82	3 (±4)
4125	ND	8.60	17.41	26.64	34.84	8.19	27.10	4.02	3.03	R3	90	3 (±4)
North Dana I-43												
1800	5.24	9.98	15.88	26.38	31.56	7.11	28.13	-	-	R0	24	1 (<5)
2030	5.21	9.98	15.93	26.43	31.48	7.06	28.07	-	-	R0	31	1 (<5)
2075	5.26	9.98	15.87	26.38	31.56	7.16	28.02	-	-	R0	24	1 (<5)
2225	5.21	9.77	16.03	26.38	31.56	7.26	27.82	-	-	R0	34	1 (<5)
2465	5.22	9.67	16.18	26.43	31.61	7.36	27.77	-	-	R0	40	1 (<5)
3025	5.21	9.72	16.18	26.43	31.62	7.42	27.82	-	•	R0	42	1 (<5)
3325	5.26	9.72	16.28	26.49	31.64	7.52	27.82	-	-	R0	46	1 (<5)
3480	5.26	9.88	16.13	26.43	31.64	7.42	27.92	•	-	R0	40	1 (<5)
3720	6.39	9.36	16.69	26.43	32.89	8.00	27.25	5.55	5.24	R1	65	2 (±5)

Sample Depth(m)	Reflections from glycolated samples (°2θCuKα radiation)					Reflections from air-dried samples		BB1	BB2	Ordering types	%I in I/S	Method (error)

North Dama I-43 Continued.

Sample Depth(m)								BB1	BB2	Ordering types	%I in I/S	Method (error)
3915	7.11	8.80	16.94	26.52	33.72	7.98	27.20	4.97	4.90	R1	71	3 (±4)
4155	7.64	ND	17.46	26.60	34.83	8.13	26.84	4.28	2.84	R3	90	3 (±4)
4470	7.16	8.80	17.07	26.54	34.45	7.98	27.20	4.46	ND	R1	85	3 (±4)
5230	7.57	8.65	17.31	26.49	34.88	8.03	26.95	4.00	2.88	R3	90	3 (±4)

North Trinity H-71

Depth(m)												
1525	5.21	9.83	15.72	26.34	31.51	7.11	27.90	-	-	R0	14	1 (<5)
1875	6.90	8.90	17.16	26.60	33.64	8.13	27.30	4.93	5.03	R1	69	3 (±4)
1925	5.21	ND	15.98	26.38	31.46	7.26	27.72	-	-	R0	33	1 (<5)
2145	7.26	8.90	17.20	26.58	33.96	8.24	27.15	5.14	4.70	R1	76	3 (±4)
2165	7.11	ND	17.00	26.38	33.74	8.19	27.20	5.24	4.97	R1	71	3 (±4)
2220	7.50	8.75	17.36	26.54	34.20	8.29	27.10	4.72	4.50	R1	80	3 (±4)
2350	SH	8.80	17.00	26.49	32.90	8.03	27.25	ND	ND	WR1	60	2 (±5)
2755	6.95	8.80	17.16	26.54	33.65	8.08	27.31	5.03	4.77	R1	70	3 (±4)
3345	7.44	SH	17.57	26.49	34.10	8.24	27.15	4.87	4.40	R1	79	3 (±4)
3760	5.62	ND	16.95	26.38	ND	7.88	27.25	5.59	5.74	WR1	60	2 (±5)
4250	5.78	SH	16.80	26.33	ND	7.88	27.24	5.45	ND	WR1	60	2 (±5)

Port au Port J-97

Depth(m)												
1600	5.10	9.88	16.04	26.32	31.52	7.36	27.77	ND	ND	R0	36	1 (<5)
1865	4.95	ND	16.50	26.24	ND	7.72	27.30	ND	ND	R0	58	2 (±5)

South Mara C-13

Depth(m)												
1225	5.11	ND	15.92	26.28	31.32	7.31	27.46	-	-	R0	31	1 (<5)
1440	5.16	10.03	15.82	26.23	31.34	7.40	27.64	-	-	R0	25	1 (<5)
1620	5.16	9.82	15.82	26.28	31.38	7.21	27.77	-	-	R0	24	1 (<5)
1730	5.16	10.03	15.87	26.33	31.46	7.16	28.07	-	-	R0	27	1 (<5)
1920	5.16	9.98	15.77	26.33	31.41	7.16	28.12	-	-	R0	21	1 (<5)
1975	5.11	9.82	15.88	26.33	31.32	7.39	27.82	-	-	R0	31	1 (<5)
2170	5.16	10.16	15.72	26.30	31.50	7.16	28.43	-	-	R0	15	1 (<5)
2335	5.16	9.98	15.84	26.32	31.41	7.16	28.07	-	-	R0	26	1 (<5)
2395	5.16	9.82	15.98	26.38	31.46	7.36	27.82	-	-	R0	35	1 (<5)
2455	5.11	9.88	15.82	26.32	31.36	7.26	27.82	-	-	R0	26	1 (<5)
2470	5.16	9.64	16.20	26.42	31.51	7.50	27.70	-	-	R0	46	1 (<5)
2520	5.16	9.52	16.28	26.42	31.50	7.62	27.61	-	-	R0	55	1 (<5)
2520	5.16	10.06	15.77	26.28	31.42	7.16	28.18	-	-	R0	22	1 (<5)
2610	5.16	9.02	17.00	26.54	31.30	8.00	27.26	-	-	R0	60	1 (<5)
2640	6.39	9.42	16.59	26.43	32.86	7.84	27.48	5.56	4.74	R1	65	2 (±5)
2725	6.39	9.28	16.90	26.49	32.94	7.98	27.41	5.24	ND	R1	72	2 (±5)
2775	6.12	ND	17.04	26.52	ND	7.98	27.36	5.11	ND	R1	55	2 (±5)
2850	7.01	8.80	16.95	26.54	33.56	8.02	27.19	5.03	4.42	R1	67	3 (±4)
3040	7.31	8.85	17.17	26.54	33.94	8.24	27.15	5.03	4.48	R1	76	3 (±4)
3155	7.40	8.90	17.10	26.54	34.14	8.24	27.20	4.93	4.25	R1	79	3 (±4)
3200	7.42	8.90	17.10	26.56	34.00	8.20	27.12	5.03	4.41	R1	77	3 (±4)
3300	7.36	8.90	17.26	26.54	34.00	8.19	27.20	4.82	4.64	R1	77	3 (±4)
3385	7.42	9.01	17.16	26.54	34.00	8.24	27.20	4.92	4.48	R1	77	3 (±4)
3495	7.42	8.95	17.26	26.54	34.04	8.24	27.15	5.03	4.27	R1	78	3 (±4)
3560	7.42	8.65	17.16	26.54	34.08	8.24	27.20	5.03	4.27	R1	78	3 (±4)
3640	7.16	9.21	17.00	26.54	33.70	8.20	27.30	4.97	4.69	R1	71	3 (±4)
3745	7.63	8.90	17.50	26.64	34.38	8.34	27.05	4.92	4.30	R1	83	3 (±4)
3820	7.42	9.11	17.10	26.59	34.04	8.22	27.25	5.03	4.55	R1	78	3 (±4)

Sample Depth(m)	Reflections from glycolated samples (°2θCuKα radiation)					Reflections from air-dried samples		BB1	BB2	Ordering types	%I in I/S	Method (error)
South Mara C-13 Continued.												
3925	6.75	9.30	16.85	26.54	33.46	8.00	27.40	5.17	4.76	R1	65	3 (±4)
4040	7.26	9.11	17.05	26.52	33.92	8.13	27.20	5.03	4.66	R1	75	3 (±4)
4235	7.31	ND	17.28	26.58	34.18	8.03	27.15	4.42	4.23	R1	80	3 (±4)
4330	7.62	ND	17.38	26.60	34.50	8.19	27.00	3.99	ND	R3	85	3 (±4)
4425	7.31	ND	17.10	26.49	34.04	8.19	27.20	5.03	4.25	R1	78	3 (±4)
4495	7.30	ND	17.05	26.42	34.00	8.08	27.04	4.71	4.40	R1	77	3 (±4)
4650	7.21	ND	17.07	26.38	33.65	8.08	27.20	5.14	4.19	R1	69	3 (±4)
4710	7.11	ND	17.28	26.42	33.72	8.14	27.20	5.06	4.10	R1	71	3 (±4)
4740	7.16	ND	17.28	26.48	33.69	8.03	27.10	4.82	4.19	R1	70	3 (±4)
4890	6.85	ND	17.17	26.48	33.40	8.04	27.25	5.03	4.47	R1	64	3 (±4)
4955	7.11	ND	17.26	26.48	33.58	8.00	27.16	5.14	4.26	R1	68	3 (±4)
5010	7.06	ND	17.05	26.48	33.56	8.05	27.20	4.93	4.50	R1	67	3 (±4)
South Tempest G-88												
1425	5.21	10.03	15.67	26.23	31.44	6.96	27.87	-	-	R0	15	1 (<5)
1630	5.11	9.93	15.82	26.33	31.48	7.01	27.72	-	-	R0	22	1 (<5)
1830	5.26	9.77	15.96	26.38	31.54	7.16	27.66	-	-	R0	30	1 (<5)
2035	5.16	9.72	16.06	26.33	31.66	7.42	27.51	-	-	R0	37	1 (<5)
2330	5.16	9.57	16.24	26.38	31.66	7.42	27.61	-	-	R0	42	1 (<5)
2640	5.21	9.84	15.96	26.38	31.46	7.26	27.82	-	-	R0	31	1 (<5)
2670	5.21	9.88	16.03	26.38	31.64	7.26	27.87	-	-	R0	37	1 (<5)
2725	5.21	9.88	16.08	26.38	ND	7.36	27.92	-	-	R0	38	1 (<5)
3085	6.70	9.36	16.75	26.43	33.30	7.98	27.41	5.18	5.10	R1	63	3 (±4)
3385	6.60	9.31	16.80	26.43	33.20	7.88	27.41	5.40	5.00	R1	65	2 (±5)
3780	7.06	9.06	17.00	26.38	33.75	7.93	27.10	4.88	4.82	R1	72	3 (±4)
3945	7.16	SH	17.51	26.54	33.70	8.03	26.95	4.82	4.40	R1	71	3 (±4)
4370	7.21	SH	17.26	26.59	33.90	7.98	27.00	4.56	4.58	R1	75	3 (±4)
Voyager J-18												
1845	5.21	10.14	15.72	26.32	31.52	7.11	28.28	ND	ND	R0	13	1 (<5)
2640	7.00	8.85	17.10	26.58	33.61	7.77	26.94	5.01	4.76	R1	68	3 (±4)
2735	7.06	8.65	17.05	26.54	33.76	7.72	27.05	5.03	5.09	R1	72	3 (±4)
West Flying Foam L-23												
1450	5.21	9.93	15.87	26.38	31.48	7.21	27.56	-	-	R0	25	1 (<5)
1610	5.16	ND	16.08	26.33	31.51	7.42	27.30	-	-	R0	35	1 (<5)
1850	5.21	ND	16.03	26.38	31.56	7.48	27.41	-	-	R0	33	1 (<5)
2350	5.26	9.80	16.00	26.43	31.68	7.38	27.86	-	-	R0	30	1 (<5)
2625	5.21	9.72	15.98	26.38	31.64	7.47	27.82	-	-	R0	29	1 (<5)
2875	5.21	ND	16.13	26.43	31.56	7.42	27.66	-	-	R0	39	1 (<5)
3070	5.26	9.67	16.13	26.38	31.74	7.52	27.66	-	-	R0	38	1 (<5)
3325	5.21	ND	16.24	26.43	31.62	7.57	27.46	-	-	R0	43	1 (<5)
3640	5.16	8.95	17.10	26.43	31.54	8.08	27.31	-	-	R0	60	2 (±5)
3965	7.52	9.06	17.16	26.54	34.14	8.19	27.20	4.72	4.58	R1	80	3 (±4)
4255	7.62	8.95	17.31	26.60	34.10	8.24	27.15	4.82	4.42	R1	79	3 (±4)
4460	7.62	8.96	17.34	26.54	34.83	8.29	27.15	4.78	4.15	R1	83	3 (±4)
Whiterose J-49												
1050	5.16	SH	15.82	26.28	31.36	7.24	27.68	-	-	R0	25	1 (<5)
1200	5.24	9.76	15.86	26.36	31.48	7.18	27.77	-	-	R0	25	1 (<5)
1535	5.24	SH	16.08	26.33	31.46	7.36	27.51	-	-	R0	37	1 (<5)
1825	5.16	SH	16.13	26.38	31.38	7.52	27.48	-	-	R0	41	1 (<5)

Sample Depth(m)	Reflections from glycolated samples (°2θCuKα radiation)					Reflections from air-dried samples		BB1	BB2	Ordering types	%I in I/S	Method (error)
Whiterose J-49 Continued.												
2020	5.21	9.60	16.28	26.36	31.46	7.54	27.56	-	-	R0	47	1 (<5)
2325	5.21	9.72	15.96	26.38	31.42	7.31	27.87	-	-	R0	34	1 (<5)
2655	7.16	8.70	17.26	26.59	33.84	8.13	27.25	4.76	4.21	R1	74	3 (±4)
2880	7.53	8.70	17.41	26.64	34.00	8.24	27.10	4.96	4.43	R1	77	3 (±4)
3570	7.72	8.90	17.36	26.59	34.38	8.24	27.10	4.40	4.10	R1	83	3 (±4)
3920	7.67	8.84	17.26	26.59	34.30	8.19	27.15	4.30	4.04	R1	82	3 (±4)
4530	SH	8.65	17.46	26.59	34.54	8.24	27.10	ND	3.99	R3	86	3 (±4)

SH=shoulder; ND=not determined; BB1 and BB2 as defined in the text (section 3.4.3); methods used to estimate the proportion of I-layers in I/S: (1)=Šrodoń, 1981; (2)=Reynolds, 1980 and Hower, 1981; (3)= Šrodoń, 1984; (4)=Šrodoń, 1980. Error in estimation of proportion of I-layers are indicated in brackets as reported by the original authors. Ro=random I/S; WR1=weakly-ordered; R1=R1-ordered; R3=R3-ordered I/S. Sample depth represents the middle part of the composite sample interval.